Understanding the Determinants of Pathogenicity in Group A *Streptococcus*

Thesis submitted in accordance with the requirements of the University of Liverpool for the degree of Doctor of Philosophy by

Jenny Clarke

February 2019

Abstract

Background: *Streptococcus pyogenes* is an important human pathogen responsible for clinical manifestations ranging from mild superficial infections such as pharyngitis to serious invasive infections such as necrotising fasciitis and sepsis. The drivers of these different disease phenotypes are not known. The M surface protein encoded by the *emm* gene is used to type GAS isolates and is used as an epidemiological marker; over 230 *emm* types have been described to date. Using *in vitro* and *in vivo* models of GAS infection the aim of this thesis was to consider the different pathogenic mechanisms GAS employs to cause serious acute infection, host-immune evasion and chronic infection.

Methods: *In vitro* characteristics such as susceptibility to opsonophagocytosis, complement deposition, and whole blood survival were characterised for a range of *emm* types across outbreak and non-outbreak isolates. These findings were translated to murine infection models of GAS. The role of streptolysin in determining disease outcome *in vivo* was investigated, by using two different clinical lineages: the emergent hypervirulent outbreak *emm* type 32.2 isolates including the development of an isogenic deletion mutant of streptolysin, that result in sepsis, and the *emm* type 1.0 isolates that cause septic arthritis. Finally, the local host immune response in the knee joints during arthritic GAS infection was characterised using flow cytometry and cytokine quantification.

Results: The *emm*32.2 isolate was able to resist opsonophagocytosis, survive in whole blood, produce large quantities of highly haemolytic SLO and result in the rapid development of sepsis in the murine infection models. By contrast, the *emm*1.0 isolate was susceptible to opsonophagocytosis, was not able to survive in whole blood and produced lower levels of SLO which led to translocation of bacteria to the joints. Importantly, sepsis associated strains that were attenuated by deletion or inhibition of SLO also translocated to the joint, confirming the key role of SLO in determining infection niche. The characterisation of the immune response in the joint during infection showed a highly pro-inflammatory immune response with an influx of neutrophils, macrophages, and associated cytokines early in the infection which may ultimately contribute to the severe joint damage caused during GAS septic arthritis.

Conclusion: The findings throughout this thesis have implications for the future of vaccine design and therapeutics for GAS. By understanding the mechanisms of infection, the varying virulence characteristics and the proceeding host response it provides a foundation with which to target specific bacterial and host proteins.

Acknowledgments

Firstly, I would like to thank my PhD supervisors, Aras Kadioglu, Neil French and Dean Everett, who have provided invaluable support and guidance throughout my research. Aras, thank you for your advice and consistent encouragement, I am sincerely grateful that I was able to complete my PhD in your lab and I look forward to continuing to work with you in the future. I have been privileged to have you as a supervisor, mentor and friend. Neil, I am grateful that your door was always open and for all the support you have provided for my next adventure into medical school. Dean, I would also like to thank you for your support and for hosting me in your lab in Malawi at the start of this journey.

I would also like to thank Dr. Neil Blake, Dr. Steve Christmas and Dr. Dan Neill who have kindly offered their guidance and advice throughout my PhD.

A huge thankyou goes to various members of IGH who made a significant impact on my life. Laura and Vicky for your friendship, curly hair and dancing. Suzy for your cheese and wine nights, Flick and Korean makeup advice. Yasmina for the sleepovers, late night chats and letting me wear your clothes. Simon for all the times you said 'chin up kid'. Thank you for an incredibly supportive lab group: Emma, Hind, Hajar, Laura J, Becca, Murielle, Elaine, Laura T, Alice, Marie and Shadia.

To Mansoor and Amirah, I am so grateful for your friendship. You both mean a lot to me and I am so thankful that I can call you my family. Rana and Abdullah your cuddles have been greatly appreciated after a long day in the lab.

To both my Mum and Dad, it's hard to know where to start. Both of you have always been so supportive of my dreams no matter how crazy, ambitious or small they are. Whether it was as a little girl watching Dad climb over walls to get me the best conkers, or Mum searching high and low for my favourite type of colouring pens. Dad for taking me to every university open day up and down the country and supporting me every time I call up with a new idea or plan even if I interrupt the rugby. Mum for being my best friend, for spending hours daily on the phone with me through both good and harder times and for all the care packages you still send me. I couldn't have done any of this without you!

My two big brothers Lee and Carl and my big sister Emma. Thank you for all the love, support and chats. Also, thank you for my beautiful nieces and nephews who are all growing up to be amazing young people.

Bob my loyal Jack Russel, I wouldn't have made it this far without your company and cuddles, especially during long nights of school work. Buzz my little chihuahua, you have been a light through some dark times, thank you for the adventures we have been on. Bronwen my sassy cat, thank you for always keeping me on my toes.

My partner, Matt, thank you for being my person. You are my biggest fan and always believe in me. I am so very grateful for your friendship, love, and laughter. We have been on so many adventures together, but my favourite will always be sat eating skittles with you at the beginning of our PhDs or as I always say 'when we were babies'. I can't wait for what's next bestie.

I would like to dedicate this thesis to a very special little boy, Abdullah, who sadly passed away during my PhD. Your smile and laughter will be remembered forever. Sweet dreams my Aboody xxx

Table of Contents

1. General Introduction 1

1.1 Background of GAS infections 2

1.1.1 Bacteriology 2

1.2 Clinical manifestations 4

1.2.1 Asymptomatic carriage 5

1.2.2 Pharyngitis and scarlet fever 7

1.2.3 Severe group A Streptococcal infections 8

1.2.4 Septic arthritis 9

1.2.5 Post-streptococcal disorders 10

1.3 Therapeutic approaches 11

1.4 Vaccines 12

1.5 Epidemiology 14

1.5.1 Disease burden 14

1.5.2 Outbreaks 15

1.5.3 Molecular epidemiology 16

1.6 Virulence factors 17

1.6.1 CovR/CovS transcriptional regulator of virulence 18

1.6.2 M protein 18

1.6.3 Hyaluronic acid capsule 20

1.6.4 Secreted extracellular virulence factors 21

1.6.5 Superantigens 28

1.7 Host response to severe group A Streptococcal infections 29

1.7.1 Innate immune cells in defence against GAS 29

1.7.2 Evasion of innate immune responses 31

1.7.3 Adaptive immunity against GAS 32

1.8 Animal models of group A Streptococcal infections 34

1.8.1 Models of nasopharyngeal colonisation 35

1.8.2 Models of soft tissue and wound infection 36

1.8.3 Models of systemic infection 37

1.8.4 Models of bone and joint infection 38

1.8.5 Transgenic mice 39

1.9 Research aims 41

2. Materials and Methods 42

2.1 Microbiology 43

2.1.1 Bacterial strains 43

2.1.2 Standard media 45

2.1.3 Viable count of bacteria (Miles and Misra Method) 46

2.1.4 Preparation of bacterial stocks 47

2.1.5 Growth curves 48

2.1.6 *Emm* typing GAS isolates 48

2.2 Tissue culture 51

2.2.1 HL60 cell culture 51

2.2.2 Differentiating HL-60 cells 52

2.2.3 J774.2 cell culture 52

2.3 Peripheral blood neutrophil isolation 54

2.3.1 Volunteer recruitment 54

2.3.2 Isolation 54

2.3.3 Purification 55

2.4 Opsonophagocytosis killing assay 56

2.4.1 Opsonisation 56

2.4.2 Phagocytosis 57

2.4.3 Analysis 58

2.5 Blood survival assay 59

2.6 Murine models of invasive GAS infection 59

2.6.1 Murine strains 59

2.6.2 Preparing GAS inoculum 59

2.6.3 Intranasal route of infection 60

2.6.4 Intravenous infection 61

2.6.5 Details of isolates used in virulence testing 62

2.6.6 Virulence testing 63

2.6.7 Infection studies: Blood, lung, and nasopharyngeal tissue 63

2.6.8 Monitoring murine behaviour 64

2.7 Murine models of septic arthritis 65

2.7.1 Arthritic index 65

2.7.2 Joint tissue 65

2.7.3 *In vivo* recovery of bacteria from joints 66

2.8 Streptolysin specific ELISA 67

2.9 Haemolytic activity assay 68

2.10 Construction of GAS mutants 69

2.10.1 Single knockout of SLO and SpeA 69

2.11 Liposomes 72

2.12 Cell population studies 73

2.12.1 Flow cytometry 73

2.13 Cytokine capture and analysis 75

2.14 Statistical analysis 75

3. Characterising the phenotypic response of GAS isolates *in vitro* 76

A. Introduction 77

3.1 *Emm* type 32.2 outbreak in Liverpool 77

3.2 Opsonophagocytosis killing assays 79

3.3 Rationale **80**

B. Results **81**

3.4 Confirmation of *emm* type and clinical profile of GAS isolates **81**

3.5 Opsonophagocytosis killing assay - peripheral blood neutrophils **83**

3.6 Opsonophagocytosis killing assay – differentiated HL-60 cells **86**

3.7 Opsonophagocytosis killing assay – J774.2 macrophage cells **88**

3.8 Comparison of OPKA with capsule thickness and complement deposition **91**

3.9 Isolates chosen for *in vivo* modelling **93**

3.10 Whole blood and serum survival assays **95**

C. Discussion **97**

4. Investigating the pathogenesis of group A *Streptococcus* using *in vivo* infection models **104**

A. Introduction **105**

4.1 *In vivo* models of GAS **105**

4.1.1 Model of invasive infection 105

4.1.2 Model of septic arthritis 106

4.2 Rationale **106**

B. Results **108**

4.3 Intranasal route of infection **108**

4.3.1 Virulence testing using low intranasal volume dose 108

4.3.2 Virulence testing using high intranasal volume dose 109

4.4 Intravenous route of infection **113**

4.4.1 Survival comparison during invasive disease 113

4.4.2 Progression of infection during invasive disease 117

4.4.3 Weight loss during invasive disease 123

4.4.4 Bacterial arthritis phenotype after intravenous infection 125

4.5 Kinetics of septic arthritis **126**

4.5.1 Progression of infection in the knee joints 126
4.5.2 Severity of arthritis 129
4.6 Host-adapted *emm* type 1.0 (isolate 101910) 131
4.6.1 Comparison of bacterial load in the blood and spleen 131
4.6.2 Comparison of joint bacterial burden and severity 134
C. Discussion 137
5. Streptolysin production and activity is central to *in vivo* pathotype and disease outcome 143
A. Introduction 144
5.1 Introduction to GAS virulence factors 144
5.2 Secreted bacterial toxins: Streptolysin 144
5.3 Rationale 145
B. Results 146
5.4 Streptolysin- Enzyme-Linked Immunosorbent Assay 146
5.5 Comparison of streptolysin production and activity 147
5.5.1 *Emm* type 32.2 isolate 112327 and *emm* type 1.0 isolate 101910 147
5.5.2 Comparison of SLO with selection of other isolates 151
5.6 *In vivo* recovered *emm* type 1.0 isolate 101910 has reduced production and activity of SLO 153
5.6.1 *In vitro* passaging host-adapted *emm* type 1.0 155
5.7 Concentration and activity of streptolysin has significant impact on virulence *in vivo* 158
5.8 Streptolysin deficient mutant 164
5.8.1 Streptolysin deficient *emm* type 32.2 isolate 112327 during invasive infection 166
5.8.2 Streptolysin deficient *emm* type 32.2 causes septic arthritis 168
5.8.3 Streptolysin deficient supernatant from *emm* type 32.2 170
5.9 Liposomes as a decoy target receptor for Streptolysin 174

5.9.1 Incubation with liposomes sequesters streptolysin..... 174

5.9.2 Liposomes used *ex vivo* increase survival with *emm* type 32.2 invasive disease176

5.10 *In vivo* liposome study 178

5.10.1 Single treatment of liposomal mixture 178

5.10.2 Double treatment of liposomal mixture..... 180

C. Discussion 184

6. Group A *Streptococcus* dependent septic arthritis in murine knee joints: The local immune response..... 191

A. Introduction..... 192

6.1 Host response in septic arthritis 192

6.2 Bacterial superantigens and septic arthritis..... 193

6.3 Rationale..... 193

B. Results 194

6.4 GAS systemic infection in mice results in fast knee joint infiltration which evolves to a more chronic form..... 194

6.5 Local inflammatory response and immune cell recruitment in knee joints 196

6.5.1 Cytokines..... 196

6.5.2 Immune cells 198

6.6 Effect of host-adapted *emm* type 1.0 101910 during re-infection 202

6.6.1 Immune cell recruitment 202

6.6.2 Comparison of immune cell recruitment..... 204

6.7 Identification of T regulatory cells during chronic infection of the knee joints. 206

6.8 Role of CCR5 and CXCR3 CD4+ T cells in the knee joint 209

6.8.1 CCR5/CXCR3 T cells in knee joint during infection with *emm* type 1.0 isolate 101910..... 209

6.8.2 CCR5/CXCR3 T cells in knee joint during infection with host-adapted *emm* type 1.0 isolate 101910 213

6.9 Spe A deficient *emm* type 1.0 isolate 101910 215

6.9.1 Effect of Spe A on progression of septic arthritis 216

6.9.2 Comparison of immune cells..... 218

C. Discussion 220

7. General discussion..... 229

7.1 *Emm* 32.2 resistance to opsonophagocytosis 230

7.2 Murine models of GAS..... 231

7.3 SLO the key to distinct *in vivo* pathotypes 233

7.4 Host-adapted GAS..... 234

7.5 Host-pathogen interactions during GAS septic arthritis 236

7.6 Summary 237

8. References 239

Abbreviations

Ab	Antibody
APC	Allophycocyanin
APC- Cy7	Allophycocyanin/Cyanine dye7
BAB	Blood agar base
BHI	Brain heart infusion
BSA	Bovine serum albumins
C3	Complement component 3
CFU	Colony forming units
DMEM	Dulbecco's Modified Eagle' Medium
DMSO	Dimethyl-sulphoxide
DPBS	Dulbecco's phosphate-buffered saline
EDTA	Ethylenediaminetetraacetic acid
ELISA	Enzyme-linked immunosorbent assay
FACS	Fluorescence-activated cell sorting
FBS	Fetal Bovine Serum
FI	Fluorescent index
FITC	Fluorescein isothiocyanate
Flincr	Florescent index increase
FOXP3	Forkhead box P3
GAS	Group A Streptococcus
HBSS	Hanks' Balanced Salt Solution
Ig	Immunoglobulin
IL	Interleukin
IN	Intranasal

INF	Interferon
IV	Intravenous
IVC	Individually ventilated cages
IVIG	Intravenous immunoglobulin
MFI	Mean fluorescence intensity
MLST	Multi locus sequence type
MHC	Major histocompatibility complex
NaOH	Sodium hydroxide
NCTC	The National Collection of Type Cultures
NP	Nasopharynx
OD	Optical density
OPK	Opsonophagocytic killing
OPKA	Opsonophagocytic killing assay
PBS	Phosphate-buffered saline
PCR	Polymerase chain reaction
PE	Phycoerythrin
PE-CY7	Phycoerythrin/Cyanine dye7
RBC	Red blood cell
RPMI	Roswell Park Memorial Institute medium
SEM	Standard Error of Mean
SLO	Streptolysin O
SLS	Streptolysin S
Th	T-helper cells
TO	Thiazole orange
UK	United Kingdom

List of figures

Figure 1 – Diagram of GAS with associated cell wall and excretory proteins. 3

Figure 2 – Range of group A Streptococcal diseases. 5

Figure 3 – Routes of bacterial infection in the joint, adapted from [60]. 9

Figure 4 - Prevalence of rheumatic heart disease in children aged 5–14 years (circles represent indigenous populations) [93] 14

Figure 5 – The range of virulence factors produced by group A *Streptococcus* [3]. . 17

Figure 6 – Colonies of group A *Streptococcus* grown on 5% blood agar 20

Figure 7– Predicted three-dimensional structure of Streptolysin. 23

Figure 8 – Generalized mechanism of pore formation by streptolysin. 24

Figure 9 – Evasion strategies of GAS to the innate immune system [175]. 31

Figure 10 – Animal models of group A *Streptococcus* [213]. 34

Figure 11 – Density gradient seperation of peripheral blood leukocytes. 55

Figure 12 - Intranasal dosing of bacterial inoculum into mice, published in [263]. .. 60

Figure 13 - Schematic diagram of a transverse section of a mouse-tail showing 61

Figure 14 – Histogram plot of outbreak and invasive GAS cases that were collected at the same time in Merseyside. 77

Figure 15 - Maximum likelihood phylogeny of the 48 GAS isolates based on core genome SNPs. 79

Figure 16 - Effect of different dilutions of intravenous immunoglobulin in opsonophagocytosis killing assay using freshly derived peripheral blood neutrophils. 84

Figure 17 - Sensitivity to opsonophagocytosis by freshly derived peripheral blood neutrophils. 85

Figure 18 - Sensitivity to opsonophagocytosis by differentiated HL-60 cells. 87

Figure 19 - Sensitivity to opsonophagocytosis by J774.2 macrophages. 89
Figure 20 - Percent killing by J774.2 macrophage cells versus capsule thickness and complement deposition. 92
Figure 21 – Comparison of capsule thickness, complement deposition, and OPK survival between isolates chosen for *in vivo* infection studies. 94
Figure 22 – Survival of *emm* type 32.2 (isolates 112327 and 102029) and *emm* type 1.0 (isolate 101910) in whole blood and serum over 24 hours. 96
Figure 23 - Comparison of survival of mice when infected with different isolates in a model for GAS pneumonia. 111
Figure 24 - Schematic representation of systemic infection model with GAS. 113
Figure 25 - Comparison of survival of mice when infected with different isolates in a model for GAS bacteraemia. 115
Figure 26 – Bacterial burden in blood of mice when infected with different isolates in a model for GAS bacteraemia. 119
Figure 27 – Direct comparison of bacterial burden in blood of mice when infected with different isolates in a model for GAS bacteraemia at 24 hours. 120
Figure 28 - Bacterial burden in spleen of mice when infected with different isolates in a model for GAS bacteraemia. 122
Figure 29 – Percent weight loss of mice when infected with different isolates in a model for GAS bacteraemia. 124
Figure 30- Schematic representation of osteomyelitis and septic arthritis model with GAS. 125
Figure 31 – Comparison of bacterial numbers in the knee joints and blood after intravenous infection with *emm* type 1.0 isolate 101910. 128

Figure 32 - Arthritic index score of knee joints during infection with *emm* type 1.0 isolate 101910. 130

Figure 33 – Comparison of bacterial burden in blood and spleen after intravenous infection with *emm* type 1.0 isolate 101910 and *in vivo* recovered *emm* type 1.0 isolate 101910. 133

Figure 34 - Comparison of knee joint CFU and arthritic index after intravenous infection with *emm* type 1.0 isolate 101910 and *in vivo* recovered *emm* type 1.0 isolate 101910. 136

Figure 35 – Streptolysin ELISA standard curve. 146

Figure 36- Comparison of streptolysin production and activity *emm* type 32.2 isolate 112327 and *emm* type 1.0 isolate 101910. 149

Figure 37 - Growth kinetics of *emm* type 32.2 isolate 112327 and *emm* type 1.0 isolate 101910. 150

Figure 38- Comparison of streptolysin production and activity in other *emm* type 32.2 isolates and *emm* type 6.0 isolates..... 152

Figure 39- Comparison of streptolysin production and activity in *emm* type 1.0 isolate 101910 grown *in vitro* or recovered from *in vivo*..... 154

Figure 40 - Comparison of streptolysin production and activity in *in vivo* recovered *emm* type 1.0 isolate 101910 and after subsequent growth *in vitro* 156

Figure 41 – Growth kinetics of *in vivo* recovered *emm* type 1.0 isolate 101910 and after subsequent *in vitro* passaging. 157

Figure 42- Analysis of SLO concentration and activity in challenge inoculum. 159

Figure 43- Schematic diagram of the method used to switch the supernatants of *emm* type 32.2 (isolate 112327) and *emm* type 1.0 (isolate 101910) before intravenously infecting mice. 160

Figure 44 - Effect of concentration and activity of secreted SLO on virulence *in vivo.* 162

Figure 45 - Percentage weight loss of mice during invasive infection with *emm* type 1.0 isolate 101910 and *emm* type 32.2 isolate 112327. 163

Figure 46 – pGEM®-T Vector (3000bp) Map and sequence reference points including list of restriction sites with corresponding base pairs. 165

Figure 47 – Allelic replacement of streptolysin gene with aad9 Spectinomycin resistance gene, using pGEM®-T Vector. 165

Figure 48 - SLO deficiency increases *in vivo* survival and switches phenotype. 167

Figure 49 - Comparison of knee joint CFU after intravenous infection with *emm* type 32.2 isolate 112327 and isolate ΔSLO 112327 and *emm* type 1.0 isolate 101910. . 169

Figure 50 - Effect of concentration and activity of SLO-containing and SLO-depleted supernatant on virulence *in vivo.* 172

Figure 51 – Liposomes reduce concentration of streptolysin in supernatant of challenge doses. 175

Figure 52 - Effect of incubation of liposomes with challenge dose of bacteria before invasive infection. 177

Figure 53 – Effect on virulence of sequestration of SLO by cholesterol: sphingomyelin (Ch: Sm) liposomes *in vivo*. 179

Figure 54 – Effect on bacterial load of sequestration of SLO by cholesterol: sphingomyelin (Ch: Sm) liposomes at 24 h. 180

Figure 55 – Effect on virulence when using two dose treatments of cholesterol: sphingomyelin (Ch: Sm) liposomes *in vivo*. 182

Figure 56 – Comparison of blood CFUs after one and two treatments of cholesterol: sphingomyelin (Ch: Sm) liposomes *in vivo.* 183

Figure 57 – Comparison of bacterial numbers in the knee joints and blood after intravenous infection with *emm* type 1.0 isolate 101910. 195
Figure 58 – Cytokine profiles measured in knee joints of infected animals (pg/joint). 197
Figure 59 – Phenotypic characterization of cells recruited into the knee joints of animals infected with *emm* type 1.0 isolate 101910. 200
Figure 60 – Gating strategy for the analysis of neutrophils, macrophages, B-cells and CD4+ T-cells in knee joints. 201
Figure 61 – Phenotypic characterisation of cells recruited into the knee joints of animals infected with *in vivo* recovered *emm* type 1.0 isolate 101910 203
Figure 62 – Comparison of cells recruited into the knee joints of animals infected with *emm* type 1.0 isolate 101910 and *in vivo* recovered *emm* type 1.0 isolate 101910. 205
Figure 63 – Identification of T regulatory cells recruited into the knee joints. 207
Figure 64 – Gating strategy for the analysis of T regulatory cells in knee joints. ... 208
Figure 65 – Phenotypic characterisation of populations of T cells recruited into the knee joints of animals infected with *emm* type 1.0 isolate 101910 211
Figure 66 – Gating strategy for the analysis of CXCR3+/CCR5+ CD4+ T-cells in knee joints. 212
Figure 67 – Phenotypic characterisation of populations of T cells recruited into the knee joints of animals infected with *in vivo* recovered *emm* type 1.0 isolate 101910 214
Figure 68 – Allelic replacement of Spe-A gene with aphA3 Kanamycin resistance gene, using pGEM®-T Vector. 215

Figure 69 – Comparison of bacterial CFU in the knee joints and the arthritic index after intravenous infection with *emm* type 1.0 isolate 101910 and ΔSpeA 101910. 217
Figure 70 – Comparison of cells recruited into the knee joints of animals infected with *emm* type 1.0 isolate 101910 and Δ SpeA 101910..... 219

List of tables

Table 1 – Current vaccine candidates for group A *Streptococcus* 13

Table 2 – List of GAS isolates and the associated clinical data used for this study. . 43

Table 3 – Volume of bacteria, IVIG, and opsonisation buffer used in opsonised and non-opsonised wells. 57

Table 4 - Mouse strain, bacterial dose, and volumes used for different models of infection..... 62

Table 5 – Description and score used to assess the development of infection in murine models. 64

Table 6 – Primers used in single knockout of SLO and SpeA in GAS..... 71

Table 7 – Antibodies and dilutions used for FACs analysis of different cell types... 74

Table 8 – Selection of isolates chosen for study, with respective disease category and *emm* type. 82

Table 9 – Comparison of percent killing by J774.2 macrophages 90

Table 10 - Comparison of survival of mice when infected with different isolates in a model for GAS pneumonia 112

Table 11 - Comparison of survival of mice when infected with different isolates in a model for GAS bacteraemia..... 116

Table 12 – Comparison of survival of mice using a Log-rank (Mantel-Cox) analysis when intravenously infected (50 µl) with *emm* type 1.0 isolate 101910, *emm* type 1.0 isolate 101910 bacteria re-suspended in supernatant from *emm* type 32.2 isolate 112327 or re-suspended in supernatant from isolate ΔSLO 112327 challenge dose (**$p < 0.01$). 173

1. General Introduction

1.1 Background of GAS infections

The clinical importance of Streptococci was first highlighted in 1879 when Louis Pasteur isolated the organism from the uterus and blood of women with puerperal fever [1, 2]. Friedrich Julius Rosenbach then later refined the name streptococcus; he examined isolates from suppurative lesions and named the species *Streptococcus pyogenes* (Gr., *pyo, pus,* and *genes,* forming) [1]. *Streptococcus pyogenes* also known as group A *Streptococcus* (GAS) is one of the most phenotypically diverse of any human pathogen, and has a varied range of clinical manifestations [3]. GAS causes mild superficial infections such as pharyngitis and more severe invasive infections such as necrotising fasciitis and sepsis [3]. In addition to this, repeated GAS infection can also lead to autoimmune diseases including acute rheumatic fever, and rheumatic heart disease [3].

1.1.1 Bacteriology

GAS is a Gram-positive, non-motile, non-sporeforming cocci that occur in pairs or chains [4] (Figure 1). It is β-haemolytic when grown on agar enriched with 5% horse blood. Prominent microbiologist Rebecca Lancefield introduced the initial classification of GAS based on specific group A carbohydrates on the cell wall [5]. The group A carbohydrate is made up of a polyrhamnose core with an immunodominant N-acetylglucosamine (GlcNAc) side chain [6]. This has been important in the development of rapid diagnostic tests in the laboratory and for use in the clinic [7]. The rapid latex agglutination test is based on latex beads coated with antibodies that react with the specific carbohydrate antigens on the cell wall of streptococci species. If the carbohydrate antigen is present, the latex beads clump providing a visual positive result that enables subsequent typing into streptococcal

groups A, B, C, D, F and G from primary culture plates [8]. The Streptococcal M protein may also be used to determine GAS serotypes [9]. The M protein is coded by the *emm* gene and through advancements in sequencing technology can be used as an epidemiological marker to identify GAS isolates [10]. Over 200 *emm* types have been identified, and although a large number there is a distinct prevalence in the distribution of serotypes [11, 12]. Steer *et al*., analysed the global distribution of *emm* types and found that *emm* type 1.0 is the most common globally, and this *emm* type has also been found to be more likely in invasive infections [10, 12]. Importantly, it was also found that there were significant differences in *emm*-type distribution between high-income countries and lower and middle-income countries (LMICs) throughout Africa and the Pacific [12]. The reasons for the contrasting epidemiology is not fully understood [12].

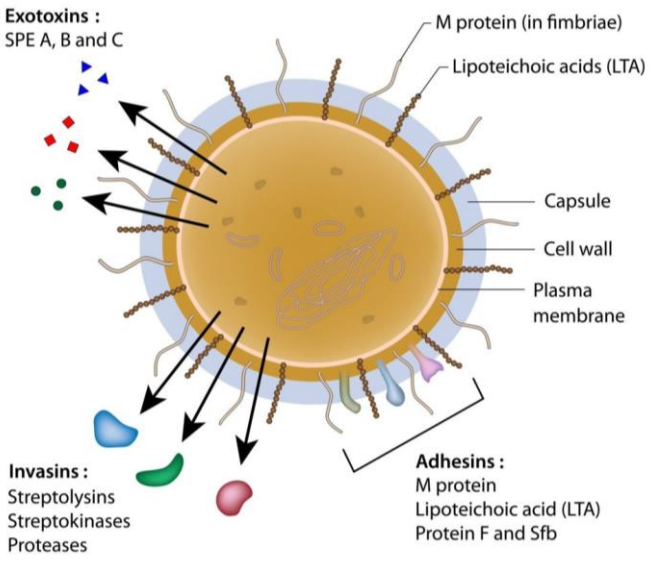

Figure 1 – Diagram of GAS with associated cell wall and excretory proteins.
GAS is encapsulated by a hyaluronic acid capsule and has several other important cell wall associated proteins including the M protein. GAS also has an array of important secretory proteins which are key in establishing infection and evading the host response. Adapted from [Alila Medical Image].

GAS has a genome size of approximately 1.8 to 1.9 Mb, with five to six highly conserved rRNA operons, and a core group of virulence genes [13-15]. GAS has a pan-genome comprised of 3,451 with 1,221 constituting the core genome (present in ≥99% of 118 isolates [16-19]. All GAS isolates are polylysogenic, containing multiple prophages or prophage-like elements [16-18]. Many prophages encode one or two virulence factors such as DNAses, pyrogenic superantigens or adhesins [13].

1.2 Clinical manifestations

There are a broad range of GAS related diseases across a clinical spectrum of both benign and serious infections which include pharyngitis, impetigo, cellulitis, scarlet fever, bacteraemia, pneumonia, streptococcal toxic shock syndrome (STSS) and necrotizing fasciitis [3] (Figure 2). Also, GAS infection can trigger serious post infectious immune-mediated disorders, including acute post streptococcal glomerulonephritis (APSGN), acute rheumatic fever (ARF), and rheumatic heart disease (RHD) [3].

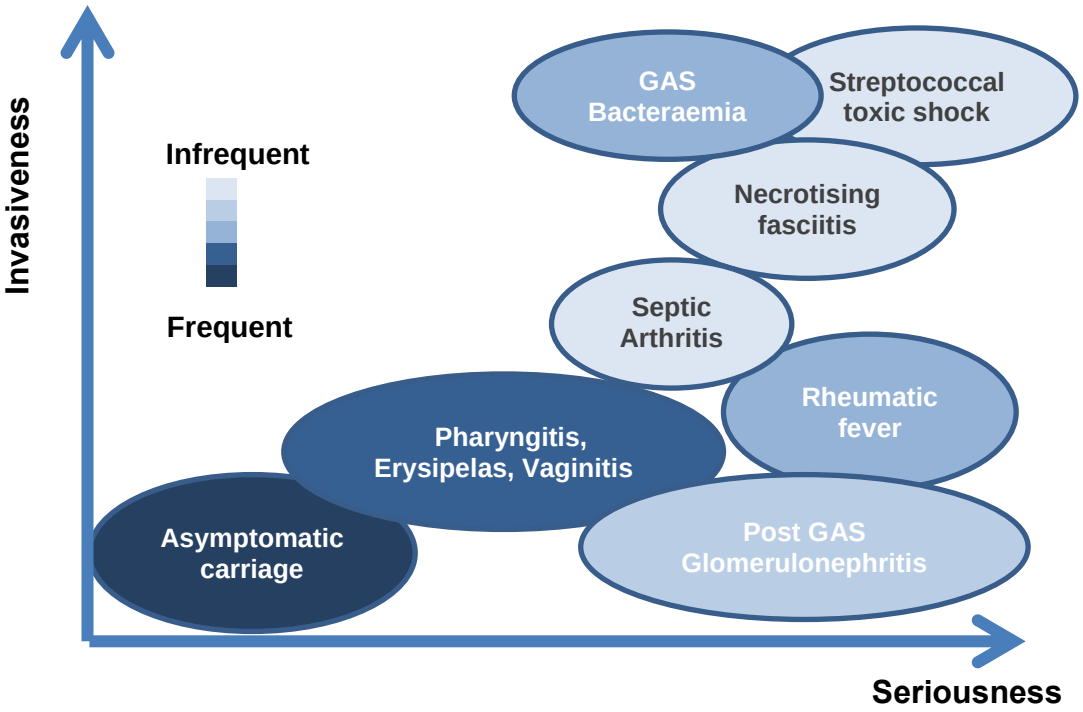

Figure 2 – Range of group A Streptococcal diseases.

GAS infections range in both seriousness of clinical phenotype (x-axis) and (invasiveness y-axis). Within both parameters there are differences in frequency of infection types.

1.2.1 Asymptomatic carriage

Asymptomatic carriage of GAS was first identified during outbreaks of GAS infection, where numerous individuals were found to be harbouring GAS in the pharynx yet were asymptomatic [20, 21]. The classical features of carriage can be defined as the confirmed presence of GAS in the posterior pharynx, with no signs or symptoms of acute infection and an absence of serological antibody rise after serial blood testing [22-24]. A large meta-analysis of studies reporting GAS infection, found that in children who lacked clinical symptoms, GAS was detected in the pharynx 12% of the time [25]. The study also found that the prevalence of GAS in

children who presented with a sore throat was 37% [25]. Asymptomatic carriage of GAS ranges from 8-40% in the school aged population [21].

There have been several theories proposed as to how GAS is asymptomatically carried. The first hypothesis is based on the idea that the normal bacterial flora of the pharynx produces β-lactamase that shields GAS from the effects of penicillin [26, 27]. These studies showed that the predominant bacteria isolated from around one-third of patients were *Bacteroides melaninogenicus*, *Bacteroides oralis*, *Bacteroides ruminicola*, and *Staphylococcus aureus* [24]. Further studies have supported this theory where there have been higher eradication rates of GAS when β-lactamase producing organisms harbouring in the pharynx have first been cleared by antimicrobials [28, 29]. GAS has been found to internalise into cell types such as epithelial cells and macrophages during acute invasive infections, thereby explaining why GAS persists even after prolonged intravenous antibiotic treatment [30-32]. In addition to this, penicillins which are frequently used to treat GAS infections are unable to penetrate host cell membranes [33].

The ability of GAS to be transmitted by carriers is somewhat inconclusive, as it is generally regarded that although infection from carriers can occur it is substantially less likely than transmission from a person with an active infection [21]. GAS carriers may play some role in providing a reservoir for invasive infection. A case control study looking at risk factors for paediatric invasive disease found that invasive infection was related to other children living in the home [34]. In addition to this, the study of an outbreak found an increase in the carriage of invasive GAS strains among school-aged children [35]. Carriage of GAS may also have some role

in perpetuating invasive infection, a study by Medina *et al*., found that increased intracellular survival may have some effects on bacterial virulence [36]. The study showed how GAS could be transported around the body after ingestion by neutrophils [36]. This and similar work may be able to explain how necrotizing fasciitis occurs when there is no entry wound or trauma for GAS to invade [37].

1.2.2 Pharyngitis and scarlet fever

Pharyngitis, an infection of the throat, is the most common clinical manifestation of GAS infection [38]. GAS is the causative agent of up to 40% of overall pharyngitis cases in children and 15% of adult cases [25, 39, 40]. The initial presentation of pharyngitis begins with an abrupt onset of fever and sore throat. Complications with GAS pharyngitis can result from direct extension of infection to other adjacent structures or by haematogenous spread to other sites in the body [38]. Severe complications can include otitis media, bacteraemia, pneumonia and meningitis [3]. There is also the risk of further inflammatory complications after the acute infection; these include acute rheumatic fever and post-streptococcal glomerulonephritis [39]. GAS pharyngitis is self-limiting, however antibiotic treatment is justified to shorten the duration of the infection and to prevent post infection syndromes like rheumatic fever [39, 41]. Penicillin is the main course of treatment, and most clinical isolates causative of pharyngitis have remained susceptible to penicillin [38].

Scarlet fever is a clinical syndrome of GAS, which is characterised by a rash alongside a GAS infection, which is most commonly pharyngitis [39]. The rash is made up of minute papules, resulting in a distinctive sandpaper feel to the skin [39]. Many studies have implicated the role of toxins in the pathogenesis of scarlet fever,

and more specifically a group of related streptococcal pyrogenic exotoxins (SPEs); SpeA, SpeC and SSA, are associated with outbreaks of scarlet fever [42-45]. There has been a recent resurgence of scarlet fever cases in the UK [46]. The reasons behind the resurgence are largely unexplained and investigations into the possible causes have largely focused on the potential expansion of a single clonal lineage or a genetic element which renders the population more susceptible [46]. Other hypotheses include a return to natural cyclical patterns of disease, up until the widespread use of antibiotics in the 1960's there were more frequent scarlet fever outbreaks [46].

1.2.3 Severe group A Streptococcal infections

Severe GAS infections affect 663000 people per year globally and are associated with a diversity of invasive diseases such as life-threatening bacteraemia, pneumonia, necrotizing fasciitis, myonecrosis and streptococcal Toxic Shock Syndrome (STSS) [47]. This is largely due to the ability of GAS to breach epithelial barriers, primarily in the lung and skin [3]. The mortality rate for invasive infection ranges from 8-23% within 7 days [48-50]. This increases to 23-81% in cases where the patient develops STSS post infection [3, 48, 49]. During the past decade there has been an increase in the number of cases of severe GAS infections [51, 52]. Prompt antimicrobial therapy with high-dose penicillin and clindamycin is required and in the case of necrotizing fasciitis surgical clearance of infected tissue is also required [53].

1.2.4 Septic arthritis

Septic arthritis is an inflammatory disease of the joints which primarily affects children under 15 or adults over 55 years of age with an estimated incidence of around 6 cases per 100,000 persons per year [54]. GAS is isolated in up to 20% of septic arthritis cases and is the second most common cause of infectious arthritis after S*taphylococcus aureus* [55-58]. The joints become infected when the bacteria enter the synovium. GAS can enter the joints by the following routes: (1) Haematogenously, with the consequent clumping of the bacteria in the synovial capillaries; (2) infected contagious foci; (3) neighbouring soft tissue sepsis; and (4) by direct inoculation due to trauma or during joint surgery (Figure 3) [59].

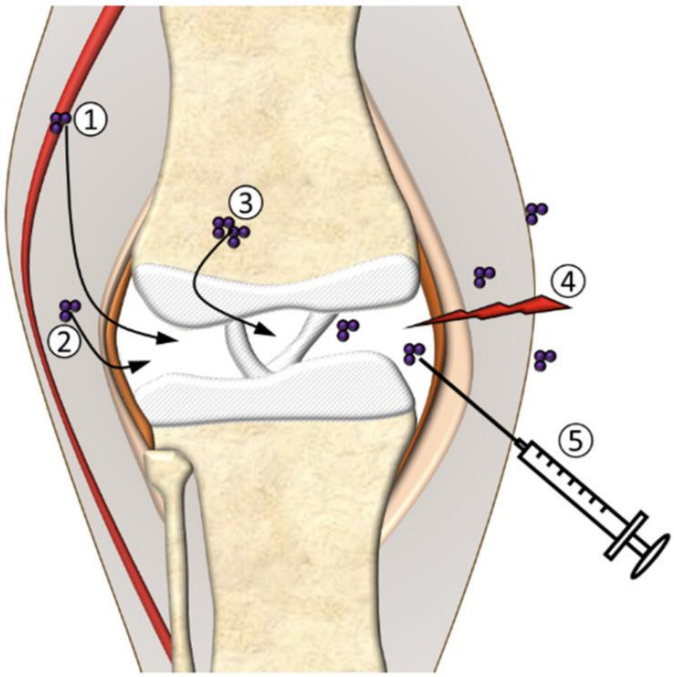

Figure 3 – Routes of bacterial infection in the joint, adapted from [60].
Bacteria can enter the joint through a number of routes: (1) Haematogenous spread; (2) from neighbouring infected tissue; (3) as a consequence of infection in the bone; (4) due to trauma; (5) or during invasive treatment/diagnostics [60].

The joints have several features that promote/enhance bacterial adherence and colonisation. The synovium is highly vascularised with no limiting basement plate which allows easy access by bacteria, and once the bacteria are able to colonise the joint the low fluid shear conditions enhance bacterial adherence and invasion [56, 59]. In addition, the production of host matrix proteins may facilitate the attachment of bacteria in the joint [61]. Joint destruction usually begins at the cartilage-synovium junction, with pannus formation and then cartilage and bone destruction [54]. Prompt antimicrobial therapy and removal of purulent material via needle aspiration is required for successful management [54, 59].

1.2.5 Post-streptococcal disorders

GAS infection may result in a number of post immune sequelae, which include acute rheumatic heart fever/ rheumatic heart disease (ARF/RHD), acute poststreptococcal glomerulonephritis (APSGN), and paediatric autoimmune neuropsychiatric disorders [62]. Most cases of rheumatic fever follow another GAS infection, commonly pharyngitis [62, 63]. A correct diagnosis requires the presence of elevated antibodies to anti-streptolysin O over normal levels and a positive throat culture for GAS [62, 63]. Post immune sequelae often occurs in children and adolescents and there has been a resurgence in the number of reported cases, as seen with other types of GAS infections over the past 30 years [3, 63-65]. There has been no link found between *emm* types and the outcome of ARF and RHD [3]. ARF and RHD occur due to autoimmune mechanisms related to molecular mimicry i.e. the production of antibodies that recognise both the host and microbial antigens [66]. Molecular mimicry has been shown to initiate and potentiate the development of symptoms associated with ARF and RHD [66]. GAS also has a large repertoire of antigens and

superantigens that are able to stimulate B and T cell responses to auto-antigens [67-70]. APSGN is due to the formation of immune-complexes in the kidney, which result in symptoms such as oedema and decreased levels of complement components in the serum. ASPGN is commonly associated with *emm* types 1, 4, 12, 49, 55, 57, and 60 [3]. Some studies have shown that GAS infection is temporally associated with obsessive-compulsive disorder and Tourettes's syndrome traits, termed paediatric autoimmune neuropsychiatric disorders [3, 66]. This area of research has gained more attention recently and some studies have highlighted the potential for anti-neuronal antibodies [3]. Vaccine development however, remains to be the main focus for reducing the number of cases of post GAS infections [63].

1.3 Therapeutic approaches

Treatment options vary slightly for the different types of the diseases caused by GAS but in general antimicrobial therapy is needed in almost all cases [71]. Although GAS pharyngitis is self-limiting, antibiotic treatment is still recommended for individuals with symptomatic pharyngitis where GAS has been confirmed as the causative agent [3]. Most advisory groups recommend penicillin as the treatment choice for GAS pharyngitis, because of its narrow spectrum and because GAS has remained remarkably susceptible to β-lactam antibiotics [3]. First-generation cephalosporins are acceptable in people who are allergic to penicillin. In patients that have GAS bacteraemia or STSS, penicillin G is administered intravenously (i.v.) (3 to 4 million units i.v. every 4 h) plus clindamycin (600 to 900 mg i.v. every 6 to 8 h) for 10 to 14 days [72]. For cases of necrotising fasciitis prompt surgical exploration and often debridement or fasciotomy is required alongside antibiotic therapy [53].

1.4 Vaccines

Research into producing a safe and effective vaccine to prevent GAS infections has been ongoing for several decades [73]. There has been strong evidence to show that natural infection with GAS results in protective immunity, with this being ascribed to the accumulation of protective antibodies most commonly against type-specific regions of the M protein or other conserved antigens [74]. Early studies in the 1970's by Fox *et al*., showed that volunteers immunised with purified M protein preparations showed some level of protection during subsequent challenge infections [75, 76]. However, others have argued that repeated GAS infections raise antibodies against conserved antigens, which may explain the immunity acquired by adults [74]. One of the limiting factors of GAS vaccine development is due to the major concern that GAS vaccine antigens may contain autoimmune epitopes that could trigger ARF [77]. Another impediment, is due to the complexity of the molecular epidemiology of GAS with geographic differences in the prevalence and burden of specific diseases and *emm* types [74, 78].

GAS vaccines can be divided into M protein-based and non-M protein-based vaccines. The vaccines that have entered clinical investigation are the N-terminal M protein-based multivalent vaccines (26-valent and 30-valent vaccines) and conserved M protein vaccines (the J8 vaccine and the StreptInCor vaccine) [77, 79]. There are a variety of other vaccine candidates that are at various stages of development (Table 1).

Table 1 – Current vaccine candidates for group A *Streptococcus*

Vaccine candidates are grouped as non-M protein vaccines, Type-specific M protein vaccines-N-terminus based and M protein vaccines-conserved C-repeat based.

Antigen	Advantages	Disadvantages	Stage
Non-M protein Vaccine			
Group A Carbohydrate **[80]**	Highly conserved and prevents colonisation	Potential trigger of autoimmunity	Preclinical
C5a peptidase **[81-83]**	Potential high *emm* type coverage. No implication in autoimmune side effects	None reported	Preclinical
Type-specific M protein vaccines-N-terminus based			
Hexavalent tandem antigen **[84]**	Protective in humans No autoimmunity observed	Low *emm* type coverage	Successful in phase I and phase II completed
26-valent combination of tandem antigens (StreptAvax™) **[85, 86]**	Protective in humans No autoimmunity observed	Limited *emm* type coverage	Successful in phase I and phase II completed
30-valent combination of tandem antigens **[87]**	Increased *emm* type coverage	Limited *emm* type coverage	Preclinical
M protein vaccines-conserved C-repeat based			
StreptinCor **[88-90]**	Induced cellular and humoral responses Cross-reaction against four non-vaccine M types shown No autoimmunity observed	Limits of *emm* type coverage unknown	Preclinical
P145 and derivatives J8 and J14 **[91]**	Human antibodies against P145 cross-react with different *emm* types	Limited *emm* type coverage despite cross-reactivity	Preclinical
Multivalent J14 **[92]**	Broader *emm* type coverage	Limits of *emm* type coverage not known	Preclinical

1.5 Epidemiology

1.5.1 Disease burden

The global burden of disease caused by GAS is not well established [12]. Global estimates suggest that there are at least 517,000 deaths each year due to severe GAS diseases (acute rheumatic fever, rheumatic heart disease, post-streptococcal glomerulonephritis, and invasive infections) [93]. The prevalence of severe GAS disease is at least 18.1 million cases, with 1.78 million new cases each year [93]. The greatest burden is due to rheumatic heart disease, with a prevalence of at least 15.6 million cases, with 282 000 new cases and 233 000 deaths each year (Figure 4) [63, 93].

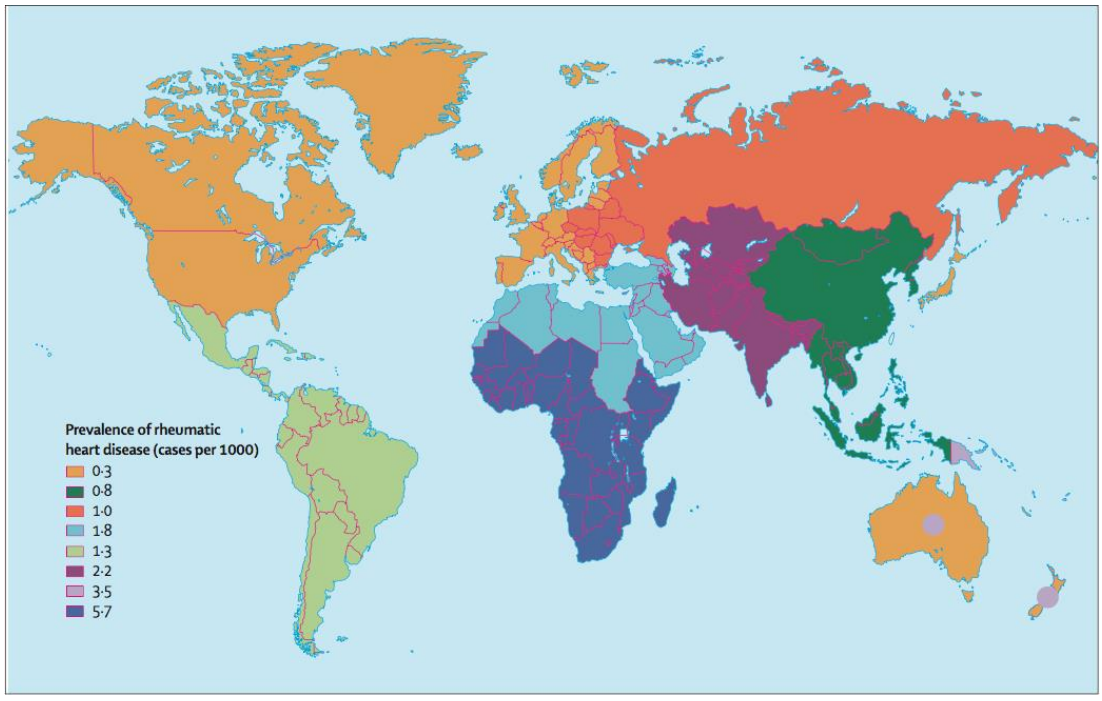

Figure 4 - Prevalence of rheumatic heart disease in children aged 5–14 years (circles represent indigenous populations) [93]

Global disease burden of rheumatic heart disease. The circles within Australia and New Zealand represent indigenous populations.

The burden of invasive GAS diseases (bacteraemia/STSS) globally is high, with at least 663,000 new cases and 163,000 deaths each year [47]. In addition, there are over 600 million cases of pharyngitis reported annually, the majority of which (550 million cases) are in developing countries [94]. In European countries, 8% of all GP consultations are for pharyngitis, with 15% of school aged children in developed countries developing pharyngitis annually, which has a significant impact on the economy through loss of school and work days [94]. In LMICs, levels of pharyngitis infection in school children are five-to ten-fold higher [95].

1.5.2 Outbreaks

GAS disease is ordinarily as a consequence of asymptomatic carriage or recent acquisition from a close contact, it also has the ability to cause outbreaks [3]. An outbreak of GAS is defined when two or more cases of GAS infection occur within 1 year and are related by person or place, which are of the same *emm* type [96]. Throughout the literature, small-scale localised outbreaks of GAS pharyngitis have been described, examples include outbreaks in military training centres due to overcrowding and hospital-acquired puerperal sepsis outbreaks [97, 98]. Large-scale outbreaks also occur through the emergence of dominant clones [99, 100]. The increase in invasive GAS disease burden since the 1980's has been closely correlated with the emergence of the M1T1 clone, which has disseminated globally and now accounts for the majority of clinical isolates in developed regions [3, 99, 100]. Since 2011, there has been an increase in the number of scarlet fever cases in Hong Kong (>10 fold increase in incidence) and the Chinese Military of Health reported a combined 110,000 cases of scarlet fever in 2011 to 2012 [101, 102]. The reason for

this surge is unclear, however recent studies have suggested that toxin acquisition and multi-drug resistance might have contributed [3, 101].

1.5.3 Molecular epidemiology

Studies of molecular epidemiology of GAS have progressed from the study of single genes to population-based genomic comparisons [103]. There have been many large scale *emm*-typing surveillance studies undertaken over the last decade in almost all global regions, which have shown that the epidemiology of GAS differs significantly between developing and developed regions [103]. In developing countries, the *emm* type found is far more diverse than in developed countries [12]. A significant percentage of GAS isolates belong to a few *emm* types in developed countries, most notably *emm* type 1, 3, 12, and 28, which account for around 40% of disease in these countries [3]. There are also significant associations of *emm t*ypes with particular disease manifestations. Examples include the association of *emm* types 1, 3, and 49 with invasive disease and *emm* types 2, 4, 6, 12, and 44/61 with superficial disease [103]. A recent large-scale analysis of 3,615 genomes by Nasser *et al.,* delineated the nature and timing of molecular events that led to the on-going global epidemic caused by *emm* protein 1 (M1) GAS [104].

1.6 Virulence factors

As an obligate human pathogen, GAS is protected by a multitude of surface bound and secreted virulence factors that work not only to protect against host immune defences but also contribute directly to host damage (Figure 5) [9, 51, 105-107].

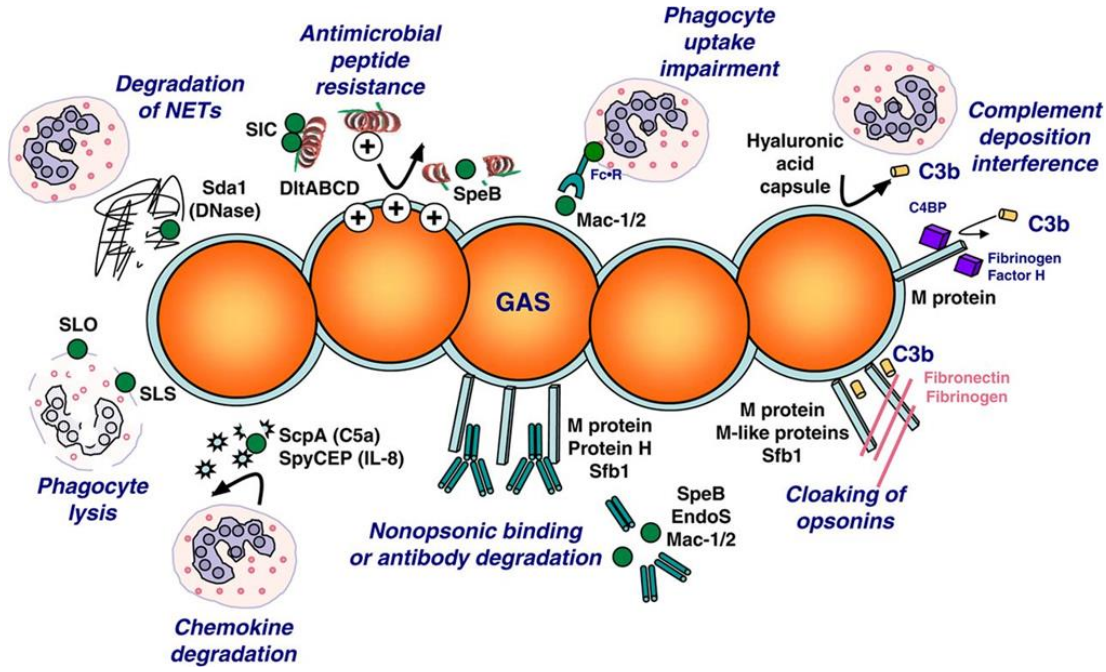

Figure 5 – The range of virulence factors produced by group A *Streptococcus* [3].

The collection of virulence factors that GAS expresses in order to bypass the host innate immune response. The secreted proteases SpyCEP/ScpC and ScpA degrade the chemokines IL-8 and C5a, inhibiting phagocyte recruitment to the site of infection. Surface-associated M protein binds Fc domains of Ig and the complement-regulatory proteins C4BP and factor H to interfere with complement deposition. Antimicrobial peptide resistance is mediated by hyaluronic acid capsule. Ig and antimicrobial peptides are degraded by SpeB. Secreted Sda1 DNase activity degrades NETs. SLS and SLO mediate lysis and apoptosis of neutrophils and macrophages [3].

1.6.1 CovR/CovS transcriptional regulator of virulence

GAS encodes a two-component master of virulence regulator called the control of virulence regulator the CovR/S, which controls the transcription of several important virulence factors [108]. CovS recognises external signals (elevated Mg^{2+}, temperature, low tissue oxygen, salt concentration) and then transduces them to the regulator protein CovR, which regulates the expression of several virulence genes [108-114]. Analysis of the CovR/S has revealed that it has an effect on transcription of up to 15% of all chromosomal genes of GAS [115]. CovR both regulates multiple virulence factors that repress the hyaluronic acid capsule operon (hasABC), and control the expression of the haemolytic exotoxins streptolysin O (SLO) and streptolysin S (SLS), a cysteine protease (SpeB), a neutrophil chemokine inhibiting protease (SpyCEP), streptokinase (Ska), an immunoglobulin modifying protein (EndoS), and a fibronectin binding protein (Fba) [108, 115, 116]. Several invasive clinical isolates have been isolated with mutations in the CovS gene, which in turn down regulates an extracellular cysteine protease SpeB, this repression permits other virulence factors to be secreted which would normally be cleaved by SpeB [110]. Selection for CovS mutants in invasive infection suggests that only GAS isolates maximally expressing important virulence factors can survive in these host sites [110].

1.6.2 M protein

The M protein encoded by the *emm* gene is considered a major determinant of virulence for GAS, it is a surface bound protein consisting of long fibrils shaped into relatively-conserved C terminal coiled-coil with a hypervariable region on the N-terminal [15, 117]. There are over 200 known *emm* types that have been identified by

N-terminal hypervariable region sequencing [118]. The M protein was identified by Rebecca Lancefield nearly 90 years ago, and since then has become one of the most well-defined molecules among the gram-positive virulence factors [117, 118].

The M protein is a highly versatile molecule and is able to bind multiple host proteins giving it a varied role in its contribution to pathogenesis [118]. One of the important functions of the M protein is to inhibit complement deposition on the bacterial surface protecting the bacteria from phagocytosis [119]. Different M proteins have developed different anti-complement strategies, highlighting the importance of this for the survival of GAS [120]. A more passive evasion of complement-mediated phagocytosis is achieved through the binding of the M protein to fibrinogen and albumin [118]. The binding of fibrinogen to the M protein also has an effect on inflammation through the activation of neutrophils and consequently inducing vascular leakage [118, 121]. The M protein has also been linked to multiple roles in adhesion and invasion of different host cells, with *emm* type being linked to specificity of cell type [122].

1.6.3 Hyaluronic acid capsule

Since its discovery it has been well documented that GAS produces colonies of a mucoid/matte phenotype (Figure 6) [123-125].

Figure 6 – Colonies of group A *Streptococcus* grown on 5% blood agar

The mucoid phenotype was later characterised as hyaluronic acid, a linear polymer of N-acetylglucosamine and glucuronic acid with a high molecular mass that is almost identical to hyaluronic acid found in the extracellular matrix of humans [123, 126]. Hyaloronic acid is synthesised by the *has*A/B/C operon, which is highly conserved among strains of GAS that have a capsule [123, 127]. Although the operon is conserved there is a large amount of variation in production of the capsule between GAS isolates [123, 126]. The CovR/S two component regulatory system is responsible for regulation of the *has* operon in response to environmental signals [123].

Early studies on the capsule found an association between virulence and capsule production and this is supported by subsequent epidemiological analysis [128, 129]. More recent work involving targeted deletions of the *has*A gene found that there was reduced virulence in systemic infection models and airway challenge models in mice [130, 131]. Capsule-deficient mutants are more susceptible to complement-mediated phagocytosis; this increase in resistance to phagocytosis is believed to be the major mechanism by which the capsule increases pathogenicity [132].

1.6.4 Secreted extracellular virulence factors

GAS produces a wide variety of extracellular products, many of which are secreted proteins that are considered to be virulence factors. The total number of these potential virulence factors far exceeds that of many other pathogens [3].

Streptokinase

Streptokinase (Ska) is a single-chain 414 amino acid protein secreted by GAS as well as group C and G Streptococci [133, 134]. Ska non-enzymatically converts inactive plasminogen, a key component of the fibrinolytic system, to produce proteolytically active plasmin [135]. The generation of active plasmin at the infection site is thought to lead to activation of host matrix metalloproteinases leading to fibrinolysis and degradation of the extracellular matrix, this could provide a mechanism by which GAS can spread from the initial site of infection [133, 135]. In addition to this, Ska has also been shown to activate the complement cascade, which may play a role in post-infectious diseases [133]. Expression of Ska is under tight negative control by the CovRS regulatory system, with phosphorylated CovR repressing the expression of Ska [3].

Cysteine proteinase

SpeB, also known as streptococcal pyrogenic erythrogenic toxin B, is produced as an inactive zymogen that must undergo autocatalytic cleavage, followed by loss of a cysteine residue to become active [133]. Although SpeB is one of the most studied virulence factors of GAS, its multiple roles in pathogenicity are not well understood [136]. SpeB has a broad specificity and is able to degrade host proteins like cytokines and complement components, as well as some GAS proteins such as SLO and DNase [137]. A key role of SpeB in invasive infections may be its ability to enhance bacterial spread through degradation of the tissue and further dissemination of other virulence factors throughout intracellular spaces [138]. There have been a number of studies that have proposed that SpeB has a modulating effect on the host response both in inducing inflammation and also having anti-inflammatory properties [133, 139]. SpeB has shown to inhibit neutrophil infiltration to the site of infection whilst also preventing degradation of neutrophil traps, and it both activates and inhibits complement activation [137, 140]. The control of SpeB is highly complex, and is managed through both environmental indicators and intrinsic regulators including the protease B regulator (RopB), the multiple gene regulator protein (Mga) and the CovR/S regulatory system [3, 109, 133].

Streptolysin O

The haemolysin SLO (69 KDa) is well established as having cell and tissue destructive activity, and is part of the family of cholesterol dependent cytotoxins that also includes perfringolysin, pneumolysin, and listeriolysin O [141-143]. SLO is 571 residues in length, however 70 residues are cleaved from the N-terminus before the protein is secreted, these 70 residues have been shown to have no effect on toxin activity [144]. The molecule is composed of four discontinuous domains and is rich in β -sheets (Figure 7) [144].

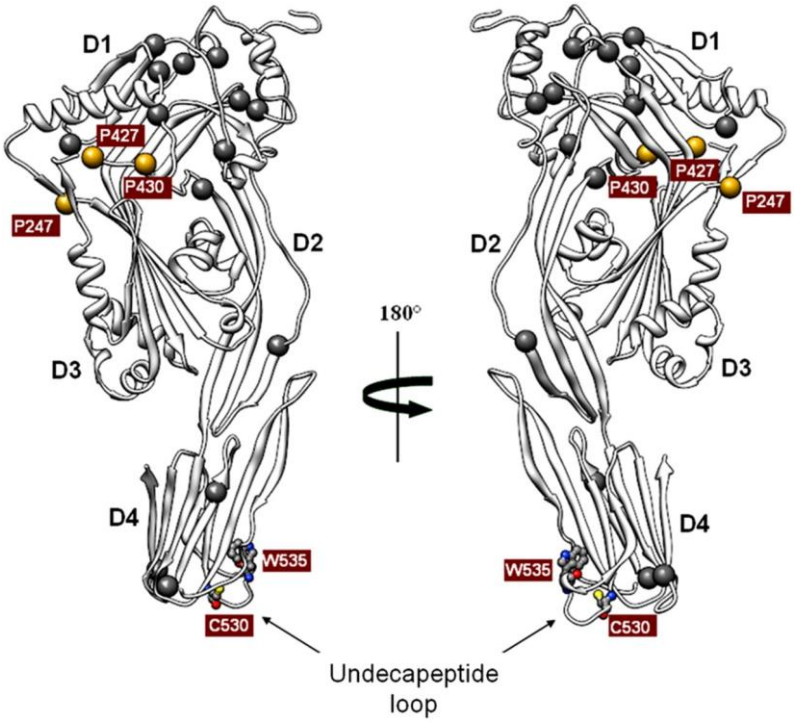

Figure 7– Predicted three-dimensional structure of Streptolysin.

The image shows a ribbon representation of the water-soluble SLO monomer lacking the first unfolded 71 amino acids in two orientations rotated 180° relative to each other [145].

SLO is a highly conserved protein secreted by nearly all clinical isolates of GAS, and acts against a wide number of eukaryotic cell types including macrophages, neutrophils, and erythrocytes, by interacting with cholesterol in target cell membranes to form pores, with sufficiently high doses of SLO resulting in complete cell lysis [145-148]. Pore formation by SLO follows a series of steps. Firstly, soluble monomeric SLO binds to cholesterol-containing membranes. Once toxin is bound, ring shaped oligomers form and lipids are removed from within the 'pre-pore' ring and once the pore complex is formed, cell lysis occurs (Figure 8) [149].

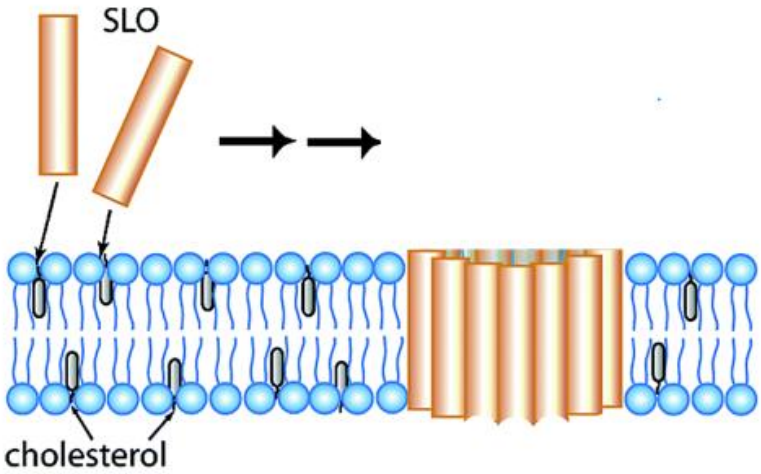

Figure 8 – Generalized mechanism of pore formation by streptolysin.
Soluble Streptolysin binds to cholesterol containing membranes, which leads to oligomerization and insertion of an aqueous pore into the plasma membrane. Adapted from [150].

SLO is produced alongside another streptococcal product the NAD-glycohydrolase (nga) which is transferred into the cytoplasm of host cells, the delivery of NADase results in major changes in the cell which enhances pathogenicity and intracellular survival [151]. SLO has a number of other biological effects on the host that act at different stages throughout infection, such as its ability to cause hyper-stimulation and cell-meditated apoptosis of host immune cells such as neutrophils [152, 153].

Although most GAS isolates encode the gene for SLO, the production of SLO is tightly regulated, as shown in studies that have seen variation in cytotoxicity within and between *emm* types [154]. Early studies with SLO demonstrated that the purified toxin was lethal to mice and rabbits when injected intravenously, mainly due to cardiotoxicity [155]. More recently, there have been studies to assess the effects of biologically relevant concentrations of SLO in *in vivo* models. Limbago *et al.,* found that SLO-deficient GAS resulted in attenuated skin infections and similarly Zhu *et al.,* reported a reduction in virulence when using SLO-deficient GAS in an invasive wound infection model [156, 157].

Streptolysin S

Streptolysin S (SLS) is another haemolysin produced by GAS. SLS is an oxygen stable cytotoxin that forms hydrophilic pores in a variety of cell types [147]. SLS can also form pores in sub-cellular organelles [133, 147]. SLS has been shown to contribute to the pathogenicity of GAS through cellular cytotoxicity, activation of the inflammatory response and inhibition of phagocytosis. Like SLO, SLS-deficient mutants have shown a decrease in virulence in *in vitro* and *in vivo* studies [133]. Although this is the case recent studies have shown that naturally occurring mutants of SLS are still capable of causing severe soft tissue infections and pharyngitis [158].

Serine Proteinase

The serine proteinase SpyCEP, is a proteolytic enzyme that cleaves and inactivates neutrophil chemokines [133]. A range of pathogenic streptococci produce homologs of SpyCEP suggesting that it could have more than one role in pathogenicity [133]. Although SpyCEP deficient mutant studies have shown varying results, it has been demonstrated that SpyCEP reduces bacterial clearance and allows bacterial dissemination in systemic infection [159]. SpyCEP is believed to be under control by the CovR/CovS two-component regulatory system [160].

DNases

GAS encodes up to four DNases (SdaD2, Sda1, SpdI1, SdaB) which are secreted as extracellular products, and are considered to be major contributors to virulence [133]. Arguably the most important for virulence being the bacteriophage-encoded SdaD2, a potent DNase produced by the M1T1 globally disseminated clone [104]. SdaD2 has the ability to protect GAS from neutrophils through the degradation of neutrophil extracellular traps [161].

Streptococcal inhibitor of complement

Streptococcal inhibitor of complement (SIC) is a 31 kDa protein found in *emm* type 1.0 strains of GAS [133]. SIC interferes with complement-mediated lysis by inhibiting the formation of the membrane attack complex. *In vivo* studies in a sepsis model have found that SIC enhances bacterial dissemination and promotes bacterial proliferation in the blood [162]. In addition, SIC also plays a role in adherence and colonisation interrupting host cells ability to effectively clear the bacteria [163].

Superoxide dismutase

Superoxide dismutase (SodA) is a metalloprotein that converts superoxide anions to oxygen and hydrogen peroxide. SodA plays a major role in detoxifying oxidative bursts produced by the host response [133].

1.6.5 Superantigens

Superantigens (SAgs) are a group of extracellular protein toxins produced by a small number of bacterial species and some viruses [164-166]. The main distinguishing feature of SAgs is their ability to simultaneously bind to the major histocompatibility complex (MHC) class II on antigen presenting cells and the T cell receptor on T cells [164]. SAgs are able to attach to MHC class II in a number of different ways, that can be peptide dependent, peptide independent or a combination [164, 167]. By establishing stable binding efficiency, a small amount of SAg is needed to cause vast amplification of T-cell signalling [105]. The super antigen-MHC complex interacts with the T cell outside of the recognition site of antigenic peptides [164]. SAgs interact with the variable (V) part of the beta chain of the TCR [168]. The human genome encodes around 50 TCR V beta elements, and super antigens are estimated to be able to activate up to 20% of the T cell pool [54]. The SAg SpeA has been shown to stimulate V beta 2, 4, 8, 12 , 14, 15 [165, 168]. The streptococcal SAgs Spe A, Spe H, Spe I, and SSA are more closely related to the staphylococcal SAgs than any other streptococcal SAg [165]. All SAgs were derived from a common ancestor, genes for these toxins are all located on mobile genetic elements so it is assumed they arose through horizontal gene transfer from *S. aureus* [165]. SAgs are thought to be involved in a number of GAS diseases [169]. In particular the SpeA gene was found in a high percentage (40-90%) of isolates associated with invasive disease and only a small number (15-20%) of those isolates from non-invasive disease [170]. A recent study looking at the M1T1 strain showed that the acquisition of SpeA was an important step in the evolution of hyper virulence [104].

1.7 Host response to severe group A Streptococcal infections

The development/refinement of effective and safe vaccines and therapeutics against GAS lies heavily on the knowledge about the immune systems response to combat GAS infection [171]. In recent years there has been a large contribution of studies on the basic principles of GAS innate and adaptive immune defences, and more research has focused on dissecting the individual immune components involved.

1.7.1 Innate immune cells in defence against GAS

Upon detection of GAS in the host, the immune system launches a complex response which, initially depends on the recruitment and fine activation of neutrophils, macrophages, and dendritic cells (DCs) [172-174]. The innate immune response is activated through the interaction of pattern recognition receptors (PRRs) with GAS-derived pathogen associated molecular patterns (PAMPs), such as GAS-derived nucleic acids and secretory proteins [175].

The primary line of defence comes from tissue resident macrophages and polymorphonuclear neutrophils (PMNs) which effectively phagocytose invading bacteria [176]. There have been a number of studies that have used diphtheria toxin mediated depletion of macrophages to address the direct role of macrophages in the clearance of GAS, whereby it was found in these studies that there was an increase in GAS dissemination and a significant decrease in host survival [173, 177]. Tissue resident macrophages also rely on the recruitment of new macrophages to the site of infection, with TNF-α a major pro-inflammatory cytokine that acts to facilitate the rapid chemotactic relocation of macrophages to the infected tissue [175]. Similarly, mice depleted of DCs also fail to control bacterial dissemination, DCs are a

significant source of IL-12 and IFN-γ (macrophage activating cytokine) which serve to enhance macrophage antimicrobial function [175]. Macrophages and DCs produce a number of PMN recruitment factors, including IL-1β and CXCL1 (IL-8 in humans) [178]. The production of IL-1β is strongly dependent on GAS-derived SLO, however there has been little evidence to suggest that this cytokine is required for successful defence [178]. *In vivo* and *in vitro* studies have shown PMNs to play a vital role in host protection [179-181]. PMNs control bacterial infections mainly through the production of antimicrobial peptides and reactive oxygen species. In addition, GAS induces an extensive formation of neutrophil extracellular traps (NETs) which immobilise the bacteria and are key in limiting bacterial dissemination [182, 183].

1.7.2 Evasion of innate immune responses

Many of the virulence factors already discussed in this chapter employ a number of strategies to evade the innate response and more specifically phagocytosis (Figure 9).

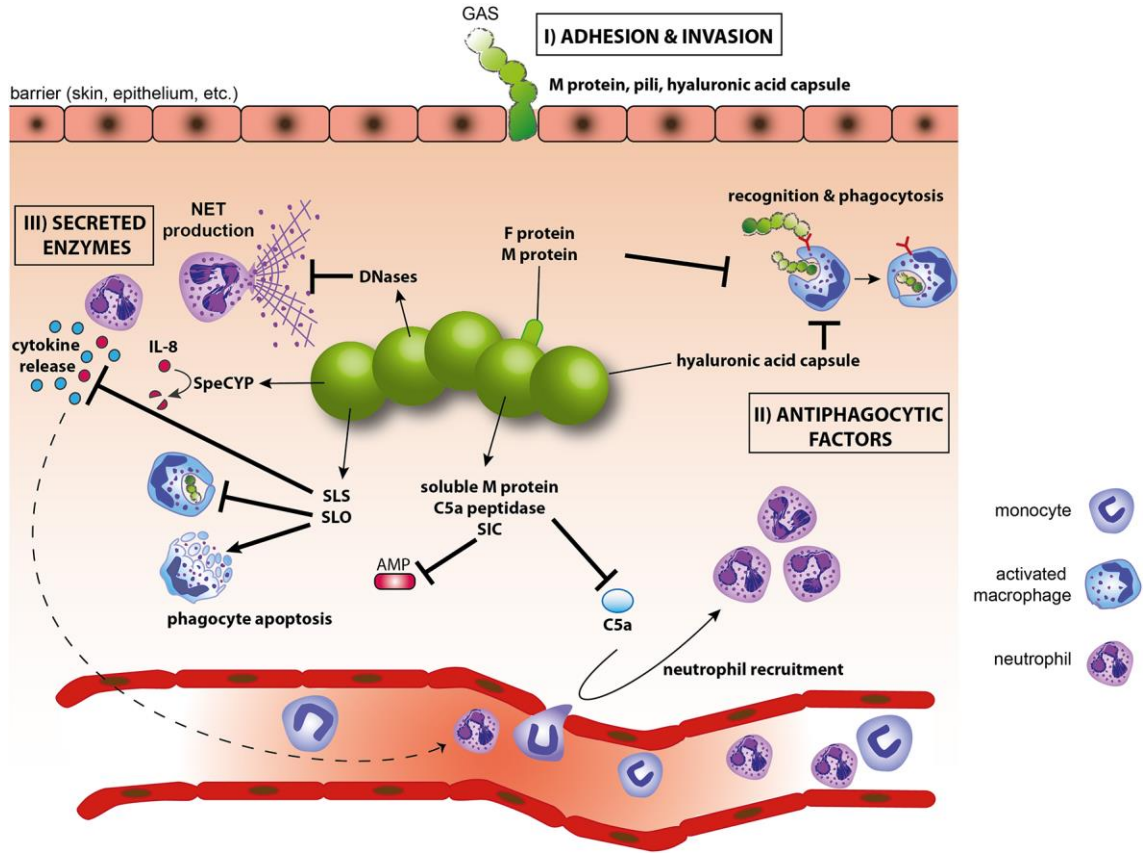

Figure 9 – Evasion strategies of GAS to the innate immune system [175].

(I) Adhesion and/or invasion; (II) SLO, hyaluronic acid capsule and M-proteins interfere with phagocytosis; (III) Secreted GAS virulence factors inhibit complement activation and antimicrobial peptides prevent phagocyte recruitment, induce apoptosis of phagocytes (SLO), and interfere with cytokines or cytokine production.

GAS can increase its survival by the expression of SLO within the phagosome to inhibit its transportation to lysosomes and also facilitate the escape of GAS [184, 185]. SLO also has a more general function in the induction of cell death of immune cells like macrophages and PMNs [153, 186]. The production of SLS has also been shown to limit the recruitment of neutrophils, by blocking the production of chemokines [182]. DNases work to degrade NETs and free entrapped GAS, promoting bacterial dissemination [161, 181, 187]. GAS is able to breakdown blood clot formation through the proteinase streptokinase, which activates plasminogen [135]. Another proteinase SpeCYP cleaves and inactivates key neutrophil chemoattractant (IL-8) [188]. There also a number of strategies that impede the complement system via C5a peptidase and SIC [162, 189-191].

1.7.3 Adaptive immunity against GAS

The humoral response to a range of cell bound and secreted streptococcal antigens have been investigated both in terms of pathogenesis and from a clinical standpoint [192-197]. Antibody titres to a variety of secreted and extracellular products, such as DNases (anti-DNase B) and streptolysin O (ASO) underpin serologic tests used in the diagnose of GAS diseases [171, 198]. Numerical differences in antibody titres to different antigens have been observed in the sera of patients with different body site infections [199]. A number of studies have showed the overwhelming protective effect of antibodies [194, 197, 200-203]. The M protein is arguably the most studied GAS antigen, antibodies are often raised specific to the M protein and opsonise GAS for phagocytosis, in addition to this antibodies provide *emm*-type specific protection [204]. Paradoxically however these antibodies are very often found in healthy people, who would have been exposed to GAS in their lifetime [205, 206].

Nonetheless, a key study showed the relative importance of the adaptive immune system in those people who lack the signalling adaptor MyD88 (required for activation of the innate response), who are very susceptible to GAS infections at a young age but decreased in adulthood [207]. Another consideration is the successful use of intra-venous poly-specific immunoglobulins (IVIG) as a therapy in severe GAS infections [198].

There has been very little research in the area of T-cell responses to GAS infections. Cleary *et al*., showed a significant contribution of IL-17 producing Th17 cells in the clearance of GAS during pharyngitis [208-210]. Further to this, it was shown that these cells developed after repeated immunisation, implying that the cells were antigen-specific [208-210]. There has been a recent study that identified cellular Th1/Th17 memory responses in children and adults, with IgG3 levels increased [211]. This is an interesting finding as IgG3 has been shown to be the most potent activator of the complement cascade (via C1q binding-classical pathway) [211, 212].

1.8 Animal models of group A Streptococcal infections

In vivo models of GAS infection have proved to be challenging to develop. As GAS is a human adapted pathogen, many of its key virulence factors are only active against human cells and receptors, as is the case with the secreted virulence factor Ska (human plasminogen activator) [135, 213]. Another issue derives from the versatility of GAS as a pathogen as it is able to cause a broad range of diseases by very different mechanisms, and infect a number of different tissue compartments in the host [213]. Finally, GAS has extensive strain diversity with no GAS isolate considered representative of the population [214]. Despite these challenges there are number of useful animal models that have been developed to explore different disease types and pathogenic mechanisms (Figure 10).

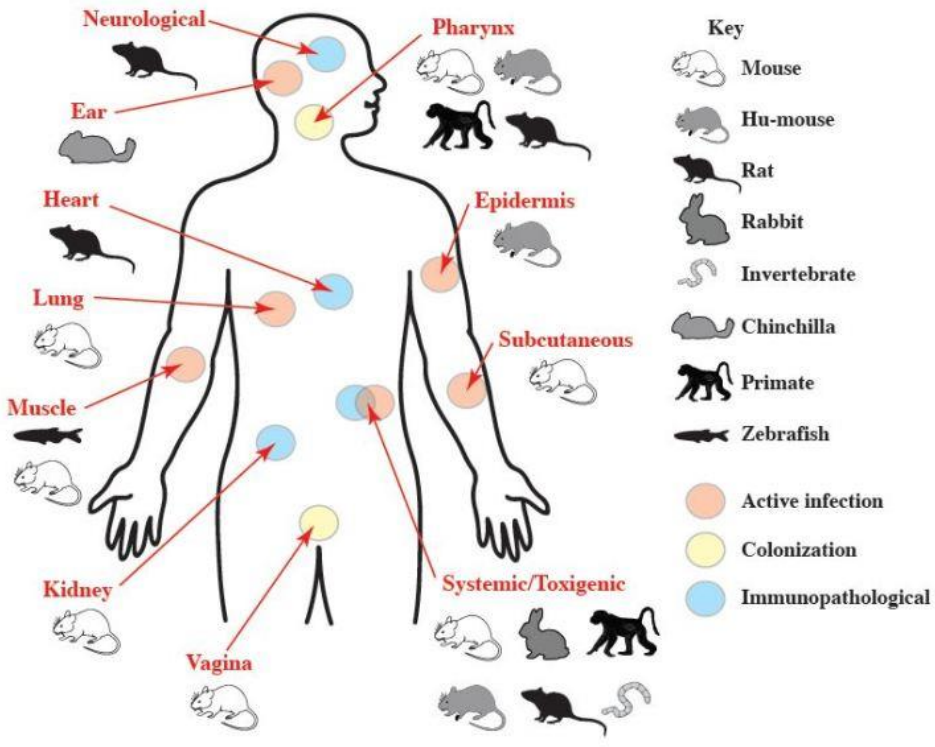

Figure 10 – Animal models of group A *Streptococcus* [213].

Key represents the different types of animals used in the various models and whether the model is of an active infection, carriage (colonisation model) or immune mediated.

1.8.1 Models of nasopharyngeal colonisation

The nasopharyngeal mucosa is one of the principal sites of GAS asymptomatic colonisation, and is a common site for infection (pharyngitis) [9]. It is also a primary reservoir for the maintenance and transmission of GAS, and as a result there has been considerable interest in the development of animal models to study the disease process at this site [3]. Development has been challenging as rodents lack a homologue for the key infection site in the pharynx, the Waldeyer's ring, and instead possess nasal associated lymphoid tissue (NALT) which shares some similarity to the tonsils [215]. Indeed, a number of groups have used murine models to investigate GAS colonisation and infection in the upper respiratory tract [130, 215-219]. There is not one widely accepted model used, instead each model varies depending on strain, sex, or age of animal used. A key difference between the models is the dose volume used to establish an infection, as it needs to be a large enough volume to establish an infection but not so that it enters the lung [213, 215]. One of the major disadvantages is the limited number of GAS isolates that will effectively colonise the nasopharynx of mice and of those that do the duration of colonisation is often short (up to 7 days) [213]. Despite this, the models developed have been particularly useful in examining passive and active mucosal immunisation and also the adaptive host response following colonisation [201, 220, 221].

1.8.2 Models of soft tissue and wound infection

One of the most commonly used models for the analysis of GAS virulence factors is a subcutaneous wound infection model [213]. The infection results in a highly inflamed lesion in the soft tissue where there is a high level of bacterial proliferation followed by extensive recruitment of inflammatory cells [222]. Typically, bacteria are injected into the tissue and a lesion forms 12 hours post-infection which is characterised by the infiltration of neutrophils and other leukocytes [223]. By 24 hours, the lesion ulcerates with the margins continuing to expand up until day 3 [213]. Resolution of the wound occurs between day 8 and 14 [213]. Many different GAS strains have been shown to be virulent in this model and strains fall into two general classes; those that remain localised to the site of infection and eventually resolve, and those that subsequently invade into the vasculature system resulting in systemic infection [156, 223]. Interestingly, studies looking at spontaneous mutations in the CovR/CovS two component regulatory system have shown that a primarily localised strain can switch into a more invasive strain [224]. Some of the key limitations of this model are due to general differences in the anatomy of murine cutaneous tissue in comparison to humans [213]. However, this model has proven valuable for exploring the host innate response and further to this has a proven utility in monitoring the GAS transcriptome during growth in a soft tissue environment [225-227].

1.8.3 Models of systemic infection

Severe systemic GAS infections result from the ability of the bacterium to migrate to normally sterile sites of the host such as the blood stream [3, 228]. There is co-ordinated expression of multiple GAS virulence factors which lead to tissue destruction, bacterial proliferation and subsequently hyper inflammation [3, 9, 186]. The mechanisms that underpin GAS invasive disease, such as virulence factor expression and the dysregulation of the host response, are the subject of intense research [3]. In murine models, the different types of systemic disease models can be distinguished from each other by their route of inoculation, which may be intravenously (IV), intraperitoneally (IP), or intranasally (IN) [213]. The IV route of infection introduces bacteria directly into the vasculature system whereas the IN and IP route require the bacteria to breach tissue barriers in order to invade the blood stream [213]. Studies using an IN route of infection in a mouse model have shown that systemic infection is initiated by flooding of the alveoli with bacteria followed by breaching of endothelial barriers into the blood [130, 219]. Further to this, lung infection models developed in rats explored the direct tissue damage caused by SpeB and SLO which then allow bacteria to cross into the blood stream [229]. IP infection is typically much slower than IV injection of bacteria and it takes longer for the bacteria to disseminate through the host [230]. Virulence of strains in systemic infection is often examined by observing survival of the animals and by examining the kinetics of clearance or proliferation of bacteria in the vasculature system by enumeration of CFUs from the blood and highly perfused organs such as the spleen [213].

1.8.4 Models of bone and joint infection

There have been relatively few *in vivo* studies on bacteraemia induced septic arthritis, and all but one study with GAS were confined to infection with *Staphylococcal aureus* [54, 231-240]. There have been a number of studies using group B *Streptococcus* in models of septic arthritis, that have effectively shown that different strains of mice have varying susceptibility to infection due to the immune responses ability to control the infection [241-244]. Although bacteraemia induced septic arthritis is regarded as the best model for replicating human disease, as often bacteria enter the joints through haematogenous seeding, many studies with GAS use a direct method to introduce bacteria into the joint [61]. Directly initiating infection in the joint and the bone (osteomyelitis) can be useful for examining the role of bacteria induced by foreign materials such as in the case of orthopedic-implant-associated infections [245]. Mouse studies have generally been accepted as good models for septic arthritis and osteomyelitis; and it has been shown that the progression of infection and in particular the erosive profile of the joints is very similar to that described in human infection [54].

1.8.5 Transgenic mice

As described previously, many GAS virulence factors only interact with human host receptors and cells. One way to circumvent this limitation is by the use of transgenic mice which express human host cells of interest [246].

In patients with STSS there is extensive immune activation, which has been linked primarily due to the action of SAgs [168]. The relationship between SAgs and the T cell response is important in characterising how the host response contributes to the clinical outcome in patients with STSS [247]. Characterising the role of SAgs in murine models has proven difficult, as mice are unable to produce a robust response to SAgs *in vivo* [248]. Early studies used sensitising agents such as D-galactosamine (D-galN), which render the mice more susceptible to the action of SAgs, however this method skewed the clinical phenotype towards the liver [249]. There have now been a number of studies that have utilised mice expressing human MHC-II molecules in infection models and also in early phase vaccine efficacy trials [250-252]. When using transgenic mice in a STSS infection model it highlighted the extra-hepatic pathology that is seen in STSS but that is not demonstrated in earlier studies due to the sensitising technique using D-galN [248]. Different polymorphisms in the MHC-II gene were analysed to see if there were any effects on the outcome of infection or altered interactions with SAgs [253, 254]. Early studies, showed the potential for preferential binding of SpeA to MHC class DQ molecules compared to DR alleles, which could be contributing to host susceptibility of infection [253]. A more recent study complemented this data and displayed that mice expressing DQ alleles outputted 10-fold more CFUs compared to mice expressing the DR alleles [255].

Kasper *et al.*, presented a study using HLA-DR4 and HLA-DQ8 transgenic mice in a nasopharyngeal infection model [255, 256]. The results provided evidence that acute infection in the upper respiratory tract is enhanced notably in mice expressing human MHC-II molecules [255, 256].

1.9 Research aims

The aim of this PhD project is to understand the mechanisms of pathogenesis of GAS using a range of *in vitro* and *in vivo* models of infection.

1. Use *in vivo* models to assess different disease types in GAS
    a. Consider the virulence of different GAS isolates from various *emm* types (outbreak, non-outbreak, invasive and non-invasive) by analysing key phenotypic characteristics
    b. Use information regarding each isolate from *in vitro* assays to develop different models of invasive and non-invasive infection (carriage, pneumonia, sepsis and septic arthritis)

2. Investigate the role of streptolysin in invasive disease pathogenesis
    a. Study the role of streptolysin in septic arthritis and invasive disease
    b. Compare the effects of streptolysin from various GAS isolates and compare this with an isogenic knockout mutant of streptolysin

3. Characterise the local host response to infection in septic arthritis
    a. Determine the kinetics of infection of GAS-induced septic arthritis
    b. Investigate the local immune response in the joint over the course of infection

2. Materials and Methods

2.1 Microbiology

2.1.1 Bacterial strains

All GAS strains used in this study were supplied by the Royal Liverpool University Hospitals Trust and Alder Hey Children's Hospital. A full list of the isolates along with the date of collection, age of patient, sex of patient, type of collection, isolate ID, age and disease category can be found in Table 2.

Table 2 – List of GAS isolates and the associated clinical data used for this study.

Sex denoted as either male (M) or female (F) and / where information was not available

Date collected	Age	Sex	Type	Store ID	Category age	Disease category
06/01/2010	84	M	Blood culture	101007	adult	Invasive
05/01/2010	47	M	Blood culture	101008	adult	Invasive
11/02/2010	69	M	Blood culture	101257	adult	Invasive
10/03/2010	39	F	Blood culture	101452	adult	Invasive-outbreak
01/04/2010	78	M	Blood culture	101563	adult	Invasive
15/04/2010	70	M	Blood culture	101640	adult	Invasive
25/04/2010	29	M	Blood culture	101700	adult	Invasive-outbreak
30/04/2010	34	F	Blood culture	101724	adult	Invasive
08/05/2010	65	F	Blood culture	101767	adult	Invasive
25/05/2010	37	M	Left hip pus	101910	adult	Invasive
25/05/2010	24	F	Blood culture	101911	adult	Invasive
09/06/2010	87	F	Blood culture	101967	adult	Invasive-outbreak
18/06/2010	51	M	Blood culture	102018	adult	Invasive
20/06/2010	43	M	Blood culture	102029	adult	Invasive-outbreak
23/07/2010	61	M	Blood culture	102256	adult	Invasive
04/08/2010	76	M	Blood culture	102314	adult	Invasive
23/08/2010	41	F	Blood culture	102434	adult	Invasive-outbreak
13/11/2010	58	F	Blood culture	102920	adult	Invasive-outbreak
05/12/2010	45	M	Blood culture	103045	adult	Invasive-outbreak
25/04/2011	53	F	Blood culture	111617	adult	Invasive-outbreak
10/09/2011	56	F	Blood culture	112327	adult	Invasive-outbreak
12/12/2011	42	M	Blood culture	112844	adult	Invasive-outbreak

01/03/2012	51	M	Blood culture	121324	adult	Invasive-outbreak
31/03/2012	71	M	Blood culture	121511	adult	Invasive-outbreak
08/09/2012	18	M	Blood culture	122397	adult	Invasive-outbreak
/	/	/	/	126214	child	Invasive
/	/	/	/	126215	child	Invasive
/	/	/	/	126216	child	Invasive
/	/	/	/	126217	child	Invasive
/	/	/	/	126218	child	Invasive
11/12/2012	3	M	/	127250	child	non-invasive
11/05/2012	3	M	/	127251	child	non-invasive
24/05/2012	4	F	/	127263	child	non-invasive
28/05/2012	4	F	/	127286	child	non-invasive
18/04/2012	14	F	/	127371	child	non-invasive
29/04/2012	20	M	/	127577	adult	non-invasive
25/11/2012	20	F	/	127655	adult	non-invasive
06/09/2012	21	F	/	127656	adult	non-invasive
08/06/2012	21	M	/	127657	adult	non-invasive
18/04/2012	29	M	/	127745	adult	non-invasive
08/01/2013	29	F	/	127746	adult	non-invasive
26/02/2013	29	M	/	127755	adult	non-invasive
22/03/2013	33	M	/	127783	adult	non-invasive
14/05/2012	35	M	/	127784	adult	non-invasive
24/05/2012	35	F	/	127785	adult	non-invasive
06/12/2012	35	F	/	127786	adult	non-invasive
30/04/2012	36	F	/	127789	adult	non-invasive
12/06/2012	37	F	/	127790	adult	non-invasive
03/04/2012	38	M	/	127793	adult	non-invasive
16/05/2012	38	F	/	127801	adult	non-invasive
17/08/2012	34	F	/	128401	adult	non-invasive
17/04/2012	39	F	/	137000	adult	non-invasive
02/05/2012	39	F	/	137027	adult	non-invasive
06/06/2012	43	M	/	137072	adult	non-invasive
11/03/2013	44	M	/	137081	adult	non-invasive

2.1.2 Standard media

Blood agar base (BAB) culture plates

16 grams of BAB medium (Sigma) was mixed with 400 ml of distilled water and autoclaved. Following autoclaving the media was allowed to cool until it had reached 56°C. 20 ml of sterile defibrinated horse blood (Sigma) was added and evenly mixed. The media was then poured into sterile petri dishes (90 mm), and left to dry overnight. The plates were inverted and stored at 4°C for 1-2 weeks.

BAB culture plates +5% v/v horse blood with gentamicin

BAB culture plates were prepared as above. Immediately after the addition of horse blood, 2 μg/ml of gentamicin (Sigma) was added and the media gently mixed.

Brain heart infusion (BHI) culture plates

20 grams of BHI medium (Sigma) was mixed with 400 ml of distilled water and autoclaved. After the media had cooled it was then poured into sterile petri dishes (90 mm), and left to dry overnight. The plates were inverted and stored at 4°C for 1-2 weeks.

Todd Hewitt Broth +0.5% yeast (THY)

14.4 g of Todd Hewitt broth (Sigma) plus 2 g of yeast (Sigma) was mixed with 400 ml of distilled water an autoclaved. The medium was stored at room temperature.

2.1.3 Viable count of bacteria (Miles and Misra Method)

The Miles & Misra method is an accurate method for determining the number of colony forming units (CFU) present in a given sample [257]. The number of CFU found can then be used to calculate the CFU/ml or mg of a sample. 20 µl of a sample (e.g aliquot, dose, blood or tissue homogenate) for testing was added to 180 µl sterile PBS and serially diluted (10-fold) until dilutions of 10^6 or higher if using more concentrated stocks. Agar culture plates were divided into six sections, and 60 µl (3 × 20 µl spots) of each dilution was plated into the sector. Plates were incubated at 30°C 5% CO_2 for 16 hours. After incubation, sectors in which contained 30-300 CFU were counted and the CFU/ml or CFU/mg were calculated.

To calculate numbers of CFU in liquid dose:

$$\frac{CFU}{ml} = average\ number\ of\ colonies\ in\ sector\ \times\ dilution\ factor\ \times \frac{1000}{60}$$

To calculate numbers of CFU in tissue:

$$\frac{CFU}{mg} = \frac{CFU}{ml} \times \frac{ml\ of\ PBS\ tissue\ was\ homegnised\ in}{tissue\ weight}$$

2.1.4 Preparation of bacterial stocks

GAS from laboratory bead collections were streaked for isolation on BAB culture plates and grown overnight at 37°C (5% CO_2). One colony from the culture plates was used to inoculate 7.9 ml of THY media supplemented with 100 µl of glucose in a sterile universal tube. The inoculum was incubated statically for 16-18 hours at 37°C (5% CO_2). 200 µl of the overnight broth was added to 8 ml of fresh THY (supplemented with glucose) and incubated statically at 37°C (5% CO_2), until it reached mid exponential phase. Depending on the strain this length of time varied but was approximately four hours. 1.6 ml of 100% glycerol was added to the 8 ml of resulting broth, to make 20% glycerol stocks. They were then vortexed and placed on ice before being dividing into 500 µl of single use aliquots in sterile cryotubes. The aliquots were stored at -80°C, and after 24 hours aliquots were thawed and numbers of GAS / ml determined used the Miles and Misra method. Stocks produced using this method contained around 10^8 CFU/ml. Sometimes more concentrated stocks were needed and so were made using the same method but with a slight modification. Following overnight culture 5 ml of the broth was added to 200 ml fresh THY media (supplemented with glucose) and incubated statically at 37 °C (5% CO_2), until it reached mid exponential phase. Following this the culture broth was centrifuged at 1500 x g for 15 minutes and the supernatant discarded. The pellet was re-suspended in 8 ml fresh THY media (supplemented with glucose). The proceeding steps were the same as previous.

2.1.5 Growth curves

The OD_{550} of 200 µl of 10^5cfu/ml bacteria in THY media (supplemented with glucose) was determined every 30 minutes for a total of 24 hours using a BMG labtech FLUOstar OMEGA microplate reader.

2.1.6 *Emm* typing GAS isolates

Genotyping using the *emm* gene is an accurate method of determining the M type of GAS [258]. The *emm* gene is amplified using PCR and then sequenced, it can then be compared to the CDC database of *emm* types. The system relies upon the use of the two highly conserved primers to amplify a large portion of the *emm* gene.

DNA extraction

GAS from laboratory bead collections were streaked for isolation on BAB culture plates and grown overnight at 37°C (5% CO_2). One colony from the culture plates was used to inoculate 7.9 ml of THY media supplemented with 100 µl of glucose in a sterile universal tube. The inoculum was incubated statically for 16-18 hours at 37 °C (5% CO_2). DNA was then extracted from the overnight using the DNeasy Blood & Tissue Kit (Qiagen) as per protocol. The concentration and purity of each extraction was then measured using the NanoDrop® 1000 spectrophotometer (Thermo Fisher Scientific, Inc.). Measurements were taken following manufacturer protocols and done in triplicate. Concentrations were determined using an undiluted sample.

Amplification of *emm* gene

The two highly conserved primers:

Forward primer [TATTSGCTTAGAAAATTAA]

Reverse primer [GCAAGTTCTTCAGCTTGTTT]

ReadyMix Taq PCR reaction mix (Sigma P4600) was used to prepare the samples along with the primers for amplification in the PCR machine. 1 µl of template DNA was added to each PCR tube at a concentration of 5 ng/µl.

The PCR machine was run using the following conditions:

1. 94°C for 1 min
2. 94°C for 15 s
3. 46.5°C for 30 s
4. 72C for 1 min 15 s
5. Cycle to step 2 (x 10)
6. 94°C for 15 s
7. 46.5°C for 30 s
8. 72°C for 1 min 15 s with a 10 s increment for each of the subsequent 19 cycles
9. Cycle to step 6 (x 20)
10. 72°C for 10 min
11. 15°C hold

Confirmation of amplification

The PCR product was run on an agarose gel to confirm that the amplification had been successful. A 1% gel was prepared by dissolving 1 g of agarose powder in 100 ml of Tris/Borate/EDTA buffer (TBE). Ethidium bromide was added to the gel to allow visualisation of the gel under ultraviolet light. 1 x loading dye (Thermo Scientific) was added to the samples before they were loaded into the wells. The gel was run at 6 V/cm for 45 minutes. The PCR should show products ranging from 800 bp - 1200bp. The remaining PCR reaction was purified using Wizard® SV Gel and PCR Clean-Up System (A9281) – as per manufactures protocol. The concentration and purity of each sample was measured using the NanoDrop® 1000 spectrophotometer (Thermo Scientific). Measurements were taken following manufacturer protocols and done in triplicate. Concentrations were determined using an undiluted sample.

Sending samples for Sanger sequencing

Samples were first diluted with DEPC-treated water so that there was 1 μg/ml per 100 bp. The *emm*_seq primer forward primer was used for sequencing at a concentration of 3.2 mM, a minimum of 5 μl was needed per reaction.

Designation of *emm* type

The Streptococci group A subtyping Blast 2.0 Server (National Centres for Disease Control, Biotechnology Core Facility Computing Laboratory) was used to query the sequences and retrieve the *emm* type of the sample.

2.2 Tissue culture

2.2.1 HL60 cell culture

The HL-60 cell line was first established from a patient with promyelocytic leukaemia in 1977 [259]. The defining feature of this cell line is that it is composed of undifferentiated haemopoeitic cells that can undergo differentiation into functional polymorphonuclear - like cells upon chemical induction [259]. Induction using DMF (N,N-dimethylformamide) results in granulocytic differentiation yielding 44% myelocytes/metamyelocytes and 53% PMNs.

Media

RPMI 1640 (Sigma, UK) was used for all HL-60 cell culture. Media was supplemented with 20% fetal bovine serum (FBS) (Gibco) to help maintain growth.

Establishing and maintaining HL-60 culture

1 ml aliquots of frozen HL-60 cells were thawed quickly in a water bath and rapidly diluted in 15 ml of RPMI media for a 10 min centrifugation step at 300 x g. The supernatant was discarded and the above step repeated. The cell pellet was then re-suspended in 10 ml of media and transferred to a T-25 tissue culture flask (BD Biosciences) and placed upright in a tissue culture incubator at 37°C (5% CO_2). 48 hours later the cell suspension was moved to a T-50 culture flask (BD Biosciences) and an extra 10 ml of media was added. At 72 hours the flask was observed for turbidity, as an indication of cell growth. The cells were then tested for viability using trypan blue and a haemocytometer to assure >80% cell viability. To ensure viability during maintenance and differentiation, growing flasks of cells were maintained every 24 hours.

2.2.2 Differentiating HL-60 cells

DMF (Fisher) was used to differentiate HL-60 cells into PMN-like phagocytic cells. 750 µl of DMF was carefully added to a T-75 tissue culture flask (BD Biosciences) containing 80 ml of fresh media. Growing, undifferentiated cells were tested for cell number and viability, and 20 ml of cell suspension at a concentration of 2 x 10^5 cells/ml was carefully transferred to the flask containing media and DMF. Cell viability of >90% only was used for differentiation. 4 days following chemical induction, cell morphology of undifferentiated cells changed towards PMN-like cells as demonstrated by granularity and a lobe like shape, indicating that the cells were ready for use.

2.2.3 J774.2 cell culture

J774.2 is a murine derived macrophage cell line [260].

J774.2 media

Dulbecco's Modified Eagle Medium (Sigma) was used for all J774.2 macrophage cell culture. Medium was supplemented with 10% FBS and 5% antibiotic/mycotic (10,000 units penicillin, 10 µg streptomycin + 25 µg amphotericin B/ml (Sigma)) solutions to maintain growth and prevent contamination. Additionally, DMEM supplemented with 10% FBS without the addition of antibiotic/mycotic solution was prepared for use in phagocytosis assays.

Establishing and maintaining J774.2 culture

Frozen cell aliquots were quickly thawed in a 37°C water bath and centrifuged at 300 *x* g for 10 minutes. The supernatant was discarded and cells re-suspended in 10 ml sterile PBS for another wash (300 *x* g for 10 minutes). The supernatant was then discarded, the resulting cell pellet re-suspended in 15 ml of medium and added to a T-75 tissue culture flask for overnight incubation at 37°C (5% CO_2). The following day, viable cells had attached to the tissue culture flask. Medium was carefully removed from the flask and the cells washed once with 10 ml of DPBS. 15 ml of fresh medium was added, and the cell culture maintained by washing cells and replenishing medium every two days. The cell line was split as soon as macrophage attachment to the flask reached 50% confluence, judged by assessing the flask using an inverted microscope. Medium was removed, and cells washed with 10 ml DPBS. 8 ml of medium was added to the flask and a cell suspension created by gently detaching cells using a cell scraper. 1 ml of the resulting cell suspension was added to 14 ml fresh medium.

2.3 Peripheral blood neutrophil isolation

2.3.1 Volunteer recruitment

Healthy adult volunteers were invited to give informed consent to a study in Liverpool (UK) involving blood donation. The only criterion is that the volunteer had been feeling healthy and well in the last week and had no serious medical conditions (ethics number: RETH000685).

2.3.2 Isolation

50 ml of peripheral blood was obtained from healthy volunteers and collected in 50 ml falcon tubes containing heparin (10 units/ ml). PMNs from peripheral blood were isolated using sequential sedimentation in dextran followed by gradient density centrifugation, which relies on components of blood being separated by their ability to pass through histopaque. Firstly, heparinised blood was transferred into dextran solution (Sigma) at a ratio of 1:2, and slowly inverted to mix. Following incubation at room temperature for 30 minutes the blood separates. The upper phase was then carefully layered into a 15 ml falcon tube containing 7 ml of Histopaque 1077 (Sigma). The tube was centrifuged at 700 x g for 30 minutes to allow for separation to occur. Following centrifugation, a clear white band was seen containing the PMN population (Figure 11). The layers above the PMN population were carefully removed using a pasteur pipette and the PMNs transferred to a 50 ml falcon tube.

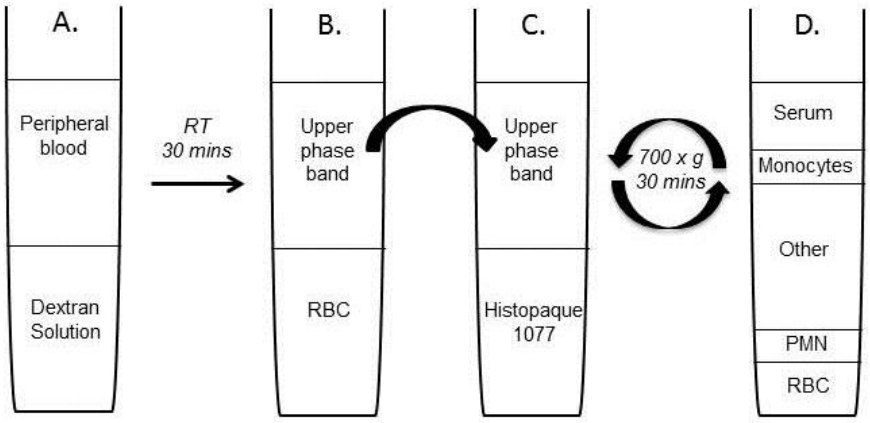

Figure 11 – Density gradient seperation of peripheral blood leukocytes.
(A) Peripheral blood is layered on top of dextran solution. Following incubation, (B) red blood cells separate out, and (C) the upper phase band is layered on top of histopaque 1077. Following centrifugation (D) the neutrophils are separated into a distinct band.

2.3.3 Purification

The tube containing the PMNs was brought up to 30 ml with Hanks buffered salt solution Mg^{2+}-/Ca^{2+}- (HBSS-/-) (Gibco) and washed by centrifuging at 200 x g for 10 minutes, after which the supernatant was discarded. The cells were re-suspended in 20 ml of red blood cell (RBC) lysis buffer (eBioscience) and left at room temperature for a maximum of 15 minutes. Next the cells were re-suspended in 30 ml HBSS-/- for another washing step. Finally, the cell pellet was re-suspended in 10 ml HBSS-/- and the cell number and viability checked using trypan blue and a haemocytometer. Freshly isolated cells were used within two hours of density separation to ensure maximum viability.

2.4 Opsonophagocytosis killing assay

Opsonophagocytosis killing assays (OPKs) first published by Romero-Steiner *et al.*, [261] were initially used to evaluate the efficacy of vaccine candidates for pneumococcus. The assay is based on pathogen-specific monoclonal antibodies which stimulate opsonisation of the target microbe, and deposit C4b and C3b fragments onto the surface of the target, this enhances phagocytosis by immune cells [262]. The effector cells used in the assay can be PMNs isolated from fresh whole blood, differentiated HL-60 cells or, J774.2 cells. Modifications were applied to the method to account for the differences in these three cell types. The opsonophagocytosis assay can be divided into three stages: opsonisation, phagocytosis and analysis.

2.4.1 Opsonisation

A 500 µl aliquot of GAS was thawed and diluted in 5 % opsonisation buffer (OB) to reach 1 x 10^5 CFU / ml. Opsonisation buffer was composed of 5% FBS and Hanks buffered salt solution Mg^{2+}+/Ca^{2+}+ (HBSS+/+). Intravenous immunoglobulin (IVIG) (Gamunex) was used as a source of pathogen-specific antibody. The diluted bacterial suspension (final concentration of 4 x 10^3) and IVIG at a concentration of 1:4, diluted in 5% OB was added to a 96 well plate. Additionally, the bacterial suspension was added to a 96 well plate with 5% OB only as a non-opsonised control. The plate was then added to an orbital shaker (180 RPM) at 37 °C for 20 minutes to allow for opsonisation to occur. Table 3 shows the amounts of bacterial suspension, IVIG and 5% OB added.

Table 3 – Volume of bacteria, IVIG, and opsonisation buffer used in opsonised and non-opsonised wells.

	Opsonised	Non-opsonised
Bacteria (10^5 CFU/ml)	40 µl	40 µl
IVIG	40 µl	0 µl
5%-OB	80 µl	120 µl
Total volume	160 µl	160 µl

2.4.2 Phagocytosis

For J774.2 macrophages

Medium was removed from the well containing 1 x 10^5 adhered macrophages and replenished with 50 µl fresh medium. 10 µl of baby rabbit complement (PelFreeze) and 20 µl of opsonised bacteria suspension (containing 5x10^2 bacteria) was then added to the wells. Final well volume of 80 µl/well.

For differentiated HL-60 and freshly derived PMNs

10 µl of baby rabbit complement and 20 µl of opsonised bacteria suspension (containing 5 x 10^2 bacteria) were added into wells of a 96-well plate. 20 µl of cell suspension (containing 5 x 10^4 cells) was then added giving a multiplicity of infection (m.o.i) of 1:50 (1 bacteria to 50 phagocyte). Final well volume of 80 µl/well.

Control reactions

Control wells included the use of non-opsonised bacteria and wells without complement.

Incubation time

For all cell types, cells were incubated for 45 minutes at 37°C on an orbital shaker (180 RPM).

Culturing

Following incubation, 10 µl from each well was plated in duplicates onto BHI agar plates and incubated for 16-18 hours at 30 °C.

2.4.3 Analysis

After incubation, CFU on BHI plates were counted. In order to determine the efficacy of killing of opsonised bacteria by the phagocytes, the number of bacterial CFU in the bacterial dose (opsonised bacteria and complement) was compared to the number of CFU recovered from the reaction wells with cells (opsonised bacteria, complement and phagocytes). The killing index was then calculated as follows:

$$Percent\ killing = 100 - \left(\frac{Average\ effector\ cell\ CFU\ count}{Average\ no\ effector\ cell\ CFU\ count}\right) x100$$

2.5 Blood survival assay

300 µl of heparinised blood or serum was added to 250 CFU of bacterial frozen stocks in PBS and incubated at 37°C at 180rpm. At specified time points, 100 µl of the mixture was plated onto BHI agar plates for CFU enumeration and incubated at 37°C overnight. A killing percentage was determined by comparison of the original CFU and the CFU counted at the time points.

2.6 Murine models of invasive GAS infection

2.6.1 Murine strains

In all experiments 5-7 week old female CD1 mice (Charles River) were used. Mice were allowed to acclimatise for one week and were always kept in groups of five in individually micro-isolator cage racks. All *in vivo* experiments were conducted following guidelines from the University of Liverpool Animal Welfare and Ethics Review committee and under authority of UK Home Office Project Licence (P86DE83DA).

2.6.2 Preparing GAS inoculum

Once stocks were prepared (see 2.1.4) and the viable number of GAS / ml in each aliquot was determined, doses for infection studies could be prepared. Aliquots of frozen stocks were thawed at room temperature and centrifuged at 13,000 x g for 2 minutes. The supernatant was discarded, and the resulting cell pellet re-suspended in 1 ml sterile PBS for another centrifugation at 13,000 x g for 2 minutes, following which the supernatant was discarded and the cell pellet re-suspended in 1 ml sterile

PBS. The bacterial suspension was then diluted in sterile PBS to establish the desired infection dose.

2.6.3 Intranasal route of infection

Mice were first lightly anaesthetised using 2.5% v/v inhaled isoflourance (1.6-1.8 L O_2 / min) in an anaesthetic box. The lack of reflex reactions confirmed anaesthesia. Once anaesthetised, the mice were scruffed and the bacterial suspension administered equally in small droplets into both nostrils allowing each droplet to be inhaled before administering the next. Following infection, the dose was measured for viable cell count as described using the Miles and Misra.

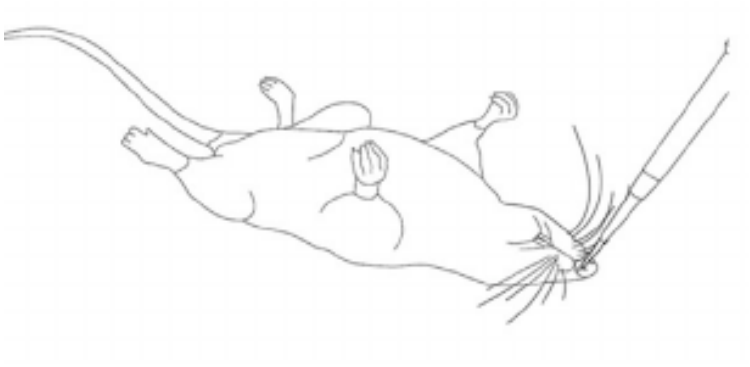

Figure 12 - Intranasal dosing of bacterial inoculum into mice, published in [263].

2.6.4 Intravenous infection

Mice were first placed into a heat box (37°C) for 2-5 minutes to allow for vasodilation of veins to occur. Mice were then placed in a restrainer to allow access to the tail veins. The tails were first sterilised using 70% ethanol, before using an insulin syringe to inject 50 µl of required dose into the dorsal tail vein as shown in Figure 13. If the infection is performed correctly the vein should blanche as the substance is injected.

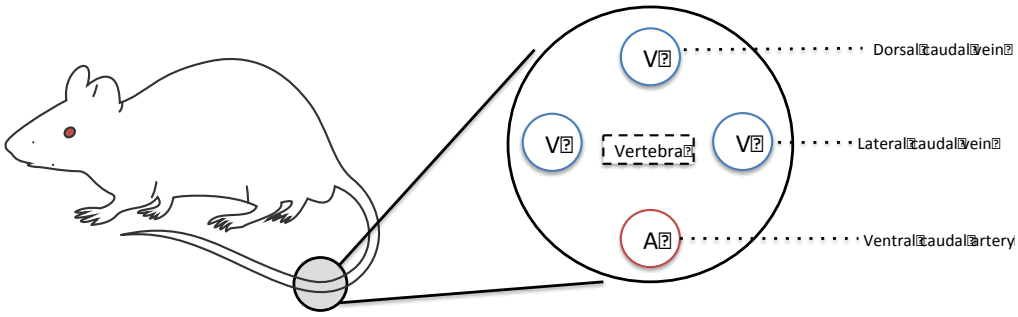

Figure 13 - Schematic diagram of a transverse section of a mouse-tail showing the various veins.

2.6.5 Details of isolates used in virulence testing

The intranasal route of infection is typically used to instil bacteria into the lungs to establish invasive pneumonia or to the nasopharynx to establish a carriage like infection, depending on the dosage and volume. The intravenous route of infection is used to establish bacteraemia and then onto clearance of infection or septicaemia, depending on the dosage. A summary of bacterial strains used to establish different infection models is detailed in Table 4.

Table 4 - Mouse strain, bacterial dose, and volumes used for different models of infection.

Model	Mouse Strain	Bacterial isolate	Dose (Tested for all isolates)	Volume
Carriage	CD1	112327 (*emm* 32.2)	1 x 10^6 CFU	10 µl
		102029 (*emm* 32.2)	1 x 10^7 CFU	
		101910 (*emm* 1.0)	1 x 10^8 CFU	
Pneumonia	CD1	112327 (*emm* 32.2)	1 x 10^6 CFU	50 µl
		102029 (*emm* 32.2)	1 x 10^7 CFU	
		101910 (*emm* 1.0)	1 x 10^8 CFU	
Bacteraemia	CD1	112327 (*emm* 32.2)	1 x 10^6 CFU	50 µl
		102029 (*emm* 32.2)	1 x 10^7 CFU	
		101910 (*emm* 1.0)	1 x 10^8 CFU	

2.6.6 Virulence testing

During virulence testing a small number of mice are used to assess the virulence of each isolate for different doses and route of infection. Following infection, mice were monitored and scored using the scoring system as described in 2.6.8 every 2-3 hours, if mice reached “lethargic ++” stage it was assumed they would progress to moribund. Mice were then humanely culled. If mice did not reach this stage they were culled after 7 days.

2.6.7 Infection studies: Blood, lung, and nasopharyngeal tissue

Blood was collected by either cardiac puncture immediately following death or, on live mice, by removal of a small volume from the tail vein and immediately placed into eppendorf tubes containing 2 µl heparin to avoid blood clotting. Blood samples were assessed for CFU using the Miles and Misra method.

Lungs and the nasopharynx were harvested and placed into a universal containing 3 ml sterile PBS. Tissue was initially mechanically disrupted with an Ultra-Turrax T8 homogeniser (IKA) until completely disintegrated. The resulting homogenate was rinsed through a 40 µm pore diameter cell sieve with 3 ml PBS. The sieve was flushed twice with the homogenate. The resulting homogenate was briefly vortexed and two 20 µl samples were taken and assessed for CFU using the Miles and Misra method.

2.6.8 Monitoring murine behaviour

During infection, the physical appearance of mice was assessed every 2-3 hours once they started to show signs of illness. The scoring system used to assess the health and wellbeing of the mice is detailed in Table 5.

Table 5 – Description and score used to assess the development of infection in murine models.

Score	Description
Normal	Mouse moving around cage normally, rearing up when cage opened, normal coat and normal social interactions.
Hunched +	Slightly arched around middle, walking on tiptoes.
Hunched ++	Very arched around middle, round appearance, walking on tiptoes, holding head down..
Starry+	Coat is slighty piloerect and not well maintained around head and neck.
Starry ++	Coat is considerably piloerect and unmaintained all over.
Lethargic +	Sluggish behaviour, less curious and not interacting with other mice.
Lethargic ++	Not moving at all unless encouraged.
Moribund	Not moving even when encouraged, ungroomed, and laboured breathing.

2.7 Murine models of septic arthritis

5-7 week old CD1 mice were intravenously infected with 50 µl of 10^7 CFU of bacteria. Mice were observed for symptoms of septic arthritis and were scored using the scoring system as previously described (see 2.6.8) as well as an arthritic specific scoring system. Blood tissue and knee joints were taken at time of culling for CFU enumeration using Miles and Misra and cell extraction from the knee joints. These experiments were performed in duplicate.

2.7.1 Arthritic index

All mice were labelled and monitored individually using the previously described scoring system (2.6.8) as well as using a clinical evaluation of arthritis scoring method previously described elsewhere [264]. Limbs were inspected visually at regular intervals (6, 12, 24, 48, 72 hours post injection). Arthritis was defined as visible erythema and/or joint swelling of at least one joint. To evaluate the intensity of arthritis, a clinical scoring (arthritic index) was carried out by using a system where macroscopic inspection yielded a score of 0 to 3 points for each limb (1 point = mild swelling and/or erythema; 2 points = moderate swelling and erythema; 3 points = marked swelling and erythema and occasionally ankylosis). The arthritic index was constructed by dividing the total score by the number of animals used in each experiment group.

2.7.2 Joint tissue

Knee joints were harvested, and the surrounding muscle tissue removed as much as possible and placed into a universal containing 3 ml sterile PBS. Tissue was initially

mechanically disrupted using scissors followed by homogenisation with an Ultra-Turrax T8 homogensiser until completely disintegrated. The resulting homogenate was rinsed through a 40 μm pore diameter cell sieve with 2 ml PBS. The sieve was flushed twice with the homogenate. The resulting homogenate was briefly vortexed and two 20 μl samples were taken and assessed for CFU using the Miles and Misra method.

2.7.3 *In vivo* recovery of bacteria from joints

Using an insulin syringe, 50 μl of bacterial inoculum was injected intravenously into two CD1 mice. The mice were monitored to ensure that 24 hours following injection they were at least a score of 1 on the arthritic index. The mice were humanely culled, the knee joints removed, and the tissue prepared as previously described above. One colony from the culture plates was used to inoculate 7.9 ml of THY media supplemented with 100 μl of glucose in a sterile universal tube. The inoculum was incubated statically for 16-18 hours at 37°C (5% CO_2). 200 μl of the overnight broth was added to 8 ml of fresh THY (supplemented with glucose) and incubated statically at 37°C (5% CO_2), until it reached mid exponential phase (around 4 hours). 1.6 ml of 100% glycerol was added to the 8 ml of resulting broth, to make 20% glycerol stocks. They were then vortexed and placed on ice before being dividing into 500 μl of single use aliquots in sterile cryotubes. The aliquots were stored at -80°C, and after 24 hours aliquots were thawed and numbers of GAS CFU / ml determined used the Miles and Misra method.

2.8 Streptolysin specific ELISA

Prior to analysis samples were thawed at room temperature and SLO quantification was performed by ELISA. Plates (R&D systems) were coated with 1 μg/well monoclonal SLO antibody (Abcam) in PBS (Peprotech) at 4 °C overnight. Plates were washed at each step with Peprotech washing buffer. After blocking for 2 hours (Peprotech blocking buffer), samples were added to the wells and incubated for 2 hours at room temperature. The plate was washed five times and incubated with rabbit IgG polyclonal anti-SLO antibody (Abcam) for 2 hours. Anti-rabbit IgG alkaline phosphatase conjugate secondary antibody (Abcam) was diluted to 1:5000 in blocking buffer, and after washing (x5), was added and incubated for 30 mins. After washing, alkaline phosphatase yellow liquid substrate (PNPP) was added and incubated for 30 mins in the dark, to stop the reaction 1 M Sodium Hydroxide (NaOH) was used. The plate was loaded on to a Multiskan Spectrum (Thermo) and the absorbance measured at 405nm. All ELISAs were carried out with control wells which had all reagents added except samples or diluted SLO. Duplicate samples of each time point were measured on a single plate and repeated independently. Each plate contained six two-fold dilutions of a known concentration of SLO. The results were analysed using Sigma Plot and a standard curve developed to generate concentrations in ng/ml.

2.9 Haemolytic activity assay

The haemolytic activity of streptolysin in culture supernatant was measured as previously described, with minor modifications [99]. Bacteria-free supernatants were incubated at room temperature for 10 minutes with 20 mmol/l of dithiothreitol (Sigma). Supernatant was aliquoted into two tubes; 25 µg of water-soluble cholesterol (inhibitor for SLO activity) was added to one. Both tubes were incubated at 37°C for 30 minutes, followed by the addition of 2% sheep erythrocytes/PBS suspension to each sample and further incubation at 37°C for 30 minutes. PBS was added to each tube the samples were centrifuged at 3000 x g for 5 minutes. Each sample was transferred to a 96-well plate and the OD540 nm was measured.

2.10 Construction of GAS mutants

2.10.1 Single knockout of SLO and SpeA

Knockout mutants of strains *emm* type 32.2 (isolate 112327) and *emm* type 1.0 (isolate 101910) were constructed through double-crossover allelic replacement of *slo* with *aad9* (encoding spectinomycin resistance) and *speA* with *aphA3* (encoding kanamycin resistance) respectively. Regions directly upstream and downstream of *slo* (~ 1000 bp each) were amplified by PCR using primers SLO112327-up-F and SLO112327-up-R, SLO112327-down-F and SLO112327-down-R respectively, which introduced BamHI restriction sites into the PCR products (Table 6). Regions directly upstream and downstream of *speA* (~ 1000 bp each) were amplified by PCR using primers SpeA101910-up-F and SpeA101910-up-R, SpeA101910-down-F and SpeA101910-down-R respectively, which introduced BamHI restriction sites into the products (Table 6). These fragments were stitched together in a second round of PCR using primers SLO112327-up-F and SLO112327-down-R for *slo* regions (*slo* fragment) (Table 6), and using primers SpeA101910-up-F and SpeA101910-down-R for *speA* regions (*speA* fragment) (Table 6) generating 2 kb fragments with a central BamHI site, which then were ligated into pGEM-T vector (Promega), generating pGEM-T-Δ*slo*-2kb and pGEM-T-Δ*speA*-2kb respectively. These plasmids were transformed into *E. coli* DH5α competent cells (ThermoFischer Scientific). The *aad9* and the *aphA3* genes, encoding the spectinomycin and the kanamycin resistance respectively, were amplified by PCR using primers aad9-F and aad9-R, aphA3-F and aphA3-R respectively (Table 6). PCR products were then sub-cloned into pGEM-T-Δ*slo*-2kb and pGEM-T-Δ*speA*-2kb respectively, generating pGEM-T-Δ*slo::aad9* and pGEM-T-Δ*speA::aphA3* plasmids respectively, which were interrupted into their *slo* fragment and *speA* fragment respectively, providing a

means of positive selection of transformants. The generated plasmids pGEM-T-Δ*slo::aad9* and pGEM-T-Δ*speA::aphA3*, were transformed into *emm* type 32.2 (isolate 112327) and *emm* type 1.0 (isolate 101910) respectively, by electroporation as previously described [265]. Transformants were recovered on THY agar supplemented with spectinomycin for MGAS112327Δ*slo::aad9* or with kanamycin for MGAS101910Δ*speA::aphA3*, at 37°C in 5% CO_2 for up to 72 h. Allelic replacement of *slo* with *aad9* and *speA* with *aphA3*, were identified by PCR of chromosomal DNA using primers SLO112327-up-F and SLO112327-down-R, SpeA101910-up-F and SpeA101910-down-R respectively (Table 6) and the PCR products were sequenced to confirmed authenticity of the insertions.

Table 6 – Primers used in single knockout of SLO and SpeA in GAS.

Primer sequences in bold correspond to BamHI restriction site.

Name	Sequence 5'>3'
SLO112327-up-F	GCTAGCGGAGATACTCCTGGAGC
SLO112327-up-R	CTGA**GGATCC**CATGTCCTTCATACCTTTTTATC
SLO112327-down-F	CATG**GGATCC**TCAGGACTGGTTCAAGAG
SLO112327-down-R	GCGCGAGACACACTGGTCCTGAC
SpeA101910-up-F	GCATGTTTTGCGTCCCATCGGCAG
SpeA101910-up-R	CTGA**GGATCC**CATTAATATTCCTCCATTTTATATC
SpeA101910-down-F	AATG**GGATCC**TCAGCTTTTTGCTTTTGGCAAC
SpeA101910-down-R	GGCGCGCTCTGGAGGTAAGTAATG
aad9-F	GAACTAGT**GGATCC**CCCGTTTG
aad9-R	CAATACGGGATAATACCGCGC
aphA3-F	CAAGCTGG**GGATCC**GTTTGA
aphA3-R	TCAAGCA**GGATCC**ATCGATAC

2.11 Liposomes

Liposomes were constructed by M. Pouget. Liposomes were generated with cholesterol and sphingomyelin from egg yolk (Sigma) and dissolved in chloroform at 100 and 50mg/ml respectively. Lipids were mixed together with cholesterol at 66 mol/% proportion and then evaporated with nitrogen gas for 30 min. For Cholesterol: Sphingomyelin (Ch:Sm) large and small liposomes, hydration was carried out by the addition of PBS and incubated at 55°C for 30 mins with vortexing. To obtain small unilamellar particles, the liposome preparation was then subsequently sonicated for 30 min at 4°C. Fluorescent Ch:Sm liposomes were hydrated in 250mM carboxyfluorescein (Sigma) and incubated at 55°C for 30 min with vortexing. To eliminate carboxyfluorescein, the preparation was diluted in PBS and applied to a Sephadex G-25 column in PD-10 (GE Healthcare).

Particle concentration and size distribution of the liposomes generated were evaluated using the NanoSight NS300 instrument (Malvern) and using Nanoparticle Tracking Analysis (NTA) software. Videos were recording at camera level 13. The post-acquisition settings were with a minimum detection threshold of 7, automatic blur and automatic minimum expected particle size. Liposome preparations were diluted 1:1000-1:2000 in PBS and for each sample three 60 sec videos were recorded and analysed.

2.12 Cell population studies

2.12.1 Flow cytometry

Samples were thawed at room temperature and then centrifuged at 400 x g for 5 minutes. The cell pellet was re-suspended in 200 μl of FACs buffer (PBS with 2% FBS) and plated into a round bottom 96 well plate and washed with FACs buffer before being incubated with a 1/200 dilution of purified anti-CD16/CD32 Fc blocking antibody (eBiosciences) for 30 minutes at room temperature. Following incubation with blocking antibody, cells were washed with FACs buffer, cell surface markers were stained using a combination of monoclonal antibodies conjugated with fluorochromes (eBiosciences/BD Biosciences) (Table 7). After 30 minutes incubation, the cells were washed twice with FACs buffer and were re-suspended in 250 μl, the whole sample was acquired using a BD FACSCanto TM flow cytometer (BD Biosciences).

Table 7 – Antibodies and dilutions used for FACs analysis of different cell types.

Target Cell	Antibodies	Dilution
Neutrophils	CD45- FITC	1/200
	GR1-AF700	1/400
Macrophages	CD45- FITC	1/200
	F4/80- PE-CY7	1/400
B cells	CD45- FITC	1/200
	CD19- APC	1/400
	CD22-PE	1/400
CD4+ T cells	CD45- FITC	1/200
	CD4- PE	1/400
T regulatory cells	CD45- FITC	1/200
	CD4- AF700	1/400
	Foxp3- PE	1/300
CXCR3+ T cells	CD45- FITC	1/200
	CD4- PE	1/400
	CXCR3- PE-CY7	1/400
CCR5+ T cells	CD45- FITC	1/200
	CD4- PE	1/400
	CCR5- APC	1/200

2.13 Cytokine capture and analysis

Supernatant from the cell suspensions were collected and stored at -80 °C. Using R&D systems ELISA kits, levels of IL-1β, IL-6, IL-8, TNF-α, and RANTES were determined as per manufacturer's instructions. Plates were read with a FLUOStar Omega plate reader and analysed with the MARS Data Analysis interface (BMG Labtech, Germany).

2.14 Statistical analysis

Data is presented as means ± standard error of the mean. Distribution of data was first assessed using D'Agostino and Pearson omnibus normality test. All data throughout was non-normally distributed, a Mann-Whitney U-test was used to compare CFU counts between two groups, or a one-way ANOVA followed by a Kruskall-Wallis multiple comparisons test if more than two groups were compared. For *in vivo* experiments groups of five mice per time point or dose were used and were performed in duplicate on separate occasions. Survival study data was plotted into a Kaplan-Meier estimator and analysed for statistical difference compared to control groups using a log-rank test. Differences between data sets were designated significant if $p < 0.05$ (*).

3. Characterising the phenotypic response of GAS isolates *in vitro*

A. Introduction

3.1 *Emm* type 32.2 outbreak in Liverpool

An *emm* type 32.2 invasive GAS outbreak occurred in Liverpool from January 2010 to September 2012. The Respiratory and Vaccine Preventable Bacteria Reference Unit (RVPBRU) in the United Kingdom (UK) confirmed a total of 14 cases of *emm* type 32.2 invasive GAS infections in the Merseyside area [266]. The *emm* 32.2 genotype was responsible for 32% (14/44) of all invasive GAS cases reported during this time period (Figure 14) [266]. There have not been any further *emm* type 32.2 invasive GAS cases reported.

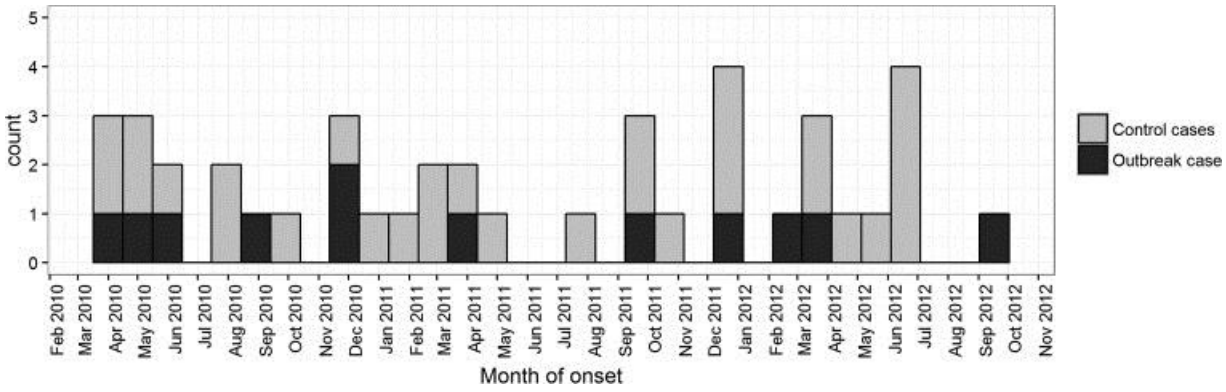

Figure 14 – Histogram plot of outbreak and invasive GAS cases that were collected at the same time in Merseyside.

Taken from Cornick *et al.*, 2016. Histogram plot of all invasive GAS cases in Liverpool from January 2010 to December 2012 reported to the Respiratory and Vaccine Preventable Bacteria Reference Unit of Public Health England.

Following a Liverpool Health Partners award, all 14 *emm* type 32.2 outbreak isolates, 15 non-*emm* type 32.2 invasive GAS isolates (randomly selected from the 30 non-outbreak invasive GAS cases available) and a random sample of 20 non-invasive pharyngitis GAS isolates supplied by the Royal Liverpool University Hospitals Trust and Alder Hey Children's Hospital were subjected to whole genome sequencing.

We previously published work that demonstrated by using core and accessory genome analysis, that the emergent *emm* type 32.2 isolates encoded a combination of 19 genes not identified in other isolates circulating in the same community during the same time frame (Figure 15) [266]. A subset of the 19 unique genes have well characterised roles in virulence and pathogenesis, namely genes encoding a Mga-like regulatory protein, Myr positive regulator, LepA, a trypsin resistant surface protein T6, and a hyaluronidase, HylP [106, 266]. Within the phylogeny, the *emm* type 32.2 outbreak isolates form a distinct clade, which are clearly separated from the non-outbreak isolates (Figure 15). The phylogeny indicates that the *emm* type 32.2 isolates are genetically distinct from the other isolates circulating within the same population during the same time frame [266].

Figure 15 - Maximum likelihood phylogeny of the 48 GAS isolates based on core genome SNPs.

Each branch is annotated with the isolate source followed by the *emm* type. R, the GAS reference sequence Streptococcus pyogenes HKU16; C, control iGAS cases; N, control non-invasive isolates; and O, outbreak *emm*32.2 iGAS cases. (Right) The absence (grey) or presence (black) of accessory genes in each strain. Taken from Cornick *et al.*, 2016.

3.2 Opsonophagocytosis killing assays

Opsonophagocytosis killing assays (OPKs) first published by Romero-Steiner *et al.*, were developed to evaluate the efficacy of vaccine candidates for pneumococcus [261]. The assay is based on pathogen-specific monoclonal antibodies that stimulate the opsonisation of the target microbe resulting in the deposition of C4b and C3b fragments onto the microbe which enhances phagocytosis by immune cells. The effector cells used in the assay can be polymorphonuclear neutrophils (PMNs)

isolated from fresh whole blood, differentiated HL-60 cells (human promyelocytic leukemia cells) and, J774.2 cell line (BALB/C monocyte macrophages).

3.3 Rationale

To consider further the differences in the *emm* type 32.2 outbreak isolates, a range of *in vitro* assays were used to assess different pathogenic characteristics that could be linked to enhanced virulence.

B. Results

3.4 Confirmation of *emm* type and clinical profile of GAS isolates

Emm sequence typing was performed in accordance with RVPBRU guidelines on each isolate to confirm the *emm* type. All of the outbreak invasive GAS cases were confirmed as *emm* type 32.2. The non-outbreak invasive isolates consisted of 12 different *emm* types. The Merseyside outbreak *emm* type 32.2 isolates (n = 14) were selected for this study alongside a selection of non-*emm* type 32.2 isolates. Invasive (n = 2) and non-invasive (n = 2) of each *emm* type 6.0 and *emm* type 89.0 isolates were selected and an additional well studied invasive *emm* type 1.0 isolate (Table 8).

Table 8 – Selection of isolates chosen for study, with respective disease category and *emm* type.

Isolate	Disease category	*emm* type
112327	Invasive-outbreak	st32.2
103045	Invasive-outbreak	st32.2
102920	Invasive-outbreak	st32.2
112844	Invasive-outbreak	st32.2
101452	Invasive-outbreak	st32.2
101967	Invasive-outbreak	st32.2
101008	Invasive-outbreak	st32.2
111617	Invasive-outbreak	st32.2
121324	Invasive-outbreak	st32.2
121511	Invasive-outbreak	st32.2
122397	Invasive-outbreak	st32.2
101700	Invasive-outbreak	st32.2
102029	Invasive-outbreak	st32.2
101910	Invasive	st1.0
126215	Invasive	st6.0
137027	Non invasive	st6.0
127785	Non invasive	st6.0
127784	Non invasive	st6.0
127746	Non invasive	st89.0
137081	Non invasive	st89.0
101724	Invasive	st89.0
137072	Non invasive	st89.0

3.5 Opsonophagocytosis killing assay - peripheral blood neutrophils

Firstly, polymorphonuclear neutrophils (PMNs) were used as the effector cell, PMNs were isolated from the peripheral blood of healthy adult volunteers (n = 3) in Liverpool (UK). It was tested whether there were any differences between a representative subset of the *emm* type 32.2 isolates in their ability to resist killing to PMNs, following opsonisation with intravenous immunoglobulin (IVIG) and complement. The protocol was optimised initially to ensure the final dilution of IVIG was suitable for effective opsonisation of GAS. Two *emm* type 32.2 isolates (101452 and 102029) were used at three different IVIG concentrations (1:4, 1:8, and 1:16). For both isolates the amount of killing decreased as the dilutions of IVIG increased (Figure 16). The concentration of 1:4 IVIG gave the optimum killing range of between 20-40% for both isolates and as such was chosen to continue with throughout the study.

6 different *emm* type 32.2 isolates were used to assess resistance to opsonophagocytosis by PMNs. There were large amounts of variation in between independent experiments which could be due to variability in the PMNs collected and inter-person variation. A much larger sample size would have been needed to standardise the percent killing. The percent killing was compared between isolates using a one-way ANOVA followed by a Kruskall-Wallis multiple comparisons test and there were no significant differences across the *emm* type 32.2 isolates. Due to the large amount of variability and the limited number of healthy volunteer recruits, the rest of the isolates chosen for the study were not tested in the assay.

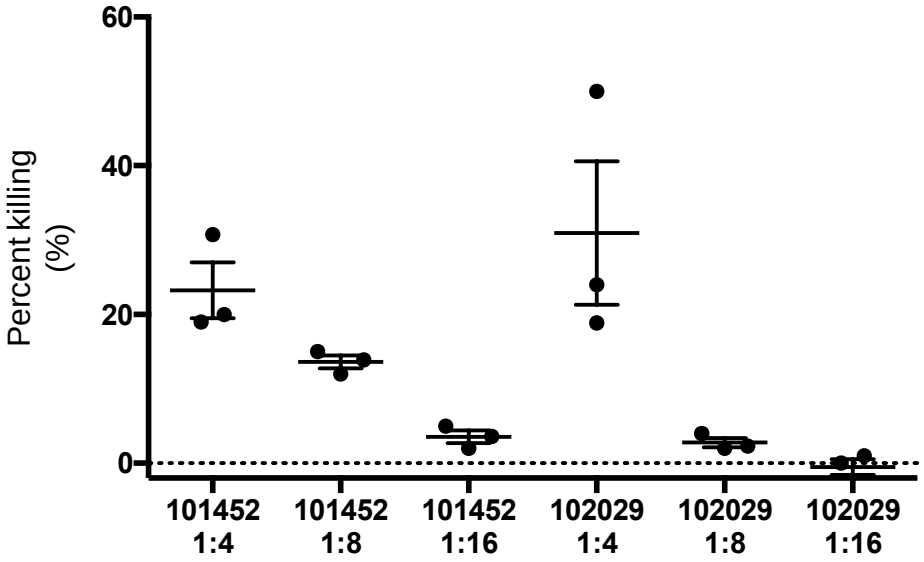

Figure 16 - Effect of different dilutions of intravenous immunoglobulin in opsonophagocytosis killing assay using freshly derived peripheral blood neutrophils.

Percent killing of *emm* 32.2 isolates 101452 and 102029 by peripheral blood neutrophils (volunteer donor blood n = 3) after opsonisation with complement and IVIG at three different final dilutions (1:4, 1:8, 1:16). Percent killing was calculated by comparing CFUs between the effector cell and non-effector cell control. Displayed as mean ±SEM.

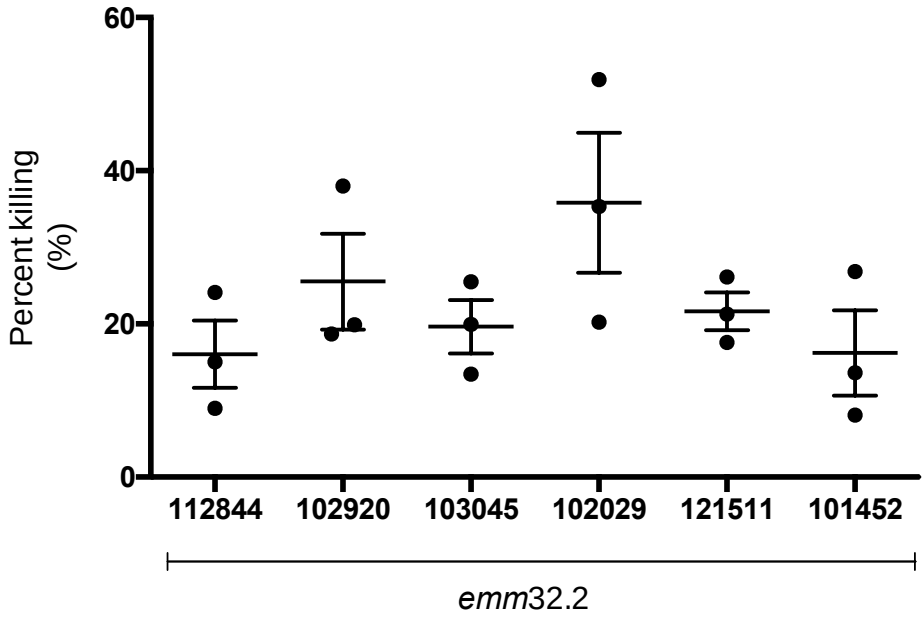

Figure 17 - Sensitivity to opsonophagocytosis by freshly derived peripheral blood neutrophils.

Percent killing of subset of *emm* 32.2 isolates (n = 6 Isolates: 112844, 102920, 103045, 102029, 121511, 101452) by peripheral blood neutrophils (volunteer donor blood n = 3) after opsonisation with complement and IVIG (1:4). Percent killing was calculated by comparing CFUs between the effector cell and non-effector cell control. Displayed as mean ±SEM.

3.6 Opsonophagocytosis killing assay – differentiated HL-60 cells

To consider whether the variation in killing between the isolates was due to inter-person variation of the PMNs, the HL-60 cell line differentiated into PMN-like granulocytic cells were used as the effector cells. 8 *emm* type 32.2 isolates, two *emm* type 6.0 isolates (non-invasive) and two *emm* type 89.0 isolates (non-invasive) were used in the assay. The assay was carried out in triplicate and over three independent days.

The average killing of *emm* type 32.2 (10%) was not statistically significantly different to the average killing of the non-invasive isolates (7%) (Figure 18). As seen with freshly isolated PMNs there were high amounts of variation in between experiments and in some cases the assay had failed to show any killing. It can be determined from this that PMNs may not be the most appropriate effector cell in this assay due to the large amount of variation observed.

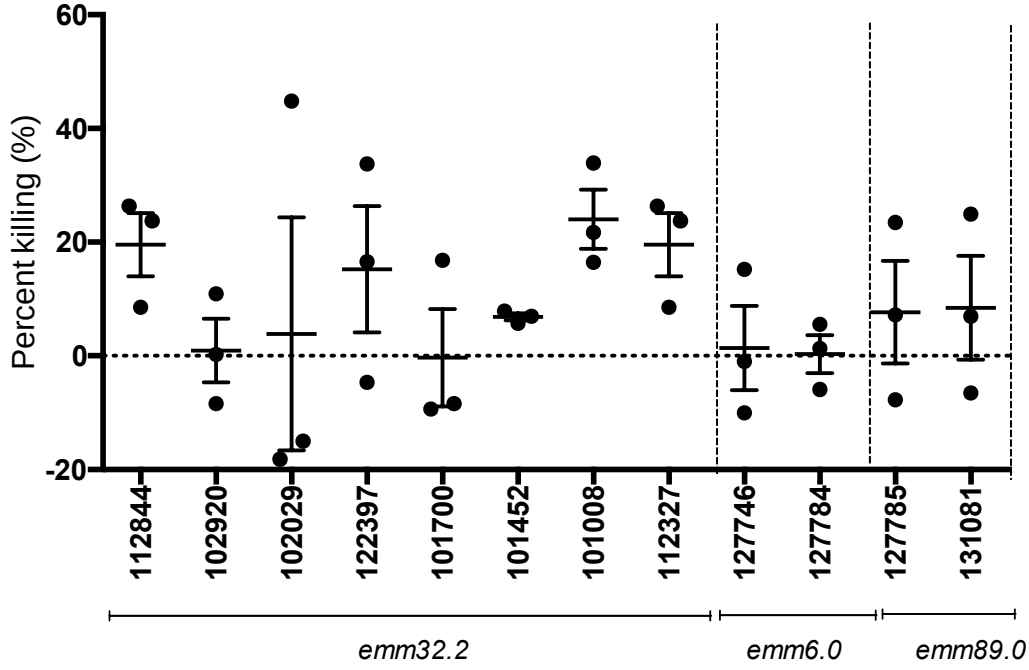

Figure 18 - Sensitivity to opsonophagocytosis by differentiated HL-60 cells.

Percent killing of a subset of *emm* 32.2 isolates (n = 6 isolates: 112844, 102920, 103045, 102029, 121511, 101452), *emm* 6.0 isolates (n = 2 isolates: 127746 and 127784) and *emm* 89.0 isolates (n = 2 isolates: 127785 and 131081) by the HL-60 cell line differentiated into PMN-like granulocytic cells, after opsonisation with complement and IVIG (1:4). Percent killing was calculated by comparing CFUs between the effector cell and non-effector cell control. Displayed as mean ±SEM.

3.7 Opsonophagocytosis killing assay – J774.2 macrophage cells

Studies have previously shown that macrophages are important in the early host immune defence against GAS [173, 175, 177]. The full set of *emm* type 32.2 isolates (n = 14), a subset of *emm* type 6.0 (n = 4), *emm* type 89.0 (n = 4), and *emm* type 1.0 (n = 1) isolates were tested in their ability to resist opsonophagocytosis using the J774.2 macrophage cell line (Figure 19). The assay was carried out in triplicate and over three independent days.

When using PMNs either from healthy blood donors or the HL-60 cell line there were large amounts of variation in between independent assays (>2 stdev of the mean), which was not the case when using J774.2 macrophages as the effector cells, making the assay more reliable and reproducible. First, considering only the *emm* type 32.2 isolates there was variation within the *emm* type in the ability to resist opsonophagocytosis. In particular, *emm* type 32.2 isolates 112844, 102920, 103045 and 102029 were more susceptible to killing than the other *emm* type 32.2 isolates (significant differences shown in Table 9). There were no patterns in the ability to resist opsonophagocytosis when *emm* 32.2 isolates were arranged temporally in line with the clinical outbreak data. Within the *emm* type 6.0 and *emm* type 89.0 isolates there was less variation, the invasive isolate in both groups had a lower mean percent killing than the non-invasive isolates. Although there was considerable variation within the *emm* type 32.2 isolates, generally, the mean percent of killing by macrophages in *emm* type 32.2 isolates (30% killing) was lower than non *emm* type 32.2 isolates (37% killing) (Figure 19).

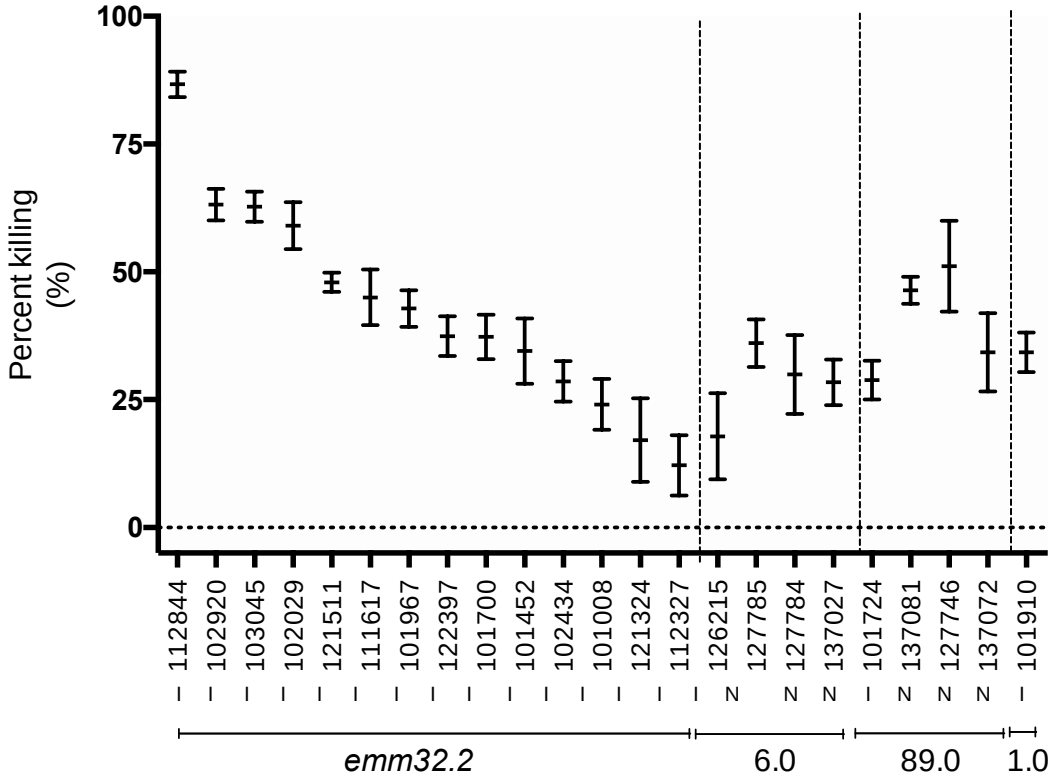

Figure 19 - Sensitivity to opsonophagocytosis by J774.2 macrophages.

Percent killing of all *emm* 32.2 isolates (n = 14) and a representative subset of *emm* 6.0 isolates (n = 4), *emm* 89.0 isolates (n = 4), and *emm* 1.0 isolates (n =1) by the J774.2 macrophage cell line, after opsonisation with complement and IVIG (1:4). I, represents invasive isolates and N, represents non-invasive isolates as determined by the clinical data. Percent killing was calculated by comparing CFUs between the effector cell and non-effector cell control. Displayed as mean ±SEM.

Table 9 – Comparison of percent killing by J774.2 macrophages

Pair wise comparison of isolates used in J774.2 OPKA, analysed using a one-way ANOVA and Kruskal-Wallis multiple comparisons test. Significance indicated by *p < 0.05 **p < 0.01 *** p < 0.005 **** p < 0.0001

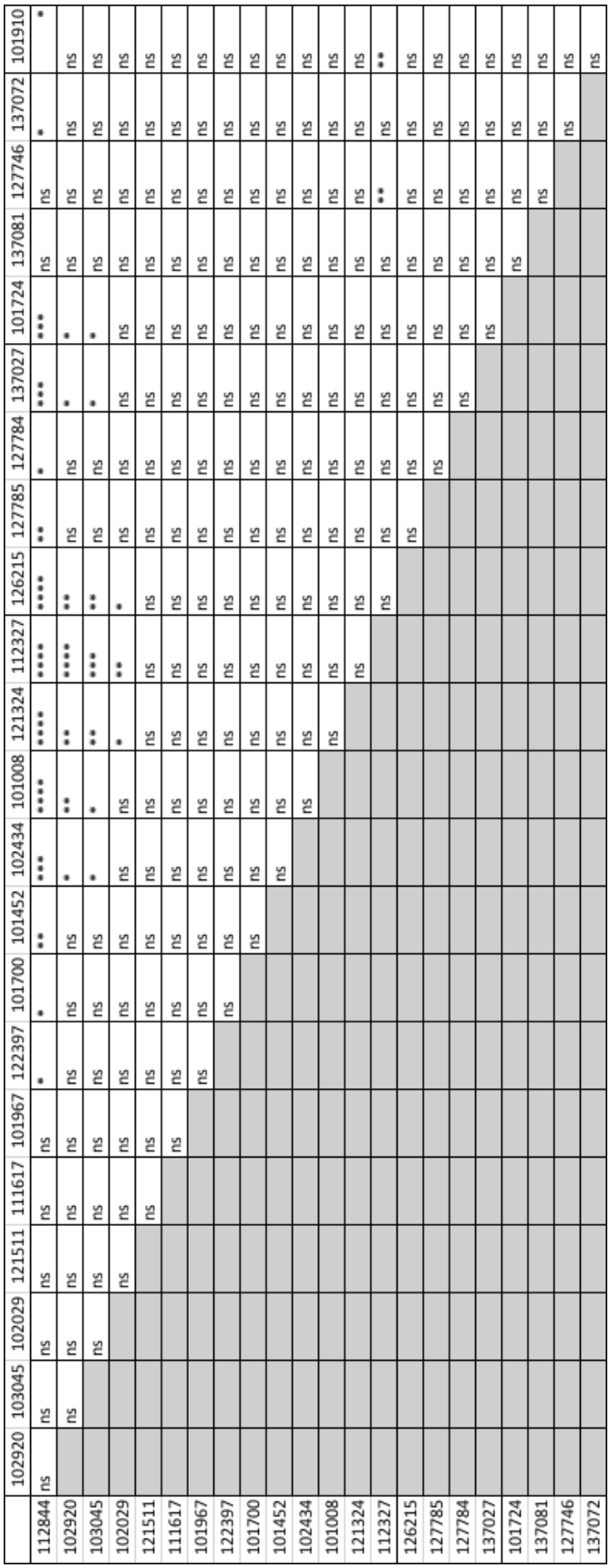

3.8 Comparison of OPKA with capsule thickness and complement deposition

In addition to the ability of outbreak and non-outbreak isolates to resist opsonophagocytosis, differences in capsule thickness and complement deposition were also assessed. Invasive *emm* type 32.2 isolates had thicker capsules than non-invasive isolates (regardless of *emm* type) and had less complement deposited on their surface on average. The size of the capsule and complement deposition are inversely proportional, with smaller capsule isolates exhibiting more complement deposition on their surface. The Pearson correlation coefficient (r) after $\log_{10}$ transformation was -0.5845 ($r^2 = 0.3416$; $p = 0.0027$).

Data from the capsule thickness assays and complement deposition were compared with the J774.2 OPKA results, to identify possible correlations between them. Although there was no significant correlation between capsule thickness and OPK, there was a positive association between the two (r = 0.20) (Figure 20). There was no significant correlation between complement deposition and OPK (Figure 20).

A.

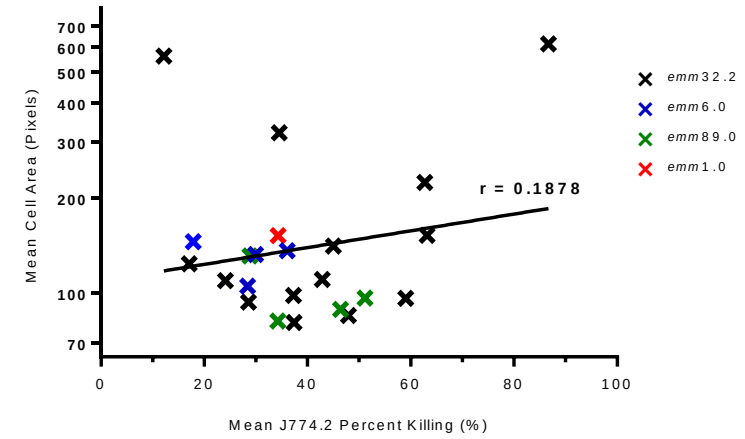

B.

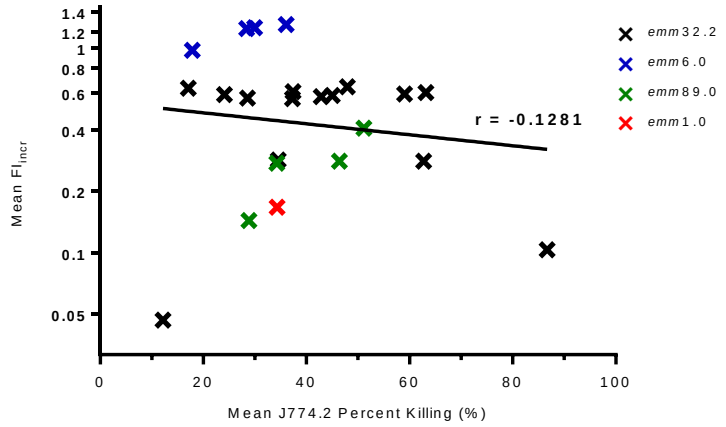

Figure 20 - Percent killing by J774.2 macrophage cells versus capsule thickness and complement deposition.

A) Comparison between capsule thickness (Pixels) and mean percent killing by J774 macrophages. The Pearson correlation coefficient (r) after $\log_{10}$ transformation of capsule thickness values was 0.1878 (95% CI: -0.2434 to 0.5569; $r^2 = 0.03525$; $p = 0.3909$). B) Comparison between complement deposition (FI) and mean percent killing by J774 macrophages on a logarithmic scale. The Pearson correlation coefficient (r) after $\log_{10}$ transformation of mean FI_{incr} was -0.2278 (95% CI: -0.5851 to 0.2036; $r^2 = 0.05190$; $p = 0.2958$). Black crosses represent *emm* 32.2 isolates, blue *emm* 6.0, green *emm* 89.0 and red *emm* 1.0. Data provided by M. Alsahag and analysed by J. Clarke.

3.9 Isolates chosen for *in vivo* modelling

To consider further the virulence of this diverse set of strains two representative isolates from the *emm* type 32.2 outbreak isolates and an *emm* type 1.0 isolate were chosen to use further in *in vitro* assays and *in vivo* infection modelling.

All three isolates chosen were from an invasive clinical phenotype but had distinct differences in the *in vitro* assays described. *Emm* type 32.2 isolate 112327 had a significantly thicker capsule than *emm* type 32.2 isolate 102029 and *emm* type 1.0 isolate 101910 (Figure 21a). *Emm* type 32.2 isolate 112327 also had significantly lower complement deposition (Figure 21b) and was more resistant to killing (Figure 21c) in comparison to both other isolates (*emm* type 32.2 isolate 102029 and *emm* type 1.0 isolate 101910).

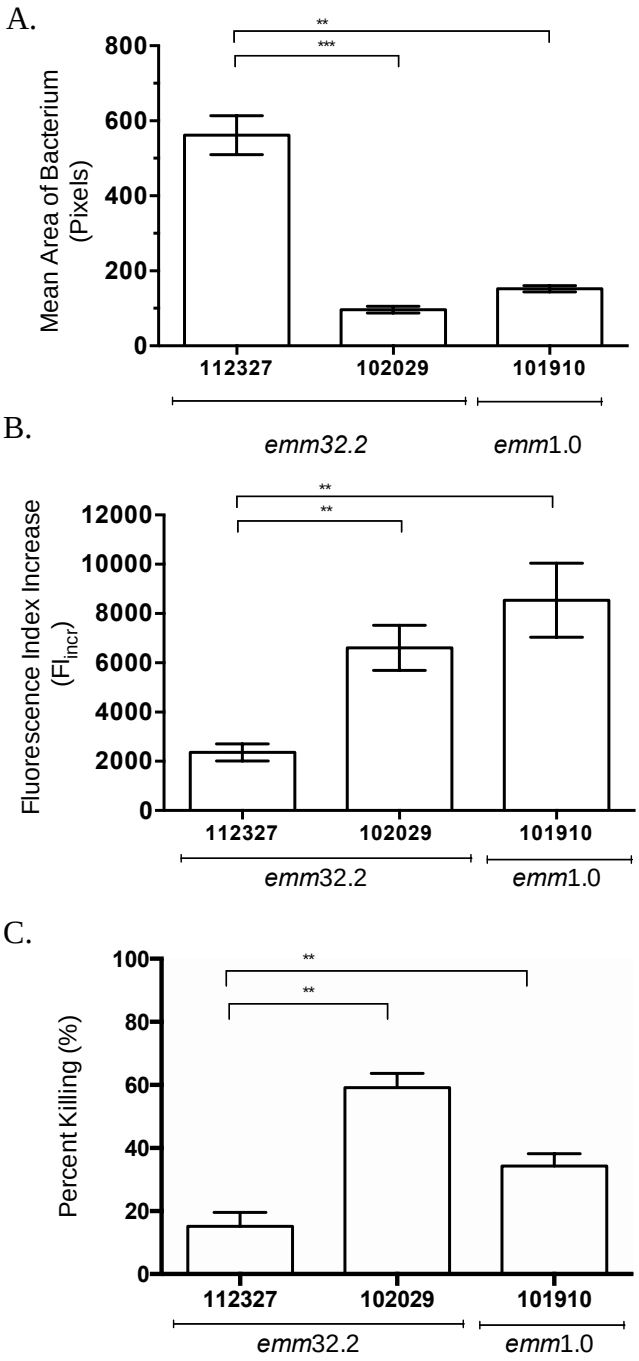

Figure 21 – Comparison of capsule thickness, complement deposition, and OPK survival between isolates chosen for *in vivo* infection studies.

Comparison between *emm* 32.2 isolates 112327 and 102029 and *emm* 1.0 isolate 101910 of A) capsule thickness (mean-pixels) B) complement deposition (Fi) and C) percent killing by macrophages. Analysed using a two-tailed Mann Whitney U-test, ** $p < 0.01$, ***$p < 0.005$.

3.10 Whole blood and serum survival assays

To compare *emm* type 32.2 isolates 112327 and 102029 and *emm* type 1.0 isolate 101910's ability to replicate in blood and serum, survival assays over 24 hours were performed. All three isolates were grown either in whole blood or serum taken from healthy volunteers (n = 3) and incubated for 24 hours, at 0, 2, 4, 6, and 24 hours samples of blood and serum were taken for CFU enumeration.

During growth in whole blood there was an initial decrease across all three isolates in the number of CFUs at 2 hours in comparison to 0 hours, CFUs of both *emm* type 32.2 isolates then begin to increase up to 6 hours where there is a significantly higher bacterial load for isolate 112327 and 102029 in comparison to *emm* type 1.0 isolate 101910 (**$p < 0.001$). For isolate 101910 there is an initial decrease between 0 and 4 hours, there is then a slight peak in CFUs at 6 hours. At 24 hours, there are significantly higher bacterial numbers for the *emm* 32.2 isolates which have continued to increase, in comparison to *emm* type 1.0 which is being cleared from the blood (**$p < 0.001$).

During growth in serum, both *emm* type 32.2 isolates proliferate between 0 and 6 hours, whereas with *emm* type 1.0 isolate 101910 there is a reduction in CFUs at 4 hours which then increases again at 6 hours. After 6 hours, the bacterial load of all three isolates increases in the serum, and there are no significant differences between the number of CFUs.

A.

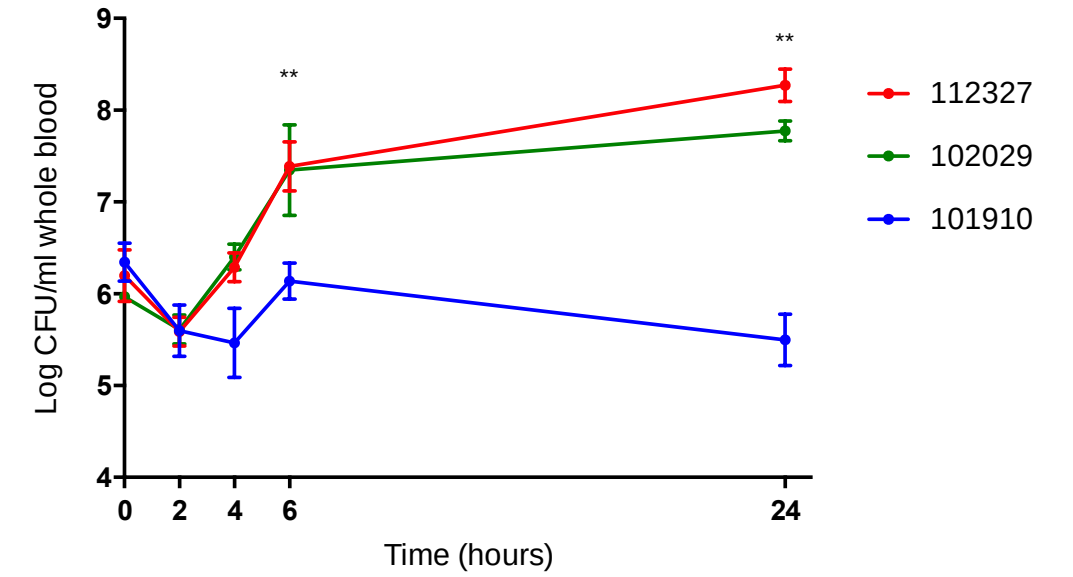

B.

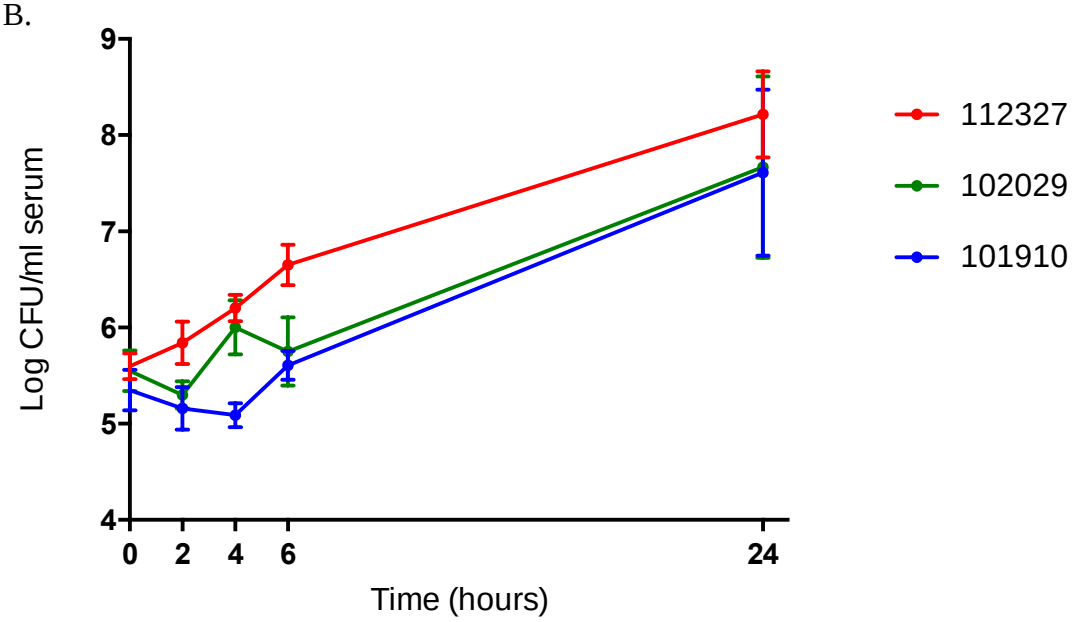

Figure 22 – Survival of *emm* type 32.2 (isolates 112327 and 102029) and *emm* type 1.0 (isolate 101910) in whole blood and serum over 24 hours.

Growth of *emm* type 32.2 isolates 112327 (red) and 102029 (green), and *emm* type 1.0 isolate 101910 (blue) in A) whole blood and B) serum. Results are reported as means ± S.E.M and were analysed using a two-tailed Mann Whitney U-test, ** $p < 0.01$.

C. Discussion

In vitro experiments were carried out to characterise the pathogenic phenotype of *emm* type 32.2 isolates obtained from an outbreak of invasive GAS in Liverpool. They were compared with other invasive isolates of GAS obtained from bacteraemia or pharyngitis cases during the same time frame (*emm* type 6.0, *emm* type 89.0 and *emm* type 1.0). Experiments that assessed the bacteria's ability to resist killing by phagocytosis, capsule thickness, complement deposition and whole blood/serum survival were performed on the isolates. The experiments clearly show that *emm* type 32.2 isolates (isolate 112327 and 102029) are unique in that they show a wide range of variability within the *emm* type and results suggest that they would be more invasive in an *in vivo* model.

Protection against GAS infection is mediated by phagocytosis, usually enhanced by bacteria-specific antibodies, with resistance to such killing linked to increased virulence of the bacteria [175]. The HL-60 OPKA was originally developed at the Centres for Disease Control and Prevention (CDC) to determine the opsonising efficacy of pneumococcal vaccine induced antibodies [261]. The assay was later modified to measure the ability of granulocytes to kill opsonised pathogens in the presence of stimulants [267, 268]. In this study, the assay was modified from the validated pneumococcal OPKA which makes use of baby rabbit complement as the exogenous source of complement and either freshly isolated PMNs, DMF-differentiated HL-60 cells, or J774 murine macrophages as the exogenous source of phagocytic effector cells to be able to assess resistance to killing by a range of GAS isolates. IVIG was used as the opsonin in all three assays, IVIG is derived from up to 3000 blood donors and includes both antibodies generated either naturally through

exposure to pathogens and those generated after vaccination [269]. Many studies have shown that IVIG contains antibodies against a wide range of common bacterial and viral pathogens [193, 270]. Due to its broad specificity, IVIG can also be administered in the clinic prior to diagnostic results [271], as well as directly included in a specific treatment regime [272]. In this study IVIG was successfully used to opsonise all GAS isolates in the assays, however there can be lot-to-lot variation in the neutralising titres of pathogen specific immunoglobulin [273]. It may also be important to consider that the IVIG dilution factor of 1:4 chosen for the experiments had more variation in killing than the dilution factor of 1:8 trialled during optimisation, it would be good to consider in the future if this had an effect on the variation observed.

Firstly, PMNs derived from fresh whole blood were used as the phagocytic effector cell. The assay demonstrated the limitations in using fresh whole blood from volunteers. There are natural variations in complement and neutrophil activity that exist between individuals, making the data variable and difficult to reproduce [274, 275]. This has been described in studies that have attempted to modify the traditional Lancefield assay, which measures the growth and survival of GAS in whole blood from an immune individual or in non-immune whole blood supplemented with serum from an immune individual [276]. There are high amounts of inter-donor variation and differences between the exposure level of people to GAS [274]. Our data showed that the variation between independent experiments was too high to be able to draw any valid conclusions about the data. In addition to this, the protocol used for the isolation of PMNs precludes the isolation of the most immature neutrophils, as their low-density results in them being deposited in the PBMC fraction after density

centrifugation, and these immature neutrophils have been shown to have decreased function in comparison to more mature populations [277].

Since studies by Martinez *et al*. reported that *in vitro* differentiated HL-60 cells showed comparable effectiveness in the phagocytosis of pneumococci to PMNs isolated from multiple donors, efforts have been made to improve the efficacy of phagocytes used for OPKAs [278]. Appropriate differentiation inducers should derive HL-60 cells into cells which successfully mimic genuine PMNs that circulate in the blood [279]. However, it has been underlined that the HL-60 line displays extensive heterogeneity that is further compounded by subsequent variability after differentiation, rendering the cell line unstable [280, 281]. Our results did not show any statistically significant differences in between isolates as the variation was so high between independent experiments (Figure 18).

Next the J774.2 murine macrophage cell line was used as the phagocytic effector cell; all isolates were tested using this assay and the variation between independent experiments was minimal. Previous studies have also used the J774.2 cell line to assess opsonophagocytosis of isogenic mutants of GAS isolates [265]. Within the *emm* type 32.2 isolates there were large amounts of variation in the ability of the bacteria to resist killing, notably 112844, 102920, 103045, 102029 were more susceptible to killing. Generally, *emm* type 32.2 isolates were more resistant to killing by macrophages (30% killing) than non *emm* type 32.2 isolates (37% killing), although this was not statistically significant (Figure 19).

Several other *in vitro* experiments were also performed to further compare the phenotypic characteristics of *emm* type 32.2 isolates with other *emm* type isolates. The experiments included capsule thickness and complement deposition quantification assays. The capsule is an essential virulence factor for GAS and nearly all GAS isolates (except acapsular *emm* type 6.0) possess a hyaluronic acid (HA) capsule [124, 126]. Numerous studies have suggested that the capsule obstructs access to surface epitopes by antibodies and thereby inhibits phagocytosis, it has also been demonstrated that the capsule enhances resistance to complement deposition on the surface further increasing resistance to phagocytosis [132, 282]. Moreover, *in vivo* studies have also demonstrated that the expression of the GAS capsule is essential for full virulence in a model of invasive infection [283, 284]. The activation of the classical and alternative complement pathway leads to opsonisation of the bacteria with C3b and its cleavage fragment iC3b [285]. Complement receptors on neutrophils and macrophages bind both of these resulting in phagocytosis [285]. In order to evade complement mediated phagocytosis, bacteria prevent or resist the deposition of C3b onto the surface [3, 120, 285]. A known way to resist complement deposition [3] is through the presence of the capsule and in this present study it was demonstrated that the isolates which had a thicker capsule also had less complement deposited on the surface ($R^2 = 0.34$, $p = 0.0027$) (Figure 21). In addition to this the amount of complement on the surface of *emm* type 32.2 isolates was significantly lower than *emm* type 6, 89, and 1.0 isolates ($p < 0.005$). From the capsule and complement data it was hypothesised that *emm* type 32.2 isolates which had a thick capsule and low complement deposition would be more resistant to killing by phagocytes. There was a positive association between capsule thickness and phagocytic killing yet none between complement deposition and killing. This could

be due to the wide range of variability seen between isolates not only across *emm* types but also within the same *emm* types. There have been other studies that have also seen variance in the synthesis of the capsule among GAS isolates of the same *emm* type [286]. The *in vitro* characteristics were used to select isolates for *in vivo* model development. Two isolates from *emm* type 32.2 were chosen that differed significantly in their capsule thickness, complement deposition and resistance to OPK and an *emm* 1.0 type isolate which was also significantly different in all three characteristics to the resistant *emm* type 32.2 isolate (112327).

Through previous high-resolution pan-genome analysis it was found that the *emm* type 32.2 isolates encoded a combination of 19 genes that were not identified in any of the other isolates collected at the same time [266]. A selection of the 19 genes have well known functions in pathogenesis, including Mga-like regulatory protein, Myr positive regulator, LepA, a trypsin resistant surface protein T6, and a hyaluronidase, HylP [266]. Mga is a critical global regulator of many GAS virulence factors and is key in regulating the expression of the *emm* gene which encodes the anti-phagocytic M protein. Previous studies have also shown that Mga directly regulates the C5a peptidase which cleaves C5a, and thereby inhibits recruitment of phagocytic cells to the site of infection [287-289]. The presence of an alternative Mga regulator within the outbreak isolates could lead to increased expression of key virulence factors that could explain why *emm* type 32.2 isolates are more successful in evading phagocytosis. In addition to this, the outbreak isolates also possess the Myr regulator protein which is known to directly contribute to resistance to phagocytosis through controlling the expression of the M protein [290]. LepA (also known as SipA) and tee6 gene encoding the T6 protein are both involved in pilus

structures which play an important role in tissue adherence and biofilm formation [266, 291]. Lastly, the *hlyP* gene encoding hyaluronidase is a key virulence factor as it is thought to enhance bacterial spread in host tissues through the breakdown of hyaluronic acid of the extracellular matrix [292]. Given that a number of these genes have been implicated in virulence and evasion of phagocytosis, it could be that they contribute to increased virulence of the isolates and further explain why *emm* 32.2 isolates are more resistant to killing by phagocytes. To confirm this further investigation would be needed which would include deletion of the chosen genes to identify any differences in pathogenesis.

Before *in vivo* modelling, all three isolates were assessed to measure the survival in whole blood and serum. When present in the blood, bacteria need to be able to withstand both the bactericidal activity of the complement system and phagocytosis. Whole blood killing assays can be used to emulate the dynamics of host pathogen interactions in the blood [293]. Further to this, by assessing phenotypic traits of the bacteria and the dynamics of the host response in *in vitro* assays it provides an opportunity to find a suitable test to measure correlates of immunity/protection particularly when determining the efficacy of vaccines and therapeutics. As expected, the *emm* type 32.2 isolate 112327 which has the thickest capsule, larger amounts of complement deposition and was the most resistant to OPK was able to proliferate in the blood. Unexpectedly, the *emm* type 32.2 isolate 102029 was also able to survive in the blood (Figure 22), even though in our previous assays showed little resistant to OPK. *Emm* type 1.0 isolate 101910 was successfully cleared from the blood by 48 hours. It was anticipated that there would be differences between the two *emm* type 32.2 isolates as seen in the OPKA, it’s possible that the extra genes

present in all the outbreak isolates are providing an advantage to successfully proliferating in the blood. There were no differences between the isolates survival in serum indicating that the clearance is cell dependent.

An important consideration is that the OPKA and whole blood killing assay may not give the full representation of what is happening during GAS infection. Being an *ex vivo* assay it does not explore other host factors such as cytokines and chemokines which could be acting on the neutrophils and macrophages. Further work should be done to explore the kinetics of infection with the *emm* type 32.2 outbreak isolates in comparison with *emm* type 1.0 in an *in vivo* model.

4. Investigating the pathogenesis of group A *Streptococcus* using *in vivo* infection models

A. Introduction

4.1 *In vivo* models of GAS

Animal models of infection that mimic human disease have become a crucial component in research into bacterial pathogenesis. For GAS the development of *in vivo* animal models has been challenging, firstly, it is an obligate human pathogen so is exquisitely adapted to the human host and secondly it is able to cause a broad range of diseases that result from different pathogenic mechanisms [213]. In addition to this there is no single strain, even within the same *emm* type, that can be considered representative of the population due to extensive strain diversity, which can reflect differences in virulence *in vivo* [213].

4.1.1 Model of invasive infection

Invasive GAS infection results from haematogenous spread of bacteria into normally sterile sites of the host, which in serious cases results in sepsis and streptococcal toxic shock [218]. In mice, the various models of systemic infection can be separated based on the route of inoculation, which may be intravenously, intranasally, or intraperitoneally. The intravenous route directly introduces bacteria into the blood stream, whereas the intranasal route requires bacteria to invade across the lung epithelium. Murine models of systemic infection have utility for modelling human disease, in particular for assessing virulence and host responses to infection [204].

4.1.2 Model of septic arthritis

Septic arthritis is an inflammatory disease of the joint and is considered a secondary infection, as the most common cause is through bacteria spreading from the bloodstream into the joint [54]. There are several well-developed murine models for septic arthritis with S. *aureus*, which closely mirrors the clinical phenotype of septic arthritis in humans, in particular the erosion of the joint. It is widely accepted that the best method to initiate septic arthritis is by the intravenous route of infection, as the majority of bacterial joint infections in humans originate from the bloodstream [54]. The kinetics of septic arthritis in GAS infection has not been well studied and there is only one published model that uses an intravenous route of infection to initiate arthritis, the major issue with this model is the large dose volume (0.5 ml) which is not representative of the normal infection dose [238].

4.2 Rationale

In Chapter 3 variation between *emm* types in the ability to resist opsonophagocytosis was observed. To consider further the virulence of this diverse set of strains two isolates were chosen from the *emm* type 32.2 outbreak and one from the *emm* type 1.0 isolates, to use in *in vivo* infection modelling. All three isolates were from an invasive clinical phenotype but had distinct differences in the *in vitro* assays used to assess virulence (capsule thickness, complement deposition, and opsonophagocytosis killing). *Emm* type 32.2 isolate 112327 had a significantly thicker capsule, lower complement deposition and was more resistant to killing, in comparison to *emm* type 32.2 isolate 102029 and *emm* type 1.0 isolate 101910.

The use of two different routes of infection and challenge dose concentrations were explored to examine virulence *in vivo*. Two models of infection were developed; a systemic invasive disease model and a reliable septic arthritis model. Next, the models were used to explore the progression of each of the disease types.

B. Results

4.3 Intranasal route of infection

The intranasal route of infection introduces bacteria to the upper airway of the respiratory tract and can be used to introduce bacteria directly into the lung. A lower volume dose allows the bacteria to remain in the upper airway whereas a high-volume dose results in dissemination of the bacteria into the lung [294]. The ability of the chosen GAS isolates to colonise nasal–associated lymphoid tissue (NALT) in the nasopharynx when using a 10 µl challenge dose was examined. Next a high-volume dose of 50 µl was used to assess whether the different GAS isolates were able to invade across the lung epithelium and establish a systemic infection.

4.3.1 Virulence testing using low intranasal volume dose

Mice were intranasally inoculated with 10 µl of *emm* type 32.2 isolates 112327 and 102029, and *emm* type 1.0 isolate 101910 at doses 10^8 and 10^7 (n = 10). Mice were monitored for signs of infection and were considered to have survived the infection by day 7, after which they were culled, and blood and nasopharyngeal tissue were removed. During infection with all isolates and dose CFUs there was 100% survival until the end of the experiment. Following CFU enumeration no bacteria were detected in the blood and identification of GAS from the NALT tissue was not successful. In summary, there were no differences in the outcome or survival of infection between *emm* types.

4.3.2 Virulence testing using high intranasal volume dose

Next, mice were intranasally inoculated with 50 µl of *emm* type 32.2 isolates 112327 and 102029, and *emm* type 1.0 isolate 101910 at doses 10^8 and 10^7 (n = 10) a higher volume dose allows successful dissemination of bacteria into the lung. Mice were monitored for signs of infection and were considered to have survived the infection by day 7, after which they were culled, and blood and lung tissue was removed. In two of the groups mice succumbed to the infection quickly, 6 hours following infection 80% (8/10) in the group infected with 10^8 CFU of *emm* type 32.2 isolate 112327 died (after reaching "lethargic ++") (Figure 23a) and 40% of mice in the group infected with 10^8 CFU of isolate 102029 died (Figure 23b). When infected with a tenfold lower dose with these two isolates there was 100% survival. Similarly, there was 0% mortality during infection with *emm* type 1.0 isolate 101910 (Figure 23c). Due to the rapid mortality, it is unlikely the bacteria had time to invade through the lung epithelium and into the vascular system of the mice, therefore the mice were more likely to have died from a response to the high levels of toxins secreted from the bacteria at the higher inoculum doses. The remaining mice had 100% survival and were subsequently culled at the end of the 7-day survival period. Bacteria were not recovered from the blood or lungs of mice at the end of the 7-day experiment, indicating that those who survived either did not establish an infection initially or successfully cleared the bacteria.

The survival data was analysed using the Log-rank (Mantel-Cox) test analysis, which is used for the comparison of survival curves (Table 10). Infection with *emm* type 32.2 isolate 112327 at 10^8 was significantly more virulent than infection with *emm* type 1.0 isolate 101910 at both CFU challenge doses (* p-value < 0.05). There was

no significant difference between survival of mice infected with isolates from *emm* type 32.2 (112327 vs. 102029) at the higher CFU of 10^8, however, *emm* type 32.2 isolate 112327 at 10^8 CFU challenge was significantly more virulent than infection with both 112327 and 102029 at 10^7 challenge (* p-value < 0.05) (Table 10). This result implies that intranasal infection with *emm* type 32.2 is significantly more virulent than infection with *emm* type 1.0 but only when administered at a high CFU challenge dose.

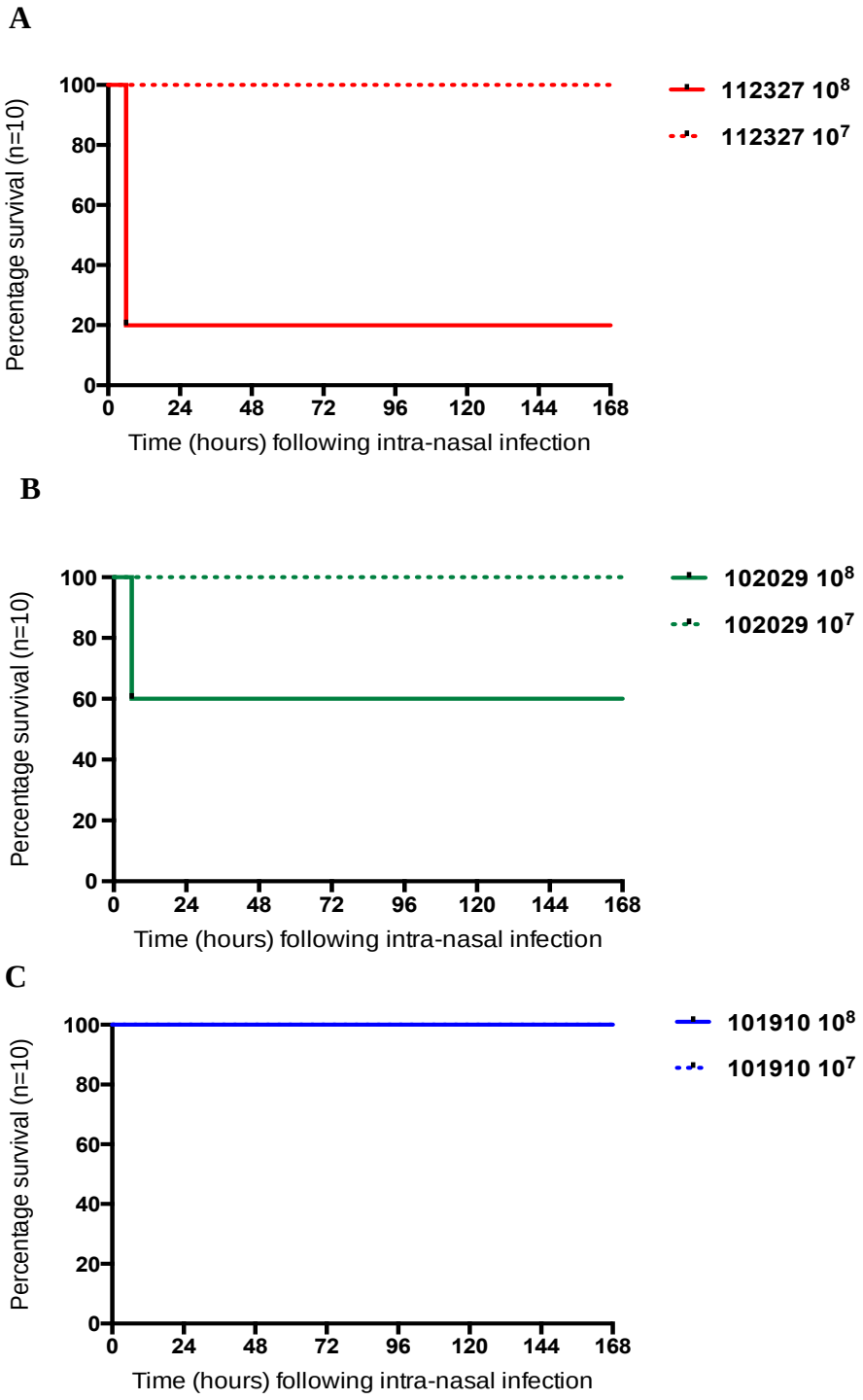

Figure 23 - Comparison of survival of mice when infected with different isolates in a model for GAS pneumonia.

Kaplan Meier plots representing percentage survival of CD1 mice (n = 10 per group) following 10^8 (solid line) and 10^7 (dashed line) CFU in 50 µl intranasal infection with isolates (A) *emm* type 32.2 isolate 112327 (red) (B) *emm* type 32.2 isolate 102029 (green) and (C) *emm* type 1.0 isolate 101910 (blue).

Table 10 - Comparison of survival of mice when infected with different isolates in a model for GAS pneumonia

Log-rank (Mantel-Cox) analysis of mice when intranasally infected (50 µl) with different isolates and dose CFUs of GAS (* p- value < 0.05).

	112327 (10^7)	102029 (10^8)	102029 (10^7)	101910 (10^8)	101910 (10^7)
112327 (10^8)	*	ns	*	*	*
112327 (10^7)		ns	ns	ns	ns
102029 (10^8)			ns	ns	ns
102029 (10^7)				ns	ns
101910 (10^8)					ns

4.4 Intravenous route of infection

The major mechanism of damage to the host during a systemic infection is through the presence of GAS proliferating in the blood stream. The intravenous route of infection directly introduces bacteria into the vasculature system, for the bacteria to be able to establish an infection it must multiply in the blood stream, bacteraemia can then progress to sepsis, which involves multiple organ dysfunction and death (Figure 24).

Figure 24 - Schematic representation of systemic infection model with GAS.

4.4.1 Survival comparison during invasive disease

The virulence of each isolate during systemic infection was determined by infecting mice intravenously with 50 µl of *emm* type 32.2 isolates 112327 and 102029, and *emm* type 1.0 isolate 101910 at doses 10^8 and 10^7 (n = 10).

Following intravenous infection, 100% of mice infected with 10^8 CFU of *emm* type 32.2 isolate 112327 succumbed to infection by 24 hours post-infection. When infected with a lower dose of 10^7 CFU, all mice showed signs of lethargy by 24 hours and succumbed to infection by 36 hours post-infection (Figure 25a). A lower CFU dose group of 10^6 CFU was included to assess whether the bacteria would still be as effective at establishing an infection, at 48 hours 20% (2/10) succumbed to infection

however 80% of the mice were able to clear the bacteria and survive to the end of the experiment. In comparison to this, infection with *emm* type 32.2 isolate 102029 resulted in only 30% mortality (3/10) at dose CFU 10^8, and 0% with dose CFU 10^7 (Figure 25b). In contrast to infection with either isolate from *emm* type 32.2, none of the mice infected with either 10^8 or 10^7 CFU of *emm* type 1.0 isolate 101910 showed any symptoms of infection and all survived (Figure 25c). There are clear differences between the ability of each isolate to establish bacteraemia, *emm t*ype 32.2 isolate 112327 is able to progress to sepsis very rapidly, on the other hand isolate 102029 of the same *emm* type is not as successful and only in high CFU challenge doses is it able to multiply in the blood stream and result in death. Infection with *emm* type 1.0 isolate 101910 did not result in the same outcome as infection with *emm* type 32.2, and none of the mice showed any characteristic symptoms of invasive infection.

The survival data was analysed using the Log-rank (Mantel-Cox) analysis, which is used for the comparison of survival curves (Table 11). Infection with *emm* type 32.2 isolate 112327 at both 10^8 and 10^7 CFU was significantly more virulent than infection with all other isolates (** $p < 0.01$). There were no significant differences in the virulence between any other isolate and dose CFU (Table 11). These initial results are consistent with earlier findings in Chapter 3; where there was a significant difference between bacterial characteristics, that are indicative of virulence, even within the same *emm* type, which are in line with the *in vivo* survival differences observed.

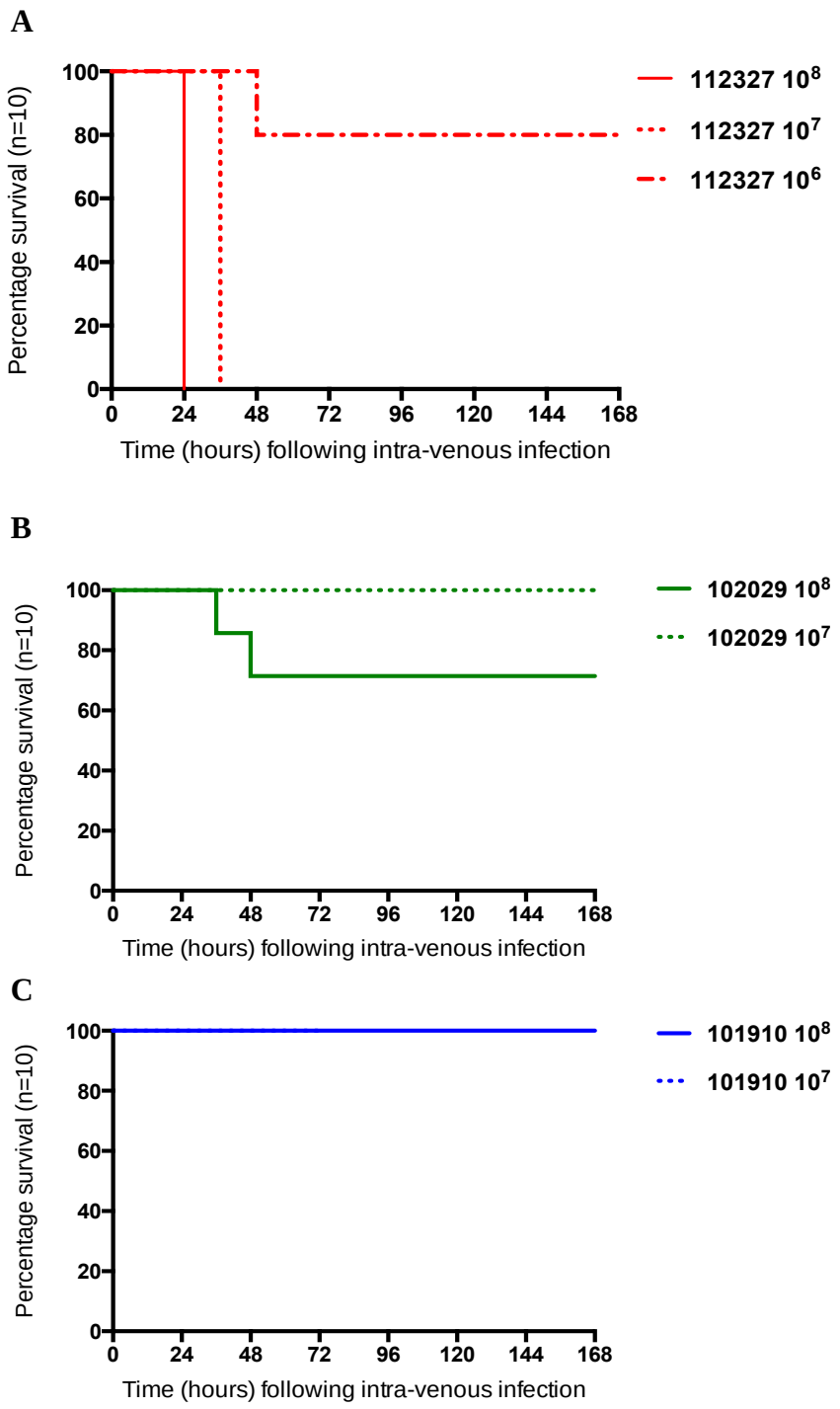

Figure 25 - Comparison of survival of mice when infected with different isolates in a model for GAS bacteraemia.

Kaplan Meier plots representing percentage survival of CD1 mice (n = 10 per group) following 10^8 (solid line), 10^7 (dashed line), and 10^6 (dotted line) CFU in 50 µl intravenous infection with isolates A) *emm* type 32.2 isolate 112327 (red), B) *emm* type 32.2 isolate 102029 (green), and C) *emm* type 1.0 isolate 101910 (blue).

Table 11 - Comparison of survival of mice when infected with different isolates in a model for GAS bacteraemia

Log-rank (Mantel-Cox) analysis of survival of mice when intravenously infected (50 µl) with different isolates and dose CFUs of GAS (** p-value < 0.01).

	112327 (10^7)	112327 (10^6)	102029 (10^8)	102029 (10^7)	101910 (10^8)	101910 (10^7)
112327 (10^8)	**	**	**	**	**	**
112327 (10^7)		**	**	**	**	**
112327 (10^6)			ns	ns	ns	ns
102029 (10^8)				ns	ns	ns
102029 (10^7)					ns	ns
101910 (10^8)						ns

4.4.2 Progression of infection during invasive disease

Based on the results from the *in vivo* virulence testing experiments, only CFU doses of 10^8 and 10^7 were selected for further investigation, in order to make direct comparisons between the different isolates.

To determine the timeline of infection, five mice were intravenously infected with 50 µl of *emm* type 32.2 isolates 112327 and 102029, and *emm* type 1.0 isolate 101910 at doses 10^8 and 10^7, CFUs were enumerated from the blood collected by tail bleeding at 3, 9 and 24 hours to assess the progression of the infection (Figure 26). Firstly, the pattern of blood CFUs were compared across all groups. Between all isolates and doses there was an increase in bacterial load in the blood from 3 to 9 hours. Initially all isolates were able to proliferate in the blood however after 9 hours differences in the pattern of blood proliferation begin to emerge across isolate types. For those infected with *emm* type 32.2 isolate 112327 at both CFU doses, there was a continued increase in bacteria load up until the time of death (Figure 26a). The average bacterial burden in the blood at time of death was mean log 5.78 CFU/ml blood. In comparison, mice infected with *emm* type 32.2 isolate 102029 the CFU levels of bacteria in the blood did not change in between 9 and 24 hours post-infection (Figure 26b). In contrast, mice infected with *emm* type 1.0 isolate 101910 do not follow the same infection pattern; they begin to clear the bacteria rapidly from the blood. The CFU load decreases from 9 hours, for CFU dose 10^8 the bacteria were cleared by 24 hours and for dose 10^7 the bacteria were cleared by 48 hours (Figure 26c).

Next the bacterial burden in the blood was compared at each time point across isolates and dose groups using a one-way ANOVA and Kruskal-Wallis multiple comparisons test. Mice infected with 10^8 CFU of *emm* type 32.2 isolate 112327 had significantly higher bacterial loads in the blood at all time points post infection in comparison to those infected with *emm* type 1 isolate 101910 (** $p < 0.01$). This was also the case by 24 hours for *emm* type 32.2 isolate 112327 infected at a ten-fold lower (10^7) CFU dose. At 24 hours mice in the group 112327 (10^8) were culled, and as expected the mean bacterial burden was highest in those mice (Figure 27). The CFU load was only marginally lower in group 112327 (10^7), which is consistent with the mice survival time being 12 hours later. There was no major variation of bacterial numbers in the blood at each time point between infection with 10^8 and 10^7 CFU of the same isolate.

There is a clear difference in blood survival, which is in line with the survival times observed. In summary, *emm* type 32.2 isolate 112327 is better adapted to survival and proliferation in the blood, and due to this there is uncontrolled bacterial proliferation resulting in sepsis and the animal succumbing to infection. When there is clearance of the bacteria from the blood, as is the case with infection with *emm* type 1.0 isolate 101910, there is 100% survival.

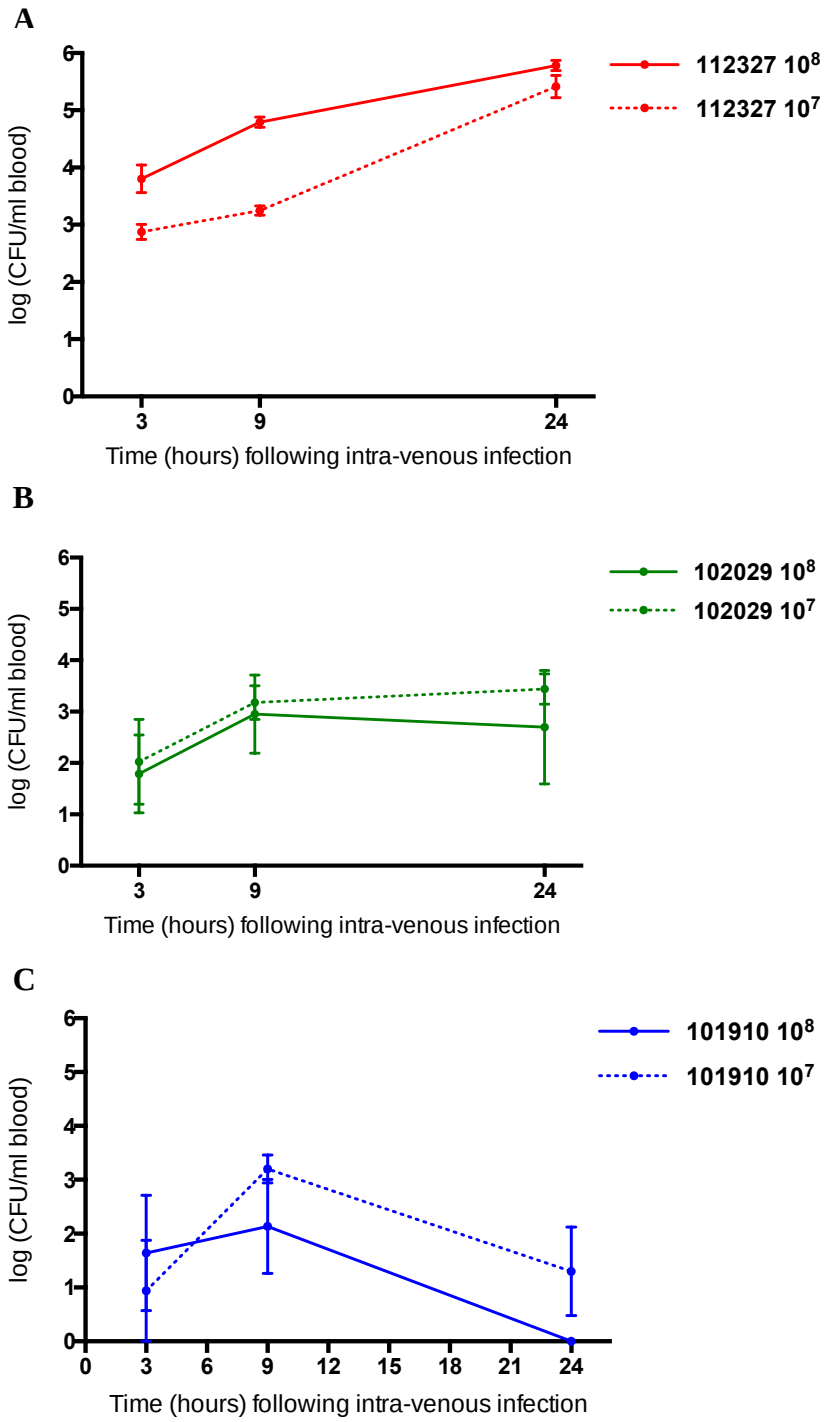

Figure 26 – Bacterial burden in blood of mice when infected with different isolates in a model for GAS bacteraemia.

The bacterial CFU in blood of CD1 mice (n = 5 per group) following 10^8 (solid line) and 10^7 (dotted line) CFU in 50 µl intravenous infection with isolates A) *emm* type 32.2 isolate 112327 (red), B) *emm* type 32.2 isolate 102029 (green), and C) *emm* type 1.0 isolate 101910 (blue) over time. Displayed as mean ± SEM.

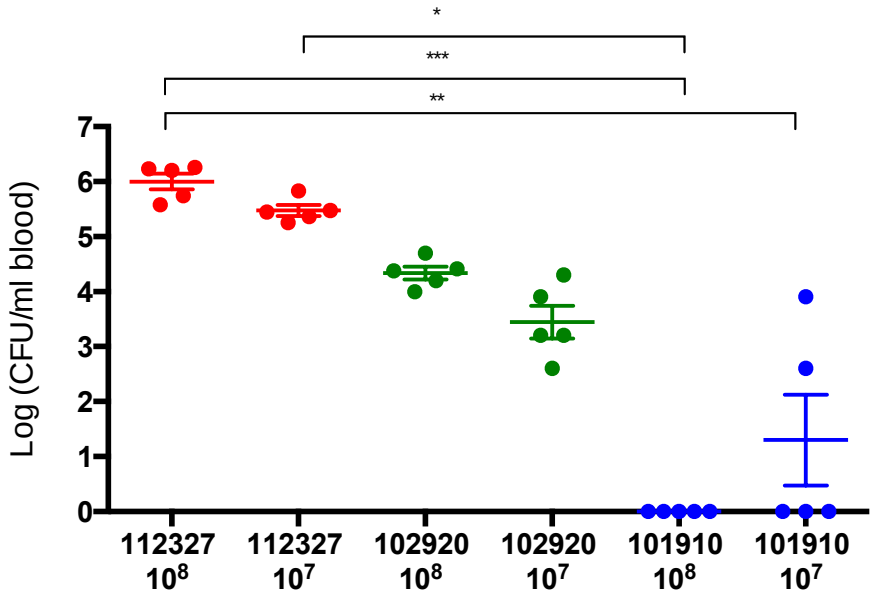

Figure 27 – Direct comparison of bacterial burden in blood of mice when infected with different isolates in a model for GAS bacteraemia at 24 hours.

The bacterial CFU in blood of CD1 mice (n = 5 per group) following intravenous infection with 10^8 and 10^7 CFU of isolates**:** *emm* type 32.2 isolate 112327 (red circles), *emm* type 32.2 isolate 102029 (green circles), and *emm* type 1.0 isolate 101910 (blue circles) was compared at 24 hours using a one-way ANOVA and Kruskal-Wallis multiple comparisons test (* $p < 0.05$ ** $p < 0.01$ ***$p < 0.005$), displayed as mean ± SEM.

To examine the rate of proliferation and clearance from the blood the progression of infection in the spleen was examined. Only the CFU dose group 10^8 was included in this analysis, as there was no major variation in bacterial numbers in the blood between this and the ten-fold lower dose group 10^7. 40 mice were intravenously infected with 10^8 CFU (50 µl) of *emm* type 32.2 isolates 112327 and 102029, and *emm* type 1.0 isolate 101910. Five mice from each group were culled at 6, 24 and 48 hours post infection and the spleen removed for CFU enumeration.

The spleen CFUs were compared between isolates using a one-way ANOVA and Kruskal-Wallis multiple comparisons test. At the earliest time point of 6 hours post infection there was no major differences in the bacterial load in the spleen between strains. At 24 hours mice infected with *emm* type 32.2 isolate 112327 had significantly higher bacterial loads in the spleen in comparison to those infected with any other isolate (** p – value < 0.01) (Figure 28). In those mice infected with *emm* type 32.2 isolate 102029, the bacterial burden did not change significantly across the time points and with *emm* type 1.0 isolate 101910 there is bacterial clearance observed in the spleen with reduced numbers at 48 hours (Figure 28).

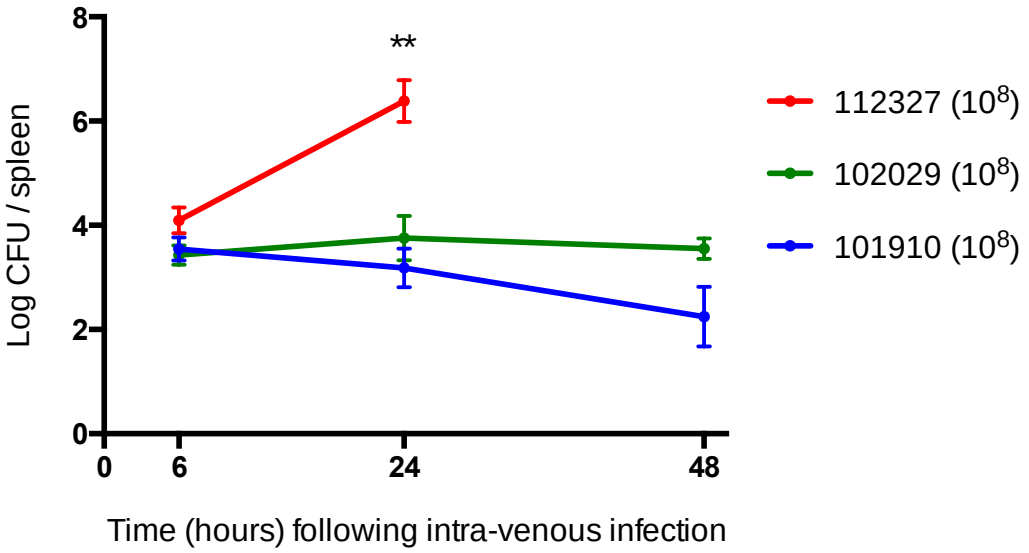

Figure 28 - Bacterial burden in spleen of mice when infected with different isolates in a model for GAS bacteraemia.

The bacterial CFU in the spleen of CD1 mice (n = 5 per group) following 10^7 CFU in 50 µl intravenous infection with isolates *emm* type 32.2 isolate 112327 (red line), *emm* type 32.2 isolate 102029 (green line) and *emm* type 1.0 isolate 101910 (blue line) over time. Analysed using a one-way ANOVA and Kruskal-Wallis multiple comparisons test (** p-value < 0.01), displayed as mean ± SEM

4.4.3 Weight loss during invasive disease

Another method used to assess the condition of animals during infection is to measure weight loss. Weight loss is used to define humane endpoints for the use of animals in experimental studies; typically, mice should not lose more than 20% of their original body weight in a short-term study. During the earlier survival study (4.4.1), all mice were weighed at the beginning of the experiment and then again every 24 hours.

At 24 hours, the mean weight loss of mice in the different groups were compared using a one-way ANOVA and Kruskal-Wallis multiple comparisons test. There were no significant differences in weight loss between dose CFU groups (10^8 and 10^7) of the same isolate (Figure 29). The percentage weight loss was significantly greater in those mice infected with *emm* type 32.2 isolate 112327 (both CFU dose group) than all other groups (Figure 29).

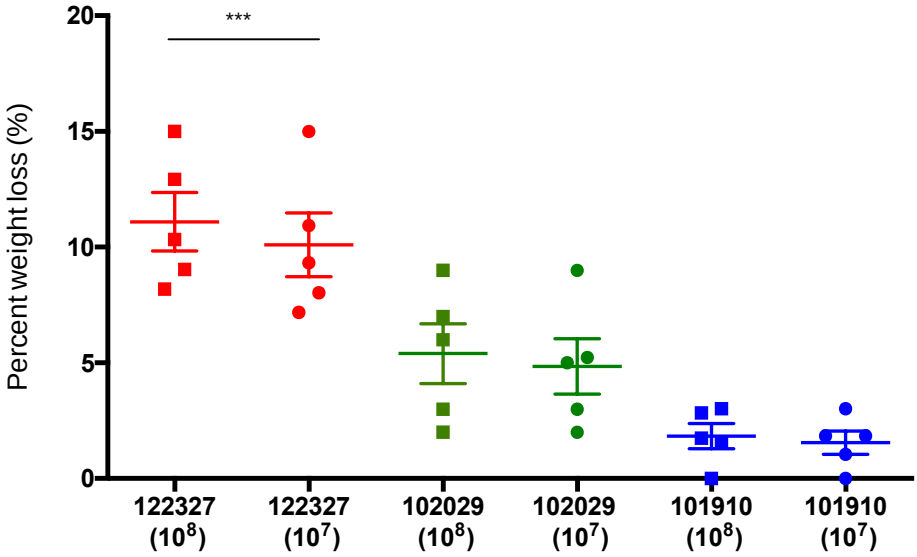

Figure 29 – Percent weight loss of mice when infected with different isolates in a model for GAS bacteraemia.

The percentage weight loss of CD1 mice (n = 5 per group) at 24 hours following 10^8 and 10^7 CFU in 50 µl intravenous infection with isolates *emm* type 32.2 isolate 112327 (red squares), *emm* type 32.2 isolate 102029 (green squares) and *emm* type 1.0 isolate 101910 (blue squares) was compared. Analysed using a one-way ANOVA and Kruskal-Wallis multiple comparisons test (*** $p < 0.005$), displayed as mean ± SEM.

4.4.4 Bacterial arthritis phenotype after intravenous infection

From earlier results in this chapter it can be concluded that *emm* type 1.0 isolate 101910 was either less well adapted to survive in blood or was able to translocate elsewhere in the host. Indeed, all mice infected with *emm* type 1.0 isolate 101910 began to show symptoms of joint deformities at 24 hours. Following CFU enumeration it was confirmed that bacteria were present in the joint, confirming that this could be used as a model for bacterial septic arthritis (Figure 30). This was an interesting outcome as this matched the clinical phenotypic data. *Emm* type 1.0 isolate 101910 was recovered from a patient who was being treated for septic arthritis of the hip joint. We have been able to replicate the human course of infection with a reliable septic arthritis animal model.

Figure 30- Schematic representation of osteomyelitis and septic arthritis model with GAS.

4.5 Kinetics of septic arthritis

To further characterise the septic arthritis model, the growth kinetics and clinical outcomes were assessed during infection. Knee joints were chosen, as they were the most commonly affected joint in this model and also the most clinically relevant. Knee joints are considered a high load bearing joint and so are more often prone to inflammation, damage, and ultimately infection [54].

4.5.1 Progression of infection in the knee joints

To determine the time line of infection within the knee joints 50 mice were intravenously infected with 10^7 CFU of *emm* type 1.0 isolate 101910. Five mice were culled immediately after infection, and 10 mice were culled at each of the following time points post infection 6, 12, 24, 48, and 168 hours to assess the progression of infection in the joints.

Bacteria were recovered successfully from the knee joint at the earliest time point of 6 hours; mean log 2.5 CFU/knee-joint, only one animal did not have any bacteria in the joint (Figure 31a). Bacterial numbers continued to increase rapidly in the knee joints, at 48 hours the maximum density of bacteria was likely reached, as the bacterial load did not greatly increase further up to 7 days. At 7 days the knee joints were severely affected by the presence of the bacteria and large abscesses and deformities had formed. Blood was also removed after the animals were culled at each time point to compare the dynamics of when the bacteria clears from the blood and enters the knee joints. Bacterial burden in the blood decreased from 6 to 24 hours until there was complete clearance at 48 hours (Figure 31b). Interestingly, the highest bacterial load in the joints corresponded with full clearance from the blood. At the

final time point of 7 days, blood was also taken to measure whether bacteria from the joints had re-entered the blood stream. In severe joint infections where abscesses form it is a possibility they can burst or leak bacteria back into the vasculature system. However, this was not observed and no bacteria were recovered from the blood.

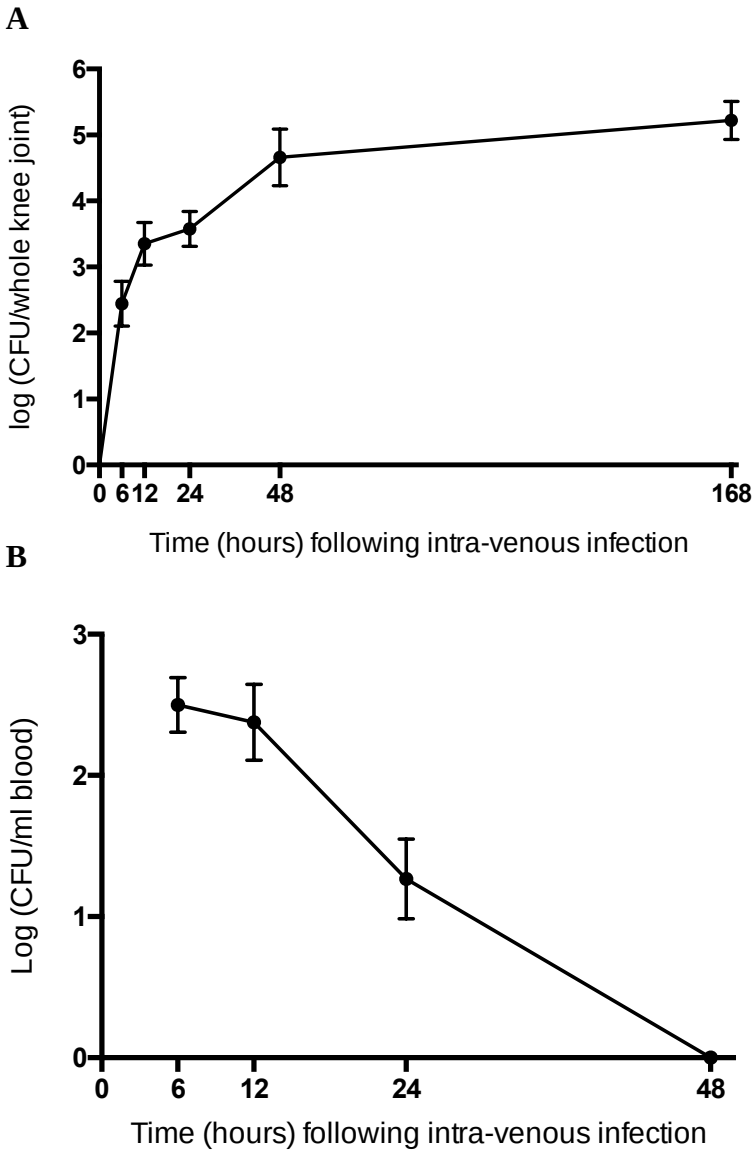

Figure 31 – Comparison of bacterial numbers in the knee joints and blood after intravenous infection with *emm* type 1.0 isolate 101910.

(A) The bacterial CFU in knee joints of CD1 mice (n = 10, knee joints n = 20) following intravenous infection with 10^7 CFU (50 μl) of *emm* type 1.0 isolate 101910 and (B) bacterial burden in blood over time. Displayed as mean ± SEM.

4.5.2 Severity of arthritis

The onset of macroscopic arthritis began at around 24 hours. The typical symptoms observed were redness, swelling, and oedematous of the knee joints. To be able to assess the progression of the external symptoms an arthritic scoring system was developed. This involved macroscopic inspection of the knee joints, in which each joint yielded a score of 0 to 3 points; 1 point = mild swelling and/or erythema; 2 points = moderate swelling and erythema; 3 points = marked swelling and erythema and occasionally ankylosis. The arthritic index was then constructed by dividing the total score by the number of animals used in each group. All animals were scored at the same time points that the knee joints and blood were sampled. There were no detectable symptoms of arthritis in any of the mice until 24 hours, in which the incidence was low and could only be measured in 25% of joints (5/20 knee joints) (Figure 32). The arthritic index gradually increased at 48 hours, the incidence of macroscopic arthritis was now 65% (13/20 joints). At 7 days the mice had severe symptoms and 90% (19/20) of knee joints were scored macroscopically, this greatly increased the arthritic index (Figure 32). In addition to scoring the knee joints, it was also noted whether animals showed any sign of macroscopic arthritis in any other joints. In 10% of cases swelling was observed in the front and hind paws, no additional limbs became affected after the initial 48 hours of disease. To ensure the welfare of the animals they were also scored using the pain scoring system and had their weight measured every 24 hours. Weight bearing was poorly tolerated in some mice and due to the set-up of the cage feeding system, wet food was supplied to counteract mild weight loss.

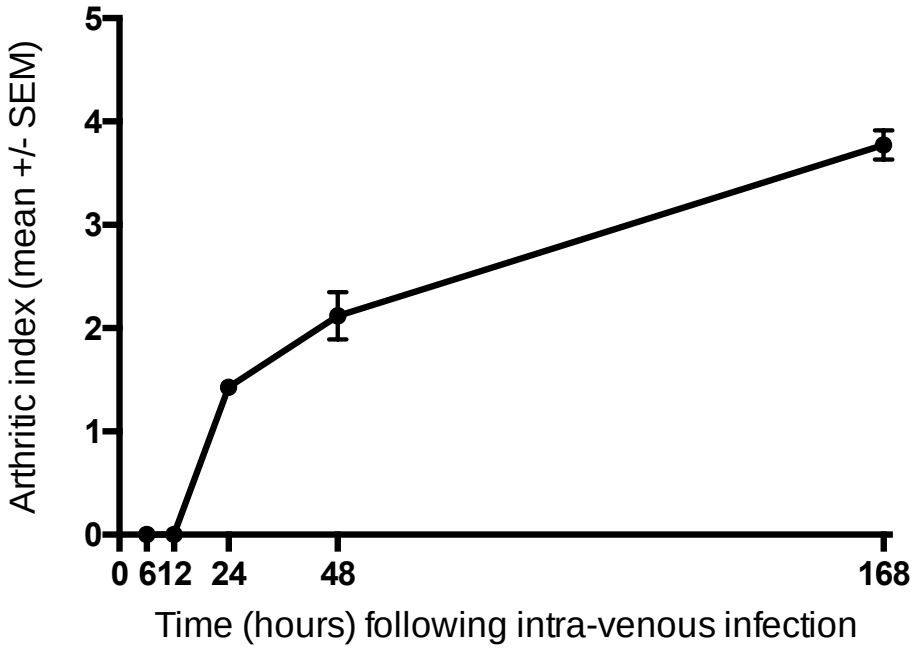

Figure 32 - Arthritic index score of knee joints during infection with *emm* type 1.0 isolate 101910.

The arthritic index (mean ± SEM) was calculated for CD1 mice (n = 10) following intravenous infection with 10^7 CFU in 50 µl with *emm* type 1.0 (isolate 101910) over time. Displayed as mean ± SEM.

4.6 Host-adapted *emm* type 1.0 (isolate 101910)

To further clarify the causes of *emm* type 1.0 isolate 101910 propensities to the joint, bacteria was recovered directly from the knee joints at 24 hours post-infection with 10^7 CFU. To compare the progression of infection in the joints with *in vivo* recovered host-adapted *emm* type 1.0 isolate 101910 compared to the previous infection with the wild type. 40 mice were intravenously infected with 10^7 CFU of host-adapted isolate 101910. Ten mice were culled at each of the following time points post infection 6, 12, 24, and 48 hours. Blood, spleen and joints were recovered for CFU enumeration. The CFUs from those infected with the host-adapted isolate were compared with the previous infection with the wildtype, to see whether there were any significant differences with the progression of the infection. During the course of the infection there was 100% survival of animals infected with the host-adapted bacteria, this was the same as with the wildtype.

4.6.1 Comparison of bacterial load in the blood and spleen

Bacterial load in the blood decreased over time during infection with the host-adapted isolate, and there was no major variation in bacterial numbers compared to the wildtype infection. Although not statistically significant the mean CFU was lower at 24 hours in the host-adapted group indicating a slightly faster rate of clearance (Figure 33a). Both infection groups had cleared from the blood by 48 hours. Similarly, the bacterial load in the spleen decreased over time during infection with *in vivo* recovered bacteria, and although there was no significant difference in splenic bacterial load at 6, 24, and 48 hours, the average mean CFU in those infected with *in vivo* recovered bacteria was lower (Figure 33b).

A slight increase in the rate of clearance of the bacteria from the vasculature system was observed during infection with the host-adapted isolate, suggesting that the bacteria is even less well adapted to surviving in the blood than *emm* type 1.0 isolate 101910. Having isolated the bacteria directly from the knee joint this could suggest the bacteria may have characteristics that have adapted to favour the joint space over the blood.

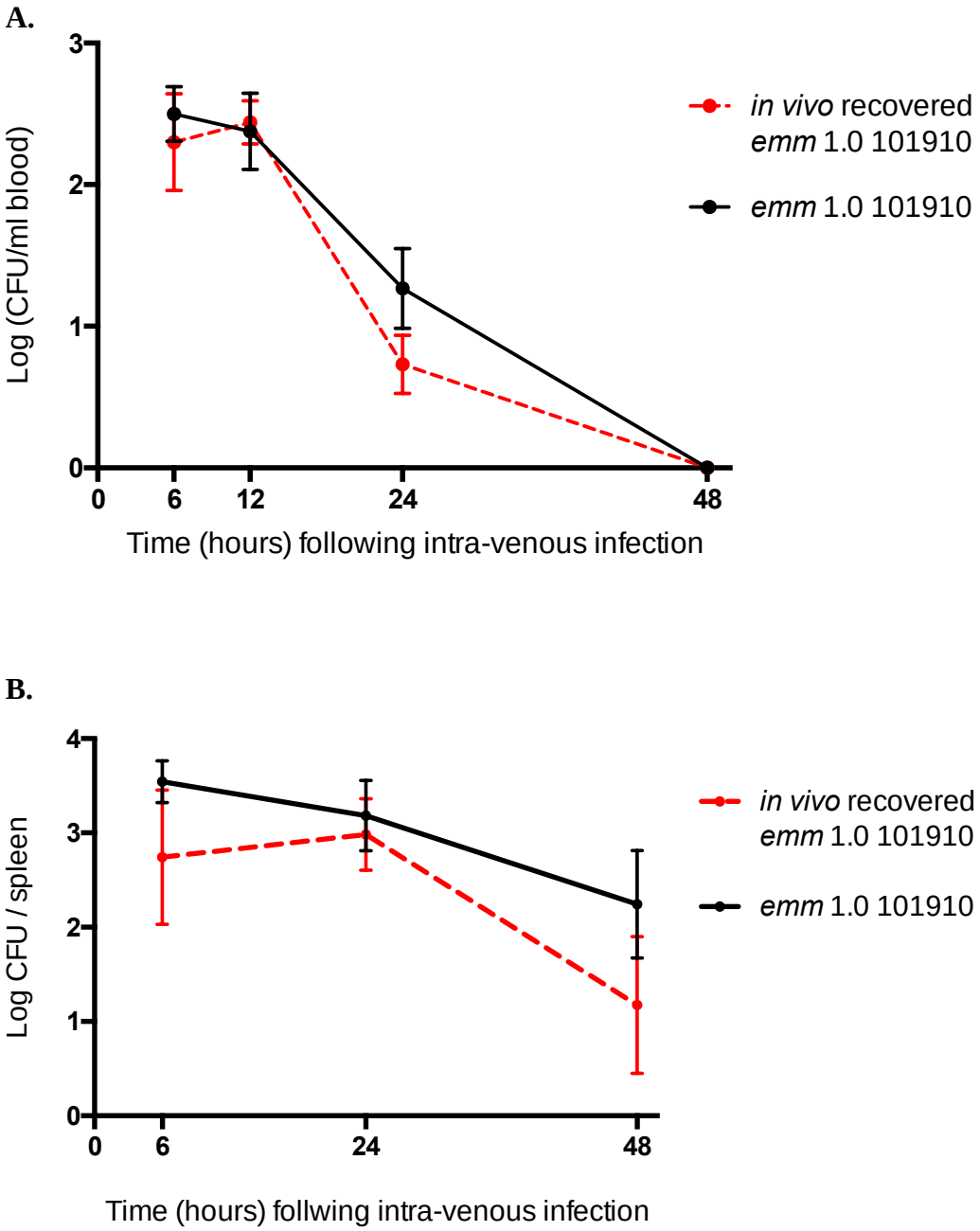

Figure 33 – Comparison of bacterial burden in blood and spleen after intravenous infection with *emm* type 1.0 isolate 101910 and *in vivo* recovered *emm* type 1.0 isolate 101910.

A) The bacterial CFU in blood of CD1 mice (n = 5) following 10^7 CFU in 50 µl intravenous infection with *emm* type 1.0 isolate 101910 (black solid line) and *in vivo* recovered *emm* type 1.0 isolate 101910 (red dashed line). B) Bacterial burden in spleen over time. Displayed as mean ± SEM.

4.6.2 Comparison of joint bacterial burden and severity

The progression of infection in the knee joints during infection with *in vivo* recovered host-adapted *emm* type 1.0 isolate 101910 was analysed, firstly by determining the joint bacterial load and secondly by calculating the arthritic index. These were both compared to results previously obtained during infection with the wild type isolate.

Bacteria was recovered from the knee joints at the earliest time point of 6 hours. When compared with the wildtype infection the host-adapted bacteria enter the knee joint at initial higher bacterial loads (Figure 34a). Bacterial numbers in the knee joints continued to increase in the host-adapted group, when compared with the wildtype. This was found to be statistically significant at 12 and 24 hours (*** $p < 0.005$). At 48 h there was a further increase in bacterial load in the host-adapted infection group, however there was no significant difference in bacterial load compared to the wildtype at this time point (Figure 34a).

To assess the severity of macroscopic arthritis, the arthritic scoring index was used and the score for mice infected with *in vivo* recovered *emm* type 1.0 isolate 101910 was compared to that previously calculated for infection with *emm* type 1.0 isolate 101910. Arthritic symptoms could be detected at 24 hours, and the severity of arthritis was the same for both groups (Figure 34b). The arthritic index increased during the infection and at 48 h mice in the host-adapted group had a significantly higher arthritic index compared to the wildtype group (* $p < 0.05$) (Figure 34b). Mice infected with the host-adapted isolate 101910 had a more serious macroscopic arthritis when assessed visually at 48 hours and the experiment was terminated, so as

not to exceed the severity threshold as outlined by the home office project licence. The arthritic score at 48 hours was similar to that at day 7 post infection with the wildtype (Figure 32),

In summary, during infection with *in vivo* recovered *emm* type 1.0 isolate 101910, bacteria enter the knee joint at higher bacterial numbers and proliferate in the joint at a faster rate compared to the wildtype. More serious macroscopic symptoms were observed at 48 hours, even though the bacterial load is not significantly higher at this time point than infection with the wildtype. These results suggest that the bacteria were better adapted to initiating infection in the joint more quickly leading to a more serious arthritic phenotype.

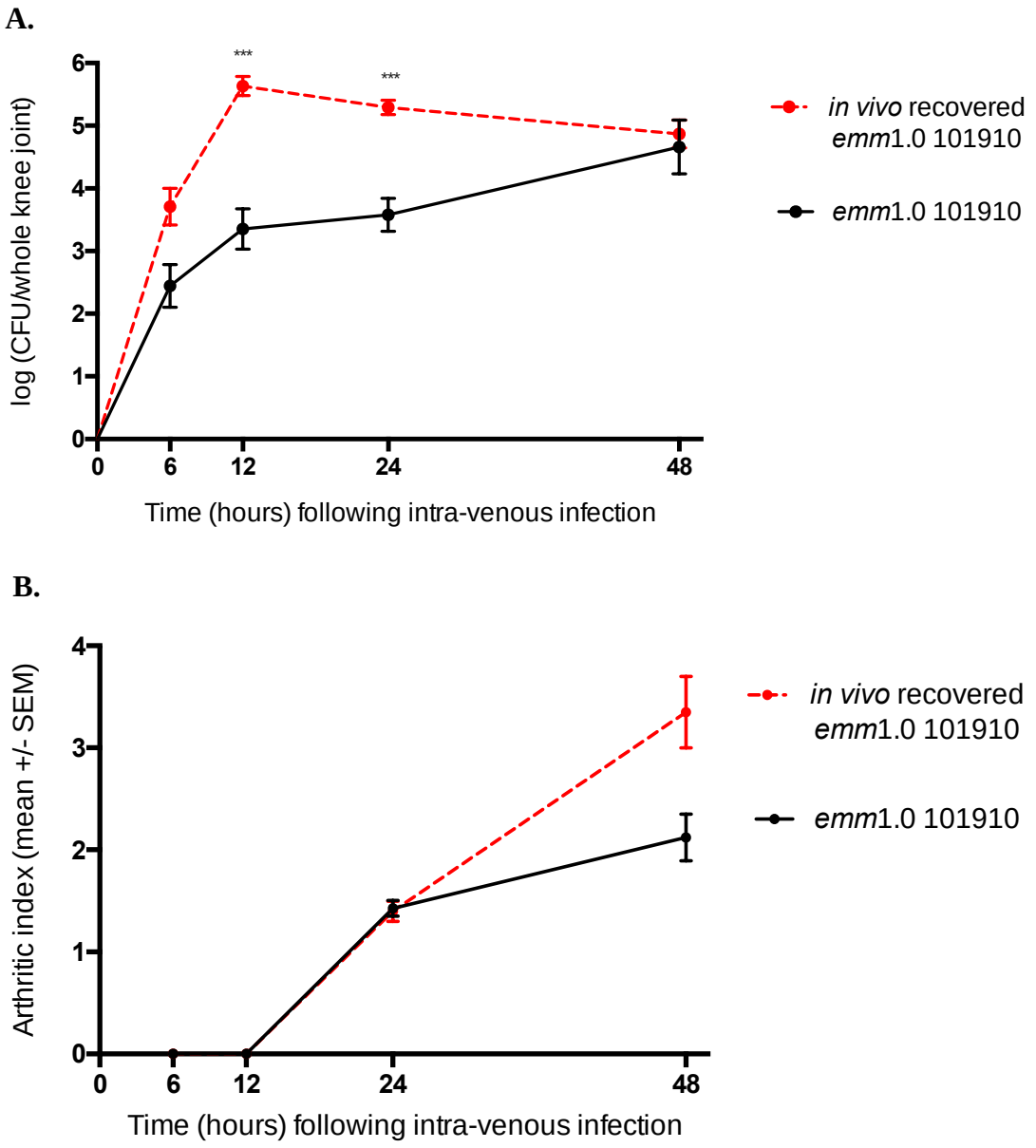

Figure 34 - Comparison of knee joint CFU and arthritic index after intravenous infection with *emm* type 1.0 isolate 101910 and *in vivo* recovered *emm* type 1.0 isolate 101910.

A) The bacterial CFU in knee joints of CD1 mice (n = 10, knee joints n = 20) and B) arthritic index score following 10^7 CFU in 50 μl intravenous infection with *emm* type 1.0 isolate 101910 (black solid line) and *in vivo* recovered *emm* type 1.0 isolate 101910 (red dashed line). ***p-value < 0.005 when analysed using a one-way Anova and Kruskal-Wallis multiple comparisons test, displayed as mean ± SEM.

C. Discussion

As outlined at the beginning of this chapter, different GAS isolates can result in diverse infection outcomes in both humans and mice. These range from subclinical non-invasive infections through to invasive disease and septic arthritis. The aim of this chapter was to investigate the virulence of *emm* type 32.2 and *emm* type 1.0 isolates using a range of doses and infection routes in order to understand how infection with different isolates can lead to very different clinical phenotypes. The data presented here shows the establishment of a suitable murine model of invasive GAS infection using *emm* type 32.2 isolate 112327, and for the first time, a model of GAS septic arthritis is described with *emm* type 1.0 isolate 101910. The infection kinetics following intranasal (10 µl dose to promote nasopharyngeal carriage and 50 µl dose to cause pneumonia) and intravenous inoculation are described for each isolate, and this data provides additional relevant information to the field.

The most common clinical manifestation of GAS is pharyngitis, which is an infection of the tonsils and surrounding tissues. This area is known as the posterior oropharynx, which includes the Waldeyer's ring collectively known as the tonsils [295]. Due to the high incidence of pharyngitis there has been considerable interest in developing animal models to attempt to replicate the disease [9]. However, mice and other rodents do not have a Waldeyer's ring homologue in the pharynx, and experimental colonization has been both challenging and limited primarily to only a few GAS isolates [213]. To test whether the isolates in this study were capable of successfully establishing colonisation in the nasopharynx of mice, mice were intranasally inoculated with 10 µl of 10^8 or 10^7 CFU of each of the isolates. There was 100% survival and no bacteria had disseminated into the lungs resulting in

pneumonia, indicating that the inoculum volume chosen was suitable for nasopharyngeal colonisation only. GAS colonies were not successfully recovered from the nasopharynx or lungs at the end of the experiment. The isolates used were not able to colonise the nasopharynx over 7 days using this model. Other studies examining GAS nasopharyngeal colonisation proposed that a strong Th17 response was responsible for the rapid clearance of GAS and increasing the length of time of colonisation was not always possible, this is in line with our findings [216].

Next, a higher volume intranasal dose of 50 µl was used to examine the effects of the bacteria disseminating into the lung. Bacterial dissemination from the lungs into the bloodstream occurred as early as 6 hours post infection after inoculation with a high CFU dose (10^8) of *emm* type 32.2 isolates 112327 and 102029. However, this was not the case when mice were infected with 10^7 CFU of those isolates- no bacteria were recovered at the end of the experiment and the mice did not show any signs of illness. There were significant differences in the survival of mice infected with *emm* type 32.2 isolates than with an *emm* type 1.0 isolate, indicating *emm* type 32.2 isolates were more virulent in a pneumonia model of infection. Previously published work, examining GAS pneumonia in a mouse model has shown that systemic infection is initiated by flooding of the alveoli with bacteria followed by breaching of endothelial barriers into the blood [130, 219]. These models showed that pneumonia was initiated dose dependently- as was the case in our experiments- with a higher CFU needed to establish a pneumonic infection [219]. One comparison to draw on is the time difference in mortality, mice in the study by Husmann *et al.*, did not establish pneumonia until 72 hours, yet there is a much more rapid time to death (6 hours) [219]. The rapid dissemination of bacteria into the vasculature system is likely

to be driven by bacteria induced damage of the lung epithelial barriers, as GAS bacteria are intrinsically capable of breaching host tissue barriers and encode a number of streptococcal proteins that are involved in the breakdown of host tissues [156]. It is widely accepted that there is significant variation in the ability of different strains to produce such proteins; the *emm* 32.2 isolates may overproduce toxins and proteins that enable quicker invasion across the epithelial barrier [3].

Invasive GAS infection results from spread of bacteria from the foci of infection to normally sterile sites, streptococcal shock-like syndrome can then occur which is one of the most severe outcomes, with an associated mortality exceeding 50% [9, 218]. In this study, a suitable model for studying the kinetics of invasive GAS disease was established and used to evaluate different GAS isolates virulence. It was shown that different strains of GAS have a varied ability to cause invasive disease. *Emm* type 32.2 isolate 112327 was the most invasive isolate and resulted in 100% mortality, during infection bacterial growth could not be controlled resulting in progressive bacterial multiplication and death. In contrast, during infection with *emm* type 32.2 isolate 102029 and *emm* type 1.0 isolate 101910, mice were able to successfully clear and survive the infection. In 30% of cases when using a higher CFU dose of 10^8 during infection with *emm* type 32.2 isolate 102029, the bacteria could not be cleared, and the mice died from the infection. Previously published work demonstrated that different strains of mice are more or less susceptible to invasive infection based on the ability of those mice to limit uncontrolled bacterial proliferation and clear the infection [218]. In addition, by ranking isolates by survival times this correlates with the control of bacterial replication, which suggests that the ability to limit bacterial growth may be a crucial factor in determining mortality.

Mice from infection with *emm* type 1.0 isolate 101910 began to clear bacteria from the blood as early as 9 hours, indicating that immunity against GAS in this model is mainly dependent on innate immune mechanisms [296]. The major cellular components involved in innate immunity, neutrophils and macrophages are potentially the most important mechanism in effectively clearing the bacteria. It was concluded in Chapter 2 that *emm* type 32.2 isolate 112327 was more resistant to opsonophagocytosis, and this is in line with how the bacteria is able to successfully evade host defences and cause significant mortality in an invasive disease model.

This study has shown that after intravenous inoculation with *emm* type 1.0 isolate 101910 mice developed septic arthritis. There have been relatively few studies on bacteraemia induced septic arthritis and all except one study with GAS bacteria are confined to infection with *Staphylococcal aureus* [231-238]. Mouse studies have generally been accepted as good models for septic arthritis and osteomyelitis; and it has been shown that the progression of infection and in particular the erosive profile of the joints is very similar to humans [54]. Considering that 30% of cases in the UK of septic arthritis are as a result of GAS, there has been little work done to study the kinetics of the disease in a reliable mouse model. The model of GAS septic arthritis described here provides additional and relevant information into the field. The study focused on dissemination of GAS to the knee joints, which are the most frequently infected joints in humans [61]. Intravenous infection of *emm* type 1.0 isolate 101910 induced septic arthritis in 90% of animals. There was 0% mortality during the experiment, suggesting that the dosage was appropriate to induce septic arthritis. Bacteria were cleared from the blood and were detected in the knee joints as early as 6 hours. The levels of bacteria peaked at 48 hours and the model was extended to 7

days. At 7 days a more chronic form of septic arthritis was observed and the effects of having bacteria in the joint over a prolonged period can be seen. Between 48 hours and 7 days the bacterial numbers do not continue to proliferate exponentially, suggesting that the localised immune response in the joint has been able to limit the progression of the infection. The associated immune response in the joint has previously been shown in S. *aureus* animal models to prevent mortality and septic shock [61].

An important point to discuss is by what mechanisms the GAS organisms sequester in the joints following bacteraemia. It is known that the synovial tissue and the subchondral bone have a rich blood supply, thereby allowing frequent passage of bacteria through the joints [231]. However, why bacteria such as GAS and *S. aureus* choose to colonise the joint space is less clear. GAS has been shown to interact with several extracellular matrix proteins, including binding to fibronectin or collagen, which may contribute to the bacteria becoming immobilised when entering the joint and ultimately expanding [297]. As previously discussed GAS is a human adapted pathogen with a very broad range of clinical disease and it is able to adapt to different sites of infection in the host [298]. *Emm* type 1.0 isolate 101910 was recovered from a patient who had septic arthritis of the hip joint in comparison to the other strains in this study (*emm* 32.2 isolates), which were both isolated from patients with an invasive bacteraemia. This suggests that *emm* type 1.0 isolate 101910 has bacterial characteristics that make it more adapted to colonising the joint space.

To consider further the role of bacterial characteristics in the propensity of the bacteria to sequester in the joints bacteria were recovered from the joint and then

mice were intravenously infected with *in vivo* recovered host-adapted *emm* type 1.0 isolate 101910. Bacteria originally isolated from the knee joint were able to induce bacterial arthritis in 100% of mice infected and that the starting CFU in the joints at 6 hours was significantly higher. Bacteria was also cleared from the blood and spleen more rapidly than with the previous infection with *emm* type 1.0 isolate 101910, which suggests it is even less well adapted to surviving in blood. In addition, the model could not be extended up to 7 days as the infection had resulted in serious deformities of the knee joints and the animals had reached the humane end point by 48 hours. A more serious acute septic arthritis model was developed by passaging the bacteria through the host, this has two implications; firstly, the bacterium may now be more adapted to the site of infection and secondly the host response in the joint may not able to limit uncontrolled bacterial proliferation.

Further work needs to be done to examine specific bacterial characteristics that may be involved in the ability of different GAS isolates to preferentially induce septic arthritis or sepsis. Understanding the molecular pathogenic mechanisms of each disease will provide a clearer picture of why there is such variation in host outcomes. In addition to this, the role of the host response in the joint should be examined to elucidate what mechanisms are involved in the initial stages of the infection in the joint and how this leads to severe joint damage. This will provide a significant amount of insight that is not currently available in the field.

5. Streptolysin production and activity is central to *in vivo* pathotype and disease outcome

A. Introduction

5.1 Introduction to GAS virulence factors

Many *emm* types of GAS cause both life threatening and self-limiting infections, implying that any given strain of GAS encodes the factors needed for establishment of more than one kind of disease, and that differential expression of these factors determines the course of infection. Defining virulence factors that are involved in determining the course of infection is crucial for understanding invasive pathogenesis.

5.2 Secreted bacterial toxins: Streptolysin

There are a number of streptococcal proteins that are involved in the destruction of host tissues and among these are two cytolysins; streptolysin S (SLS) and streptolysin O (SLO) [299]. The haemolysin SLO has been well established as having cell and tissue destructive activity, and is part of the family of oxygen-sensitive, thiol-activated toxins that includes already established virulence factors such as perfringolysin (theta toxin), pneumolysin, and listeriolysin O [141-143]. SLO is a highly conserved protein and is secreted by nearly all clinical isolates of GAS, it works by interacting with cholesterol in target cells to form pores, this is active against a number of eukaryotic cell types and sufficient doses of SLO results in cell lysis [145-148]. Early studies with SLO demonstrated that the purified toxin was lethal to mice and rabbits when injected intravenously, mainly due to cardiotoxicity [155].

More recently, there have been some attempts to assess the effects of biologically relevant concentrations of SLO in *in vivo* models. Limbago *et al.,* found that SLO-deficient GAS resulted in attenuated skin infections and similarly Zhu *et al.,* reported a reduction in virulence when using SLO-deficient GAS in an invasive model [156, 157].

5.3 Rationale

There are substantial gaps in our understanding of the contribution of the variation in SLO production to overall GAS pathogenesis. In order to address this, a custom-made ELISA was developed to compare the production of SLO between invasive *emm* type 32.2 outbreak GAS isolates and invasive *emm* type 1.0. isolates. Using an *in vivo* GAS bacteraemia model and a novel septic arthritis model, the role of SLO in establishing and maintaining different clinical pathotypes was explored. In addition, an SLO deficient mutant strain in the background of the invasive outbreak *emm* type 32.2 isolate was made and used the in *in vivo* models of infection.

B. Results

5.4 Streptolysin- Enzyme-Linked Immunosorbent Assay

A custom-made SLO enzyme-linked immunosorbent assay (SLO-ELISA) was developed using the following antibody pairs; monoclonal SLO antibody (Abcam) and polyclonal SLO antibody (Abcam). All buffers used were from the Peprotech ELISA buffers kit. A standard curve was produced to assess the sensitivity of the assay at a range of known concentrations of recombinant SLO which were from 0-200ng/ml (Figure 35).

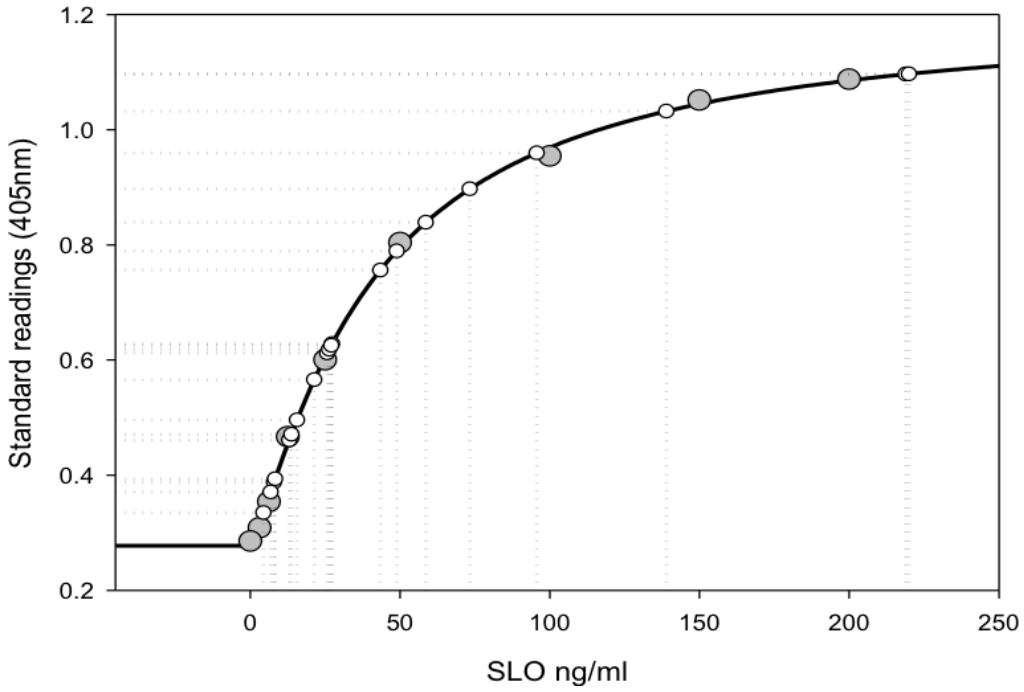

Figure 35 – Streptolysin ELISA standard curve.

Standard curve produced using known concentrations of recombinant SLO (ng/ml) (grey circles) measured at $OD405_{nm}$ and white circles shown the unknown values.

5.5 Comparison of streptolysin production and activity

To assess the production and activity of secreted SLO. Bacteria were grown in Todd Hewitt broth (supplemented with yeast and glucose) (THYG). At 2-hour time points (0, 2, 4, 6, 8, 10, 12 h) the CFUs were enumerated and SLO concentration (ng/ml) and activity was measured using the SLO-ELISA and the haemolytic assay.

5.5.1 *Emm* type 32.2 isolate 112327 and *emm* type 1.0 isolate 101910

In Chapter 4 it was determined that *emm* type 32.2 isolate 112327 and *emm* type 1.0 isolate 101910 had different clinical phenotypes. In an invasive bacteraemia model, there were very clear differences in survival of the mice, 100% of mice infected with *emm* type 32.2 (isolate 112327) succumbed to infection in contrast to 0% of those mice infected with *emm* type 1.0 (isolate 101910). Further to this, the bacterial load increased in the blood rapidly during infection with *emm* type 32.2 (isolate 112327) but cleared quickly with *emm* type 1.0 (isolate 101910). It was also observed that during infection with *emm* type 1.0 (isolate 101910), mice further developed septic arthritis alongside completely clearing the bacteria from the blood. This resulted in the hypothesis that differences in virulence could be attributed to the production of SLO, and that the *emm* type 32.2 (isolate 112327) was more likely to secrete higher amounts and more haemolytic SLO.

The concentration (ng/ml) of SLO in the supernatant was quantified using the SLO-ELISA. The concentration (ng/ml) of SLO produced by *emm* type 32.2 (isolate 112327) increased rapidly over time compared with *emm* type 1.0 (isolate 101910); whereby *emm* type 32.2 (isolate 112327) produced significantly more SLO from 6 hours onwards until the final time point at 12 hours ($p = 0.015$ - <0.0001) (Figure

36a). *Emm* type 1.0 (isolate 101910) produced a small amount of SLO initially but the concentration did not continue to increase beyond 8 hours (Figure 36a).

Next, the haemolytic activity of SLO in the supernatant was quantified using the haemolytic activity assay. The haemolytic activity of SLO secreted by isolates *emm* type 32.2 (isolate 112327) and *emm* type 1.0 (isolate 101910) followed the same pattern as that of the amount secreted; *emm* type 32.2 (isolate 112327) SLO was significantly more haemolytic from 6 hours until the final time point at 12 hours compared to *emm* type 1.0 (isolate 101910) SLO ($p = 0.028$ - <0.0001) (Figure 36b). Hence, *emm* type 32.2 (isolate 112327) secreted not only significantly more SLO than *emm* type 1.0 (isolate 101910), but also significantly more haemolytic toxin at equivalent CFU.

The growth dynamics by CFU growth over 12 hours and also optical density (OD) over 24 hours of both isolates were assessed to ensure the differences observed for SLO were not due to significant differences in bacterial growth. There was no difference in the pattern of growth between both isolates, although the OD is higher for *emm* type 32.2 (isolate 112327) this is due to it being mucoid and not due to the presence of more bacteria (Figure 37a and b). There was no significant difference in bacterial CFU growth for both isolates across all time points, with almost identical CFU loads at 10 and 12 h, which interestingly were the same time points with the greatest difference in SLO concentration and activity, suggesting that bacterial growth rate and CFU load were not responsible for observed SLO differences between isolates.

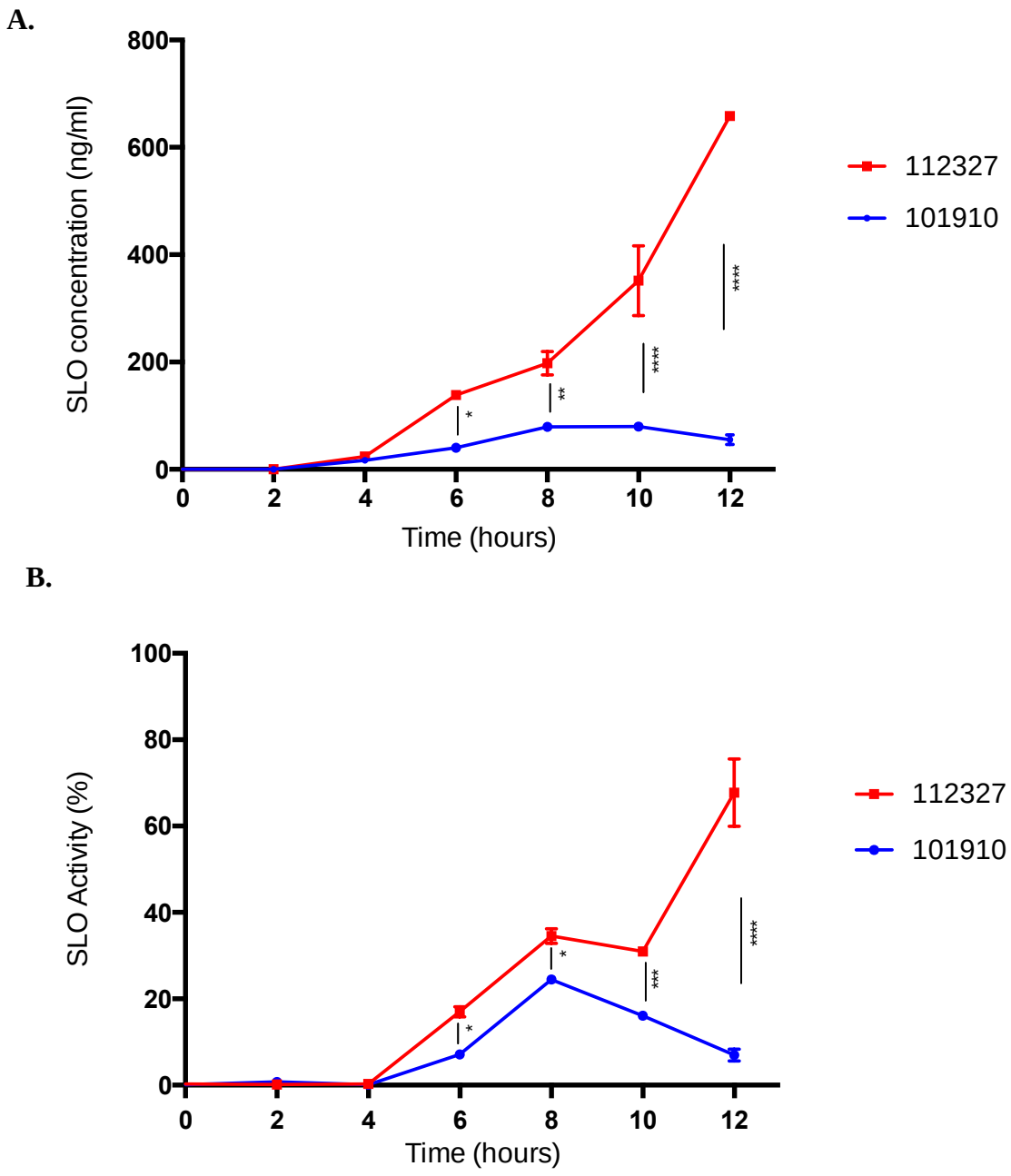

Figure 36- Comparison of streptolysin production and activity *emm* type 32.2 isolate 112327 and *emm* type 1.0 isolate 101910.

A) Concentration of streptolysin (ng/ml) secreted into the supernatant by isolates *emm* type 32.2 (isolate 112327) (red line) and *emm* type 1.0 (isolate 101910) (blue line) over time, measured by a custom made SLO-ELISA. B) SLO haemolytic activity. *p < 0.05, **p < 0.01, ***p < 0.005, and ****p < 0.001 when analysed using a two-way ANOVA and Bonferroni's multiple comparisons test.

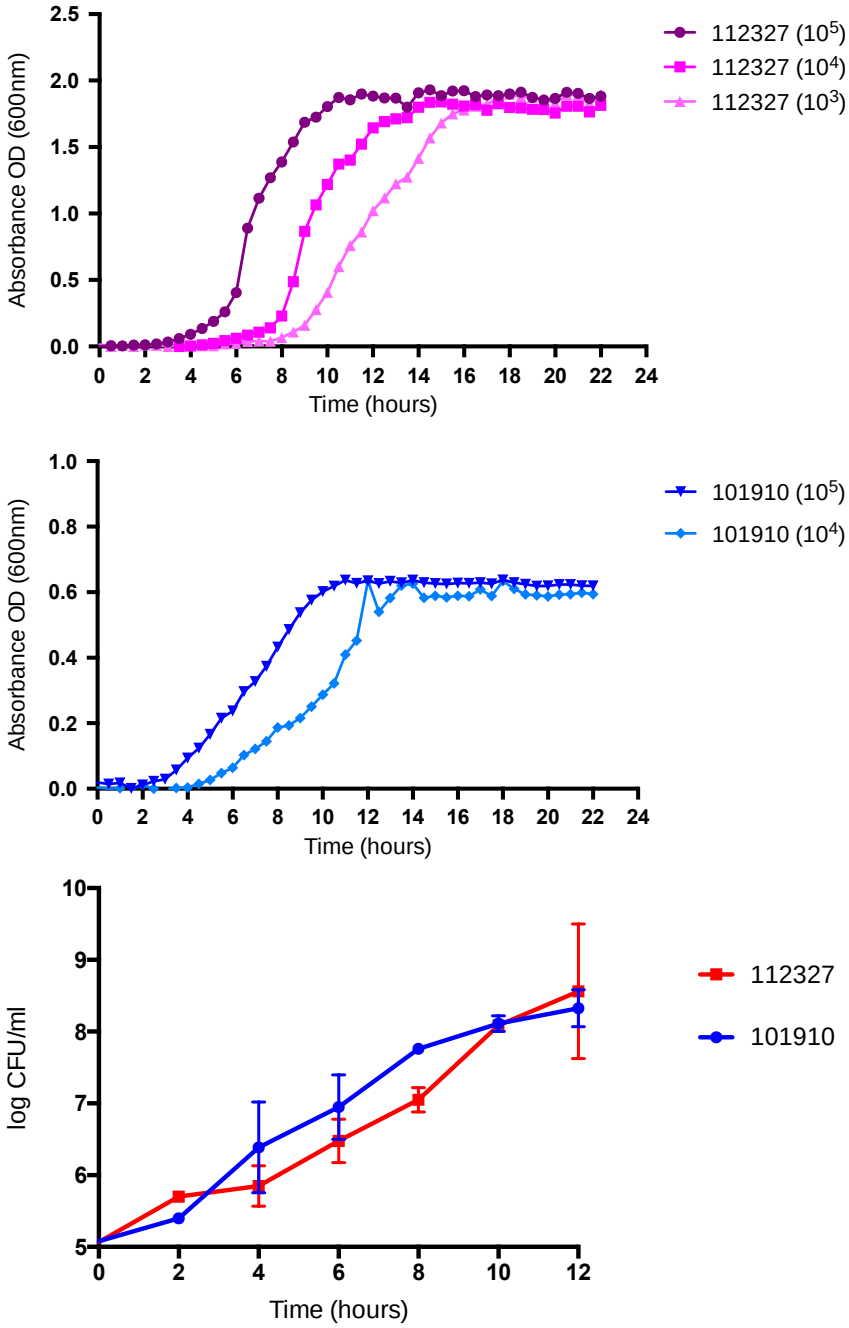

Figure 37 - Growth kinetics of *emm* type 32.2 isolate 112327 and *emm* type 1.0 isolate 101910.

Optical density (600 nm) growth curves of A) *emm* type 32.2 (isolate 112327) (red line) and B) *emm* type 1.0 (isolate 101910) (blue line) shown as OD_{600} of bacterial cultures determined every 15 minutes during a 24-hour incubation in THYG at a starting CFU count of 10^3, 10^4, or 10^5. C) The CFU count was measured every two hours for 12 hours, at a starting CFU of 10^5. This experiment was done in duplicate over two independent days.

5.5.2 Comparison of SLO with selection of other isolates

The SLO profiles of *emm* type 32.2 (isolate 112327) and *emm* type 1.0 (isolate 101910) were compared at the stationary phase with other isolates of GAS that were collected during the outbreak. We used two other *emm* type 32.2 isolates; 112844 and 102029, and a non-invasive *emm* 6.0, isolate 127785 for comparison. *Emm* type 32.2 isolate 102029 was shown in chapter 4 to be significantly less virulent than *emm* type 32.2 isolate 112327. When comparing the production of SLO between *emm* 32.2 isolates there were no significant differences at 8 and 10 hours. At 12 hours isolate 102029 produced significantly less SLO than 112327 and 112844 ($p < 0.001$) (Figure 38a). *Emm* type 32.2 isolate 102029 produced almost identical amounts of SLO as the *emm* type 6.0 isolate across all time points. *Emm* type 1.0 isolate 101910 still had the lowest production of SLO at 10 hours, although the concentration of SLO was similar at 8 and 12 hours to that of *emm* type 32.2 isolate 102029 and *emm* type 6.0 isolate 127785 (Figure 38a).

There were no significant differences between the haemolytic activity of *emm* type 32.2 isolate 102029, *emm* type 6.0 isolate 127785 and *emm* type 1.0 isolate 101910 (Figure 38b). *Emm* type 32.2 isolate 112844 was more haemolytic than *emm* type 32.2 isolate 112327 at 10 hours, although this was not significant and by 12 hours the haemolytic activity of isolate 112844 had reduced significantly (Figure 38b). There are clear similarities in the SLO profile of *emm* type 32.2 isolates 112327 and 112844, and although isolate 112844 has not been analysed in the invasive bacteraemia model they share significant similarities in the *in vitro* assays described in Chapter 2, indicating both these isolates could behave the same way *in vivo.*

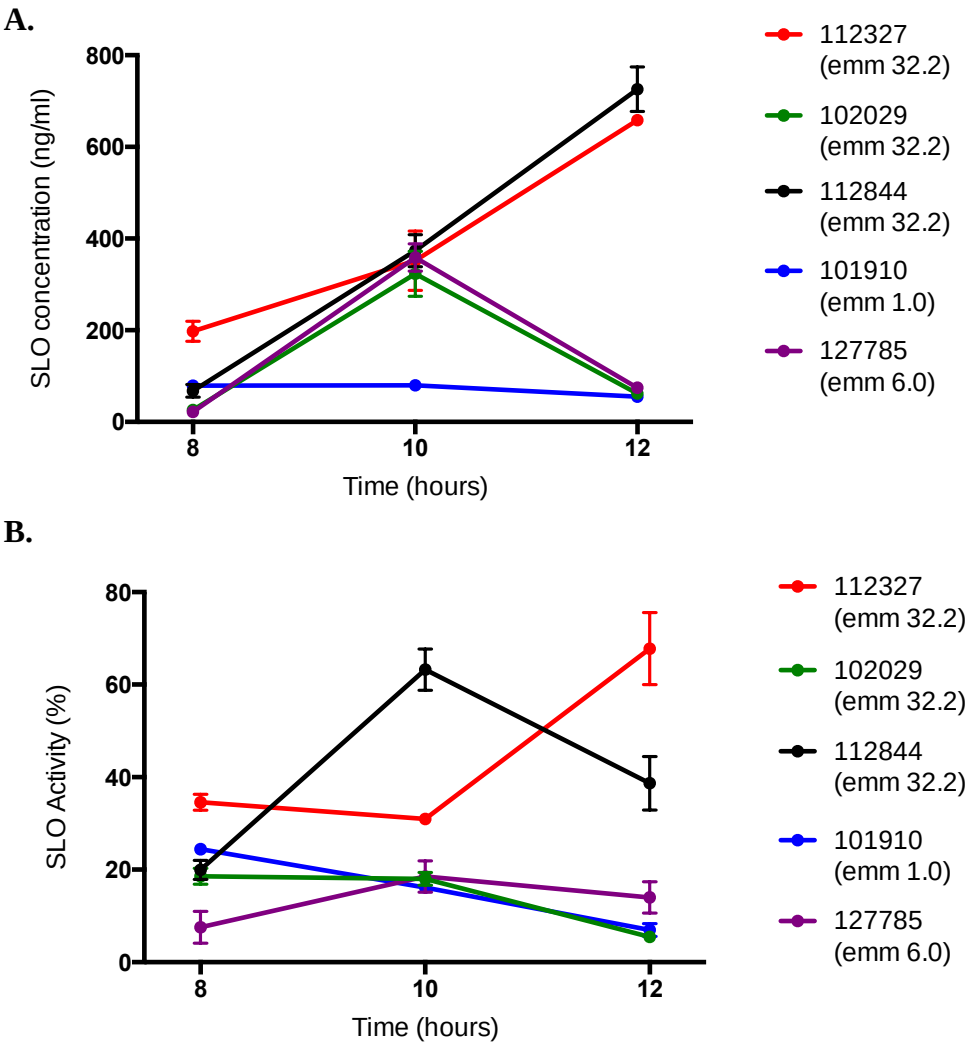

Figure 38- Comparison of streptolysin production and activity in other *emm* type 32.2 isolates and *emm* type 6.0 isolates.

A) Concentration of streptolysin (ng/ml) secreted into the supernatant at 8, 10, and 12 hours by *emm* type 32.2 isolates 112327 (red), 102029 (green) and 112844 (black), *emm* type 1.0 isolate 101910 (blue) and *emm* type 6.0 isolate 127785 (purple) (B) SLO haemolytic activity. Displayed as mean ±SEM.

5.6 *In vivo* recovered *emm* type 1.0 isolate 101910 has reduced production and activity of SLO

To further clarify the reasons for *emm* type 1.0 (isolate 101910) clearance from the bloodstream and translocation to the knee joints, bacteria were recovered from mouse knee joints at 24 h post infection, and the amount of SLO secreted into the supernatant was quantified over an *in vitro* growth phase. Host-adapted *in vivo* recovered isolate 101910 secreted significantly less SLO into the supernatant over the 12 h *in vitro* growth phase. There was significantly less SLO secreted from 6 h onward to that originally produced by isolate 101910 grown *in vitro* at equivalent CFU ($p = 0.009 – <0.0001$) (Figure 39a). In addition to producing significantly less SLO, the haemolytic activity of *in vivo* recovered bacterial SLO was also significantly lower from 6 h to 10 h, again at equivalent CFU ($p = 0.0007 – <0.0001$), with SLO activity comparable at 12 h (Figure 39b).

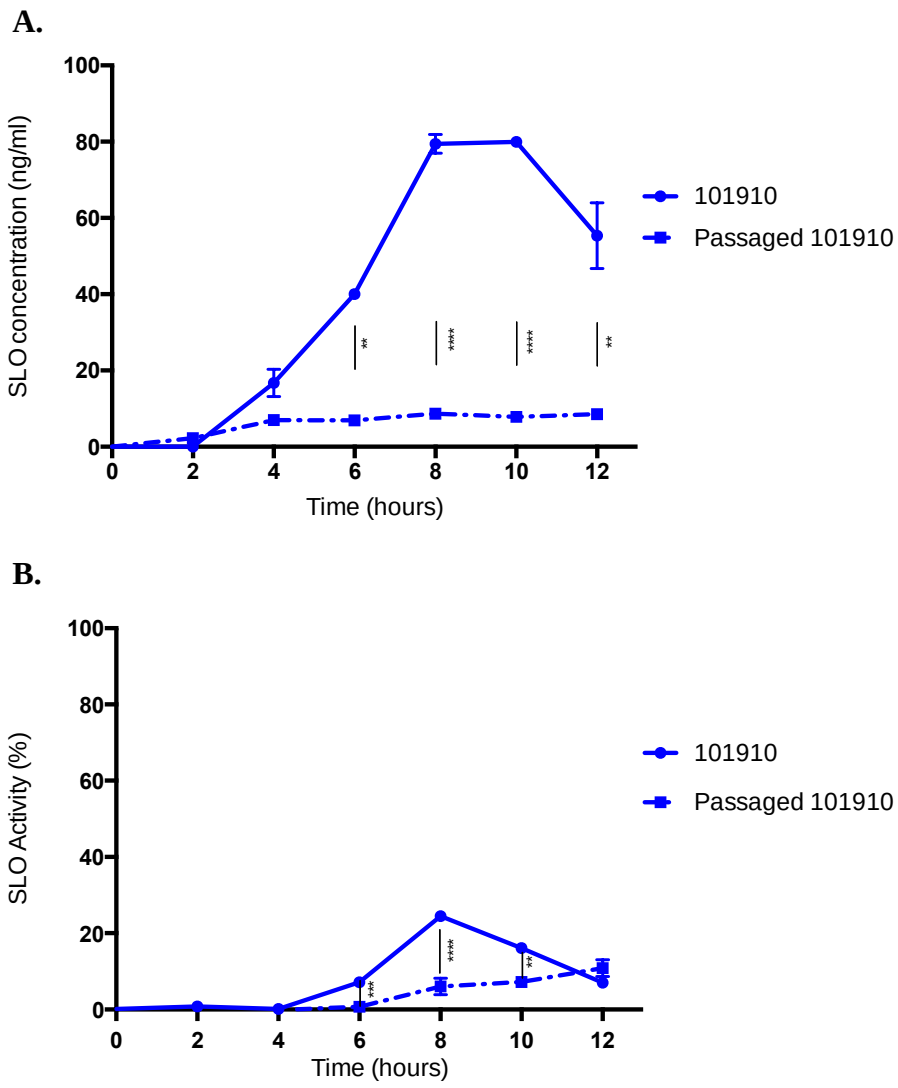

Figure 39- Comparison of streptolysin production and activity in *emm* type 1.0 isolate 101910 grown *in vitro* or recovered from *in vivo*.

A) Concentration of streptolysin (ng/ml) secreted into the supernatant by *emm* type 1.0 isolate 101910 grown *in vitro* or recovered from knee joints (P101910) and then grown *in vitro*. (B) SLO haemolytic activity. **p < 0.01, ***p < 0.005 and ****p < 0.001 two-way ANOVA and Bonferroni's multiple comparisons correction.

5.6.1 *In vitro* passaging host-adapted *emm* type 1.0

We next wanted to determine whether *in vivo* recovered *emm* type 1.0 (isolate 101910) retained its low SLO production and low SLO activity phenotype when grown over multiple times *in vitro*. *In vivo* recovered *emm* type 1.0 (isolate 101910) was subsequently passaged in THYG broth once, four, and then 10 times. Interestingly, after just one growth phase in THYG culture, the concentration of SLO had reverted to a high SLO production phenotype ($p < 0.0001$) (Figure 40a), with significantly increased haemolytic activity from 6 hours to 10 hours ($p = < 0.005$) (Figure 40b), suggesting that factors *in vivo* drive *emm* type 1.0 isolate 101910 to suppress its SLO production.

The CFUs over the growth phase were assessed to see if there were any differences in the ability to grow in culture first after *in vivo* passaging and then subsequent *in vitro* passaging. *In vivo* recovered *emm* type 1.0 isolate 101910 had lower CFU counts from 6 - 12 h, although this was not significant (Figure 41). This could be due to the bacteria being more adapted to the joint and subsequently not growing as effectively in broth. The *in vitro* passaged *in vivo* recovered bacteria CFU counts were almost identical for each *in vitro* growth phase passage number (Figure 41).

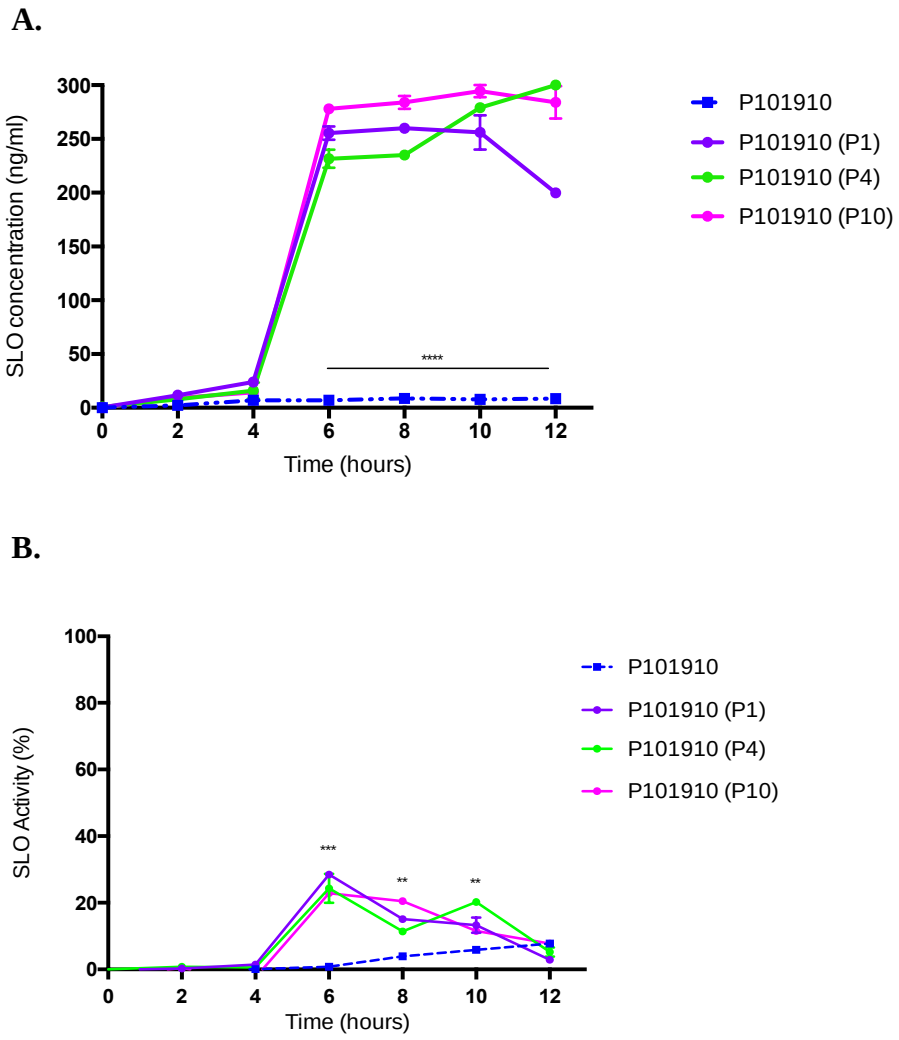

Figure 40 - Comparison of streptolysin production and activity in *in vivo* recovered *emm* type 1.0 isolate 101910 and after subsequent growth *in vitro*

A) Concentration of streptolysin (ng/ml) secreted into the supernatant by *emm* type 1.0 isolate 101910 recovered from knee joints (P101910) and then after subsequent growth *in vitro*. B) SLO haemolytic activity. **p < 0.01, ***p < 0.005 and ****p < 0.001 two-way ANOVA and Bonferroni's multiple comparisons correction.

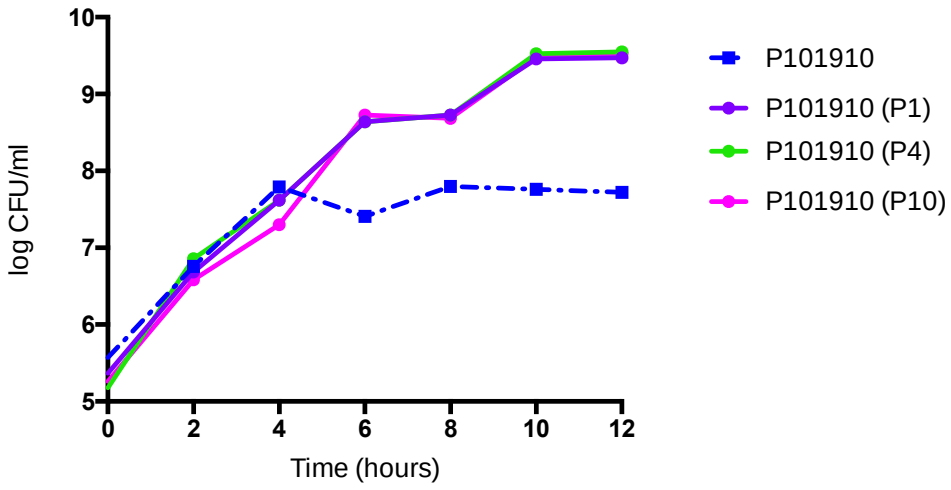

Figure 41 – Growth kinetics of *in vivo* recovered *emm* type 1.0 isolate 101910 and after subsequent *in vitro* passaging.

The CFU count was measured every two hours for 12 hours, at a starting CFU of 10^5. This experiment was done in duplicate over two independent days. Displayed as mean ±SEM.

5.7 Concentration and activity of streptolysin has significant impact on virulence *in vivo*

To investigate the effect of secreted SLO on virulence *in vivo,* the amount and activity of SLO released into the challenge inoculum (prior to infection of mice) of *emm* type 1.0 (isolate 101910) and *emm* type 32.2 (isolate 112327) was measured. At equivalent CFU challenge inoculum (1 x 10^8 per 50 μl), *emm* type 32.2 (isolate 112327) had significantly higher SLO concentration ($p = 0.012$) and haemolytic activity ($p = 0.01$) than *emm* type 1.0 (isolate 101910) (Figure 42) This had a direct effect on survival *in vivo*, where mice infected with *emm* type 32.2 (isolate 112327) all died from their infections, while those infected with *emm* type 1.0 (isolate 101910) all survived.

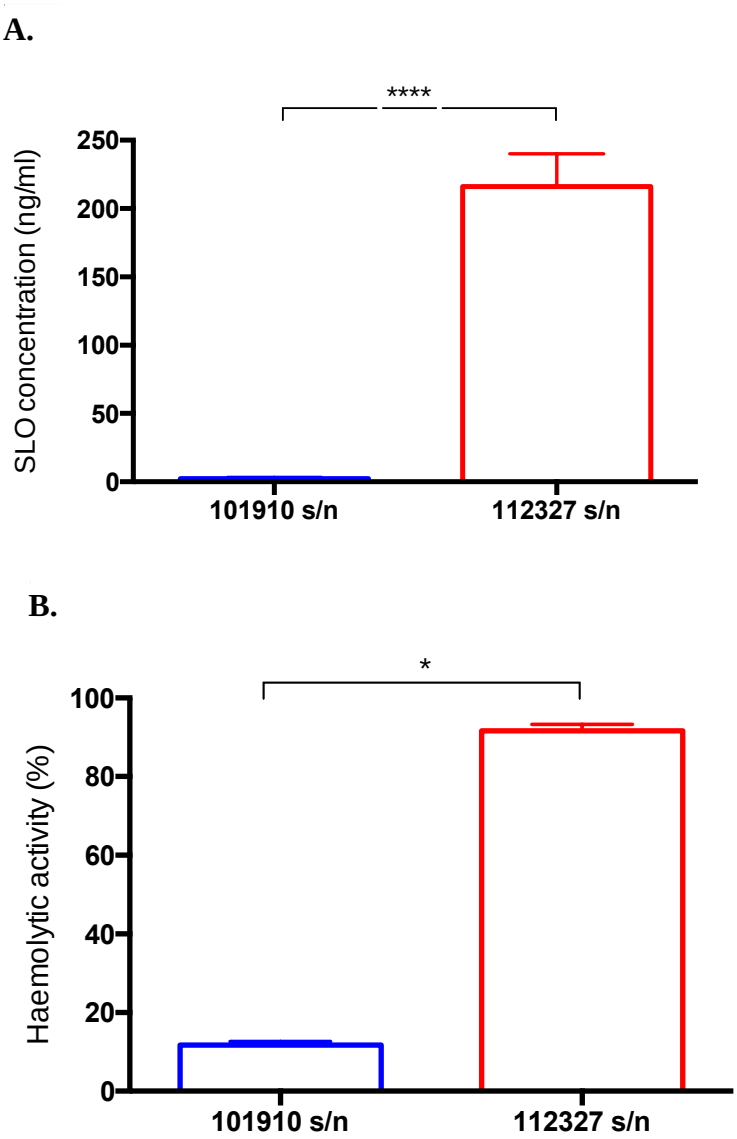

Figure 42- Analysis of SLO concentration and activity in challenge inoculum.

A) Concentration of streptolysin (ng/ml) and B) haemolytic activity in infection doses of *emm* type 1.0 isolate 101910 and *emm* type 32.2 isolate 112327, when prepared in 1 ml of PBS, incubated at room temperature for 30 minutes. *$p < 0.05$ and ****$p < 0.001$, analysed using a two-tailed Mann Whitney U-test, displayed as mean ±SEM.

To further investigate the effect of secreted SLO on infection dose and survival, the supernatants between isolates *emm* type 32.2 (isolate 112327) and *emm* type 1.0 (isolate 101910) were swapped prior to infection of the mice. Infection doses were prepared in 1 ml of PBS, incubated at room temperature for 30 minutes, immediately prior to infection bacteria were pelleted by centrifugation and the supernatants of the two challenge doses were swapped. Mice were infected with either isolate 112327 bacteria re-suspended in supernatant from isolate 101910 challenge dose or isolate 101910 bacteria re-suspended in supernatant from isolate 112327 challenge dose (Figure 43).

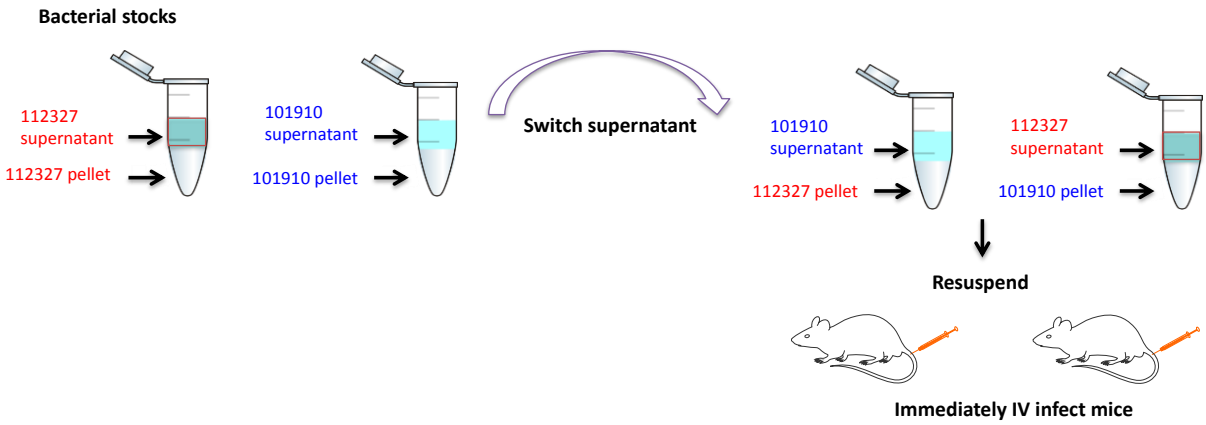

Figure 43- Schematic diagram of the method used to switch the supernatants of *emm* type 32.2 (isolate 112327) and *emm* type 1.0 (isolate 101910) before intravenously infecting mice.

In contrast to original challenge dose infections, the supernatant swap infected mice exhibited the opposite phenotype, whereby the normally non-lethal *emm* type 1.0 (isolate 101910), now killed all mice when infected with supernatant from *emm* type 32.2 (isolate 112327), and the normally lethal *emm* type 32.2 (isolate 112327) became significantly less virulent, leading to only 50% death as compared to 100% death previously (Figure 44a).

Moreover, the bacterial load in blood 24 h post-infection was determined. As previously observed, there were no CFUs of *emm* type 1.0 (isolate 101910) in blood at 24 h, but a significant 4 log increase in CFUs was observed when isolate 101910 was infected with the supernatant swap dose, clearly suggesting that the high concentration of SLO present in *emm* type 32.2 (isolate 112327) supernatant was enabling proliferation and retention of isolate 101910 in blood as compared to its normal condition of being cleared from blood (Figure 44b). In contrast, *emm* type 32.2 (isolate 112327) challenge dose with *emm* type 1.0 isolate 101910 supernatant infected mice had significantly lower CFUs in blood at 24 h in comparison to when infected with its original supernatant ($p = 0.0079$) (Figure 44b), suggesting again, that the concentration and activity of SLO is key to virulence *in vivo*, both in terms of survival and bacterial load. The general condition of the mice was assessed using percent weight loss as a factor to compare between infection groups. Although not statistically significant, when *emm* type 1.0 (isolate 101910) was infected with supernatant from *emm* type 32.2 (isolate 112327), there was more weight loss observed at 24 hours (Figure 45). Mice infected with *emm* type 32.2 (isolate 112327) and *emm* type 1.0 (isolate 101910) supernatant, had slightly lower weight loss at 24 hours (Figure 45).

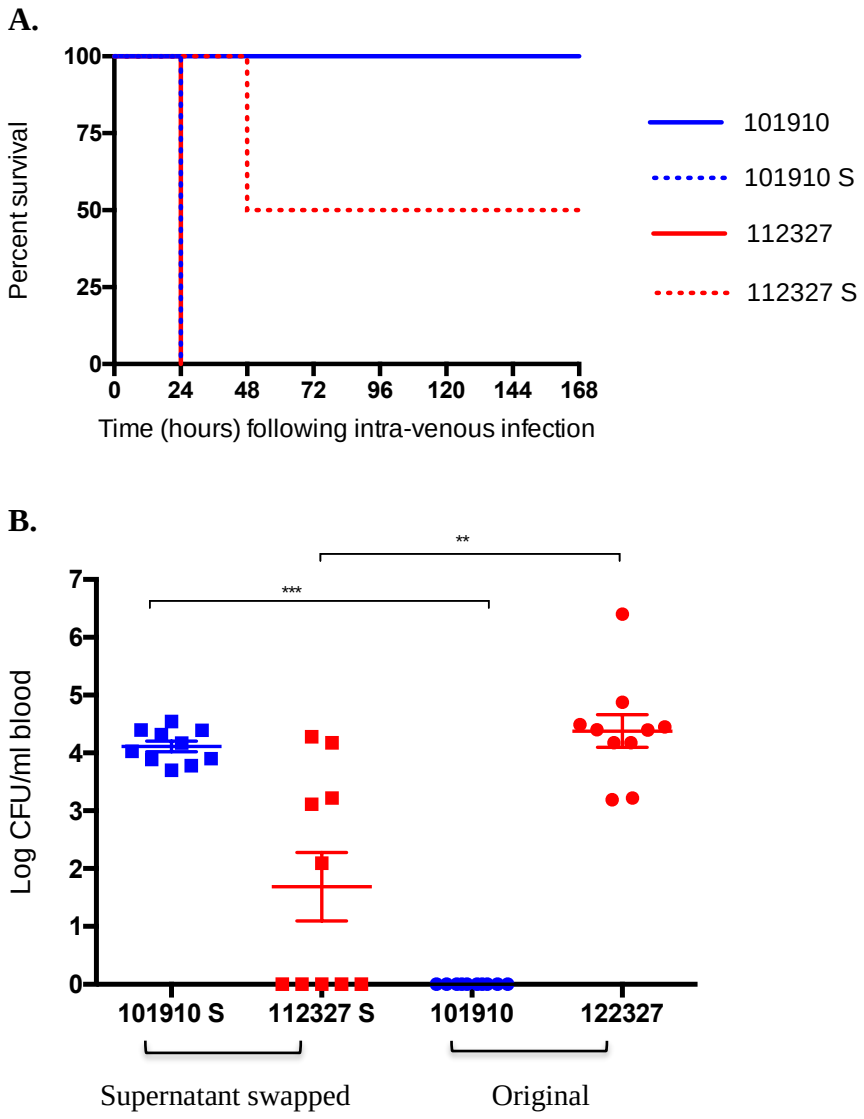

Figure 44 - Effect of concentration and activity of secreted SLO on virulence *in vivo.*

A) Kaplan Meier survival plots representing survival of CD1 mice (n = 10 per group) when intravenously infected (10^8 CFU) with *emm* type 1.0 (isolate 101910), *emm* type 32.2 (isolate 112327), *emm* type 32.2 isolate 112327 bacteria re-suspended in supernatant from *emm* type 1.0 isolate 101910 challenge dose (112327 S) or *emm* type 1.0 isolate 101910 bacteria re-suspended in supernatant from *emm* type 32.2 isolate 112327 challenge dose (101910 S). B) Bacterial burden in blood 24 hours after infection with isolates 101910 and 112327 and swapped supernatant isolates as above. Displayed as mean ±SEM, **p < 0.01 and ***p < 0.005 when analysed using a one-way ANOVA and Kruskall-Wallis multiple comparisons test.

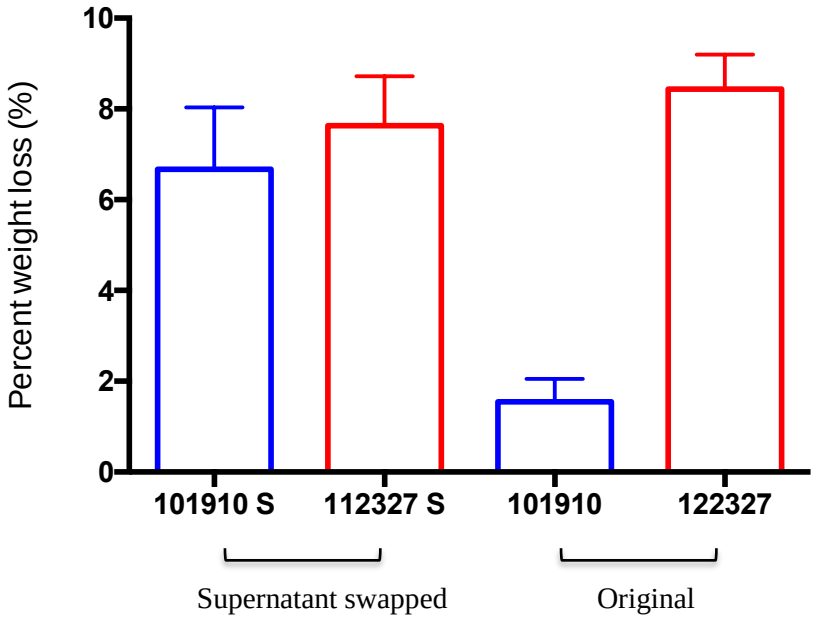

Figure 45 - Percentage weight loss of mice during invasive infection with *emm* type 1.0 isolate 101910 and *emm* type 32.2 isolate 112327.

The percentage weight loss CD1 mice (n = 10 per group) when intravenously infected (10^8 CFU) with *emm* type 1.0 isolate 101910, *emm* type 32.2 isolate 112327, *emm* type 32.2 isolate 112327 bacteria re-suspended in supernatant from *emm* type 1.0 isolate 101910 challenge dose (112327 S) or *emm* type 1.0 isolate 101910 bacteria re-suspended in supernatant from *emm* type 32.2 isolate 112327 challenge dose (101910 S). Displayed as mean ±SEM.

5.8 Streptolysin deficient mutant

To assess the role of SLO in the virulence of *emm* type 32.2 (isolate 112327) *in vivo* an isogenic SLO deletion mutant was generated where the SLO gene was deleted and replaced by a spectinomycin resistance gene through allelic exchange. Regions directly upstream and downstream of SLO (~ 1000 bp each) were amplified by PCR using primers SLO112327-up-F and SLO112327-up-R, SLO112327-down-F and SLO112327-down-R respectively, which introduced BamHI restriction sites into the PCR products. These fragments were stitched together in a second round of PCR using primers SLO112327-up-F and SLO112327-down-R for SLO regions (slo fragment), generating 2 kb fragments with a central BamHI site, which then were ligated into pGEM-T vector (Promega) (Figure 46), generating pGEM-T-Δslo-2kb (Figure 47). The plasmid was transformed into *E. coli* DH5a competent cells (ThermoFischer Scientific). Transformants were recovered on LB agar supplemented with ampicillin. The aad9 gene, encoding spectinomycin resistance, was amplified by PCR using primers aad9-F and aad9-R. PCR products were then sub-cloned into pGEM-T-Δslo-2kb generating a pGEM-T-Δslo::aad9 plasmid, which interrupted the SLO fragment, providing a means of positive selection of transformants. The generated plasmid pGEM-T-Δslo::aad9 was transformed into *emm* type 32.2 (isolate 112327) Allelic replacement of SLO with aad9 was identified by PCR of chromosomal DNA using primers SLO112327-up-F and SLO112327-donw-R, SpeA101910-up-F and SpeA101910-donw-R respectively and the PCR products were sequenced to confirm authenticity of the insertions.

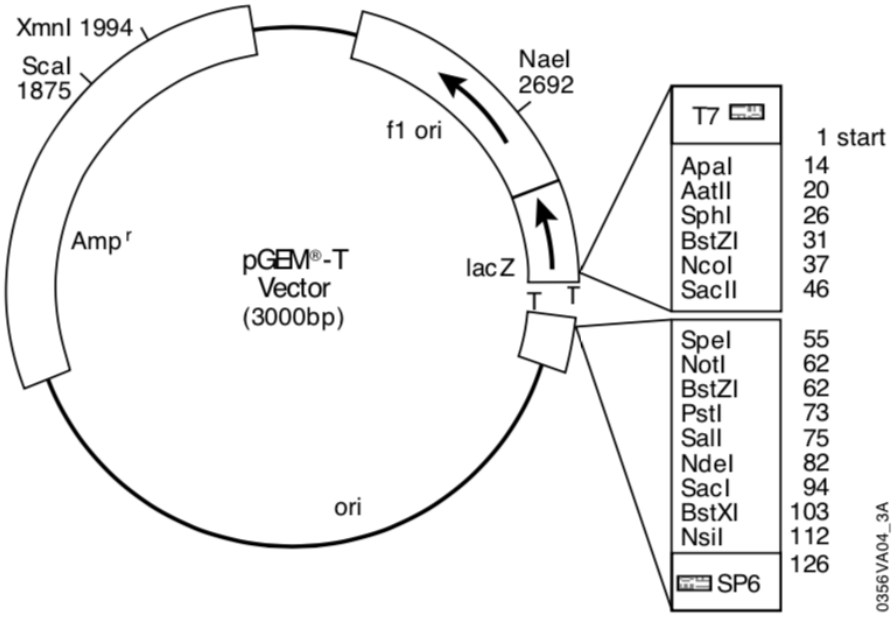

Figure 46 – pGEM®-T Vector (3000bp) Map and sequence reference points including list of restriction sites with corresponding base pairs.

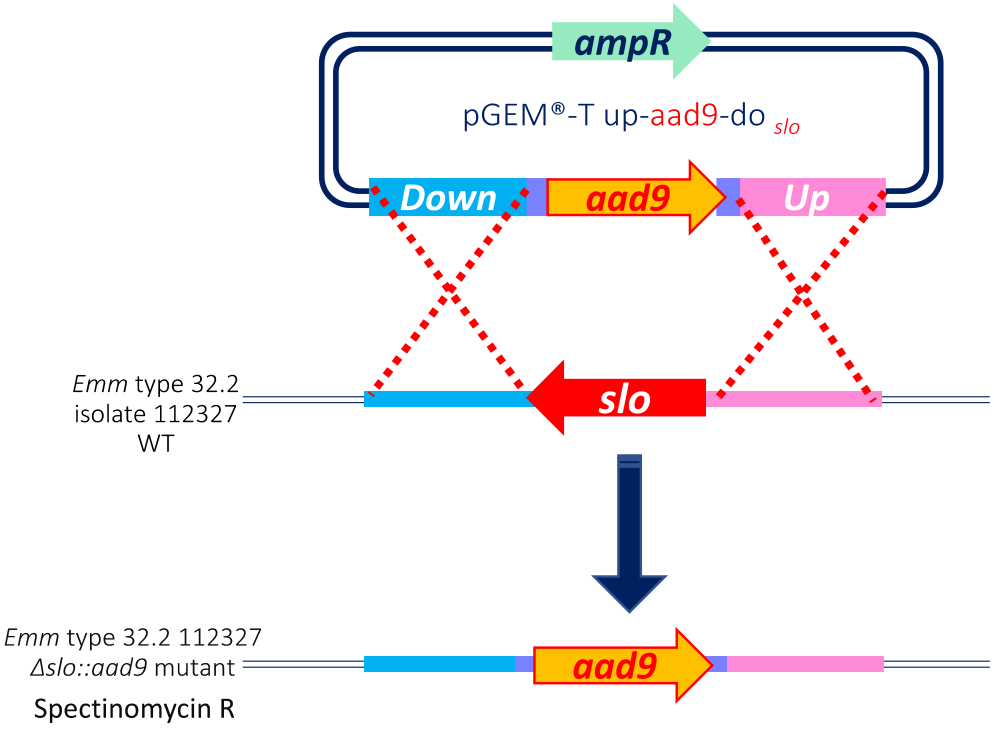

Figure 47 – Allelic replacement of streptolysin gene with aad9 Spectinomycin resistance gene, using pGEM®-T Vector.

5.8.1 Streptolysin deficient *emm* type 32.2 isolate 112327 during invasive infection

To determine whether there were any differences in virulence *in vivo* with SLO deficient *emm* type 32.2 (isolate ΔSLO 112327), an invasive infection model was used to compare survival and progression of infection alongside infection with *emm* type 32.2 isolate 112327 (wildtype). 10 mice were intravenously challenged with 10^8 CFU (50 µl) of *emm* type 32.2 isolates 112327 and ΔSLO 112327. Alongside survival times, blood CFUs were also measured at 24 h, 48 h, and at time of death.

All mice infected intravenously with 112327 ΔSLO mutant survived until the end of the experiment (96 h post infection), compared with wild type infected mice whom all succumbed to infection at 24h (Figure 48a). The survival data was analysed using the log-rank (Mantel-Cox) analysis used for the comparison of survival curves. Infection with isolate 112327 was significantly more virulent than infection with isolate ΔSLO 112327 (** $p < 0.01$). The bacterial load in blood was 3.5 log lower 24 h post infection in the mutant infection, then that observed in the mice infected with the wild type isolate ($p < 0.0001$) (Figure 48b). Furthermore, the bacterial burden of the 112327 ΔSLO mutant decreased over time and by 96 h post infection, bacteria were completely cleared from the blood (Figure 48b). Overall, in the absence of the toxin, bacteria were less able to establish an infection in the blood or were able to translocate elsewhere. Indeed, as described before during infection with *emm* type 1.0 (isolate 101910), mice infected with *emm* type 32.2 112327 ΔSLO mutant began to show joint deformities at 24 h.

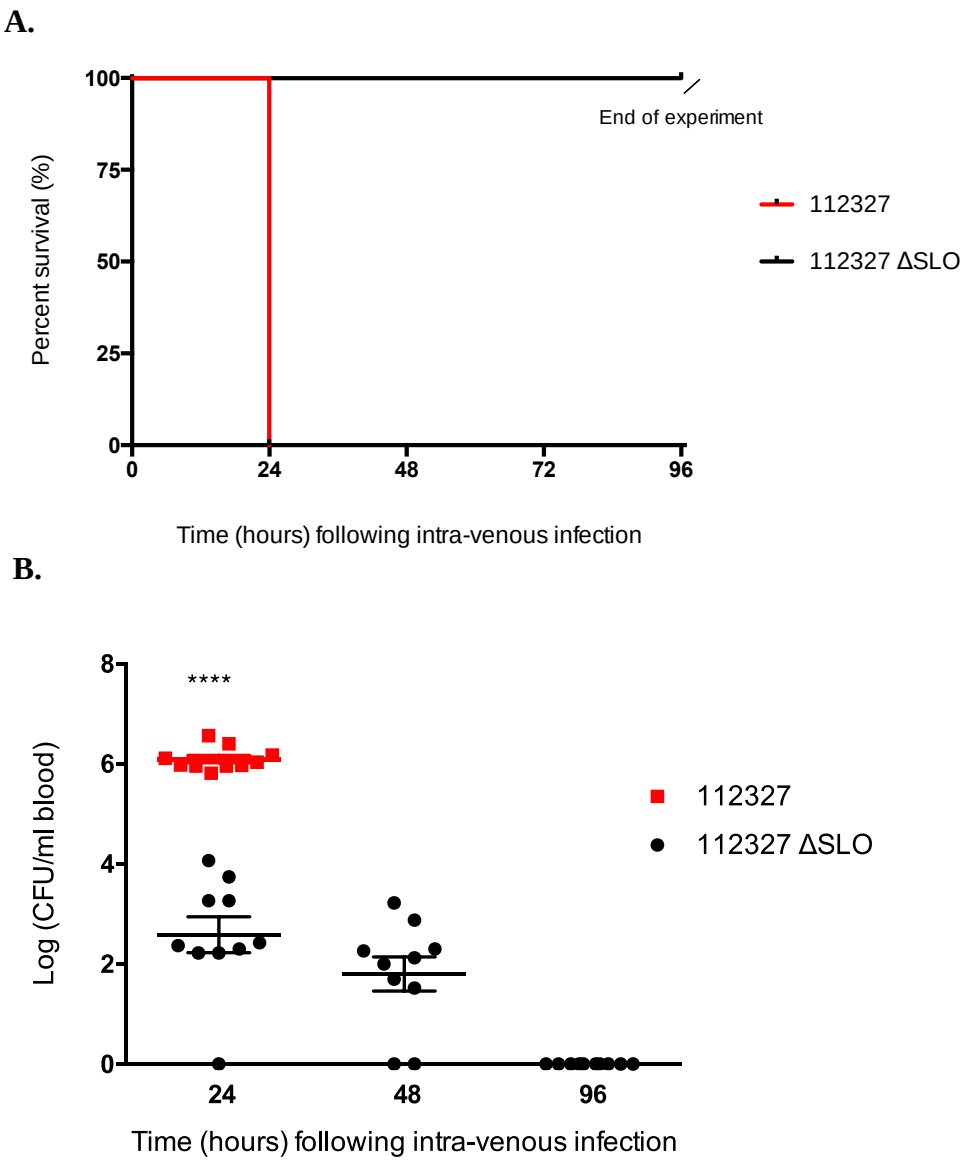

Figure 48 - SLO deficiency increases *in vivo* survival and switches phenotype.

A) Kaplan Meier plots representing percentage survival of CD1 mice (n = 10 per group) following 10^8 CFU intravenous infection with isolates *emm* type 32.2 (isolate 112327) and *emm* type 32.2 (isolate ΔSLO 112327). B) The bacterial CFU in blood for each isolate over time. Displayed as mean ±SEM, ****p < 0.001 when analysed using a Mann-Whitney U test.

5.8.2 Streptolysin deficient *emm* type 32.2 causes septic arthritis

SLO deficient *emm* type 32.2 (isolate ΔSLO 112327) was less able to proliferate in the blood. This is similar to the kinetics of the infection with *emm* type 1.0 (isolate 101910) (as seen in Chapter 4.4), *emm* type 1.0 (isolate 101910) is cleared from the blood between 24-48 h depending on the initial challenge CFU dose and is able to cause septic arthritis. To assess whether *emm* type 32.2 isolate ΔSLO 112327 was able to cause septic arthritis, 10 mice were intravenously challenged with 10^8 CFU (50μl) of *emm* type 32.2 isolate 112327 and isolate ΔSLO 112327 and *emm* type 1.0 isolate 101910, the CFUs in the knee joints were enumerated at 24 hours.

As expected there were no bacteria found in the knee joints of those mice infected with wildtype isolate 112327. Interestingly, bacteria were present in the knee joints of those mice infected with isolate ΔSLO 112327 at ~log 5 CFU/knee joint (Figure 49). There was no difference in the bacterial burden in the knee joints between isolate ΔSLO 112327 mutant and *emm* type 1.0 (isolate 101910) (Figure 49), which demonstrates that the kinetics of the infection was the same across the two different isolates. These results suggest that as well as being a key factor necessary and sufficient to virulence *in vivo*, SLO in this case is demonstrated to be the driving factor in determining the phenotypic outcome of infection.

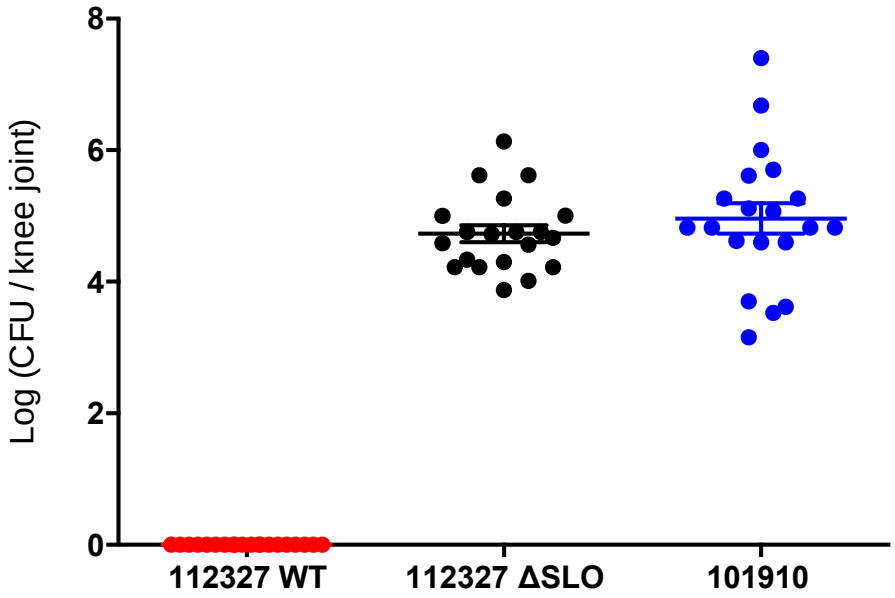

Figure 49 - Comparison of knee joint CFU after intravenous infection with *emm* type 32.2 isolate 112327 and isolate ΔSLO 112327 and *emm* type 1.0 isolate 101910.

The bacterial CFU in knee joints of CD1 mice (n = 5, knee joints n = 10) following 10^8 CFU in 50 µl intravenous infection with *emm* type 32.2 isolate 112327 and isolate ΔSLO 112327 and *emm* type 1.0 isolate 101910. Displayed as mean ± SEM.

5.8.3 Streptolysin deficient supernatant from *emm* type 32.2

Previously, the effects of switching the supernatant between *emm* type 32.2 (isolate 112327) and *emm* type 1.0 (isolate 101910) were assessed. *Emm* type 32.2 (isolate 112327) had high concentrations of SLO in the challenge inoculum and when this was co-infected with *emm* type 1.0 (isolate 101910) it resulted in a switch in the clinical phenotype; *emm* type 1.0 (isolate 101910) was now able to persist in the blood and cause mortality. To investigate further whether SLO alone was the driving factor behind the switch in clinical phenotype, mice were intravenously infected with 10^8 CFU of *emm* type 1.0 (isolate 101910), isolate 101910 bacteria re-suspended in supernatant from isolate 112327 challenge dose, and re-suspended in supernatant from Δ SLO 112327 challenge dose.

As previously demonstrated, non-lethal *emm* type 1.0 (isolate 101910) resulted in 100% mortality of mice when infected with supernatant from *emm* type 32.2 (isolate 112327). When mice were infected with 101910 bacteria re-suspended in supernatant from the mutant isolate Δ SLO 112327 challenge dose it was found that 2/5 succumbed to infection by day 4 and the rest of the mice survived till the end of the infection (Figure 50a). The survival data was analysed using the Log-rank (Mantel-Cox) analysis (Table 12). Infection with *emm* type 1.0 (isolate 101910) re-suspended in supernatant from *emm* type 32.2 (isolate 112327) challenge dose was significantly more virulent than infection with both other isolate combinations (** $p < 0.01$).

The blood CFUs were also compared at 12, 24, and 48 h to analyse the progression of infection in the blood (Figure 50b). The blood CFUs of those in infection group *emm* type 1.0 isolate 101910 (Δ SLO 112327 s/n) were compared to both other

groups. At 12 h there was no significant difference between all 3 groups, however there was a difference in the pattern of infection. As expected at 12 h, *emm* type 1.0 isolate 101910 had the lowest blood CFUs, followed by *emm* type 1.0 isolate 101910 with *emm* 32.2 mutant supernatant and *emm* type 1.0 isolate 101910 with *emm* 32.2 wildtype supernatant had the highest bacterial load in the blood. At 24 h, *emm* type 1.0 isolate 101910 with *emm* 32.2 wildtype supernatant had significantly more bacteria in the blood (4 log increase) than in both other groups (**$p < 0.01$). As seen before all bacteria had been cleared from the blood by 24 h in group *emm* type 1.0 (isolate 101910), and bacterial CFUs in group *emm* type 1.0 isolate 101910 with *emm* 32.2 mutant supernatant had significantly reduced, and bacteria were totally cleared by 48 h. These results further suggest that SLO is key to bacterial virulence *in vivo*, however there is some increase in persistence during infection with *emm* type 1.0 isolate 101910 with *emm* 32.2 mutant supernatant which could suggest there are other secreted proteins that are present in *emm* type 32.2 (isolate 112327) supernatant which are contributing to the increase in persistence of *emm* type 1.0.

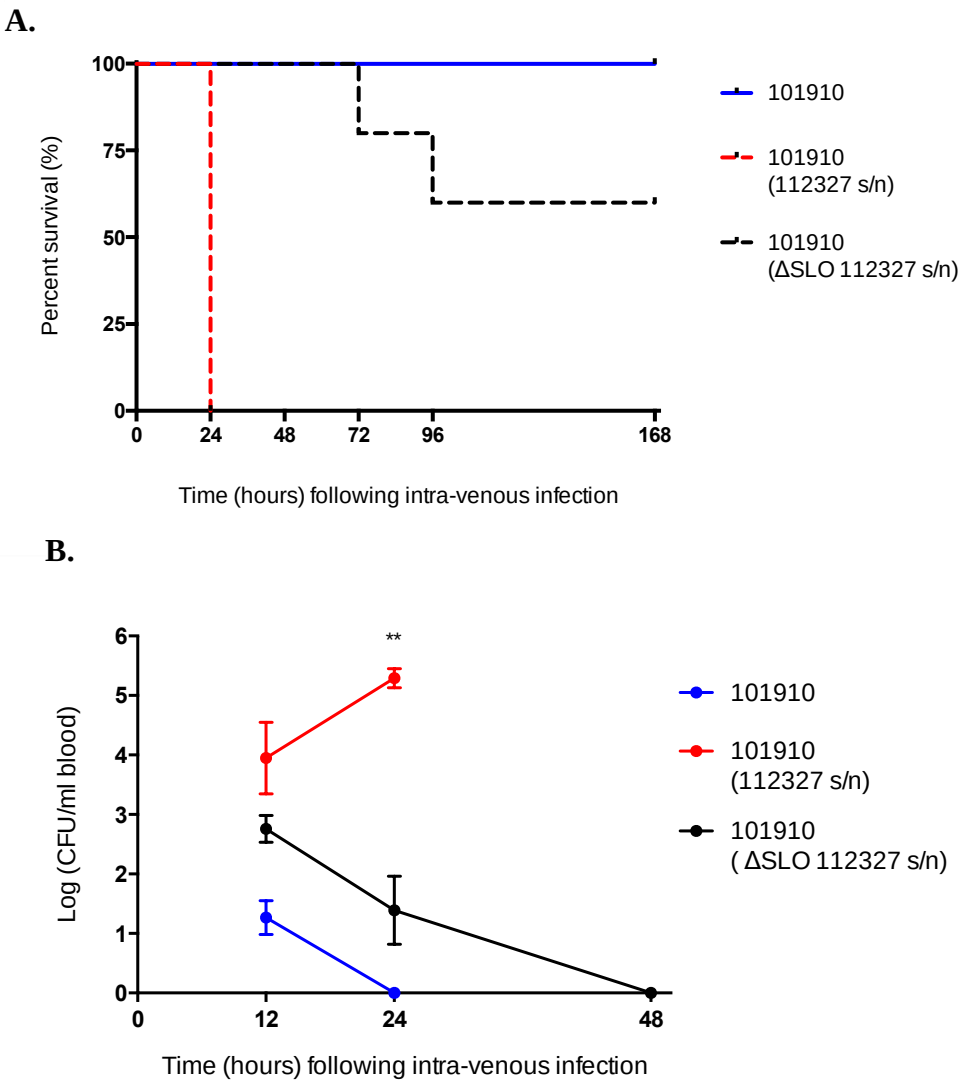

Figure 50 - Effect of concentration and activity of SLO-containing and SLO-depleted supernatant on virulence *in vivo*.

A) Kaplan Meier survival plots representing survival of CD1 mice (n = 5 per group) when intravenously infected (10^8 CFU) with *emm* type 1.0 isolate 101910, *emm* type 1.0 isolate 101910 bacteria re-suspended in supernatant from *emm* type 32.2 isolate 112327 or re-suspended in supernatant from isolate Δ SLO 112327 challenge dose. B) Bacterial burden in blood 12, 24, and 48 hours after infection. Displayed as mean ±SEM, **p < 0.01 when analysed using a one-way ANOVA and Kruskall-Wallis multiple comparisons test.

Table 12 – Comparison of survival of mice using a Log-rank (Mantel-Cox) analysis when intravenously infected (50 µl) with *emm* type 1.0 isolate 101910, *emm* type 1.0 isolate 101910 bacteria re-suspended in supernatant from *emm* type 32.2 isolate 112327 or re-suspended in supernatant from isolate ΔSLO 112327 challenge dose (p < 0.01).**

	101910 (112327 s/n)	101910 (ΔSLO 112327 s/n)
101910	**	ns
101910 (112327 s/n)		**

5.9 Liposomes as a decoy target receptor for Streptolysin

Previously published research has demonstrated the use of cholesterol rich liposomes (cholesterol: sphingomyelin liposomes; 66 mol/% cholesterol) as a method to sequester cholesterol dependent cytolysins both *in vitro* and *in vivo* [300]. It was shown that administration of cholesterol rich liposomes within 10 h after initiation of infection stopped the progression of bacteraemia caused by *S. aureus* and *S. pneumoniae* [300]. Liposomes were also able to bind strongly to SLO [300, 301]. Specially tailored cholesterol rich liposomes can thereby be used as targets to sequester secreted SLO *in vivo*. During preparation of the challenge inoculum for *in vivo* infection models it takes approximately 30 minutes from the time of preparation to infection of the mice, in this time SLO will be actively secreted into the challenge dose. It was initially determined whether liposomes were able to sequester the toxin that was secreted into the challenge dose and subsequent effect *in vivo*.

5.9.1 Incubation with liposomes sequesters streptolysin

The bacterial challenge dose used in the invasive infection model with *emm* type 32.2 (isolate 112327) and *emm* type 1.0 (isolate 101910) was incubated for 30 mins with 2 μg/ml of liposomes. After 30 mins, the liposomes were removed by centrifugation and the amount of SLO was measured in the supernatant. Liposomes were successful in reducing the concentration of the toxin. The concentration of SLO was significantly lower in *emm* type 32.2 (isolate 112327) supernatant when incubated with liposomes as compared to non-liposome control ($p = 0.003$) (Figure 51). The concentration of SLO in the bacterial challenge dose of *emm* type 1.0 isolate 101910 was low and after incubation with liposomes the concentration of SLO could not be detected using the SLO-ELISA (Figure 51).

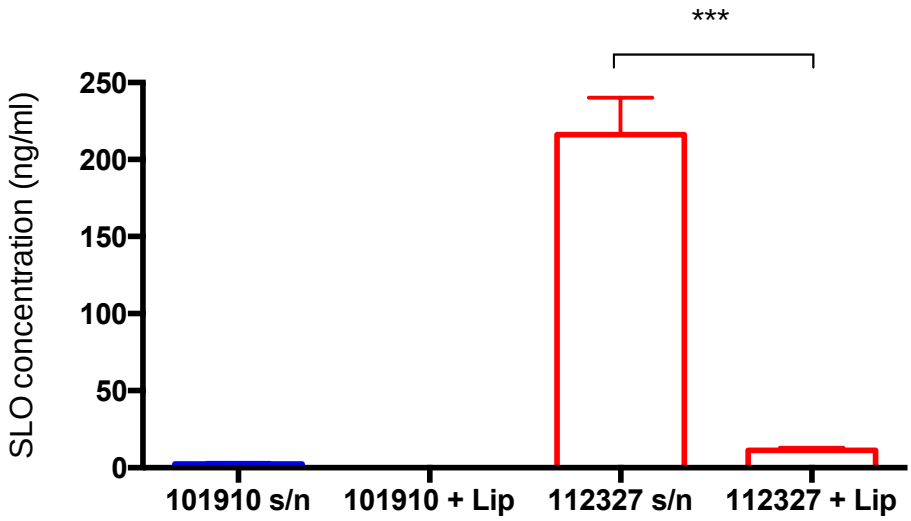

Figure 51 – Liposomes reduce concentration of streptolysin in supernatant of challenge doses.

Concentration of streptolysin (ng/ml) in infection doses of *emm* type 1.0 isolate 101910 and *emm* type 32.2 isolate 112327 before and after liposome treatment. Displayed as mean ±SEM, ***p < 0.005 analysed using a two-tailed Mann Whitney U-test.

5.9.2 Liposomes used *ex vivo* increase survival with *emm* type 32.2 invasive disease

To further investigate the effects of significantly reducing the concentration of SLO using liposomes, five mice were intravenously infected with 10^8 CFU of *emm* type 32.2 (isolate 112327) and bacteria after incubation of liposomes. When the bacterial challenge dose was incubated with liposomes prior to infection, all mice infected with liposome treated isolate 112327, survived a further 24 h as compared to non-liposome treated control challenge dose (Figure 52a). This extended survival period correlated with reduced CFU load in blood (Figure 52b).

A.

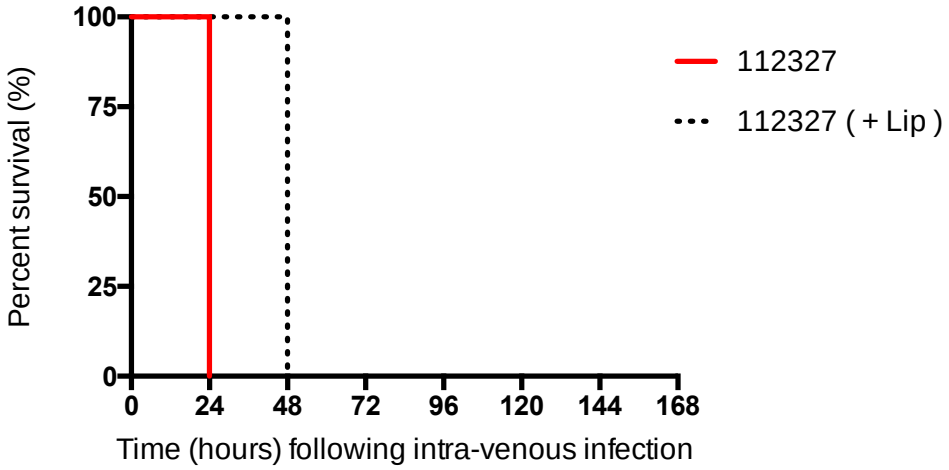

B.

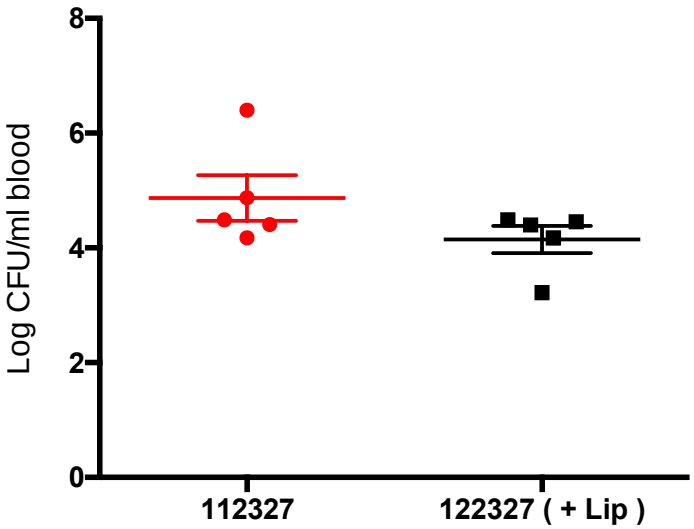

Figure 52 - Effect of incubation of liposomes with challenge dose of bacteria before invasive infection.

A) Kaplan Meier survival plots representing survival of CD1 mice (n = 5 per group) when intravenously infected (10^8 CFU) *emm* type 32.2 isolate 112327 and *emm* type 32.2 isolate 112327 bacteria after 30 min incubation with liposomes (liposomes removed prior to infection) B) Bacterial burden in blood 24 hours after infection. Displayed as mean ±SEM.

5.10 *In vivo* liposome study

In addition, the effects of giving liposomes as a treatment to invasive GAS was also considered.

5.10.1 Single treatment of liposomal mixture

The dose of liposome used in this study (150mg/kg) is known to be non-toxic from previously published work [300]. This is consistent with the findings presented here, all healthy mice treated with 150mg/kg showed no signs of ill health over a 7-day period.

A single injection of the liposomal mixture was administered at 4 h post infection. All mice that were not liposome treated succumbed to infection by 24 h, in comparison 60% of mice treated with the liposomal mixture survived an extra 24 h to 48 h (Figure 52a). There was also a reduction in the pain scores of those mice treated with the liposomal mixture (Figure 52b). The survival data was analysed using the Log-rank (Mantel-Cox) analysis, infection with *emm* type 32.2 isolate 1112327 without liposome treatment was significantly more virulent than with a single treatment of liposomes at 4 hours (* $p < 0.05$). In line with the differences in survival time, there was a considerable reduction of the bacterial load in the blood of mice that had been injected with a single dose of liposomes at 4 h in comparison to no treatment group (Figure 53). These results show that a treatment with liposomes reduces the amount of SLO secreted into the extracellular environment, leading to a considerable reduction of the bacterial burden in the blood of mice and to attenuation of invasive GAS infection.

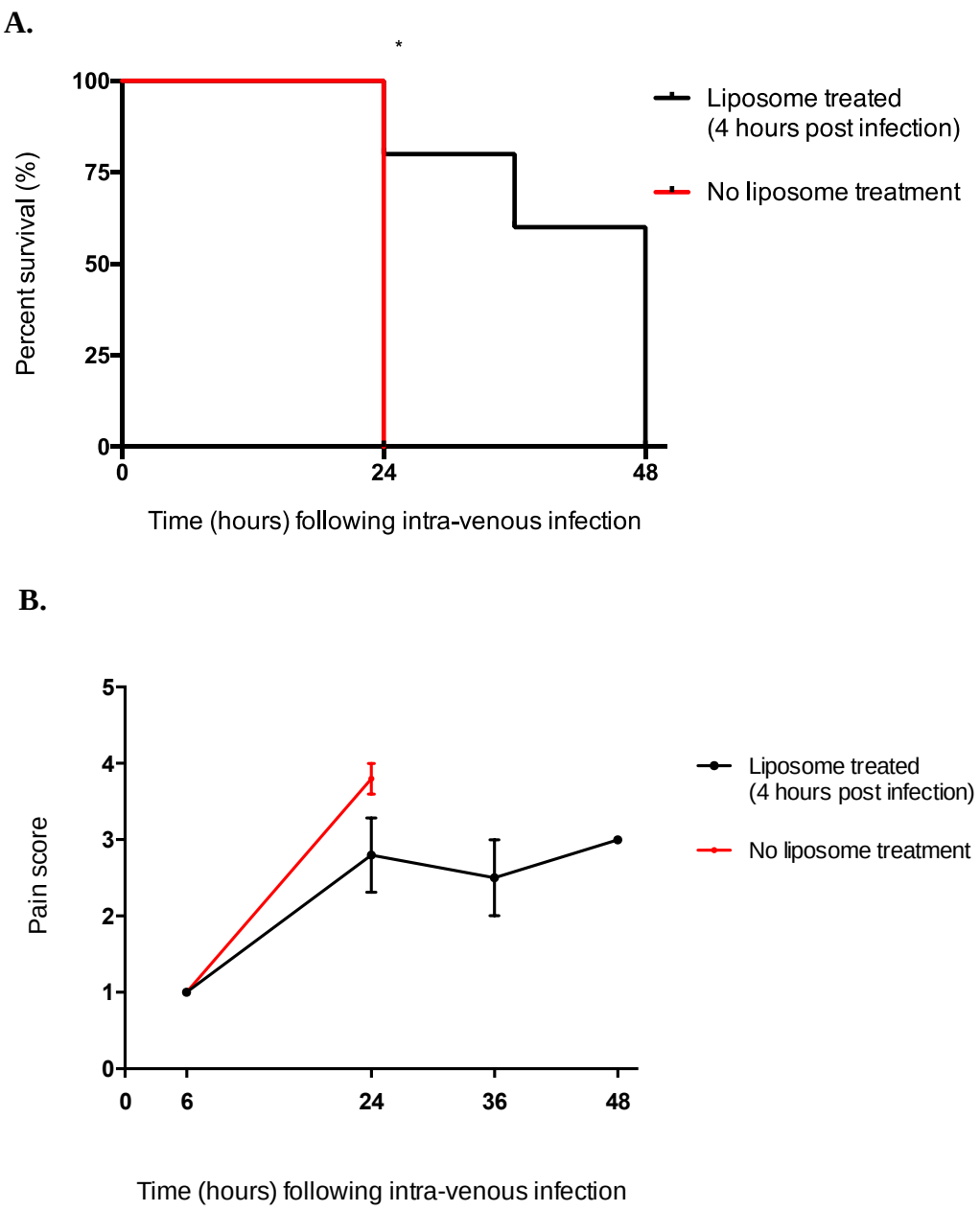

Figure 53 – Effect on virulence of sequestration of SLO by cholesterol: sphingomyelin (Ch: Sm) liposomes *in vivo*.

A) Kaplan Meier survival plots comparison representing survival of CD1 mice (n = 5 per group) when intravenously infected (10^8 CFU) *emm* type 32.2 isolate 112327 and after injection of liposomal mixture 4 h after infection. Analysed using the Log-rank (Mantel-Cox) test *$p < 0.05$. B) Pain scores of mice over time, displayed as mean ±SEM.

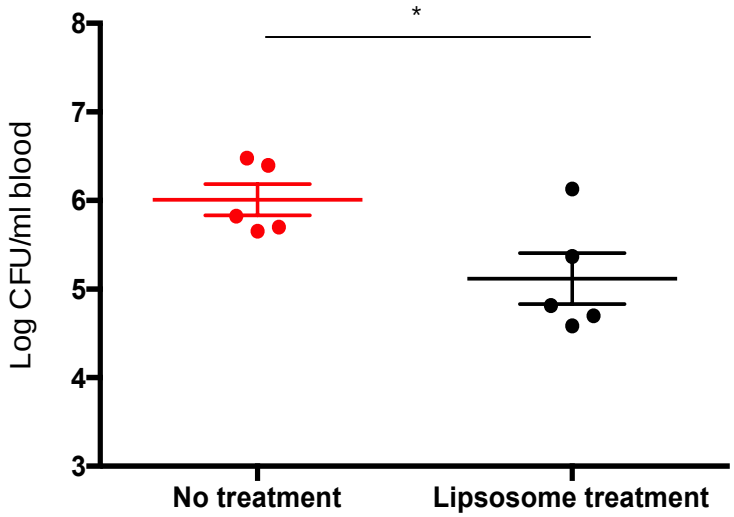

Figure 54 – Effect on bacterial load of sequestration of SLO by cholesterol: sphingomyelin (Ch: Sm) liposomes at 24 h.

The bacterial CFU in blood of CD1 mice (n = 5) following 10^8 CFU in 50 μl intravenous infection with *emm* type 32.2 isolate 112327 and after injection of liposomal mixture 4 h after infection. Analysed using One-way ANOVA and Kruskall-Wallis multiple comparisons test, *$p < 0.05$, displayed as mean ±SEM.

5.10.2 Double treatment of liposomal mixture

Previously published data showed that the half-maximal decline in the level of circulating liposomes occurred at 4 h, and ~20% of the liposomes were still circulating at 24 h after injection [300]. As the levels of liposomes in blood decreased by 50% 4 h after injection, mice were treated with liposomes twice with a 4 h interval to maintain a high level of circulating liposomes. As expected healthy mice injected with two doses of the liposomal mixture showed no signs of ill health.

Using an invasive sepsis model, five mice were injected intravenously with a lethal dose of *emm* type 32.2 (isolate 112327) (10^8 CFU). An injection of the liposomal mixture was administered at 4 h after infection followed by a second dose at 8 h. All mice that were not treated succumbed to infection at 24 h, in comparison 4/5 mice treated with the liposomal mixture survived an extra 24 h to 48 h (Figure 55a). The survival data was analysed using the Log-rank (Mantel-Cox) analysis, infection with *emm* type 32.2 (isolate 1112327) without double liposome treatment was significantly more virulent than with a double treatment of liposomes at 4 h and 8 h (* p-value < 0.05). At 24 h there was a considerable reduction of the bacterial load in the blood of mice that had been injected with a double dose of the liposomes at 4 h and 8 h in comparison to no treatment (Figure 55b). There was no significant difference between survival times, and there were no differences in the bacterial burden in the blood between single and double treatment groups at 24 hours (Figure 56).

A.

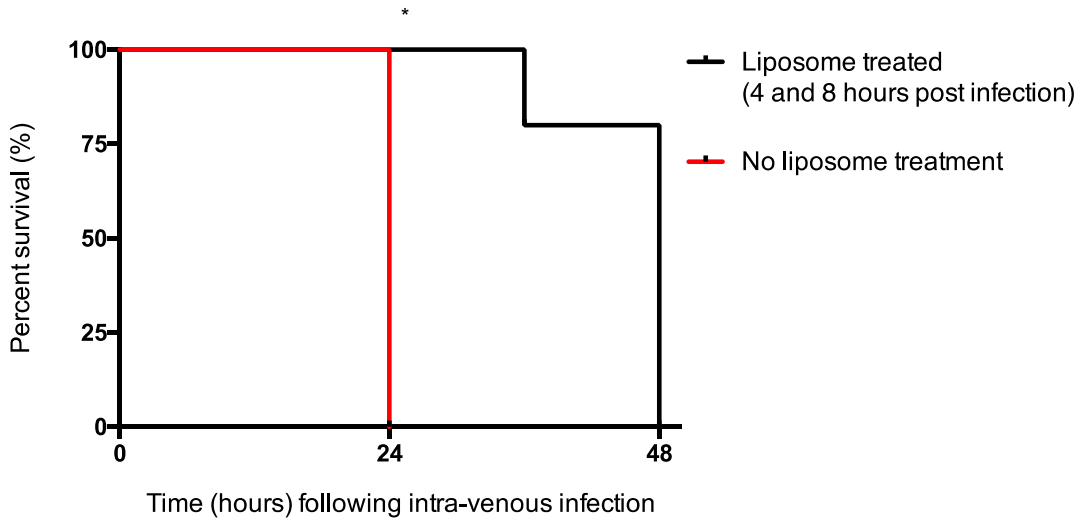

B.

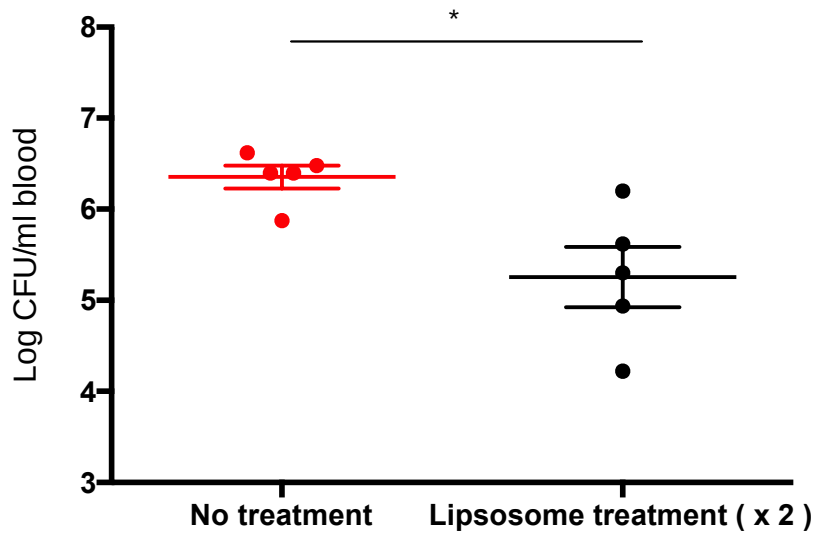

Figure 55 – Effect on virulence when using two dose treatments of cholesterol: sphingomyelin (Ch: Sm) liposomes *in vivo*.

A) Kaplan Meier survival plots comparison representing survival of CD1 mice (n = 5 per group) when intravenously infected (10^8 CFU) with *emm* type 32.2 isolate 112327 and after injection of liposomal mixture 4 h and 8 h after infection. Analysed using the Log-rank (Mantel-Cox) test (*$p<0.05$). B) Bacterial burden in the blood at 24 h post-infection. Analysed using One-way ANOVA and Kruskall-Wallis multiple comparisons test *$p < 0.05$, displayed as mean ±SEM.

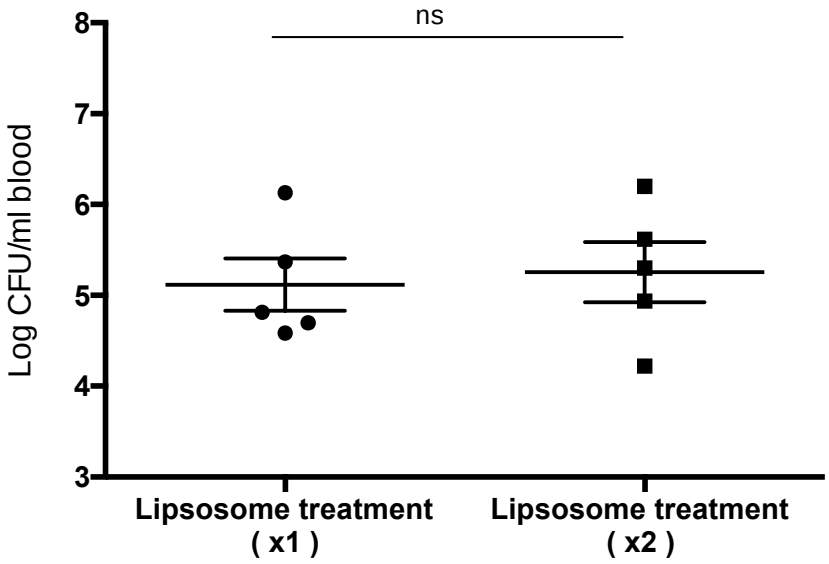

Figure 56 – Comparison of blood CFUs after one and two treatments of cholesterol: sphingomyelin (Ch: Sm) liposomes *in vivo.*

Comparison of bacterial CFU in blood (24 h) of CD1 mice (n = 5) following 10^8 CFU in 50 μl intravenous infection with *emm* type 32.2 isolate 112327 and treatment with liposomal mixture at 4 h (x 1) or at 4 h and 8 h (x 2). Analysed using a Mann-Whitney U-test, displayed as mean ±SEM.

C. Discussion

In summary, SLO production and activity drove two very distinct *in vivo* pathotypes; *emm* type 32.2 isolates which produced SLO in high levels and with high activity and *emm* type 1.0 isolates, which were the exact opposite with low levels of SLO production and of low activity. This correlated directly with their *in vivo* pathotype i.e. high virulence in bacteraemia models accompanied by short host survival (*emm* type 32.2) and low virulence in chronic septic arthritis models accompanied by long term host survival (*emm* type 1.0). Indeed, it was found that the levels and activity of SLO at time of initial infection, determined the disease phenotype, with high levels of SLO driving invasive disease and low levels sustaining chronic joint infections. When removing SLO from the *in vivo* environment, either by gene deletion or by significantly reducing SLO (by supernatant swap or liposome sequestration method), a complete reversal in the *in vivo* pathotypes of these *emm* isolates was observed, whereby normally bacteraemia causing *emm* type 32.2 isolates could be made to translocate into joints rather than killing their hosts, and septic arthritis causing *emm* type 1.0 isolates could be made highly invasive, highlighting the crucial role of SLO in determining disease phenotype and outcome *in vivo*.

SLO is a major virulence factor for GAS, expressed by nearly all strains, and with amino acid sequence homology highly conserved between strains [105]. Multiple roles in pathogenicity *in vivo* have been attributed to SLO, and recent studies have shown that SLO is important in the evasion of the host response via a number of mechanisms. Timmer *et al*., demonstrated that GAS induces rapid macrophage and neutrophil apoptosis due to the effects of SLO [153], and further work in the field has demonstrated that SLO rapidly impairs neutrophil oxidative burst preventing the

bactericidal action of neutrophils [302]. The effects of the general presence of secreted SLO in the blood stream has been less well studied however, although it has been implicated in driving inflammation, including the well documented evidence on activation of the NLRP3 inflammasome [303], hence, it would therefore seem likely that SLO production and activity is important for GAS in invasive bacteraemia infections yet there has been no studies to date to show that SLO itself could be driving disease phenotype *in vivo*. Although the SLO gene is highly conserved among all *emm* types of GAS, studies have shown that there are differences in the expression of the SLO gene which regulates the production of secreted SLO [304], and that specific invasive variants can be isolated post *in vivo* passage [305]. In addition to this, it has been shown that *in vivo* conditions can result in differential expression of certain proteins; a study looking at exotoxins SpeA and SpeB found that *in vivo* host and/or environmental signals induced SpeA gene expression and suppressed SpeB expression that could not be induced under *in vitro* conditions [306].

This study demonstrates that SLO levels and activity determine invasiveness or chronicity during infection. The role of SLO was further investigated using supernatant switching, an SLO-deficient mutant and SLO sequestration by cholesterol rich liposomes. When the supernatant of isolate 112327 was replaced with isolate 101910 supernatant, the amount of SLO in the challenge inoculum was significantly reduced and 50% of the mice challenged were able to clear the infection, a delayed invasive phenotype was observed with mortality at 48 h instead of 24 h with 112327 and its original supernatant. This demonstrated that without the initial high SLO concentration in the challenge inoculum there is an attenuation of

virulence. The bacteria may secrete SLO during the infection but the initial challenge concentration remains the key determinant resulting in clearance when concentrations are low and increased virulence with higher concentrations. Interestingly, when the experiment was reversed and the supernatant from the challenge inoculum of high SLO secreting isolate 112327 was used and co-infected with isolate 101910, there was a complete change in the clinical phenotype, whereby isolate 101910 was now able to successfully proliferate in the blood resulting in host death. Taking both of these results together, they indicate that the amount of SLO that is initially secreted is key to virulence in the early stages of infection, and it is possible for the host to successfully clear the bacteria when SLO concentrations are low. The data also suggests that the ability of the mice to survive infection is linked with the ability of the bacteria to proliferate. Early studies on SLO indicated that it was toxic when injected directly in an animal model [156, 307], in this study administrating the supernatant alone into the mice without any bacteria did not have a fatal effect. The difference between the two could be due to early studies using supraphysiological concentrations of purified SLO and/or purified SLO preparations contaminated with LPS.

To consider how the complete removal of SLO affects the progression of invasive infection, an isogenic SLO deletion mutant of isolate 112327 was made. The results demonstrated that mice infected with the SLO mutant had a significantly higher rate of survival than mice infected with the wild type bacteria. None of the mice infected with the mutant succumbed to infection where as 100% of mice infected with the wildtype died at 24 h. The SLO mutant began to be cleared from the blood as early as 24 h and was completely cleared by 96 h. Surprisingly, it was found that the SLO

deficient mutant sequestered in the knee joints causing septic arthritis as previously seen during infection with the low SLO secreting isolate 101910. The results clearly show that GAS strains lacking SLO and or low SLO producing GAS strains are severely impaired in their ability to cause bacteraemia and that lack (or reduced levels) of SLO enables the bacteria to accumulate within host joints.

There have been a number of previous studies using SLO mutants which have found that virulence is attenuated, although the relative importance of SLO would appear to be dependent on disease model used [147, 151, 156, 157]. For example, Limbago *et al*., used a subcutaneous invasive skin infection model to study the virulence of SLO-deficient mutants, where they found that although there were increased survival times of mice infected with SLO deficient strains, the absence of SLO itself did not limit dissemination from the wound into the vasculature system [156]. In contrast to this, a later study by Sierig *et al.,* found that during a skin infection model initiated by intraperitoneal infection there were no changes to survival using an SLO deficient mutant [147]. A more recent study looking at the emergence of an invasive *emm* type 89.0 clade, showed that elevated SLO producers are significantly more virulent than low SLO producers [154]. Based on the findings presented, it can be speculated that the low production of SLO (or SLO deficiency) prevents the ability of GAS to cause bacteraemia while enhancing its capability to translocate into the joints. Low SLO secreting isolate 101910 which effectively colonises the joints, adapts further to the joint by selecting for low secreting SLO variants. This is a selection pressure applied from environmental signals in the joint as when the isolate is recovered from the joints and placed under growth conditions *in vitro* it reverts to producing significantly more SLO. Moreover, deletion of SLO in isolate 112327 resulted in a

complete reversal of *in vivo* phenotype, whereby these SLO deficient isolates now caused septic arthritis.

The exact mechanism by how GAS infects the joint is not clear. The general mechanism of joint colonisation begins with haematogenous entry into the vascularised synovium. Once bacteria are in the joint space the low fluid shear conditions provide a unique opportunity for bacterial adherence and infection [61]. Different strains of bacteria that commonly infect the joint including GAS and others such as *S. aureus* have varying degrees of tropism to the joint, thought to be due to differences in adherence characteristics and toxin production [61]. Previously discussed in chapter 3, isolate 112327 is an outbreak strain with characteristics that suggest it is hypervirulent, e.g. it has 19 extra genes, five of which are associated with an increase in virulence [266]. In this current study, it was highlighted that isolate 112327 is more virulent in an invasive bacteraemia model and produced significantly more SLO which is likely to be one of the causes of its increased capacity to cause host death.

Infection with isolate 112327 results in uncontrolled bacterial proliferation in blood and rapid progression into sepsis. On the other hand, isolate 101910 which was isolated from a patient with septic arthritis and produces low concentrations of SLO, can be reduced to even lower concentrations after further selection from the joint. This implies that decreased production of SLO is beneficial during infection in the joint. Reduced or no expression of SLO could have a protective effect for the pathogen, as SLO is immunogenic and avoiding host immune cell detection could

thereby prevent immune activation and clearance, allowing GAS to continue to colonise the joint [145].

Survival of patients with GAS-bacteraemia is dependent on timely antimicrobial treatment of penicillin and clindamycin, which is administered to limit the production of toxins such as SLO [308]. Although many clinical isolates of GAS are susceptible to antibiotics it is still a future concern that antibiotic resistance to penicillin could become widespread [32]. In addition to this, the exotoxins secreted by GAS result in some of the more serious clinical phenotypes observed and so work towards limiting these effects is advantageous [3]. Previously published work has explored using cholesterol rich liposomes (cholesterol: sphingomyelin liposomes; 66 mol/% cholesterol) as a method to sequester cholesterol dependent cytolysins [300]. The liposomes have higher than *in vivo* relative concentrations of cholesterol and so act as a decoy target to sequester the toxins. It has been shown that administration of artificial liposomes within 10 h after initiation of infection stopped the progression of bacteraemia caused by *S. aureus* and *S. pneumoniae*, whereas untreated mice died within 24–33 h [300]. Furthermore, they showed that liposomes protect mice against invasive pneumococcal pneumonia [300]. Pneumolysin secreted by *S. pneumoniae* is part of the family of cholesterol dependent cytolysins along with GAS, therefore similar results were expected as they are known to have the same mechanism of action. Artificial liposomes were able to sequester SLO produced by *emm* type 32.2 (isolate 112327), and upon binding of SLO to liposomes *in vivo* there was some effective clearance of the bacteria from the host. This clearance was demonstrated by reduced bacterial load in the blood at 24 h and increased survival time. The administration of liposomes did not completely rescue mice from sepsis as the

previous study showed. This could be due to the fact that the concentration of liposomes administered and then circulating in the blood was not high enough to completely sequester SLO. Liposomes are currently used as carriers in drug delivery systems *in vivo* and are considered to be non-toxic for humans [309]. All components of the liposomal mixture used are naturally occurring lipids that are present in the outer leaflet of the plasmalemmal lipid bilayer, they are frequently exposed to the systemic circulation *in vivo* and therefore are non-immunogenic and biologically neutral [300]. It has already been discussed in previously published work that as liposomes are not bactericidal, it is unlikely that they will exert evolutionary pressure that would select for the emergence of drug-resistant bacteria and therefore it may be valuable pursuing liposome-based, toxin-sequestrating therapy for use as a treatment alongside antibiotics for life-threatening bacterial infections. Further work on this should be done to explore different dosages of liposomes and also to administer liposomes alongside antibiotic treatment.

The results presented here have important implications for our understanding of GAS pathogenesis. It can be concluded that levels and activity of SLO is key to determining whether GAS infection follows a highly invasive and virulent pattern leading to host death or whether it follows a chronic pattern of long term joint infection. The fact that these disease phenotypes are not fixed is highly interesting, as it suggests that GAS is highly sensitive to environmental signals and can change its phenotype rapidly. Indeed, by artificially effecting SLO levels, it can be shown that one disease phenotype can easily be switched into another. This has significant implications for therapy and vaccines as anti-SLO based treatments may not be the complete answer to protection against all forms of GAS infection.

6. Group A *Streptococcus* dependent septic arthritis in murine knee joints: The local immune response

A. Introduction

6.1 Host response in septic arthritis

Septic arthritis is an inflammatory disease of the joints with innate and specific immune mechanisms contributing to pathology and joint destruction [59, 61, 310]. Currently our understanding of host immunopathogenesis in septic arthritis comes from staphylococcal experimental models only [54]. Generally, the inflammatory process is characterised by the rapid recruitment of polymorphonuclear granulocytes and macrophages which is later followed by infiltration of T cells [54]. After the bacteria have successfully established an infection in the joint inflammatory cytokines (IL-1β and IL-6) are released into the joint fluid by synovial cells, which accompanies the influx of host inflammatory cells [61, 233, 311]. Phagocytosis of the bacteria by macrophages, synoviocytes and PMNs occurs and the release of other inflammatory cytokines follow including TNF-α and IL-8 [61]. The T–cell mediated (Th1) immune response has also been shown to play a role both in clearance and pathogenesis of septic arthritis and can be specifically activated by bacterial antigens through antigen presenting cells or non-specifically in the case of bacterial superantigens [312, 313]. Under most circumstances the host is able to provide a protective inflammatory response that contains the bacteria and resolves the infection, however when the infection is not quickly cleared the potent activation of the immune response and high levels of cytokine concentrations leads to irreparable joint destruction [54, 61].

6.2 Bacterial superantigens and septic arthritis

It is understood that bacterial superantigens play a major role in the potent activation of the host response during septic arthritis with *S.aureus*, leading to exacerbation of host inflammatory cell invasion, cytokine release, increased mortality rates and joint remodelling and destruction [61]. Superantigens bind to the conserved regions of the host major histocompatibility complex class II molecule and T cell receptor, and are able to activate 2-20% of all T cells [168]. The activated T cells are able to increase the release of a number of inflammatory cytokines such IFN-γ and TNF-α, which result in significant toxicity [61]. The stimulated T cells proliferate rapidly and then quickly disappear, which is believed to be due to apoptosis [61]. B cells are also stimulated by the superantigens, but their role in septic arthritis is not fully understood [234].

6.3 Rationale

Currently there are limited experimental septic arthritis models with GAS, and none that have been used to characterise the host response during infection. In this study, an arthritogenic strain of GAS was used (*emm* type 1.0 isolate 101910) to induce septic arthritis to investigate the host response over time in the knee joint. Next, an isogenic superantigen SpeA knockout in isolate 101910 was used to consider the role of superantigens in GAS septic arthritis.

B. Results

6.4 GAS systemic infection in mice results in fast knee joint infiltration which evolves to a more chronic form

As discussed in Chapter 4, when *emm* type 1.0 (isolate 101910) was intravenously injected into mice the bacteria enter and colonise the knee joint. CFUs were recovered from the knee joint as early as 6 hours and the number of bacteria continued to increase in the joint up to 72 hours. A more chronic form of the infection was observed after 72 hours and the number of bacteria remained stable up to day 7 (end of experiment) (Figure 57a). Evidence of joint swelling was visible by 24 hours and the severity of the infection, based on the arthritic index, continued to increase until the end of the experiment whereby all infected joints had severe swelling and erythema (Figure 57b).

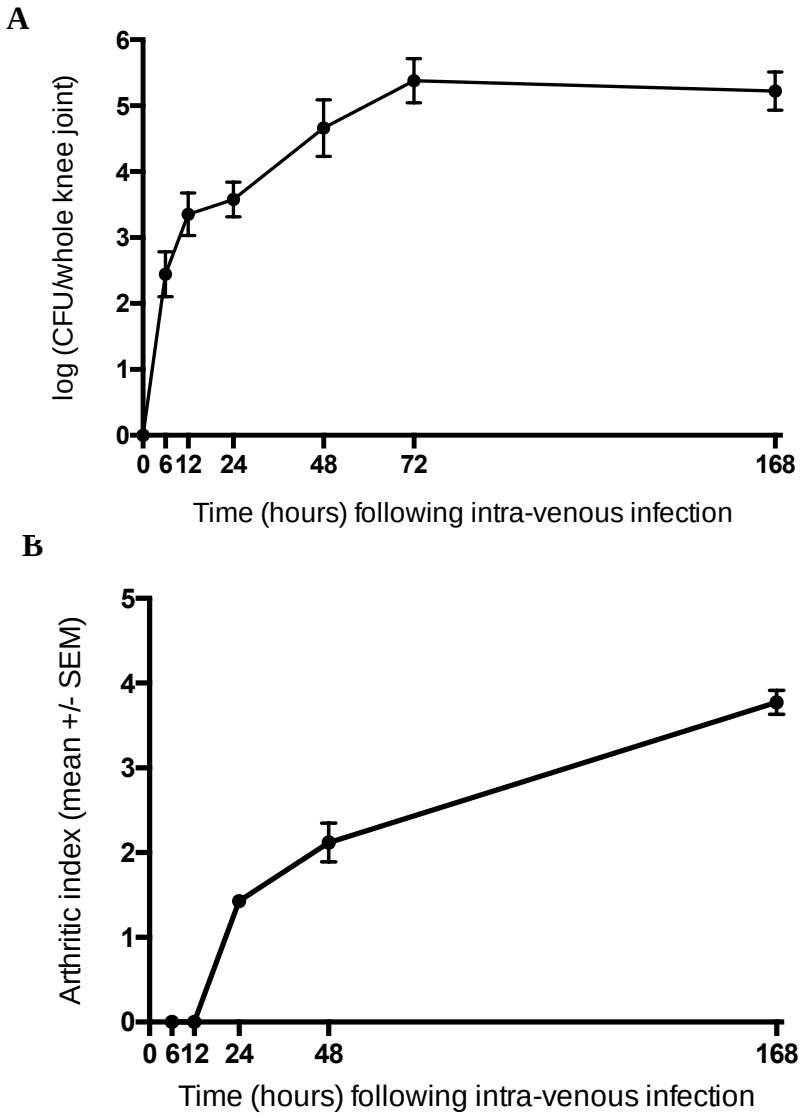

Figure 57 – Comparison of bacterial numbers in the knee joints and blood after intravenous infection with *emm* type 1.0 isolate 101910.

(A) The bacterial CFU in knee joints of CD1 mice (n = 10, knee joints n = 20) following intravenous infection with 10^7 CFU (50 μl) of *emm* type 1.0 isolate 101910 and (B) arthritic index over time. Displayed as mean ± SEM.

6.5 Local inflammatory response and immune cell recruitment in knee joints

To provide a comprehensive picture of the immune response in the knee joints during GAS-induced septic arthritis, mice were intravenously infected with *emm* type 1.0 (isolate 101910) and knee joints were removed at defined time points (n = 10) for bacterial, cellular and cytokine analysis.

6.5.1 Cytokines

Once bacteria colonise the joint they can rapidly activate an acute inflammatory response [61]. Host inflammatory cytokines IL-1β and IL-6 are initially released into the joint by synovial cells [311]. The amount of IL-1β released into the joint increased rapidly and by 24 hours there were significantly higher titres of IL-1β ($p < 0.01$), which continued to increase up to 72 hours (Figure 58a). Between 72 hours and day 7 there was a change in the cytokine profile in the joint and the amount of pro-inflammatory cytokine IL-1β returned to basal levels (Figure 58a). The same trend of an initial rise (up to 72 hours) and then decline in cytokine titres was also observed for IL-6, although this was not statistically significant (Figure 58b). Phagocytosis of the bacteria by macrophages, synoviocytes, and PMNs are associated with the release of other pro-inflammatory cytokines such as IL-8 and TNF-α [61]. The concentration of IL-8 in the knee joint did not change between 0 and 48 hours. At 72 hours, was a statistically significant increase in the amount of IL-8 in the joint ($p < 0.01$) (Figure 58c). The concentration of IL-8 decreased by day 7, although the amount present did not completely return to basal concentrations. The

levels of TNF-α in the joint peaked at 48 hours ($p < 0.01$) and the concentration in the joint remains high even at day 7 (Figure 58d).

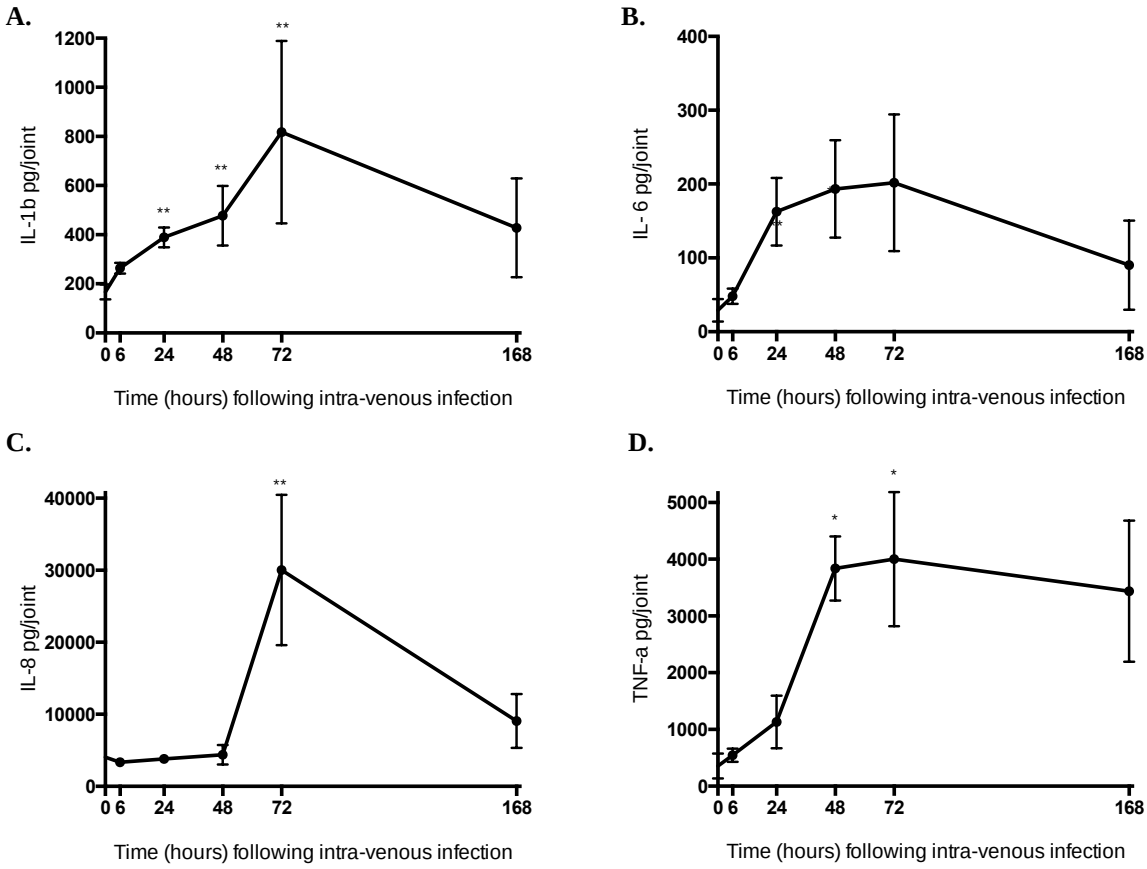

Figure 58 – Cytokine profiles measured in knee joints of infected animals (pg/joint).

A) Measurement of IL-1β, B) IL-6, C) IL-8, and D) TNF-α in knee joints of mice at 0, 6, 24, 48, 72, and 168 hours post intravenous infection with *emm* type 1.0 (isolate 101910). Samples were collected from 10 mice/time point from 2 independent experiments and data are reported as mean ± SEM. Statistical analysis was performed using a two-tailed Mann-Whitney U-test comparing single time points against time 0 (*$p < 0.05$, **$p < 0.01$).

6.5.2 Immune cells

The numbers of neutrophils, macrophages, B cells and CD4+ T cells in the joint were examined, the cell types were chosen as they have previously been identified to play a key role in the local response in the joint during bacterial septic arthritis [54, 235].

Firstly, the total number of neutrophils gated based on single cells that were positive both for CD45 and GR1 were analysed in whole knee joints (Figure 60). Neutrophil numbers did not significantly differ from basal levels over the first 72 hours of the infection (Figure 59a). At 72 hours, the number of neutrophils found in the joint was significantly higher than at time 0 ($p < 0.005$) (Figure 59a). The number of CD45 and F4/80 positive macrophages were examined in the knee joints (Figure 60). The number of macrophages in the joint significantly increased at much earlier time points in comparison to the number of neutrophils. At 12 hours the number of macrophages observed in the joint was significantly higher than at time 0 ($p < 0.05$) (Figure 59b). The number of macrophages entering the joint continued to increase over time. At 72 hours, the macrophage numbers began to decline (Figure 59b). Considering next the total number of CD45, CD19 and CD22 positive B cells found in the joint (Figure 60c) there was an interesting pattern observed which was dissimilar to the phagocytic cells examined. There was an initial increase in the number of B cells at time points 6 and 12 hours ($p < 0.01 – p < 0.05$). However, this was followed by a rapid decrease in the number of B cells over the next 72 hours (Figure 59c). By 72 hours, the number of B cells returned to the same numbers found at time 0. At day 7 the number of B cells found in the joint was even lower than before infection with GAS (p value not significant), suggesting that there could be environmental signals in the joint that are resulting in decreased numbers of B cells

(Figure 59c). Finally, CD45, CD4 positive T cells were enumerated from the knee joints (Figure 60). CD4 T cells significantly increased in numbers from 6 to 72 hours ($p < 0.05 – p < 0.001$), and at 72 hours there were 5 times the amount of CD4 positive T cells than at time 0 (Figure 60d). Similar to the pattern observed with the B cell numbers, CD4 T cells were cleared from the joint and the total number of cells at day 7 was lower than at day 0.

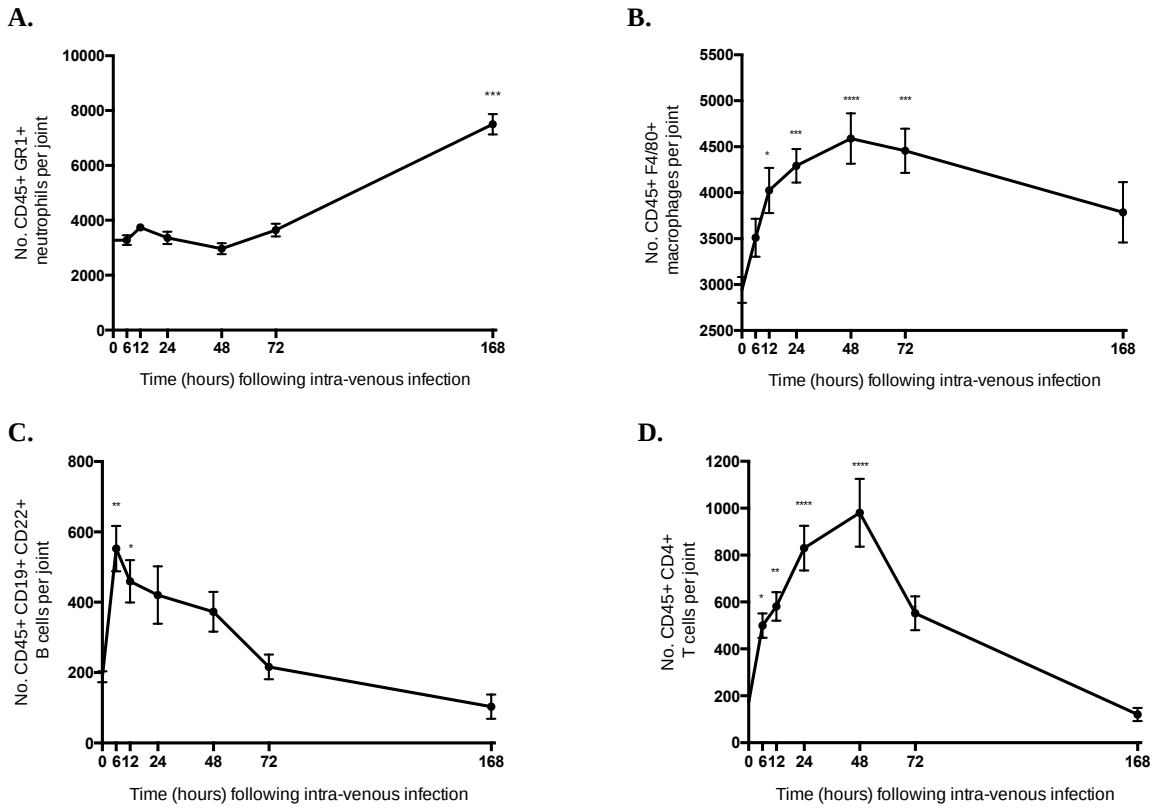

Figure 59 – Phenotypic characterization of cells recruited into the knee joints of animals infected with *emm* type 1.0 isolate 101910.

A) Measurement of neutrophils B) macrophages C) B-cells, and D) CD4 + T-cells in total knee joints of mice at 0, 6, 12, 24, 48, 72, and 168 hours post intravenous infection with *emm* type 1.0 isolate 101910. Samples were collected from 10 mice/time point from 2 independent experiments and data are reported as mean ± SEM. Statistical analysis was performed using a two-tailed Mann-Whitney U-test comparing single time points against time 0 (*$p < 0.05$, **$p < 0.01$, ***$p < 0.005$, and ****$p < 0.001$).

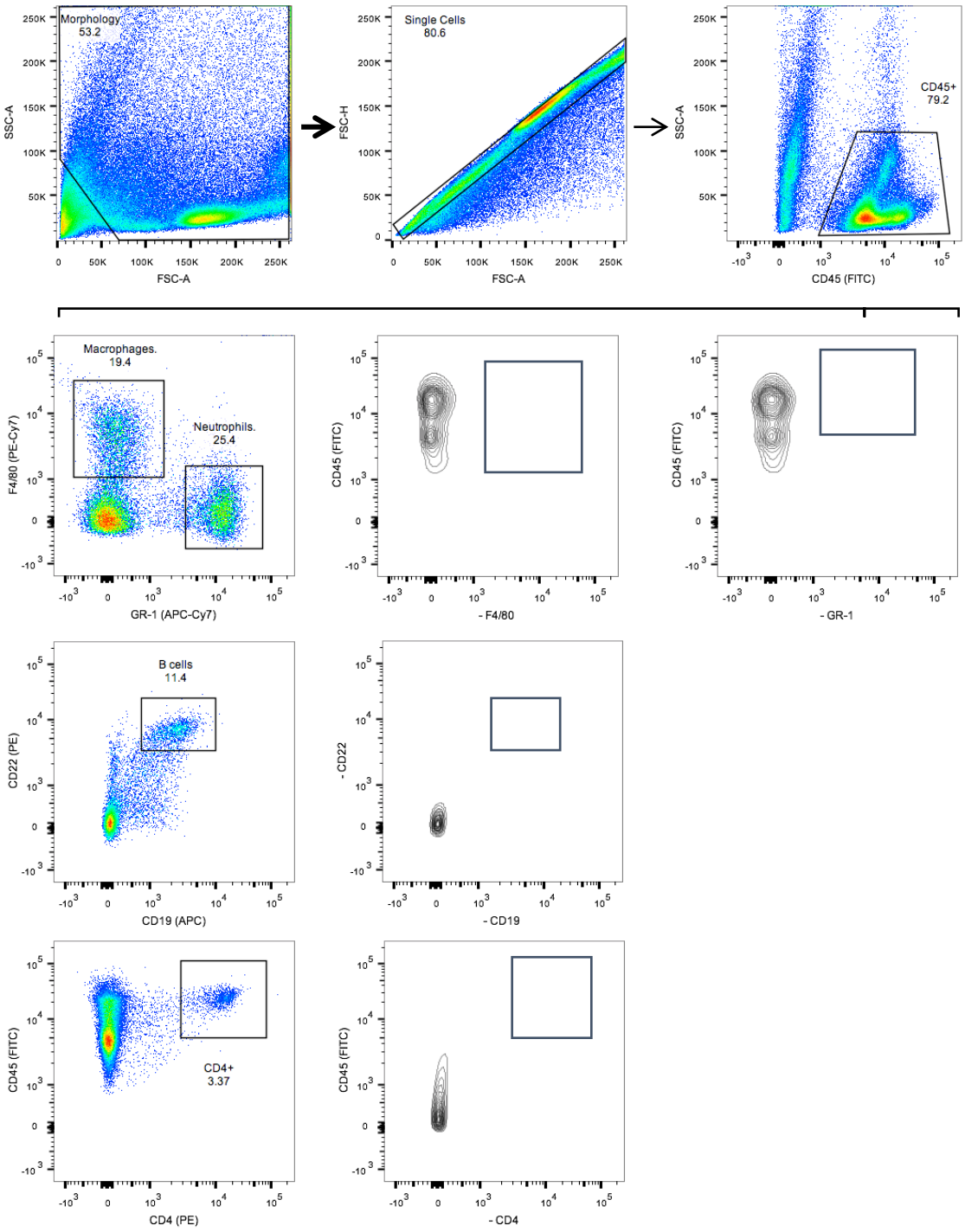

Figure 60 – Gating strategy for the analysis of neutrophils, macrophages, B-cells and CD4+ T-cells in knee joints.

The flow cytometry analysis was used to identify different immune cell subsets in knee joints of GAS intravenously infected animals. On the X and Y-axes are reported different markers utilised for the specific analysis, cell types described along with percentage of CD45+ cells. Gates identify the different cell subsets analysed. Alongside are the negative controls.

6.6 Effect of host-adapted *emm* type 1.0 101910 during re-infection

To investigate the immediate effect of knee joint recovered *emm* type 1.0 isolate 101910 during re-infection on the host response, bacterial and cellular analysis was performed on the knee joints (n = 10) over 0-48 hours. As previously described, host-adapted *in vivo*-recovered *emm* type 1.0 isolate 101910 colonises the joint at higher densities and does so more rapidly than the wildtype strain. We have also shown that host-adapted *emm* type 1.0 has significantly reduced production of the toxin SLO.

6.6.1 Immune cell recruitment

The number of neutrophils found in the joint over the course of 48 hours did not change significantly from basal levels (day 0), though a reduction in the number of cells was observed at 12 hours before an increase up to 48 hours (Figure 61a). A similar pattern was also observed with the macrophage cell numbers in the joint as they also showed a slight decrease in between 0 and 12 hours, before increasing up to 48 hours. At 48 hours there were significantly more macrophages present ($p < 0.01$) (Figure 61b). The number of B cells increased 3-fold at 6 hours ($p < 0.01$), followed by the number of cells gradually decreasing until the total amount returned to basal levels by 24 and 48 hours (Figure 61c). CD4+ T cells rapidly increased in the joint and the highest number of cells were found at the early time point of 6 hours ($p < 0.01$). The number of T cells fluctuated slightly in between 12 and 24 hours but the number of cells remained significantly higher than at time 0, whereas at 48 hours the numbers of cells in the joint were only 2-fold higher than at time 0 (Figure 61d).

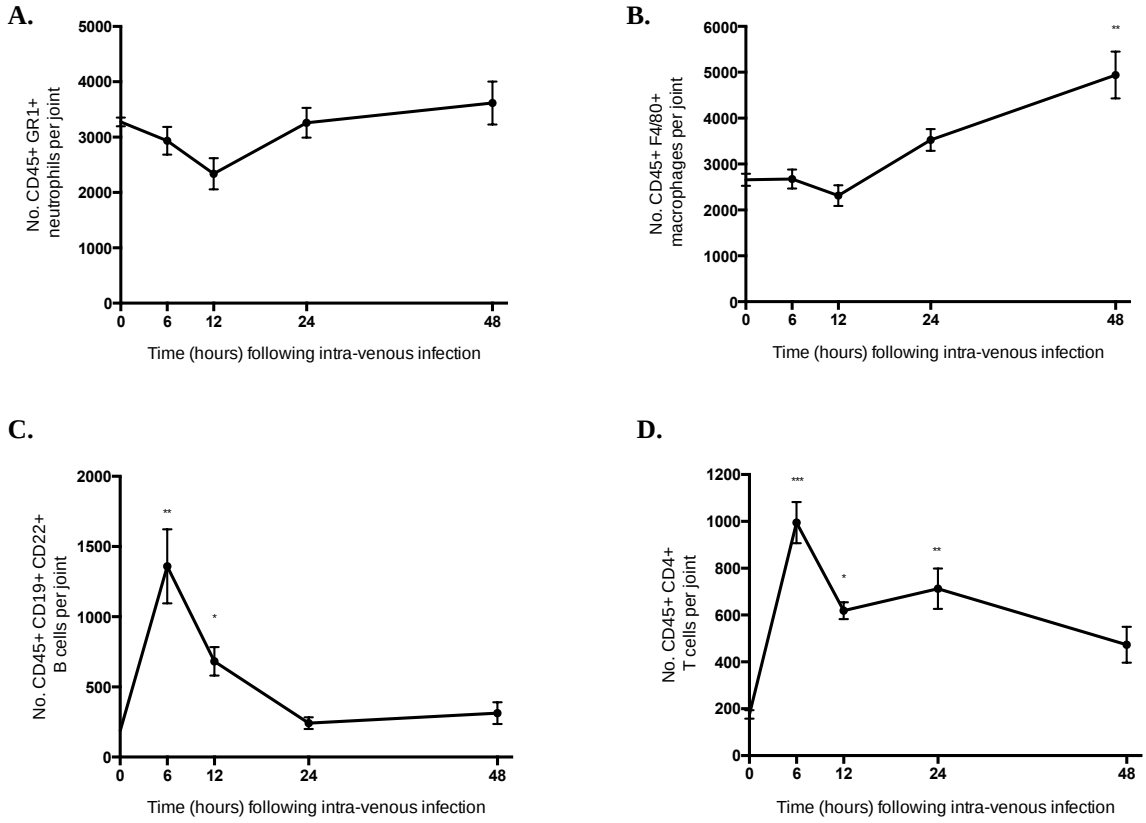

Figure 61 – Phenotypic characterisation of cells recruited into the knee joints of animals infected with *in vivo* recovered *emm* type 1.0 isolate 101910

A) Measurement of neutrophils B) macrophages C) B-cells, and D) CD4 + T-cells in total knee joints of mice at 0, 6, 12, 24, and 48 hours post intravenous infection with *in vivo* recovered *emm* type 1.0 isolate 101910. Samples were collected from 10 mice/time point from 2 independent experiments and data are reported as mean ± SEM. Statistical analysis was performed using a two-tailed Mann-Whitney U-test comparing single time points against time 0 (*$p < 0.05$, **$p < 0.01$ and ***$p < 0.005$).

6.6.2 Comparison of immune cell recruitment

The number of cells in the knee joints were compared during infection with *emm* type 1.0 isolate 101910 and host-adapted *emm* type 1.0 isolate 101910 at 0, 6, 12, 24 and 48 hours, to investigate any differences in immune cell recruitment between the two infection types.

All of the cell types analysed showed clear differences between the number of cells present in the knee joint at the early time points (0-12 hours), with CD4+ T cells alone showing any difference in cell numbers beyond 12 hours. The number of neutrophils present in the joint at 12 hours were significantly higher during infection with the wildtype bacteria in comparison to the infection with host-adapted bacteria ($p < 0.005$) (Figure 62a). The same pattern was also observed for macrophage cell numbers. At 12 hours there were significantly more macrophages recruited to the site of infection with the wildtype isolate than with the host-adapted bacteria ($p < 0.01$) (Figure 62b). For both B cells and CD4+ T cells the number of cells recruited to the joint was significantly higher at 6 hours during infection with host-adapted bacteria ($p <0.005$, $p < 0.01$). After 6 hours, the number of B cells do not significantly differ between the two infections (Figure 62c). For CD4+ T cells as the infection progressed the cell numbers returned to similar cell counts at 12 and 24 hours. At 48 hours, the number of cells in the knee joint during infection with the wildtype continued to increase, whereas with the host-adapted isolate the number of cells decline ($p < 0.01$) (Figure 62d).

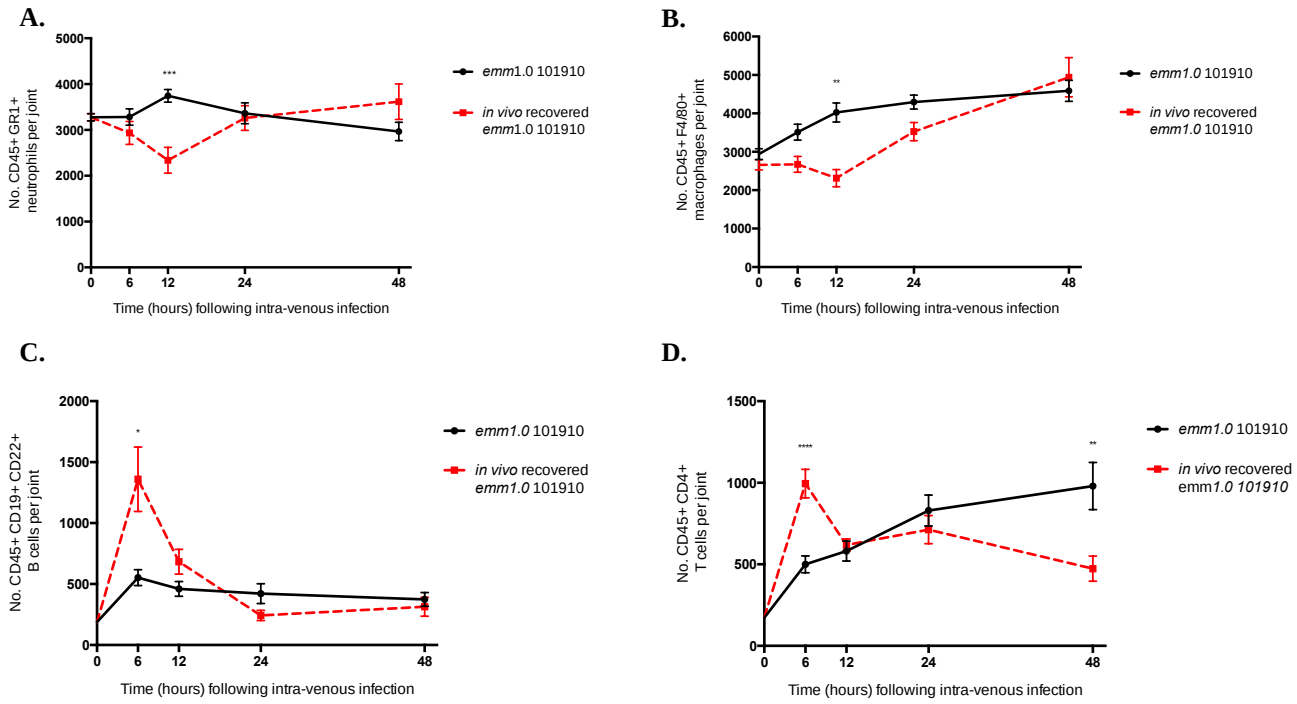

Figure 62 – Comparison of cells recruited into the knee joints of animals infected with *emm* type 1.0 isolate 101910 and *in vivo* recovered *emm* type 1.0 isolate 101910.

A) Measurement of neutrophils B) macrophages C) B-cells, and D) CD4 + T-cells in total knee joints of mice at 0, 6, 12, 24, and 48 hours post intravenous infection with *emm* type 1.0 isolate 101910 and *in vivo* recovered *emm* type 1.0 isolate 101910. Samples were collected from 10 mice/time point from 2 independent experiments and data are reported as mean ± SEM. Statistical analysis was performed using a two-tailed Mann-Whitney U-test comparing single time points for each infection type (*$p < 0.05$, **$p < 0.01$, ***$p < 0.005$, and ****$p < 0.001$).

6.7 Identification of T regulatory cells during chronic infection of the knee joints

We previously showed that CD4+ T cells are found in the knee joint during GAS septic arthritis and previous studies have shown that in experimental models with *S. aureus* they have a dualistic role in both inflammation and clearance [54]. It was further characterised which subsets of T cells are involved in the course of the infection. The extended septic arthritis model of 7 days was used to identify T regulatory cells (Tregs) (n = 5) in the knee joint during infection with *emm* type 1.0 isolate 101910 and *in vivo* recovered host-adapted isolate 101910 in comparison to naïve mice (Figure 63). Tregs were gated based on CD45+, CD4+ and FoxP3+ staining (Figure 63)

The highest number of Tregs found in the knee joints were observed in mice infected with host-adapted 101910 wherein there were significantly more cells than in the knee joints of the naïve controls ($p < 0.05$) (Figure 63). Infection with wildtype 101910 also resulted in more Tregs in the joint in comparison to the control, although this was not statistically significant (Figure 63).

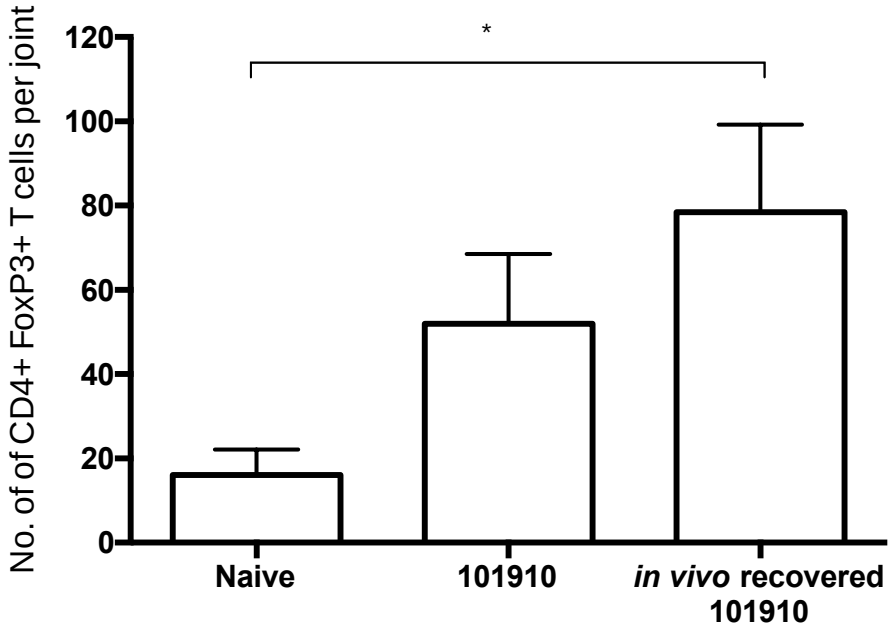

Figure 63 – Identification of T regulatory cells recruited into the knee joints.
Measurement of Foxp3+ CD4+ T-cells in total knee joints of mice at 7 days post intravenous infection with *emm* type 1.0 isolate 101910 and *in vivo* recovered *emm* type 1.0 isolate 101910. Samples were collected from 5 mice/time point from 2 independent experiments and data are reported as mean ± SEM. Statistical analysis was performed using a two-tailed Mann-Whitney U-test comparing single time points against naïve control (*$p < 0.05$).

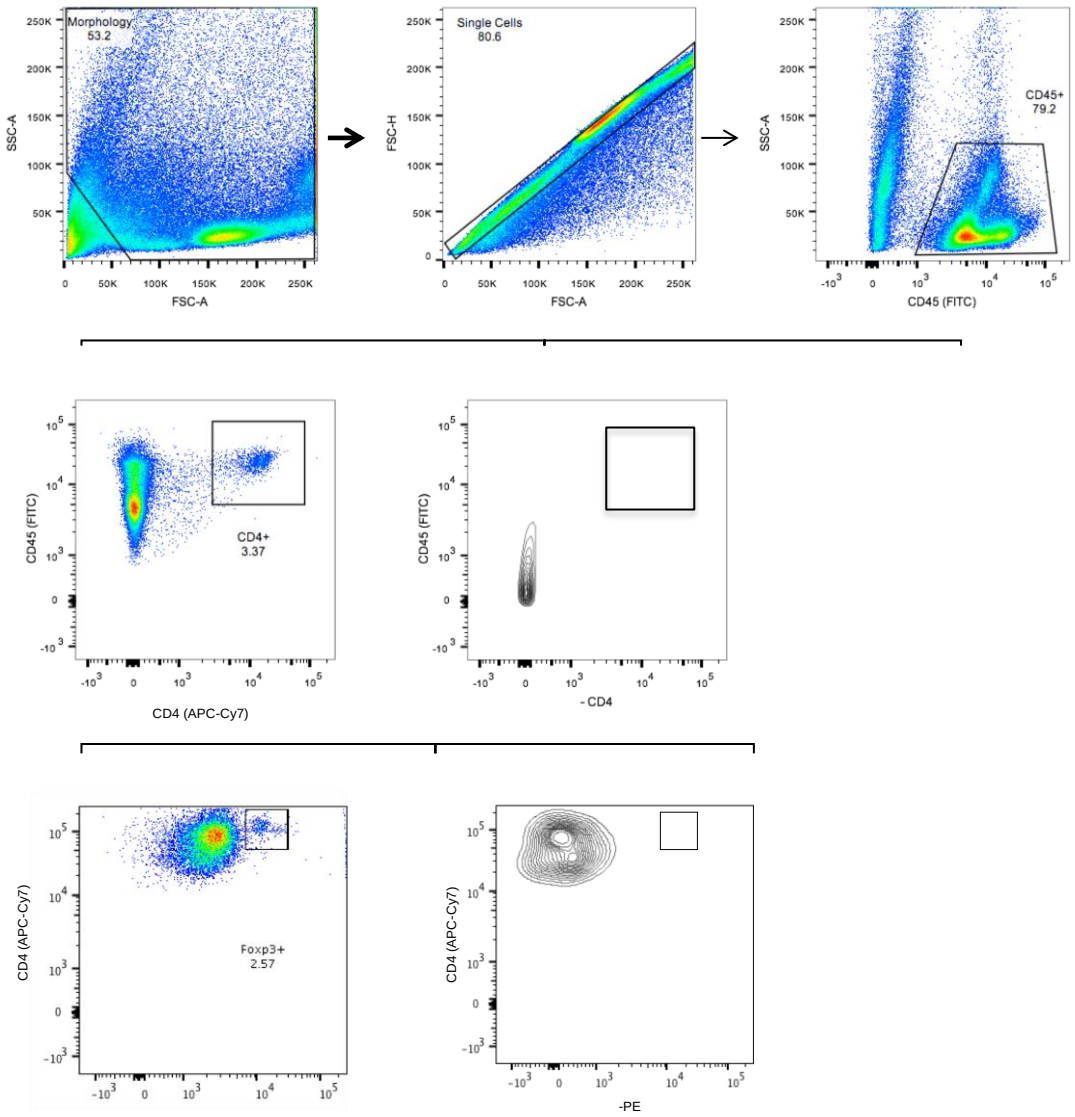

Figure 64 – Gating strategy for the analysis of T regulatory cells in knee joints. The flow cytometry analysis was used to identify different immune cell subsets in knee joints of GAS intravenously infected animals. On the X and Y-axes are reported different markers utilised for the specific analysis, cell types described along with percentage of CD45+ cells. Gates identify the different cell subsets analysed. Alongside are the negative controls.

6.8 Role of CCR5 and CXCR3 CD4+ T cells in the knee joint

CCR5 and CXCR3 are primarily expressed during a Th1 CD4+ T cell phenotype and recent studies have shown that there is selective recruitment of CD4+ T cells that express these two receptors into the synovium of people with rheumatoid arthritis [314]. Synovial fibroblasts and macrophages produce the ligands to CCR5 and CXCR3 in abundance during inflammation [315, 316]. As there was an infiltration of CD4+ T cells into the knee joints during infection with *emm* type 1.0 isolate 101910. The aim was to characterise further what types of CD4+ T cells were entering the joint and whether the rapid infiltration was linked to the production of the chemokine RANTES. The number of CCR5+ CD4+ T-cells, CXCR3+ CD4+ T-cells, CCR5+ CXCR3+ CD4 + T-cells and the chemokine RANTES were measured in total knee joints of mice at 0, 6, 12, 24, and 48 hours post infection (Figure 65). Cells were stained and gated based on the above markers (Figure 66).

6.8.1 CCR5/CXCR3 T cells in knee joint during infection with *emm* type 1.0 isolate 101910

The total number of CD4+ T cells expressing CXCR3 did not change significantly from the baseline, until the 48 hour time point. At 48 hours, there were significantly more CXCR3 T cells recorded to be present ($p < 0.005$) (Figure 65a). This corresponds to when the highest number of CD4+ T cells were found in the joint (Figure 61d) indicating that the high influx of CD4+ T cells at 48 hours predominantly express CXCR3. The number of CD4+ T cells expressing CCR5 increased in the joint, and at 12 hours there were significantly more present in the joint ($p < 0.005$). The number of cells with this phenotype continued to increase over

the time course (Figure 65b). The same pattern was also observed for double positive (CXCR3 and CCR5) CD4+ T cells, where there were significantly more found in the joint from 12 hours onwards, suggesting that the majority of CCR5 positive cells were also CXCR3 positive (Figure 65c).

The chemokine RANTES is the ligand to CCR5 and attracts cells that express the CCR5 receptor [317]. The concentration of RANTES found in the joint increased as the bacterial load in the joint increased. RANTES was found at high concentrations even at the earliest time point of 6 hours, the time point when bacteria initially colonise the joint (Figure 65d). The amount of RANTES continued to increase up to the final time point of 48 hours ($p < 0.001$) (Figure 65d), this corresponded with the increase in CCR5 positive T cells entering the knee joint. The association between the amount of RANTES and the number of CCR5 CD4+ entering the joint suggests that the chemokine could be responsible for the rise in CD4 T cells early on in infection.

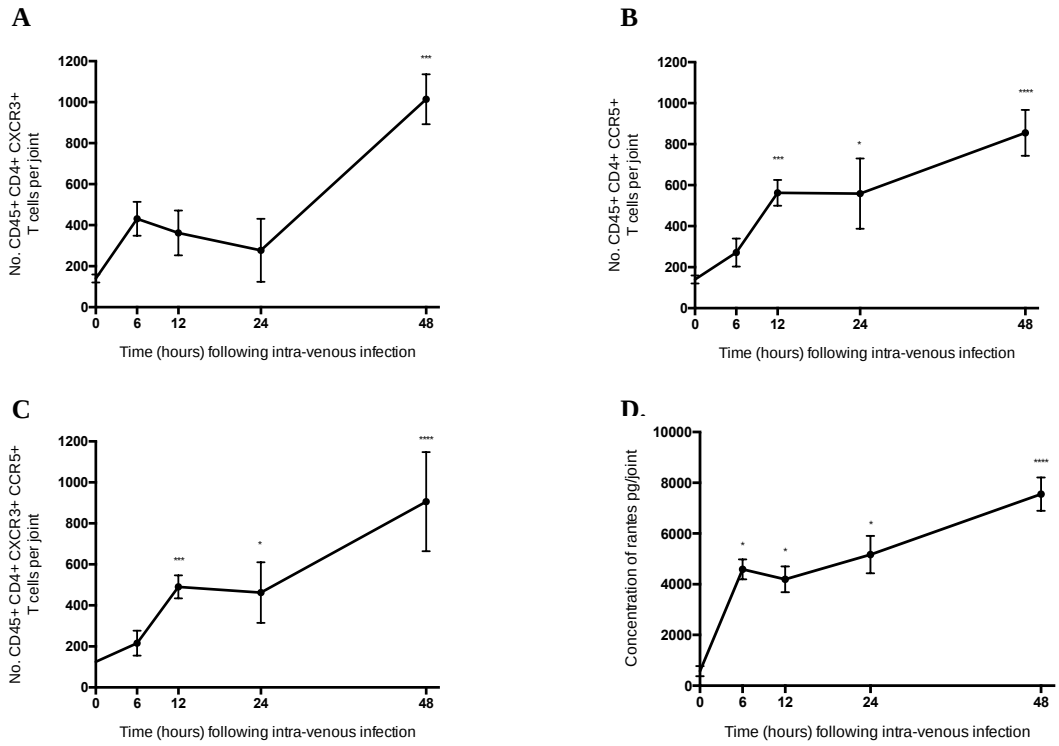

Figure 65 – Phenotypic characterisation of populations of T cells recruited into the knee joints of animals infected with *emm* type 1.0 isolate 101910

A) Measurement of CCR5+ CD4+ T-cells B) CXCR3+ CD4+ T-cells, C) CCR5+ CXCR3+ CD4 + T-cells and D) the chemokine RANTES in total knee joints of mice at 0, 6, 12, 24, and 48 hours post intravenous infection with *emm* type 1.0 isolate 101910. Samples were collected from 10 mice/time point from 2 independent experiments and data are reported as mean ± SEM. Statistical analysis was performed using a two-tailed Mann-Whitney U-test comparing single time points against time 0 (*$p < 0.05$, ***$p < 0.005$ and ****$p < 0.001$)

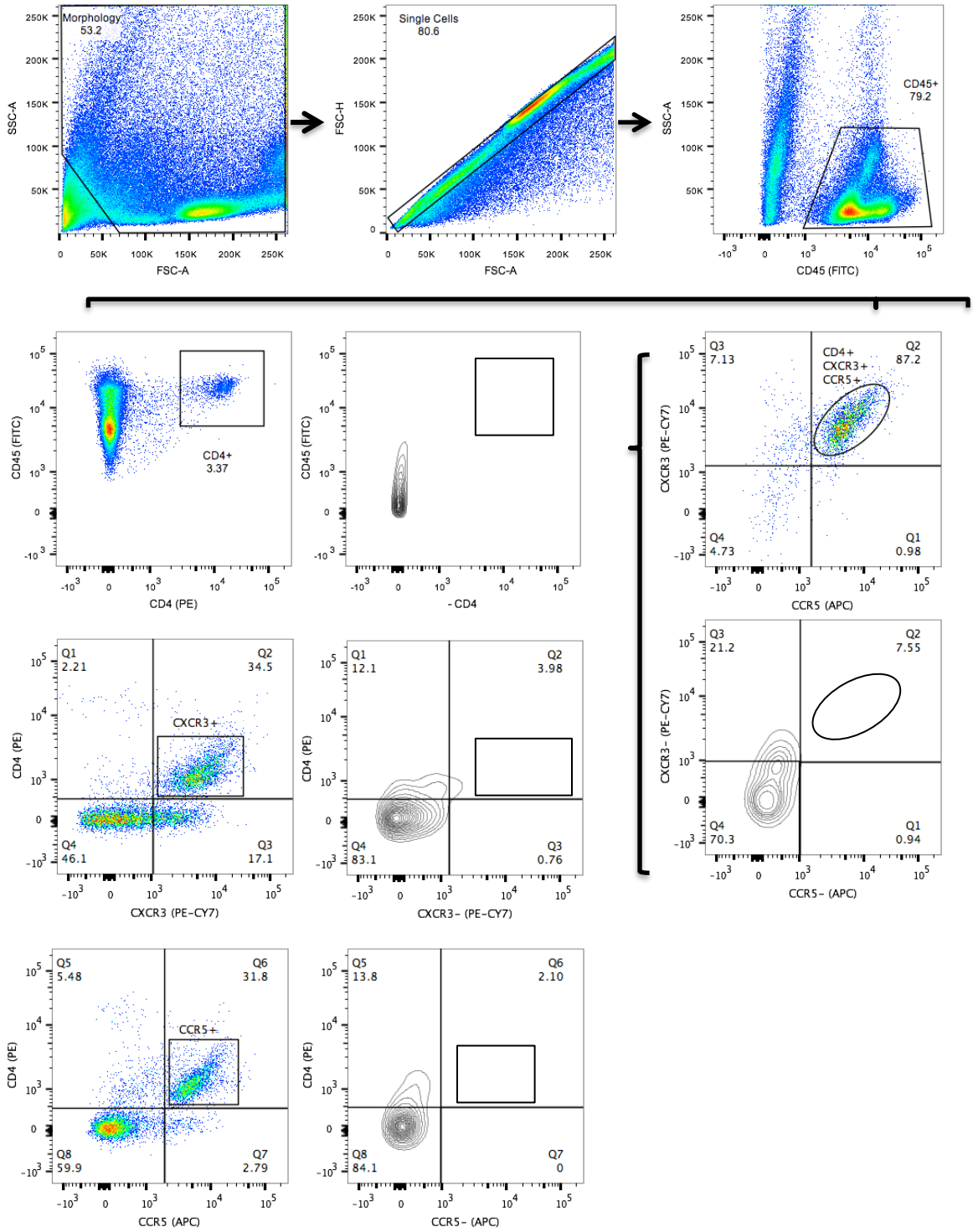

Figure 66 – Gating strategy for the analysis of CXCR3+/CCR5+ CD4+ T-cells in knee joints.

The flow cytometry analysis was used to identify different immune cell subsets in knee joints of GAS intravenously infected animals. On the X and Y-axes are reported different markers utilised for the specific analysis, cell types described along with percentage of CD45+ cells. Gates identify the different cell subsets analysed. Alongside are the negative controls.

6.8.2 CCR5/CXCR3 T cells in knee joint during infection with host-adapted *emm* type 1.0 isolate 101910

During infection with *in vivo* recovered host-adapted *emm* type 1.0 isolate 101910 there was a peak in the number of CD4+ T cells at 6 hours (Figure 61d) which also corresponded to an increase in CCR5 (Figure 67a), CXCR3 (Figure 67b) and double positive T cells (Figure 67c) in the knee joint ($p < 0.01 – p < 0.05$). After 6 hours, the number of CD4+ T cells expressing CCR5 and CXCR3 returned to similar cell numbers observed at time 0.

The chemokine RANTES was observed to rapidly increases in the joint, resulting in a significantly higher concentration at 12 hours ($p < 0.005$). RANTES continued to increase up to 48 hours ($p < 0.005$) (Figure 67d).

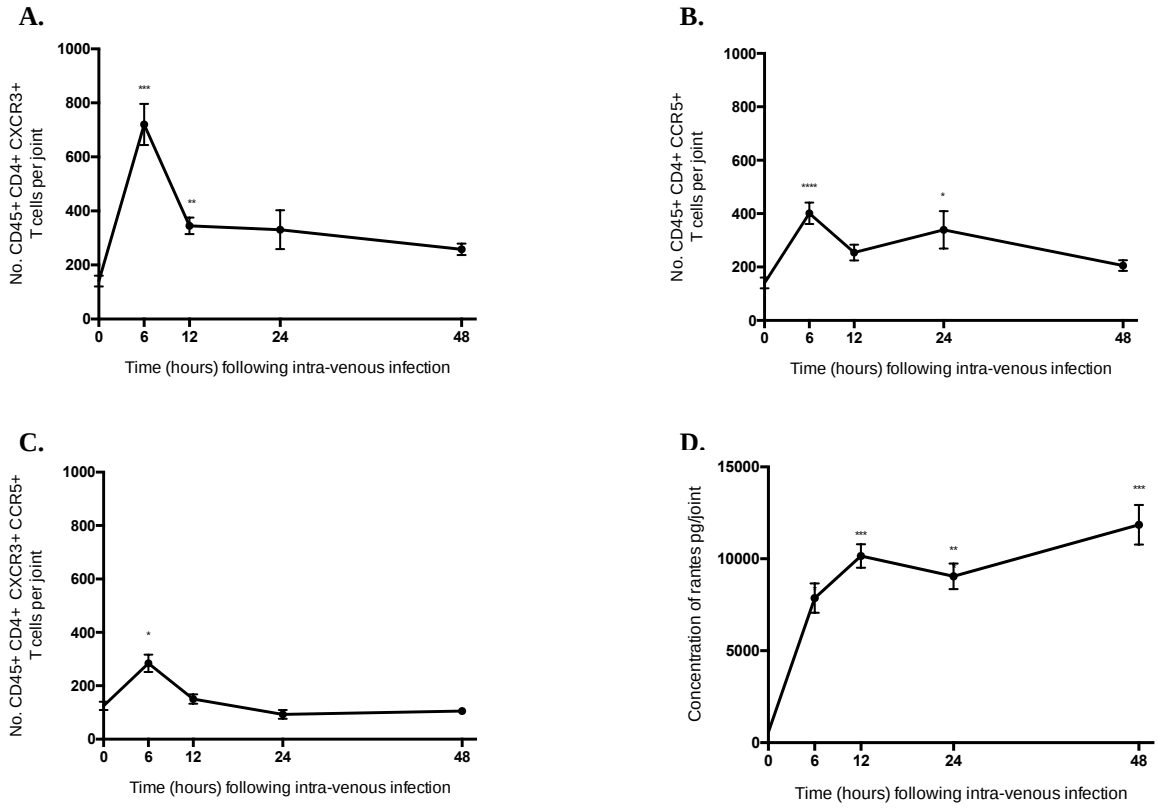

Figure 67 – Phenotypic characterisation of populations of T cells recruited into the knee joints of animals infected with *in vivo* recovered *emm* type 1.0 isolate 101910

A) Measurement of CD4+ T-cells B) CCR5+ CD4+ T-cells C) CXCR3+ CD4+ T-cells and D) CCR5+ CXCR3+ CD4 + T-cells in total knee joints of mice at 0, 6, 12, 24, and 48 hours post intravenous infection with *in vivo* recovered *emm* type 1.0 isolate 101910. Samples were collected from 10 mice/time point from 2 independent experiments and data are reported as mean ± SEM. Statistical analysis was performed using a two-tailed Mann-Whitney U-test comparing single time points against time 0 (*$p < 0.05$, **$p < 0.01$, ***$p < 0.005$ and ****$p < 0.001$).

6.9 Spe A deficient *emm* type 1.0 isolate 101910

To be able to examine the role of the superantigen SpeA in GAS-induced septic arthritis an isogenic deletion mutant was developed for further investigations in the septic arthritis murine model. An isogenic deletion mutant of *emm* type 1.0 isolate 101910 was constructed through double-crossover allelic replacement of SpeA with aphA3 (encoding kanamycin resistance). Regions directly upstream and downstream of SpeA (~ 1000 bp each) were amplified and then stitched together in a second round of PCR before they were ligated into the pGEM-T vector (Promega) (Figure 42), generating pGEM-T-ΔspeA-2kb (Figure 68).

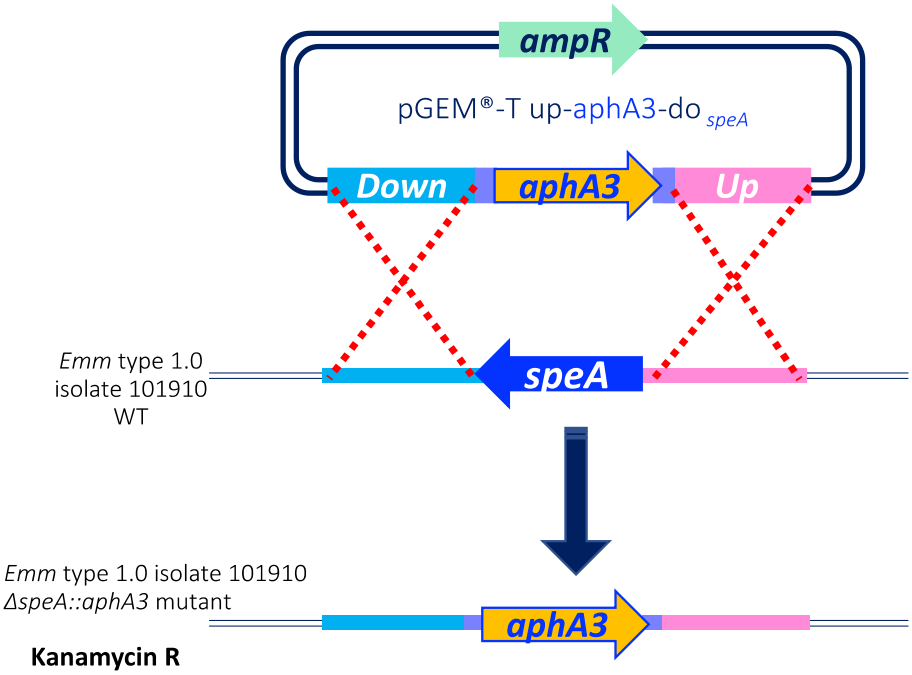

Figure 68 – Allelic replacement of Spe-A gene with aphA3 Kanamycin resistance gene, using pGEM®-T Vector.

Spe A deletion mutant of *emm* type 1.0 isolate 101910 was constructed through double-crossover allelic replacement of SpeA with aphA3 (encoding kanamycin resistance). Regions directly upstream and downstream of SpeA (~ 1000 bp each) were amplified and then stitched together in a second round of PCR before they were ligated into the pGEM-T vector generating pGEM-T-ΔspeA-2kb.

6.9.1 Effect of Spe A on progression of septic arthritis

There have been recent studies that have shown that the arthritogenicity of different strains of *S. aureus* is dependent on the superantigen profile of the bacteria [234]. To consider whether the deletion of SpeA had any effect on the progression of the infection with GAS, mice were intravenously infected with *emm* type 1.0 isolate 101910 and isolate ΔSpeA 101910 (n = 5 per time point). The arthritic index of the mice was calculated and at 6 and 48 hours the bacterial load in the knee joints were assessed.

There were no significant differences between the bacterial load of both isolates at 6 and 48 hours (Figure 69a). Although at 48 hours the CFU of ΔSpeA isolate 101910 is 1 log higher than during infection with the wildtype (Figure 69a). There were also no differences in the severity of the infection as the arthritic index for each was almost identical throughout the course of the infection (Figure 69b).

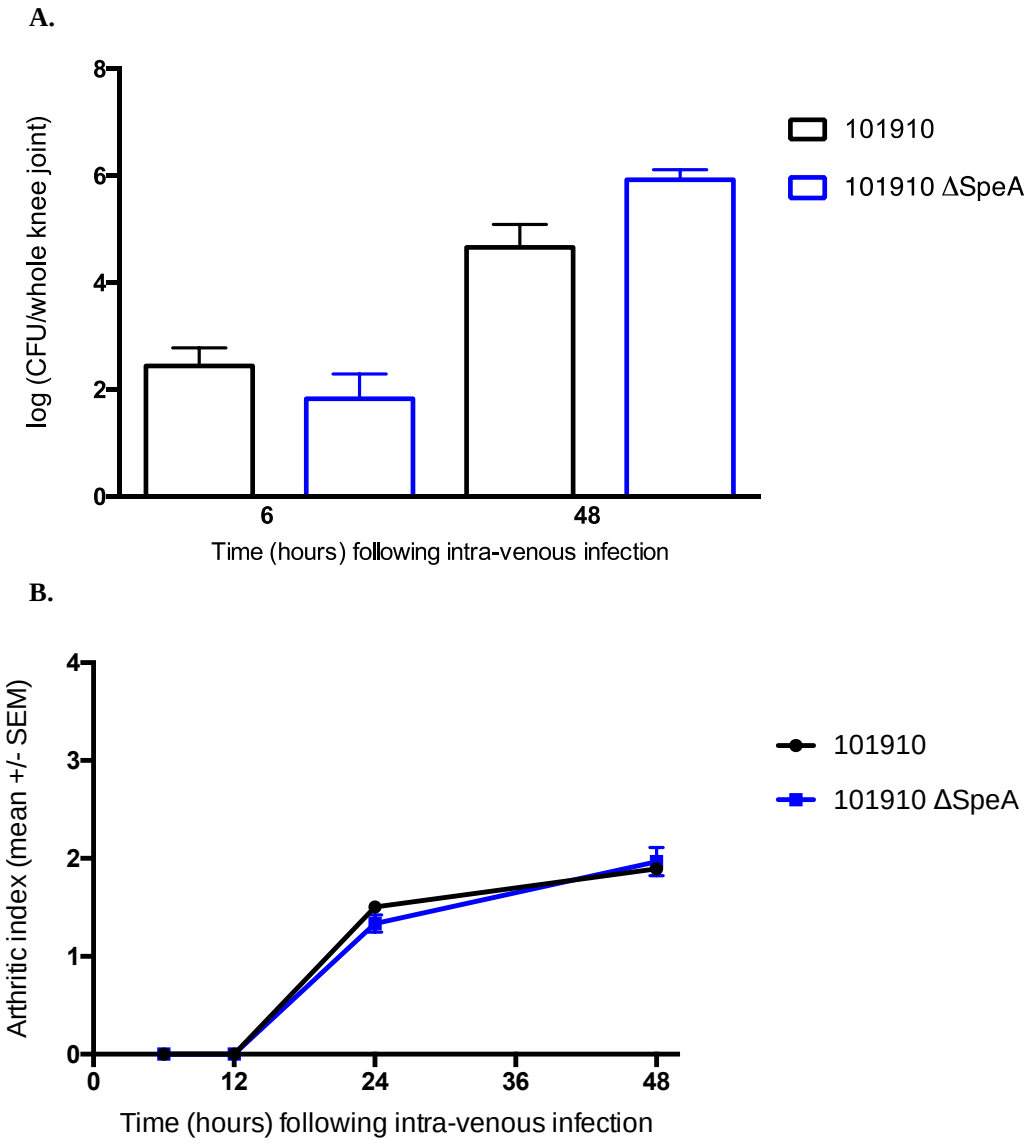

Figure 69 – Comparison of bacterial CFU in the knee joints and the arthritic index after intravenous infection with *emm* type 1.0 isolate 101910 and ΔSpeA 101910.

(A) The bacterial CFU in knee joints of CD1 mice (n = 10, knee joints n = 20) following intravenous infection with 10^7 CFU (50 μ l) of *emm* type 1.0 isolate 101910 (black lines) and Δ SpeA 101910 (blue lines). (B) Arthritic index calculation over time. Displayed as mean ± SEM.

6.9.2 Comparison of immune cells

To compare the inflammatory response in between the wildtype and Spe A mutant, the number of neutrophils, macrophages, B cells and T cells in the knee joints were analysed at 6 and 48 hours.

Firstly, the number of neutrophils in the joint was lower during infection with the mutant at both 6 (p = ns) and 48 hours ($p < 0.05$) in comparison to the wildtype (Figure 70a). There were also significantly less macrophages present in the joint during infection with the mutant at both 6 ($p < 0.01$) and 48 hours ($p < 0.001$) in comparison to the wildtype (Figure 70b). There were no differences between the number of B cells at 6 hours, though at 48 hours there was a significant rise in the number of B cells observed in the joint during infection with the mutant ($p < 0.001$) (Figure 70c). Similarly to that observed with neutrophils and macrophages there were significantly less CD4+ T cells in the knee joints during infection with the mutant at both 6 ($p < 0.01$) and 48 hours ($p < 0.01$) (Figure 70d).

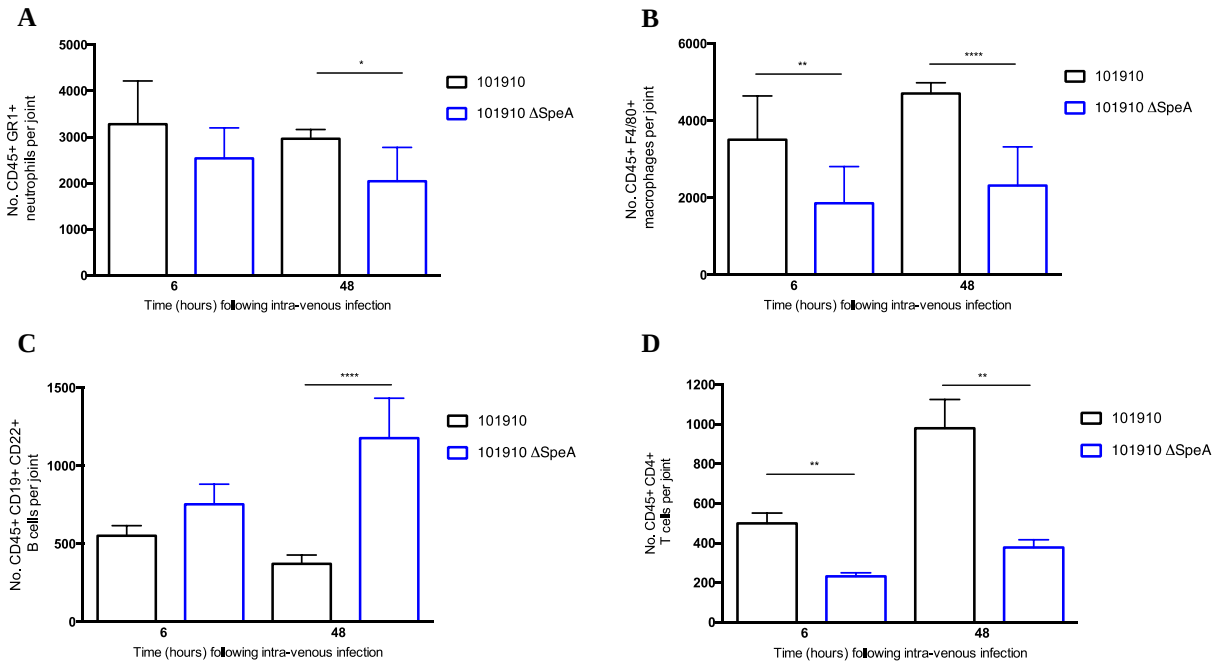

Figure 70 – Comparison of cells recruited into the knee joints of animals infected with *emm* type 1.0 isolate 101910 and Δ SpeA 101910.

A) Measurement of neutrophils B) macrophages C) B-cells, and D) CD4 + T-cells in total knee joints of mice at 6 and 48 hours post intravenous infection with *emm* type 1.0 isolate 101910 and Δ SpeA 101910. Samples were collected from 5 mice/time point from 2 independent experiments and data are reported as mean ± SEM. Statistical analysis was performed using a two-tailed Mann-Whitney U-test comparing single time points, (*$p < 0.05$, **$p < 0.01$, ***$p < 0.005$ and ****$p < 0.001$).

C. Discussion

GAS causes severe infections of the joint, that is often difficult to treat as the disease progresses quickly and often results in a chronic infection. Using the haematogenously-derived murine model of GAS septic arthritis, this study aimed to characterise the immune profile in the knee joints during infection. *Emm* type 1.0 isolate 101910 was used to initiate the infection alongside the host adapted version of this isolate (recovered from a previous knee joint infection). Multiple parameters were quantitatively measured including CFUs, arthritic index, cytokines, and immune cell recruitment across various time points. Bacteria rapidly colonised the knee joint and proliferated resulting in a potent inflammatory response which persisted.

The release of cytokines into the synovium of the joint begins as soon as bacteria colonise the knee joint at 6 hours. Pro-inflammatory cytokines IL-1β and IL-6β increase rapidly at the start of the infection, followed by a delayed rise in two other pro-inflammatory cytokines TNF-α and IL-8. As the growth of bacteria stabilises in the joint and the acute infection takes a more chronic form, the cytokine profile changes with all the cytokines measured, except TNF-α returning to baseline concentrations. These results are consistent to those observed during infection with *S. aureus* [54]. TNF-α, IL-1β and IL-6 have all been found to be significantly involved in the severe inflammation that precedes cartilage and bone destruction in *S. aureus* septic arthritis. However, these cytokines are also relevant to protect the host and are essential for clearance of bacteria from the joint [244, 264, 318]. TNF-α, IL-1β and IL-6 stimulate osteoclast differentiation through interactions with the known triad osteoprotegerin (OPG)/receptor activator of NF-Kb (RANK)/RANK

ligand (RANKL) [319]. Osteoclasts are multinucleated giant cells which resorb mineralised tissue (i.e bone) resulting in the remodelling and breakdown of bone tissue [319, 320]. All three cytokines have been found to stimulate osteoclastogenesis synergistically, with the net outcome being a net increase in RANKL activity which is also responsible for the direct stimulation of osteoclastic differentiation and inhibition of osteoclast apoptosis [319]. It is concerning that in GAS septic arthritis the levels of TNF-α continue increasing, as TNF-α is considered the most osteoclastogenic cytokine out of the three described. This could indicate why GAS induced septic arthritis in mice produces a more severe form of the infection with much more rapid joint destruction in comparison to *S. aureus in vivo* models which can be extended up to 3 months [321].

In addition, host inflammatory cells begin to enter the joint resulting in the further release of inflammatory cytokines [54]. Firstly, considering the phagocytic cells, macrophages enter the joint early after colonisation of bacteria (12 hours) and begin to increase up to 72 hours, after this they start to reduce in numbers in the knee joint. Macrophages are associated with the release of more inflammatory cytokines including IL-8 [54, 322]. This is consistent with our data as the concentration of IL-8 only increases when the number of macrophages are at the highest in the joint. The concentration of IL-8 then decreases as the number of macrophages decrease in the joint after 72 hours. IL-8 is a major neutrophil chemoattractant, and in this model, there is an increase in the number of neutrophils after a significant rise in IL-8 in the joint [60]. Neutrophils slightly peak at 12 hours with more entering the joint as the infection progresses. Neutrophil numbers continue to increase in the joint and at 7 days the number of neutrophils peak and they are also the most common immune cell

type now found in the joint. The high numbers of neutrophils still present at 7 days could be due to them being the predominant cell type found in the abscesses that form, as seen in experimental arthritis with *S. aureus* [60, 323]. *In vivo* models with *S. aureus* have also shown the dualistic properties of both neutrophils and macrophages in septic arthritis. They are indispensable in the early phase of disease and subsequent host survival but are also key mediators of tissue-destructive events [322, 323]. Studies have shown that the elimination of phagocytic cells from the site of inflammation is essential for the resolution of the acute inflammatory response, and that persistence of neutrophils and macrophages leads to subsequent tissue damage [322, 323]. Neutrophils and macrophages contribute to bone and tissue damage through the release of more pro-inflammatory cytokines, free-radicals and tissue degrading enzymes [61, 322, 323].

It has been previously reported that B cells do not play a major role in *S. aureus* infections and in particular in septic arthritis [324]. However, our results show that the number of B cells rapidly increases in the joint during the early stages of infection (6 hours) which is followed by quick suppression of B cell numbers to levels even below baseline levels. This suggests that GAS could be directly involved in suppressing B cell responses during infection than in comparable septic arthritis incidence. Another study of *S. aureus* septic arthritis also found that B cells may be important in the early stages of infection, and that *S. aureus* has a number of known mechanisms including utilisation of superantigens to supress the B cell response. The known effects of B cell responses could be underestimated in septic arthritis as recently described in the literature [321].

In contrast to B cells, T cells and their cytokines have been shown to be clearly involved in septic arthritis. The contribution of T cells was initially proposed due to the presence of CD4+ T cells found in the affected joints of mice with *S. aureus* induced arthritis [312]. We found that CD4+ T cells were recruited to the site of infection early during infection (as early as 6 hours) and the numbers continued to increase up to 72 hours after which the cell type decreased. At 7 days, there was no longer a significant increase over the number of cells at day 0. CD4+ T cells have been implicated directly in contributing to joint destruction, as *in vivo* depletion of CD4+ T cells results in a considerably milder course of staphylococcal induced arthritis [312]. T cells are specifically activated by bacterial antigens on host antigen-presenting cells or non-specifically in the case of bacterial superantigens [164, 325]. Superantigens can stimulate a large proportion of T cells, which is followed by further proliferation and secretion of cytokines [61, 240]. A considerable number of CD4+ T cells enter the joint over the course of the infection and as such work was done to characterise the subsets of T cells found in the affected joint. Tregs are a class of effective T helper cell characterised by the expression of X-linked forkhead transcriptional repressor (FoxP3). Tregs are either naturally occurring or induced by antigens and play a fundamental role in immunological tolerance [326]. We found a small peak in the number of Tregs at 7 days in the joints of mice infected with GAS *emm* type 1.0 bacteria compared to naïve control mice. An increased population of Tregs may be induced to counteract the inflammatory environment generated immediately after bacterial colonisation. Another study using an experimental model of septic arthritis with *S. aureus*, looked at the role of Th17 and Treg cells over the course of the disease [325]. They found that arthritic inflammation was induced through Th1 polarisation followed by a Th17/Treg immune response which

corresponded to tolerance, and they hypothesised that the transfer of fully active Tregs may contribute to a novel treatment strategy in septic arthritis [325].

T cells that infiltrate inflammatory sites are often activated T cells, and the mechanism of how these cells enter infected/inflamed tissues so rapidly is unclear [327]. The control of T cell migration appears to be regulated by an intricate balance of chemokines and their receptors [327, 328]. Important chemokines are usually for the CXCR3 and CCR5 receptors, including IP-10 and RANTES respectively [314, 327]. It was observed that nearly all T cells (>90%) expressed CXCR3 across all time points, and the expression of CCR5 increased over time. At 48 hours both CCR5 and CXCR3 were expressed by approximately 80% CD4+ T cells. This phenotype of T cells has also been explored in experimental models of rheumatoid arthritis and the same results were observed [314, 316, 327]. Taking together our results and previous studies with rheumatoid arthritis it could suggest that the chemokine receptor CXCR3 and CCR5 are markers for T cells associated with inflammatory diseases independent of whether this is due to an infectious agent such as GAS or an autoimmune response [327]. We also observe a significant increase in the concentration of RANTES over the course of the infection, and this increase correlates with an increase in the infiltration of CCR5 CD4+ T cells. This is consistent with other studies that have highlighted the crucial role of RANTES in mediating intensity and composition of cellular infiltration in rheumatoid arthritis [315, 317, 327].

Phenotypic heterogeneity within an infection is key to the adaptive success of GAS in specific niches [329, 330]. Studies have shown that adaptation to diverse within-

host niches drives phenotypic heterogeneity of GAS during infection and the establishment of specially adapted sub-lineages [329-332]. GAS recovered from the knee joints and then used to induce septic arthritis resulted in higher density colonisation of the joint more rapidly along with more severe joint damage. We aimed to characterise if there were any differences in the host immune response in the joints to infection with *in vivo* recovered bacteria in comparison to the wildtype. Neutrophils and macrophages did not infiltrate the joints as rapidly during infection with *in vivo* recovered bacteria and the number of cells found in the joint were significantly lower for both cell types at 12 hours. Although it has been shown that the inflammatory effects of phagocytes result in severe inflammation in the joint that precedes joint damage, it has also been observed that early infiltration by lymphocytes is key to controlling bacterial proliferation through phagocytosis. It is also important to note that bacterial proliferation and the secretion of bacterial products also have a direct effect on cell and tissue damage. The decreased number of phagocytes early in the joint could explain why there are a higher number of CFU recovered from knee joints of mice infected with *in vivo* recovered bacteria at the earlier time points. Neutrophils and macrophages continue to infiltrate the joint and by 48 hours the cell numbers are almost identical between the two infection types. There is a rapid infiltration of CD4+ T cells into the joint at the earliest time point of 6 hours, which corresponds to the time at which bacteria colonise the joint, this is significantly higher than what is observed in the wildtype infection. Interestingly after 6 hours the CD4+ T cells begin to reduce in number in the joint and at 48 hours are significantly lower than the wildtype infection. The number of Tregs in the joint were also compared and the number of Tregs found in the *in vivo* recovered joints was significantly higher than the naïve mice. This may suggest that the initial surge

in joint tissue-damaging CD4+ T cells may initiate a rise in Tregs entering the joint which then work to control the inflammation. This also corresponds to there being a significant reduction in the number of CXCR3 and CCR5 positive CD4+ T cells during infection with *in vivo* recovered bacteria even though there is more RANTES being secreted, and we have identified these cell types as being a marker of inflammation. As seen during infection with the wildtype bacteria we see a sharp rise in the number of B cells early in the infection (6 hours) and as the disease progresses the numbers of B cells are supressed to that lower of even basal levels. Examining the cell profile found in the knee joints of mice infected with *in vivo* recovered bacteria it indicates that GAS is able to circumvent the host response early on in infection and establish high density colonisation in the joint before phagocytes are able to clear the infection.

The presence of GAS initiates a strong inflammatory CD4+ T cell response but this is circumvented by infiltrating Tregs into the joint. Inflammation by lymphocytes in the joint may be reduced but the direct effect of high bacterial numbers which are not being cleared by the host response results in severe tissue damage and a much more serious arthritic phenotype. Although the molecular mechanisms are unclear this is an example of how the bacteria has adapted to successfully establishing an infection in the joint and how it has become pathoadaptive to the joint space by modulating its interaction with the host response. There have been recent studies that have also identified GAS becoming more adapted to the host niche, isolates of *emm* type 1.0 were able to bind collagen much more avidly after *in vivo* passage in a model of acute rheumatic fever [333]. We have also demonstrated in the previous chapter how

GAS is able to regulate its SLO production both *in vivo* and *in vitro* indicating there are mechanisms that GAS uses to adapt to its host during infection.

As previously described strains of GAS can produce a number of different virulence factors including superantigens which may contribute to its potential athritogenicity. The possible contribution of superantigens in septic arthritis was described by Bremell and Tarkowski who demonstrated that rats infected with superantigen producing *S. aureus* strains preferentially developed arthritis over strains lacking superantigens at a ratio of 4:1 [234]. The superantigen SpeA has commonly been associated with *emm* type 1.0 and is often found in cases of invasive disease and streptococcal toxic shock syndrome (STSS) [164, 165]. Genomic analysis of the isolates of GAS collected during the Merseyside outbreak showed that *emm* type 1.0 isolate 101910 contained the gene encoding SpeA whereas the other isolates had a different superantigen profile [266]. To consider whether SpeA had any role in the ability of isolate 101910 to induce septic arthritis we produced an isogenic deletion mutant of SpeA was developed for use in the septic arthritis murine model. Surprisingly, infection with the SpeA deletion mutant failed to attenuate virulence and we did not see any differences in the severity of arthritis by visible joint damage. There were no significant differences in the CFU counts in the knee joints, although at 48 hours the mutant did have 10-fold more bacteria in the joint. There was also less infiltration by neutrophils, macrophages and CD4+ T cells to the site of infection. Sriskandan *et al*., also found similar results in a model of GAS muscle infection, where SpeA knockout resulted in increased bacteraemia and reduced neutrophil infiltration [334]. These results were attributed to the reduced binding affinity of superantigens to murine MHC class II molecules. Further experiments

using the same model with HLA-DQ transgenic mice resulted in the animals being susceptible to SpeA [335]. These studies could explain why here there were no differences in disease outcome when using the SpeA mutant. However, there is an increase in the number of B cells found in the knee joint at 48 hours with the mutant whereas in the wildtype the numbers of B cells decrease as the infection progresses. This could suggest there is some interaction between SpeA and B cells that would need to be investigated further. Typically, SpeA is not commonly associated as being a B cell superantigen, however, the increase observed could be due to a general change in the immune profile of the joints during infection with the mutant.

Murine models have proven to be a useful way of studying the pathogenesis of GAS and in the replication of human disease including sepsis and septic arthritis. Parts of this study highlight some of the limitations in using an animal model in such that mice and humans may have differential sensitivity to certain GAS virulence factors including SpeA. To investigate further the involvement of SpeA and other superantigens in invasive disease it would be interesting to employ a transgenic strain of mice that was susceptible to the effects of superantigens. It may also be useful to investigate whether a long term chronic model of GAS septic arthritis can be developed by using different strains or gender of mice.

In conclusion, this study shows that certain strains of GAS can result in a severe septic arthritis phenotype which results in a potent immune response which may cause further damage to the joint and surrounding tissue. Interestingly, passaging GAS can result in a more pathoadaptive strain to the joint and including changes in the modulation and activation of the host immune response.

7. General discussion

Diseases caused by GAS have been well documented over the last few centuries and historically GAS was the first organism to be recognised as the cause of communicable disease [1]. In turn, hygiene and asepsis was introduced into medical practice. Medical and scientific research using GAS has had a major role in understanding the pathogenesis of infectious diseases including the development of antibiotics and in genetic engineering with the revolutionary development of the CRISPR-Cas9 system. While we have come to know a vast amount about GAS and its associated diseases, there is still much to learn, especially as GAS continues to cause outbreaks of invasive infection and scarlet fever across the globe. Also, treatment of GAS infections relies solely on antimicrobial therapy with no licenced vaccine available to limit the disease burden. The major theme of this thesis was to assess the virulence characteristics of GAS isolates collected during an outbreak of a novel *emm* type of GAS in comparison with typical circulating strains using a range of *in vitro* and *in vivo* techniques.

7.1 *Emm* 32.2 resistance to opsonophagocytosis

A standardised killing assay developed by the CDC was chosen to measure the ability of macrophages and neutrophils to phagocytose and kill different isolates of GAS in the presence of immunoglobulin (IVIG) and complement. Titrated IVIG was used as a source of pathogen specific antibody and baby rabbit complement as a source of complement, both of which are important for opsonisation of the bacteria. Phagocytes tested included a murine macrophage cell line, human neutrophil HL-60 cell line and freshly isolated human peripheral blood neutrophils. Across all types of phagocytes tested *emm* type 32.2 isolates were unique in that they showed a wide range of variability within the *emm* type and further *in vitro* assays assessing whole

blood survival suggested that they would be more invasive in an *in vivo* infection model. These findings are consistent with what has been previously shown in other *emm* types and it is widely accepted that the hallmark of virulence in GAS is in their ability to successfully resist phagocytosis and successfully proliferate in non-immune human blood [336].

7.2 Murine models of GAS

Mouse models of GAS have been widely used to assess the dynamics of host-pathogen interactions, the efficacy of therapeutic drugs and early vaccine efficacy [213]. During the development of murine models, it's important to assess the variation between mouse strain and sex associated with susceptibility [218]. In this study female CD1 mice were used. CD1 mice are an outbred strain, and although they do not provide near-uniform responses as inbred mice do, they do however represent a heterozygous population reflecting some of the natural variation seen in human host responses to infection [337]. The infecting dose and strain of bacteria is also important rendering optimisation to the specific model necessary.

Using the *in vitro* phenotypic tests as a guide to predict pathogenicity *in vivo*, different *emm* type 32.2 isolates were chosen that differed in their ability to resist phagocytosis, survive in whole blood and that had varying levels of capsule thickness and complement deposition. These isolates were used alongside a clinical isolate of a typical invasive infecting *emm* type (*emm* type 1.0) to develop murine models of carriage, pneumonia and systemic infection. In carriage and pneumonia infection models, bacteria were instilled into the host intranasally at a low-volume dose (wherby CFUs remain in the nasopharynx) and high-volume dose (CFUs enters

the lung). For systemic infection, the bacteria are administered intravenously. The data showed that phenotypic characteristics *in vitro* did predict the likely level of pathogenicity during *in vivo* infection. *Emm* type 32.2 was particularly invasive with a high mortality rate in the systemic infection model in comparison with invasive *emm* type 1.0.

In addition, a model of septic arthritis was developed using a haematogenous route of infection which is regarded as the most comparable to natural infection dynamics. There is currently only one published model of GAS septic arthritis that uses this route of infection and the major limitation is that the previous study used a significantly greater dose volume (of 500 μl) at a much higher bacterial CFU which does not necessarily reflect typical infecting bacterial quantities or volume [238]. The data presented in this thesis shows clearance from the blood, entry into the joint and then uncontrolled bacterial proliferation after only a 50 μl infecting dose volume. Using the GAS septic arthritis model, the kinetics and host interactions in the context of infection could be described as further providing a significant contribution to the field of GAS pathogenesis. The isolates of GAS used in the animal infection models were also clinical isolates that were taken from patients that had either sepsis or septic arthritis. Hence, the clinical phenotype was successfully replicated in the murine model highlighting further the importance of developing clinically relevant models of infection to study pathogenesis and host interactions.

7.3 SLO the key to distinct *in vivo* pathotypes

The role of the haemolytic exotoxin SLO in determining disease phenotype was investigated and it was found that differences in production and activity of SLO were central to *in vivo* pathotype and disease outcome in GAS infections. SLO production and activity drove two very distinct *in vivo* pathotypes: *emm* type 32.2 isolates which produced SLO at high levels and with high activity and *emm* type 1.0 isolates with low levels of SLO production and of low activity. The production and activity of SLO correlated directly with their *in vivo* pathotype i.e. high virulence in bacteraemia models accompanied by short host survival (*emm* type 32.2) and low virulence in chronic septic arthritis models accompanied by long term host survival (*emm* type 1.0). The levels and activity of SLO at the time of initial infection determined the disease phenotype, with high levels of SLO driving invasive disease and low levels sustaining chronic joint infections. When removing SLO from the *in vivo* environment, either by gene deletion or by significantly reducing/removing SLO (by supernatant swap or liposome sequestration method), there was a complete reversal in the *in vivo* pathotypes of these *emm* isolates, whereby normally bacteraemia causing *emm* type 32.2 isolates could be made to translocate into joints rather than killing their hosts, and septic arthritis causing *emm* type 1.0 isolates could be made highly invasive, highlighting the crucial role of SLO in determining disease phenotype and outcome *in vivo*.

There have been a number of studies that have shown that SLO is an important virulence factor and that removal of SLO does result in attenuation, although the outcome is highly dependent on the model of infection used [154]. The results presented here have important implications for our understanding of GAS

pathogenesis, by artificially affecting SLO levels one disease phenotype can easily be switched into another. This has significant implications for therapy and vaccines as anti-SLO based treatments may not be the complete answer to protection against all forms of GAS infection. To continue with this work, it would be relevant to develop methods to consider the mechanism by which GAS actually enters and colonises the joint. It would be interesting to identify whether GAS possess any adhesins like *S. aurues* which directly relate to its ability to adhere to certain tissues initiating the infection [54]. One way to approach this could be through genome wide association studies (GWAS), which would involve collecting and sequencing a number of GAS isolates associated with septic arthritis and using this data to highlight potentially important genes that are involved in joint colonisation which could then be validated *in vivo.*

7.4 Host-adapted GAS

The mechanisms that underlie niche adaptation in GAS are not fully understood, with many GAS strains differing in their tissue site preference [338]. Experimental studies have been used to determine that some strains exhibiting high fitness for a specific tissue site have an increase in frequency of tissue-specific adaptive alleles or regulate production of certain proteins [338]. An example of this has been shown using skin-tropic strains that are able to bind to host plasminogen via the plasminogen-binding group A Streptococcal M protein present on the cell surface, deletion of this gene or its regulatory activator results in loss of virulence at the skin [338, 339]. It has also been found that specific variants can be isolated after host passaging, isolating bacteria from an invasive blood infection resulted in increased expression of the SpeA gene [306]. This study used host adapted variants in several

ways, firstly, to consider the effect on virulence in joint-tropism infections, on the regulation and secretion of SLO and to determine any effects on the host immune response in clearing the infection when using host-adapted isolates. Considering the effect on joint infections, the data showed that variants isolated from the joint and used in the septic arthritis murine model were cleared from the blood rapidly and entered the joint more quickly and based on arthritic index scoring also produced a more serious phenotype. In addition to this, when characterising the host immune response in the joint it was found that there were significant differences in the response elicited. When inducing septic arthritis using the joint-adapted isolate there was less infiltration into the joints early on by phagocytes which could explain why there the bacteria are able to reach higher CFU densities early in the infection in comparison to the original infecting strain which is potentially limited by neutrophils and macrophages. There were also effects on the production and secretion of SLO after joint-passaging. Low SLO secreting bacteria which effectively colonise the joints, adapt further to the joint by selecting for low secreting SLO variants. This is a selection pressure applied from environmental signals in the joint as when the isolate is recovered from the joints and placed under growth conditions *in vitro* it reverts to producing significantly more SLO. These findings show that GAS is highly sensitive to environmental signals and can change its phenotype rapidly in the host, this has important implications when considering host-pathogen dynamics and transmission ability. This study also adds to the current data that shows that different strains of GAS do indeed adapt to specific niche environments in the human host. It would also be interesting to consider the expression and regulation of genes *in vivo* and so RNA-sequencing techniques would provide invaluable information in to which proteins are being transcribed in different host niches.

7.5 Host-pathogen interactions during GAS septic arthritis

GAS causes severe infections of the joint, which are often difficult to treat as the disease progresses quickly and in a high number of cases results in a severe chronic infection. Currently our only understanding of host immunopathogenesis in septic arthritis comes from staphylococcal experimental models only [54]. *Emm* type 1.0 isolate 101910 was used to initiate the infection alongside the host adapted version of this isolate (recovered from a previous knee joint infection). Multiple parameters were collected during septic arthritis induced by each isolate including CFUs, arthritic index, cytokines, and immune cell recruitment across various time points. The host response in the joint was characterised by an initial potent inflammatory response mainly dominated by neutrophils and macrophages, along with their associated cytokines. In addition to this CD4+ T cells were found to play an important role in the immune response and further T cell subsets were characterised. Overall the infection results in a highly pro-inflammatory immune response which may ultimately contribute to the severe joint damage caused. This study has provided invaluable information in to how the immune response works to clear the infection and also how it may exacerbate symptoms and joint damage. As previously discussed, the murine immune system differs in that it is not sensitive to a number of streptococcal superantigens and toxins. Therefore, further work using humanised mice and in particular those that have human MHC class II systems, would be important in highlighting which GAS proteins initiate the different aspects of the immune response.

In addition to this deciphering the direct interaction between immune cells and the host joint remodelling mechanisms would be important particularly when designing

therapeutic options. The host immune response during a septic arthritis infection provides a unique dichotomy, it is well known from murine models of *S. aureus* septic arthritis that the host response plays a role in both clearance and the pathogenesis of septic arthritis. Studies which have depleted CD4+ T cells before *S. aureus* infection found that there was a considerably milder course of infection along with a reduction in associated damage [312]. There has also been some interesting research which suggests that it is primarily the role of the largely inflammatory Th1 response that is responsible for joint damage with no positive effect on protection [61]. Further to this it has been shown that the Th2 response provides the resistance to infection without the associated bone damage [340]. It would be interesting to replicate these findings in a murine model of GAS induced septic arthritis, if a particular arm of the host response was solely responsible for exacerbated joint damage with no protective capacity this could be targeted with the aim to enhance bone and joint recovery. It would also be useful to acquire synovial joint fluid from GAS infected patients to validate the findings here in human infections.

7.6 Summary

In summary, GAS is a diverse pathogen that employs a number of different pathogenic mechanisms to initiate diverse clinical phenotypes, adapt to its host niche and evade the host immune response. It was found that isolates from a hypervirulent outbreak of GAS resulted in severe infection of the host and this correlated with the ability to resist opsonophagocytic killing. A novel septic arthritis murine model was established using isolates of GAS that were collected from a patient with septic arthritis, highlighting the specificity of GAS to different niches. The adaptability of GAS in the host was further investigated and it was shown that arthritic isolates can

become more even more specifically adapted to the joint. A key *in vivo* virulence factor of GAS, SLO, was shown to play a key role in the outcome of infection. Although SLO has been shown to be an important virulence factor in invasive disease this is the first study to show that the ability of GAS to regulate its SLO production has a subsequent effect on the *in vivo* pathotype. This finding could have particular implications on the development of treatment and vaccine strategies. It was shown that by removing SLO invasive bacteraemia was attenuated, but GAS was able to establish a more chronic infection. Using the murine model of septic arthritis, the localised immune response in the joint was characterised for the first time during infection with GAS. Septic arthritis is often associated with poor recovery and the bone damage that occurs is often irreversible. By investigating the bacterial and host mechanisms behind both infection and damage it provides new prospects for treatment and patient outcomes.

8. References

1. Ferretti, J.J. & Köhler, W., *History of Streptoccocal Research*, in *Streptococcus pyogenes: Basic Biology to Clinical Manifestations*, J.J. Ferretti, D.L. Stevens & V.A. Fischetti, Editors. 2016, University of Oklahoma Health Sciences Center

.

2. Alouf, J.E. & Horaud, T. Streptococcal research at Pasteur Institute from Louis Pasteur's time to date. *Advances in experimental medicine and biology* **418**, 7-14 (1997).

3. Walker, M.J. *et al.* Disease manifestations and pathogenic mechanisms of group a Streptococcus. *Clinical microbiology reviews* **27**, 264-301, doi:10.1128/cmr.00101-13 (2014).

4. Spellerberg, B. & Brandt, C., *Laboratory Diagnosis of Streptococcus pyogenes (group A streptococci)*, in *Streptococcus pyogenes : Basic Biology to Clinical Manifestations*, J.J. Ferretti, D.L. Stevens & V.A. Fischetti, Editors. 2016.

5. Lancefield, R.C. A seriological differentiation of human and other groups of hemolytic streptococci. *The Journal of experimental medicine* **57**, 571-595 (1933).

6. Henningham, A. *et al.* Virulence Role of the GlcNAc Side Chain of the Lancefield Cell Wall Carbohydrate Antigen in Non-M1-Serotype Group A Streptococcus. *mBio* **9**, doi:10.1128/mBio.02294-17 (2018).

7. Leung, A.K., Newman, R., Kumar, A. & Davies, H.D. Rapid antigen detection testing in diagnosing group A beta-hemolytic streptococcal pharyngitis. *Expert review of molecular diagnostics* **6**, 761-6, doi:10.1586/14737159.6.5.761 (2006).

8. Gerber, M.A., Spadaccini, L.J., Wright, L.L. & Deutsch, L. Latex agglutination tests for rapid identification of group A streptococci directly from throat swabs. *The Journal of pediatrics* **105**, 702-5 (1984).

9. Cunningham, M.W. Pathogenesis of group A streptococcal infections. *Clinical microbiology reviews* **13**, 470-511 (2000).

10. Oehmcke, S., Shannon, O., Morgelin, M. & Herwald, H. Streptococcal M proteins and their role as virulence determinants. *Clinica chimica acta; international journal of clinical chemistry* **411**, 1172-80, doi:10.1016/j.cca.2010.04.032 (2010).

11. Lancefield, R.C. Current knowledge of type-specific M antigens of group A streptococci. *Journal of immunology (Baltimore, Md. : 1950)* **89**, 307-313 (1962).

12. Steer, A.C., Law, I., Matatolu, L., Beall, B.W. & Carapetis, J.R. Global emm type distribution of group A streptococci: systematic review and implications for vaccine development. *The Lancet. Infectious diseases* **9**, 611-6, doi:10.1016/s1473-3099(09)70178-1 (2009).

13. Musser, J.M. & DeLeo, F.R. Toward a genome-wide systems biology analysis of host-pathogen interactions in group A Streptococcus. *The American journal of pathology* **167**, 1461-72, doi:10.1016/s0002-9440(10)61232-1 (2005).

14. Banks, D.J., Beres, S.B. & Musser, J.M. The fundamental contribution of phages to GAS evolution, genome diversification and strain emergence. *Trends in microbiology* **10**, 515-21 (2002).

15. Ferretti, J.J. *et al.* Complete genome sequence of an M1 strain of Streptococcus pyogenes. *Proceedings of the National Academy of Sciences of the United States of America* **98**, 4658-63, doi:10.1073/pnas.071559398 (2001).

16. Nakagawa, I. *et al.* Genome sequence of an M3 strain of Streptococcus pyogenes reveals a large-scale genomic rearrangement in invasive strains and new insights into phage evolution. *Genome research* **13**, 1042-55, doi:10.1101/gr.1096703 (2003).

17. Banks, D.J. *et al.* Progress toward characterization of the group A Streptococcus metagenome: complete genome sequence of a macrolide-resistant serotype M6 strain. *The Journal of infectious diseases* **190**, 727-38, doi:10.1086/422697 (2004).

18. Green, N.M. *et al.* Genome sequence of a serotype M28 strain of group a streptococcus: potential new insights into puerperal sepsis and bacterial disease specificity. *The Journal of infectious diseases* **192**, 760-70, doi:10.1086/430618 (2005).

19. Ding, W., Baumdicker, F. & Neher, R.A. panX: pan-genome analysis and exploration. *Nucleic acids research* **46**, e5, doi:10.1093/nar/gkx977 (2018).

20. Hartley, G., Jr., Enders, J.F., Mueller, J.H. & Schoenbach, E.B. ABSENCE OF CLINICAL DISEASE IN SPITE OF A HIGH INCIDENCE OF CARRIERS OF GROUP A HEMOLYTIC STREPTOCOCCI OF A SINGLE TYPE; FAILURE OF TYROTHRICIN TO INFLUENCE THE CARRIER RATE. *The Journal of clinical investigation* **24**, 92-96, doi:10.1172/JCI101584 (1945).

21. DeMuri, G.P. & Wald, E.R. The Group A Streptococcal Carrier State Reviewed: Still an Enigma. *Journal of the Pediatric Infectious Diseases Society* **3**, 336-42, doi:10.1093/jpids/piu030 (2014).

22. Kaplan, E.L. The group A streptococcal upper respiratory tract carrier state: an enigma. *The Journal of pediatrics* **97**, 337-45 (1980).

23. Johnson, D.R., Kurlan, R., Leckman, J. & Kaplan, E.L. The human immune response to streptococcal extracellular antigens: clinical, diagnostic, and potential pathogenetic implications. *Clinical infectious diseases : an official publication of the Infectious Diseases Society of America* **50**, 481-90, doi:10.1086/650167 (2010).

24. Kaplan, E.L., Gastanaduy, A.S. & Huwe, B.B. The role of the carrier in treatment failures after antibiotic therapy for group A streptococci in the upper respiratory tract. *The Journal of Laboratory and Clinical Medicine* **98**, 326-335 (1981).

25. Shaikh, N., Leonard, E. & Martin, J.M. Prevalence of streptococcal pharyngitis and streptococcal carriage in children: a meta-analysis. *Pediatrics* **126**, e557-e564 (2010).

26. Brook, I. The role of β-lactamase-producing bacteria in the persistence of streptococcal tonsillar infection. *Review of Infectious Diseases* **6**, 601-607 (1984).

27. Brook, I. & Gober, A.E. Recovery of interfering and beta-lactamase-producing bacteria from group A beta-haemolytic streptococci carriers and non-carriers. *Journal of medical microbiology* **55**, 1741-4, doi:10.1099/jmm.0.46796-0 (2006).

28. Smith, T.D., Huskins, W.C., Kim, K.S. & Kaplan, E.L. Efficacy of beta-lactamase-resistant penicillin and influence of penicillin tolerance in eradicating streptococci from the pharynx after failure of penicillin therapy for group A streptococcal pharyngitis. *The Journal of pediatrics* **110**, 777-82 (1987).

29. Sanders, C.C., Sanders, W.E., Jr. & Harrowe, D.J. Bacterial interference: effects of oral antibiotics on the normal throat flora and its ability to interfere with group A streptococci. *Infection and immunity* **13**, 808-12 (1976).

30. Thulin, P. *et al.* Viable group A streptococci in macrophages during acute soft tissue infection. *PLoS medicine* **3**, e53, doi:10.1371/journal.pmed.0030053 (2006).

31. Kaplan, E.L., Top, F.H., Dudding, B.A. & Wannamaker, L.W. Diagnosis of Streptococcal Pharyngitis: Differentiation of Active Infection from the Carrier State in the Symptomatic Child. *Journal of Infectious Diseases* **123**, 490-501, doi:10.1093/infdis/123.5.490 (1971).

32. Kaplan, E.L., Chhatwal, G.S. & Rohde, M. Reduced ability of penicillin to eradicate ingested group A streptococci from epithelial cells: clinical and pathogenetic implications. *Clinical infectious diseases : an official publication of the Infectious Diseases Society of America* **43**, 1398-406, doi:10.1086/508773 (2006).

33. Passàli, D., Lauriello, M., Passàli, G.C., Passàli, F.M. & Bellussi, L. Group A streptococcus and its antibiotic resistance. *Acta otorhinolaryngologica Italica : organo ufficiale della Societa italiana di otorinolaringologia e chirurgia cervico-facciale* **27**, 27-32 (2007).

34. Factor, S.H. *et al.* Risk factors for pediatric invasive group A streptococcal disease. *Emerging infectious diseases* **11**, 1062-6, doi:10.3201/eid1107.040900 (2005).

35. Cockerill, F.R., 3rd *et al.* An outbreak of invasive group A streptococcal disease associated with high carriage rates of the invasive clone among school-aged children. *Jama* **277**, 38-43 (1997).

36. Medina, E., Goldmann, O., Toppel, A.W. & Chhatwal, G.S. Survival of Streptococcus pyogenes within host phagocytic cells: a pathogenic mechanism for persistence and systemic invasion. *The Journal of infectious diseases* **187**, 597-603, doi:10.1086/373998 (2003).

37. Tart, A.H., Walker, M.J. & Musser, J.M. New understanding of the group A Streptococcus pathogenesis cycle. *Trends in microbiology* **15**, 318-25, doi:10.1016/j.tim.2007.05.001 (2007).

38. Wessels , M.R. Streptococcal Pharyngitis. *New England Journal of Medicine* **364**, 648-655, doi:10.1056/NEJMcp1009126 (2011).

39. Wessels, M.R., *Pharyngitis and Scarlet Fever*, in *Streptococcus pyogenes : Basic Biology to Clinical Manifestations*, J.J. Ferretti, D.L. Stevens & V.A. Fischetti, Editors. 2016, University of Oklahoma Health Sciences Center
(c) The University of Oklahoma Health Sciences Center.: Oklahoma City (OK).

40. Ebell, M.H., Smith, M.A., Barry, H.C., Ives, K. & Carey, M. The rational clinical examination. Does this patient have strep throat? *Jama* **284**, 2912-8 (2000).

41. Spinks, A., Glasziou, P.P. & Del Mar, C.B. Antibiotics for sore throat. *The Cochrane database of systematic reviews*, Cd000023, doi:10.1002/14651858.CD000023.pub4 (2013).

42. Yu, C.E. & Ferretti, J.J. Molecular epidemiologic analysis of the type A streptococcal exotoxin (erythrogenic toxin) gene (speA) in clinical Streptococcus pyogenes strains. *Infection and immunity* **57**, 3715-9 (1989).

43. Davies, M.R. *et al.* Emergence of scarlet fever Streptococcus pyogenes emm12 clones in Hong Kong is associated with toxin acquisition and multidrug resistance. *Nature genetics* **47**, 84-7, doi:10.1038/ng.3147 (2015).

44. Tyler, S.D. *et al.* Streptococcal erythrogenic toxin genes: detection by polymerase chain reaction and association with disease in strains isolated in Canada from 1940 to 1991. *Journal of clinical microbiology* **30**, 3127-31 (1992).

45. Silva-Costa, C., Carrico, J.A., Ramirez, M. & Melo-Cristino, J. Scarlet fever is caused by a limited number of Streptococcus pyogenes lineages and is associated with the exotoxin genes ssa, speA and speC. *The Pediatric infectious disease journal* **33**, 306-10, doi:10.1097/inf.0000000000000088 (2014).

46. Lamagni, T. *et al.* Resurgence of scarlet fever in England, 2014–16: a population-based surveillance study. *The Lancet Infectious Diseases* **18**, 180-187, doi:10.1016/S1473-3099(17)30693-X.

47. Steer, A.C., Lamagni, T., Curtis, N. & Carapetis, J.R. Invasive group a streptococcal disease: epidemiology, pathogenesis and management. *Drugs* **72**, 1213-27, doi:10.2165/11634180-000000000-00000 (2012).

48. Lamagni, T.L. *et al.* Epidemiology of severe Streptococcus pyogenes disease in Europe. *Journal of clinical microbiology* **46**, 2359-67, doi:10.1128/jcm.00422-08 (2008).

49. O'Grady, K.A. *et al.* The epidemiology of invasive group A streptococcal disease in Victoria, Australia. *The Medical journal of Australia* **186**, 565-9 (2007).

50. O'Loughlin, R.E. *et al.* The epidemiology of invasive group A streptococcal infection and potential vaccine implications: United States, 2000-2004. *Clinical infectious diseases : an official publication of the Infectious Diseases Society of America* **45**, 853-62, doi:10.1086/521264 (2007).

51. Cole, J.N., Barnett, T.C., Nizet, V. & Walker, M.J. Molecular insight into invasive group A streptococcal disease. *Nature reviews. Microbiology* **9**, 724-36, doi:10.1038/nrmicro2648 (2011).

52. Stevens, D.L. Invasive group A streptococcus infections. *Clinical infectious diseases : an official publication of the Infectious Diseases Society of America* **14**, doi:10.1093/clinids/14.1.2 (1992).

53. Stevens, D.L. *et al.* Practice guidelines for the diagnosis and management of skin and soft tissue infections: 2014 update by the Infectious Diseases Society of America. *Clinical infectious diseases : an official publication of the Infectious Diseases Society of America* **59**, e10-52, doi:10.1093/cid/ciu444 (2014).

54. Colavite, P.M. & Sartori, A. Septic arthritis: immunopathogenesis, experimental models and therapy. *The Journal of Venomous Animals and Toxins Including Tropical Diseases* **20**, 19-19, doi:10.1186/1678-9199-20-19 (2014).

55. Goldenberg, D.L. & Reed, J.I. Bacterial arthritis. *N Engl J Med* **12**, doi:10.1056/nejm198503213121206 (1985).

56. Goldenberg, D.L. Septic arthritis. *The Lancet* **351**, 197-202, doi:10.1016/S0140-6736(97)09522-6 (1998).

57. Kaandorp, C.J. *et al.* Incidence and sources of native and prosthetic joint infection: a community based prospective survey. *Annals of the rheumatic diseases* **56**, 470-5 (1997).

58. Dubost, J.J. *et al.* No changes in the distribution of organisms responsible for septic arthritis over a 20 year period. *Annals of the rheumatic diseases* **61**, 267-9 (2002).

59. García-Arias, M., Balsa, A. & Mola, E.M. Septic arthritis. *Best Practice & Research Clinical Rheumatology* **25**, 407-421, doi:10.1016/j.berh.2011.02.001 (2011).

60. Boff, D., Crijns, H., Teixeira, M.M., Amaral, F.A. & Proost, P. Neutrophils: Beneficial and Harmful Cells in Septic Arthritis. *International journal of molecular sciences* **19**, doi:10.3390/ijms19020468 (2018).

61. Shirtliff, M.E. & Mader, J.T. Acute Septic Arthritis. *Clinical microbiology reviews* **15**, 527-544, doi:10.1128/CMR.15.4.527-544.2002 (2002).

62. Cunningham, M.W., *Post-Streptococcal Autoimmune Sequelae: Rheumatic Fever and Beyond*, in *Streptococcus pyogenes : Basic Biology to Clinical Manifestations*, J.J. Ferretti, D.L. Stevens & V.A. Fischetti, Editors. 2016, University of Oklahoma Health Sciences Center
(c) The University of Oklahoma Health Sciences Center.: Oklahoma City (OK).

63. Carapetis, J.R. *et al.* Acute rheumatic fever and rheumatic heart disease. *Nature reviews. Disease primers* **2**, 15084, doi:10.1038/nrdp.2015.84 (2016).

64. Kaplan, E.L., Johnson, D.R. & Cleary, P.P. Group A streptococcal serotypes isolated from patients and sibling contacts during the resurgence of rheumatic fever in the United States in the mid-1980s. *The Journal of infectious diseases* **159**, 101-3 (1989).

65. Veasy, L.G. *et al.* Resurgence of acute rheumatic fever in the intermountain area of the United States. *N Engl J Med* **316**, 421-7, doi:10.1056/nejm198702193160801 (1987).

66. Cunningham, M.W. Rheumatic fever, autoimmunity, and molecular mimicry: the streptococcal connection. *International reviews of immunology* **33**, 314-29, doi:10.3109/08830185.2014.917411 (2014).

67. Rush, C.M., Govan, B.L., Sikder, S., Williams, N.L. & Ketheesan, N. Animal models to investigate the pathogenesis of rheumatic heart disease. *Frontiers in pediatrics* **2**, 116, doi:10.3389/fped.2014.00116 (2014).

68. Galvin, J.E., Hemric, M.E., Ward, K. & Cunningham, M.W. Cytotoxic mAb from rheumatic carditis recognizes heart valves and laminin. *The Journal of clinical investigation* **106**, 217-24, doi:10.1172/jci7132 (2000).

69. Ellis, N.M. *et al.* Priming the immune system for heart disease: a perspective on group A streptococci. *The Journal of infectious diseases* **202**, 1059-67, doi:10.1086/656214 (2010).

70. Zabriskie, J.B. Mimetic relationships between group A streptococci and mammalian tissues. *Advances in immunology* **7**, 147-88 (1967).

71. Shulman, S.T. *et al.* Executive Summary: Clinical Practice Guideline for the Diagnosis and Management of Group A Streptococcal Pharyngitis: 2012 Update by the Infectious Diseases Society of America. *Clinical Infectious Diseases* **55**, 1279-1282, doi:10.1093/cid/cis847 (2012).

72. Allen, U.D. & Moore, D.L. Invasive group A streptococcal disease: Management and chemoprophylaxis. *The Canadian Journal of Infectious Diseases & Medical Microbiology* **21**, 115-118 (2010).

73. Song, Y., Zhang, X., Lu, C., Zhang, F. & Zhu, H. Progress in development of Group A Streptococcus vaccines. *Current pharmaceutical biotechnology* **14**, 947-50 (2013).

74. Dale, J.B. *et al. Current Approaches to Group A Streptococcal Vaccine Development*. (University of Oklahoma Health Sciences Center, Oklahoma City (OK), 2016).

75. Fox, E.N., Pachman, L.M., Wittner, M.K. & Dorfman, A. Primary immunization of infants and children with group A streptococcal M protein. *Zentralblatt fur Bakteriologie, Parasitenkunde, Infektionskrankheiten und Hygiene. 1. Abt. Medizinisch-hygienische Bakteriologie, Virusforschung und Parasitologie. Originale* **214**, 352-63 (1970).

76. Fox, E.N., Waldman, R.H., Wittner, M.K., Mauceri, A.A. & Dorfman, A. Protective study with a group A streptococcal M protein vaccine. Infectivity challenge of human volunteers. *The Journal of clinical investigation* **52**, 1885-92, doi:10.1172/jci107372 (1973).

77. Steer, A.C. *et al.* Status of research and development of vaccines for Streptococcus pyogenes. *Vaccine* **34**, 2953-2958, doi:10.1016/j.vaccine.2016.03.073 (2016).

78. Dale, J.B. *et al.* Group A streptococcal vaccines: paving a path for accelerated development. *Vaccine* **31 Suppl 2**, B216-22, doi:10.1016/j.vaccine.2012.09.045 (2013).

79. Sharma, A. & Nitsche-Schmitz, D. Challenges to developing effective streptococcal vaccines to prevent rheumatic fever and rheumatic heart disease. *Vaccine (Auckl)* **4**, 39-54 (2014).

80. Sabharwal, H. *et al.* Group A streptococcus (GAS) carbohydrate as an immunogen for protection against GAS infection. *The Journal of infectious diseases* **193**, 129-35, doi:10.1086/498618 (2006).

81. Chmouryguina, I., Suvorov, A., Ferrieri, P. & Cleary, P.P. Conservation of the C5a peptidase genes in group A and B streptococci. *Infection and immunity* **64**, 2387-90 (1996).

82. Cheng, Q. *et al.* Immunization with C5a peptidase or peptidase-type III polysaccharide conjugate vaccines enhances clearance of group B Streptococci from lungs of infected mice. *Infection and immunity* **70**, 6409-15 (2002).

83. Cleary, P.P., Matsuka, Y.V., Huynh, T., Lam, H. & Olmsted, S.B. Immunization with C5a peptidase from either group A or B streptococci enhances clearance of group A streptococci from intranasally infected mice. *Vaccine* **22**, 4332-41, doi:10.1016/j.vaccine.2004.04.030 (2004).

84. Kotloff, K.L. *et al.* Safety and immunogenicity of a recombinant multivalent group a streptococcal vaccine in healthy adults: phase 1 trial. *Jama* **292**, 709-15, doi:10.1001/jama.292.6.709 (2004).

85. Hu, M.C. *et al.* Immunogenicity of a 26-valent group A streptococcal vaccine. *Infection and immunity* **70**, 2171-7 (2002).

86. McNeil, S.A. *et al.* Safety and immunogenicity of 26-valent group a streptococcus vaccine in healthy adult volunteers. *Clinical infectious diseases : an official publication of the Infectious Diseases Society of America* **41**, 1114-22, doi:10.1086/444458 (2005).

87. Dale, J.B. *et al.* Potential coverage of a multivalent M protein-based group A streptococcal vaccine. *Vaccine* **31**, 1576-81, doi:10.1016/j.vaccine.2013.01.019 (2013).

88. Guerino, M.T. *et al.* HLA class II transgenic mice develop a safe and long lasting immune response against StreptInCor, an anti-group A streptococcus vaccine candidate. *Vaccine* **29**, 8250-6, doi:10.1016/j.vaccine.2011.08.113 (2011).

89. Guilherme, L., Ferreira, F.M., Kohler, K.F., Postol, E. & Kalil, J. A vaccine against Streptococcus pyogenes: the potential to prevent rheumatic fever and rheumatic heart disease. *American journal of cardiovascular drugs : drugs, devices, and other interventions* **13**, 1-4, doi:10.1007/s40256-013-0005-8 (2013).

90. Guilherme, L. *et al.* A vaccine against S. pyogenes: design and experimental immune response. *Methods (San Diego, Calif.)* **49**, 316-21, doi:10.1016/j.ymeth.2009.03.024 (2009).

91. Hayman, W.A. *et al.* Mapping the minimal murine T cell and B cell epitopes within a peptide vaccine candidate from the conserved region of the M protein of group A streptococcus. *International immunology* **9**, 1723-33 (1997).

92. Bauer, M.J. *et al.* Evaluation of novel Streptococcus pyogenes vaccine candidates incorporating multiple conserved sequences from the C-repeat region of the M-protein. *Vaccine* **30**, 2197-205, doi:10.1016/j.vaccine.2011.12.115 (2012).

93. Carapetis, J.R., Steer, A.C., Mulholland, E.K. & Weber, M. The global burden of group A streptococcal diseases. *The Lancet. Infectious diseases* **5**, 685-94, doi:10.1016/s1473-3099(05)70267-x (2005).

94. Gerber, M.A. *et al.* Prevention of rheumatic fever and diagnosis and treatment of acute streptococcal pharyngitis. *Circulation* **119**, 1541-1551 (2009).

95. Carapetis, J.R., Steer, A.C., Mulholland, E.K. & Weber, M. The global burden of group A streptococcal diseases. *The Lancet infectious diseases* **5**, 685-694 (2005).

96. Turner, C.E. *et al.* Community outbreaks of group A Streptococcus revealed by genome sequencing. *Scientific reports* **7**, 8554, doi:10.1038/s41598-017-08914-x (2017).

97. Ramos, M. *et al.* Outbreak of Group A beta hemolytic Streptococcus pharyngitis in a Peruvian military facility, April 2012. *Msmr* **20**, 14-7 (2013).

98. Ben Zakour, N.L., Venturini, C., Beatson, S.A. & Walker, M.J. Analysis of a Streptococcus pyogenes puerperal sepsis cluster by use of whole-genome sequencing. *Journal of clinical microbiology* **50**, 2224-8, doi:10.1128/jcm.00675-12 (2012).

99. Sumby, P. *et al.* Evolutionary origin and emergence of a highly successful clone of serotype M1 group a Streptococcus involved multiple horizontal gene transfer events. *The Journal of infectious diseases* **192**, 771-82, doi:10.1086/432514 (2005).

100. Beres, S.B. *et al.* Genome-wide molecular dissection of serotype M3 group A Streptococcus strains causing two epidemics of invasive infections. *Proceedings of the National Academy of Sciences of the United States of America* **101**, 11833-8, doi:10.1073/pnas.0404163101 (2004).

101. Lee, C.F., Cowling, B.J. & Lau, E.H.Y. Epidemiology of Reemerging Scarlet Fever, Hong Kong, 2005-2015. *Emerging infectious diseases* **23**, 1707-1710, doi:10.3201/eid2310.161456 (2017).

102. Lau, E.H., Nishiura, H., Cowling, B.J., Ip, D.K. & Wu, J.T. Scarlet fever outbreak, Hong Kong, 2011. *Emerging infectious diseases* **18**, 1700-2, doi:10.3201/eid1810.120062 (2012).

103. Efstratiou, A. & Lamagni, T. Epidemiology of Streptococcus pyogenes. (2017).

104. Nasser, W. *et al.* Evolutionary pathway to increased virulence and epidemic group A Streptococcus disease derived from 3,615 genome sequences. *Proceedings of the National Academy of Sciences of the United States of America* **111**, E1768-76, doi:10.1073/pnas.1403138111 (2014).

105. Barnett, T.C. *et al.* Streptococcal toxins: role in pathogenesis and disease. *Cellular microbiology* **17**, 1721-41, doi:10.1111/cmi.12531 (2015).

106. Bisno, A.L., Brito, M.O. & Collins, C.M. Molecular basis of group A streptococcal virulence. *The Lancet Infectious Diseases* **3**, 191-200, doi:10.1016/S1473-3099(03)00576-0 (2003).

107. Reglinski, M. & Sriskandan, S. The contribution of group A streptococcal virulence determinants to the pathogenesis of sepsis. *Virulence* **5**, 127-36, doi:10.4161/viru.26400 (2014).

108. Vega, L.A., Malke, H. & McIver, K.S., *Virulence-Related Transcriptional Regulators of Streptococcus pyogenes*, in *Streptococcus pyogenes : Basic Biology to Clinical Manifestations*, J.J. Ferretti, D.L. Stevens & V.A. Fischetti, Editors. 2016, University of Oklahoma Health Sciences Center
(c) The University of Oklahoma Health Sciences Center.: Oklahoma City (OK).

109. Friães, A., Pato, C., Melo-Cristino, J. & Ramirez, M. Consequences of the variability of the CovRS and RopB regulators among Streptococcus pyogenes causing human infections. *Scientific reports* **5**, 12057, doi:10.1038/srep12057 (2015).

110. Mayfield, J.A. *et al.* Mutations in the control of virulence sensor gene from Streptococcus pyogenes after infection in mice lead to clonal bacterial variants with altered gene regulatory activity and virulence. *PLoS One* **9**, e100698, doi:10.1371/journal.pone.0100698 (2014).

111. Chiang-Ni, C., Tseng, H.C., Hung, C.H. & Chiu, C.H. Acidic stress enhances CovR/S-dependent gene repression through activation of the covR/S promoter in emm1-type group A Streptococcus. *International journal of medical microbiology : IJMM* **307**, 329-339, doi:10.1016/j.ijmm.2017.06.002 (2017).

112. Chiang-Ni, C., Nian, S.Y., Wu, J.J. & Chen, C.J. Oxygen-dependent phenotypic variation in group A streptococcus. *Journal of microbiology, immunology, and infection = Wei mian yu gan ran za zhi* **49**, 837-842, doi:10.1016/j.jmii.2014.11.010 (2016).

113. Dalton, T.L. & Scott, J.R. CovS inactivates CovR and is required for growth under conditions of general stress in Streptococcus pyogenes. *Journal of bacteriology* **186**, 3928-37, doi:10.1128/jb.186.12.3928-3937.2004 (2004).

114. Gryllos, I., Levin, J.C. & Wessels, M.R. The CsrR/CsrS two-component system of group A Streptococcus responds to environmental Mg(2+). *Proceedings of the National Academy of Sciences of the United States of America* **100**, 4227-4232, doi:10.1073/pnas.0636231100 (2003).

115. Graham, M.R. *et al.* Virulence control in group A Streptococcus by a two-component gene regulatory system: Global expression profiling and in vivo infection modeling. *Proceedings of the National Academy of Sciences of the United States of America* **99**, 13855-13860, doi:10.1073/pnas.202353699 (2002).

116. Pence, M.A. *et al.* Streptococcal inhibitor of complement promotes innate immune resistance phenotypes of invasive M1T1 group A Streptococcus. *J Innate Immun* **2**, 587-95, doi:10.1159/000317672 (2010).

117. Fischetti, V.A., *M Protein and Other Surface Proteins on Streptococci*, in *Streptococcus pyogenes : Basic Biology to Clinical Manifestations*, J.J. Ferretti, D.L. Stevens & V.A. Fischetti, Editors. 2016.

118. Smeesters, P.R., McMillan, D.J. & Sriprakash, K.S. The streptococcal M protein: a highly versatile molecule. *Trends in microbiology* **18**, 275-82, doi:10.1016/j.tim.2010.02.007 (2010).

119. Johnsson, E. *et al.* Role of the hypervariable region in streptococcal M proteins: binding of a human complement inhibitor. *J Immunol* **161**, 4894-901 (1998).

120. Ermert, D. *et al.* Virulence of Group A Streptococci Is Enhanced by Human Complement Inhibitors. *PLoS pathogens* **11**, e1005043, doi:10.1371/journal.ppat.1005043 (2015).

121. Pahlman, L.I. *et al.* Streptococcal M protein: a multipotent and powerful inducer of inflammation. *J Immunol* **177**, 1221-8 (2006).

122. Courtney, H.S., Hasty, D.L. & Dale, J.B. Molecular mechanisms of adhesion, colonization, and invasion of group A streptococci. *Annals of medicine* **34**, 77-87 (2002).

123. Wessels, M.R., *Cell Wall and Surface Molecules: Capsule*, in *Streptococcus pyogenes : Basic Biology to Clinical Manifestations*, J.J. Ferretti, D.L. Stevens & V.A. Fischetti, Editors. 2016, University of Oklahoma Health Sciences Center
(c) The University of Oklahoma Health Sciences Center.: Oklahoma City (OK).

124. Wessels, M.R., Moses, A.E., Goldberg, J.B. & DiCesare, T.J. Hyaluronic acid capsule is a virulence factor for mucoid group A streptococci. *Proceedings of the National Academy of Sciences of the United States of America* **88**, 8317-21 (1991).

125. Lancefield, R.C. & Todd, E.W. ANTIGENIC DIFFERENCES BETWEEN MATT HEMOLYTIC STREPTOCOCCI AND THEIR GLOSSY VARIANTS. *The Journal of experimental medicine* **48**, 769-90 (1928).

126. Stollerman, G.H. & Dale, J.B. The importance of the group a streptococcus capsule in the pathogenesis of human infections: a historical perspective. *Clinical infectious diseases : an official publication of the Infectious Diseases Society of America* **46**, 1038-45, doi:10.1086/529194 (2008).

127. Crater, D.L. & van de Rijn, I. Hyaluronic acid synthesis operon (has) expression in group A streptococci. *The Journal of biological chemistry* **270**, 18452-8 (1995).

128. Johnson, D.R., Stevens, D.L. & Kaplan, E.L. Epidemiologic analysis of group A streptococcal serotypes associated with severe systemic infections, rheumatic fever, or uncomplicated pharyngitis. *The Journal of infectious diseases* **166**, 374-82 (1992).

129. Todd, E.W. & Lancefield, R.C. VARIANTS OF HEMOLYTIC STREPTOCOCCI; THEIR RELATION TO TYPE-SPECIFIC SUBSTANCE, VIRULENCE, AND TOXIN. *The Journal of experimental medicine* **48**, 751-67 (1928).

130. Husmann, L.K., Yung, D.L., Hollingshead, S.K. & Scott, J.R. Role of putative virulence factors of Streptococcus pyogenes in mouse models of long-term throat colonization and pneumonia. *Infection and immunity* **65**, 1422-30 (1997).

131. Ashbaugh, C.D., Warren, H.B., Carey, V.J. & Wessels, M.R. Molecular analysis of the role of the group A streptococcal cysteine protease, hyaluronic acid capsule, and M protein in a murine model of human invasive soft-tissue infection. *The Journal of clinical investigation* **102**, 550-60, doi:10.1172/jci3065 (1998).

132. Dale, J.B., Washburn, R.G., Marques, M.B. & Wessels, M.R. Hyaluronate capsule and surface M protein in resistance to opsonization of group A streptococci. *Infection and immunity* **64**, 1495-501 (1996).

133. Hynes, W. & Sloan, M., *Secreted Extracellular Virulence Factors*, in *Streptococcus pyogenes : Basic Biology to Clinical Manifestations*, J.J. Ferretti, D.L. Stevens & V.A. Fischetti, Editors. 2016.

134. McArthur, J.D., Cook, S.M., Venturini, C. & Walker, M.J. The Role of Streptokinase as a Virulence Determinant of Streptococcus pyogenes - Potential for Therapeutic Targeting. *Curr. Drug Targets* **13**, 297-307 (2012).

135. Sun, H. *et al.* Plasminogen is a critical host pathogenicity factor for group A streptococcal infection. *Science (New York, N.Y.)* **305**, 1283-6, doi:10.1126/science.1101245 (2004).

136. Terao, Y. The virulence factors and pathogenic mechanisms of Streptococcus pyogenes. *Journal of Oral Biosciences* **54**, 96-100, doi:10.1016/j.job.2012.02.004 (2012).

137. Nelson, D.C., Garbe, J. & Collin, M. Cysteine proteinase SpeB from Streptococcus pyogenes - a potent modifier of immunologically important host and bacterial proteins. *Biol. Chem.* **392**, 1077-1088, doi:10.1515/bc-2011-208 (2011).

138. Sumitomo, T., Nakata, M., Higashino, M., Terao, Y. & Kawabata, S. Group A streptococcal cysteine protease cleaves epithelial junctions and contributes to bacterial translocation. *The Journal of biological chemistry* **288**, 13317-24, doi:10.1074/jbc.M113.459875 (2013).

139. Hynes, W. Virulence factors of the group A streptococci and genes that regulate their expression. *Frontiers in bioscience : a journal and virtual library* **9**, 3399-433 (2004).

140. Honda-Ogawa, M. *et al.* Cysteine proteinase from Streptococcus pyogenes enables evasion of innate immunity via degradation of complement factors. *The Journal of biological chemistry* **288**, 15854-64, doi:10.1074/jbc.M113.469106 (2013).

141. Berry, A.M., Yother, J., Briles, D.E., Hansman, D. & Paton, J.C. Reduced virulence of a defined pneumolysin-negative mutant of Streptococcus pneumoniae. *Infection and immunity* **57**, 2037-42 (1989).

142. Dramsi, S. & Cossart, P. Listeriolysin O. *a genuine cytolysin optimized for an intracellular parasite* **156**, 943-946, doi:10.1083/jcb.200202121 (2002).

143. Alouf, J.E. Cholesterol-binding cytolytic protein toxins. *International Journal of Medical Microbiology* **290**, 351-356, doi:https://doi.org/10.1016/S1438-4221(00)80039-9 (2000).

144. Feil, S.C., Ascher, D.B., Kuiper, M.J., Tweten, R.K. & Parker, M.W. Structural studies of Streptococcus pyogenes streptolysin O provide insights into the early steps of membrane penetration. *Journal of molecular biology* **426**, 785-92, doi:10.1016/j.jmb.2013.11.020 (2014).

145. Chiarot, E. *et al.* Targeted Amino Acid Substitutions Impair Streptolysin O Toxicity and Group A Streptococcus Virulence. *mBio* **4**, doi:10.1128/mBio.00387-12 (2013).

146. Bensi, G. *et al.* Multi high-throughput approach for highly selective identification of vaccine candidates: the Group A Streptococcus case. *Molecular & cellular proteomics : MCP* **11**, M111.015693, doi:10.1074/mcp.M111.015693 (2012).

147. Sierig, G., Cywes, C., Wessels, M.R. & Ashbaugh, C.D. Cytotoxic Effects of Streptolysin O and Streptolysin S Enhance the Virulence of Poorly Encapsulated Group A Streptococci. *Infection and immunity* **71**, 446-455, doi:10.1128/iai.71.1.446-455.2003 (2003).

148. Musser, J.M. & Shelburne, S.A., 3rd. A decade of molecular pathogenomic analysis of group A Streptococcus. *The Journal of clinical investigation* **119**, 2455-63, doi:10.1172/jci38095 (2009).

149. Walev, I., Palmer, M., Valeva, A., Weller, U. & Bhakdi, S. Binding, oligomerization, and pore formation by streptolysin O in erythrocytes and fibroblast membranes: detection of nonlytic polymers. *Infection and immunity* **63**, 1188-1194 (1995).

150. Xu, D. & Cheng, Q. Surface-Bound Lipid Vesicles Encapsulating Redox Species for Amperometric Biosensing of Pore-Forming Bacterial Toxins. *Journal of the American Chemical Society* **124**, 14314-14315, doi:10.1021/ja027897f (2002).

151. Bricker, A.L., Carey, V.J. & Wessels, M.R. Role of NADase in virulence in experimental invasive group A streptococcal infection. *Infection and immunity* **73**, 6562-6, doi:10.1128/iai.73.10.6562-6566.2005 (2005).

152. Shiseki, M. *et al.* Comparison of pathogenic factors expressed by group A Streptococci isolated from patients with streptococcal toxic shock syndrome and scarlet fever. *Microbial pathogenesis* **27**, 243-52, doi:10.1006/mpat.1999.0302 (1999).

153. Timmer, A.M. *et al.* Streptolysin O Promotes Group A Streptococcus Immune Evasion by Accelerated Macrophage Apoptosis. *Journal of Biological Chemistry* **284**, 862-871, doi:10.1074/jbc.M804632200 (2009).

154. Zhu, L., Olsen, R.J., Nasser, W., de la Riva Morales, I. & Musser, J.M. Trading Capsule for Increased Cytotoxin Production: Contribution to Virulence of a Newly Emerged Clade of emm89 Streptococcus pyogenes. *mBio* **6**, e01378-15, doi:10.1128/mBio.01378-15 (2015).

155. Howard, J.G. & Wallace, K.R. The comparative resistances of the red cells of various species to haemolysis by streptolysin O and by saponin. *British journal of experimental pathology* **34**, 181-4 (1953).

156. Limbago, B., Penumalli, V., Weinrick, B. & Scott, J.R. Role of Streptolysin O in a Mouse Model of Invasive Group A Streptococcal Disease. *Infection and immunity* **68**, 6384-6390 (2000).

157. Zhu, L. *et al.* Contribution of Secreted NADase and Streptolysin O to the Pathogenesis of Epidemic Serotype M1 Streptococcus pyogenes Infections. *The American journal of pathology* **187**, 605-613, doi:10.1016/j.ajpath.2016.11.003 (2017).

158. Yoshino, M. *et al.* Nonhemolytic Streptococcus pyogenes isolates that lack large regions of the sag operon mediating streptolysin S production. *Journal of clinical microbiology* **48**, 635-8, doi:10.1128/jcm.01362-09 (2010).

159. Kurupati, P. *et al.* Chemokine-cleaving Streptococcus pyogenes protease SpyCEP is necessary and sufficient for bacterial dissemination within soft tissues and the respiratory tract. *Molecular microbiology* **76**, 1387-1397, doi:10.1111/j.1365-2958.2010.07065.x (2010).

160. Sumby, P. *et al.* A chemokine-degrading extracellular protease made by group A Streptococcus alters pathogenesis by enhancing evasion of the innate immune response. *Infection and immunity* **76**, 978-85, doi:10.1128/iai.01354-07 (2008).

161. Walker, M.J. *et al.* DNase Sda1 provides selection pressure for a switch to invasive group A streptococcal infection. *Nat Med* **13**, 981-5, doi:10.1038/nm1612 (2007).

162. Frick, I.M. *et al.* Antibacterial activity of the contact and complement systems is blocked by SIC, a protein secreted by Streptococcus pyogenes.

The Journal of biological chemistry **286**, 1331-40, doi:10.1074/jbc.M110.178350 (2011).

163. Hoe, N.P. *et al.* Insight into the molecular basis of pathogen abundance: group A Streptococcus inhibitor of complement inhibits bacterial adherence and internalization into human cells. *Proceedings of the National Academy of Sciences of the United States of America* **99**, 7646-51, doi:10.1073/pnas.112039899 (2002).

164. Proft, T. & Fraser, J.D., *Streptococcal Superantigens: Biological properties and potential role in disease*, in *Streptococcus pyogenes : Basic Biology to Clinical Manifestations*, J.J. Ferretti, D.L. Stevens & V.A. Fischetti, Editors. 2016, University of Oklahoma Health Sciences Center
(c) The University of Oklahoma Health Sciences Center.: Oklahoma City (OK).

165. Proft, T. & Fraser, J.D. Bacterial superantigens. *Clinical and Experimental Immunology* **133**, 299-306, doi:10.1046/j.1365-2249.2003.02203.x (2003).

166. Commons, R.J. *et al.* Streptococcal superantigens: categorization and clinical associations. *Trends in molecular medicine* **20**, 48-62, doi:10.1016/j.molmed.2013.10.004 (2014).

167. Fraser, J.D. & Proft, T. The bacterial superantigen and superantigen-like proteins. *Immunological reviews* **225**, 226-43, doi:10.1111/j.1600-065X.2008.00681.x (2008).

168. Schlievert, P.M. Role of Superantigens in Human Disease. *Journal of Infectious Diseases* **167**, 997-1002, doi:10.1093/infdis/167.5.997 (1993).

169. Norrby-Teglund, A. *et al.* Evidence for superantigen involvement in severe group A streptococcal tissue infections. *Journal of Infectious Diseases* **184**, 853-860, doi:10.1086/323443 (2001).

170. Hauser, A.R., Stevens, D.L., Kaplan, E.L. & Schlievert, P.M. Molecular analysis of pyrogenic exotoxins from Streptococcus pyogenes isolates associated with toxic shock-like syndrome. *Journal of clinical microbiology* **29**, 1562-7 (1991).

171. Ferrieri, P. Immune responses to streptococcal infections. *Manual of Clinical Laboratory Immunology*, 336-341 (1986).

172. Loof, T.G., Rohde, M., Chhatwal, G.S., Jung, S. & Medina, E. The contribution of dendritic cells to host defenses against Streptococcus pyogenes. *Journal of Infectious Diseases* **196**, 1794-1803, doi:10.1086/523647 (2007).

173. Goldmann, O., Rohde, M., Chhatwal, G.S. & Medina, E. Role of Macrophages in Host Resistance to Group A Streptococci. *Infection and immunity* **72**, 2956-2963, doi:10.1128/IAI.72.5.2956-2963.2004 (2004).

174. Goldmann, O., Sastalla, I., Wos-oxley, M., Rohde, M. & Medina, E. Streptococcus pyogenes induces oncosis in macrophages through the

activation of an inflammatory programmed cell death pathway. *Cellular microbiology* **11**, 138-155, doi:10.1111/j.1462-5822.2008.01245.x (2009).

175. Fieber, C. & Kovarik, P. Responses of innate immune cells to group A Streptococcus. *Frontiers in cellular and infection microbiology* **4**, 140, doi:10.3389/fcimb.2014.00140 (2014).

176. Fieber, C. *et al.* Innate immune response to Streptococcus pyogenes depends on the combined activation of TLR13 and TLR2. *PLoS One* **10**, e0119727, doi:10.1371/journal.pone.0119727 (2015).

177. Mishalian, I. *et al.* Recruited macrophages control dissemination of group A Streptococcus from infected soft tissues. *Journal of Immunology* **187**, 6022-6031, doi:10.4049/jimmunol.1101385 (2011).

178. Harder, J. *et al.* Activation of the Nlrp3 inflammasome by Streptococcus pyogenes requires streptolysin O and NF- κ B activation but proceeds independently of TLR signaling and P2X7 receptor. *Journal of Immunology* **183**, 5823-5829, doi:10.4049/jimmunol.0900444 (2009).

179. Hidalgo-Grass, C. *et al.* A streptococcal protease that degrades CXC chemokines and impairs bacterial clearance from infected tissues. *EMBO Journal* **25**, 4628-4637, doi:10.1038/sj.emboj.7601327 (2006).

180. Navarini, A.A. *et al.* Innate immune-induced depletion of bone marrow neutrophils aggravates systemic bacterial infections. *Proceedings of the National Academy of Sciences of the United States of America* **106**, 7107-7112, doi:10.1073/pnas.0901162106 (2009).

181. Sumby, P. *et al.* Extracellular deoxyribonuclease made by group A Streptococcus assists pathogenesis by enhancing evasion of the innate immune response. *Proceedings of the National Academy of Sciences of the United States of America* **102**, 1679-1684, doi:10.1073/pnas.0406641102 (2005).

182. Lin, A., Loughman, J.A., Zinselmeyer, B.H., Miller, M.J. & Caparon, M.G. Streptolysin S inhibits neutrophil recruitment during the early stages of Streptococcus pyogenes infection. *Infection and immunity* **77**, 5190-5201, doi:10.1128/IAI.00420-09 (2009).

183. Kaplan, M.J. & Radic, M. Neutrophil extracellular traps (NETs): Double-edged swords of innate immunity. *Journal of immunology (Baltimore, Md. : 1950)* **189**, 2689-2695, doi:10.4049/jimmunol.1201719 (2012).

184. Nakagawa, I. *et al.* Autophagy defends cells against invading group A Streptococcus. *Science (New York, N.Y.)* **306**, 1037-1040, doi:10.1126/science.1103966 (2004).

185. Håkansson, A., Bentley, C.C., Shakhnovic, E.A. & Wessels, M.R. Cytolysin-dependent evasion of lysosomal killing. *Proceedings of the National Academy of Sciences of the United States of America* **102**, 5192-5197, doi:10.1073/pnas.0408721102 (2005).

186. Tsatsaronis, J.A., Walker, M.J. & Sanderson-Smith, M.L. Host responses to group a streptococcus: cell death and inflammation. *PLoS pathogens* **10**, e1004266, doi:10.1371/journal.ppat.1004266 (2014).

187. Chang, A., Khemlani, A., Kang, H. & Proft, T. Functional analysis of Streptococcus pyogenes nuclease A (SpnA), a novel group A streptococcal virulence factor. *Molecular microbiology* **79**, 1629-1642, doi:10.1111/j.1365-2958.2011.07550.x (2011).

188. Edwards, R.J. *et al.* Specific C-terminal cleavage and inactivation of interleukin-8 by invasive disease isolates of Streptococcus pyogenes. *Journal of Infectious Diseases* **192**, 783-790, doi:10.1086/432485 (2005).

189. Frick, I.M., Åkesson, P., Rasmussen, M., Schmidtchen, A. & Björck, L. SIC, a secreted protein of Streptococcus pyogenes that inactivates antibacterial peptides. *Journal of Biological Chemistry* **278**, 16561-16566, doi:10.1074/jbc.M301995200 (2003).

190. Cleary, P.P., Prahbu, U., Dale, J.B., Wexler, D.E. & Handley, J. Streptococcal C5a peptidase is a highly specific endopeptidase. *Infection and immunity* **60**, 5219-5223 (1992).

191. Terao, Y., Yamaguchi, M., Hamada, S. & Kawabata, S. Multifunctional glyceraldehyde-3-phosphate dehydrogenase of Streptococcus pyogenes is essential for evasion from neutrophils. *Journal of Biological Chemistry* **281**, 14215-14223, doi:10.1074/jbc.M513408200 (2006).

192. Basma, H. *et al.* Risk factors in the pathogenesis of invasive group A streptococcal infections: Role of protective humoral immunity. *Infection and immunity* **67**, 1871-1877 (1999).

193. Basma, H. *et al.* Opsonic antibodies to the surface M protein of group a streptococci in pooled normal immunoglobulins (IVIG): Potential impact on the clinical efficacy of IVIG therapy for severe invasive group a streptococcal infections. *Infection and immunity* **66**, 2279-2283 (1998).

194. Norrby-Teglund, A. *et al.* Relative neutralizing activity in polyspecific IgM, IgA, and IgG preparations against group A streptococcal superantigens. *Clinical Infectious Diseases* **31**, 1175-1182, doi:10.1086/317423 (2000).

195. Mascini, E.M. *et al.* Invasive group a streptococcal disease in The Netherlands: Evidence for a protective role of anti-exotoxin A antibodies. *Journal of Infectious Diseases* **181**, 631-638, doi:10.1086/315222 (2000).

196. O'Connor, S.P. *et al.* The human antibody response to streptococcal C5a peptidase. *The Journal of infectious diseases* **163**, 109-16 (1991).

197. Ma, C.Q. *et al.* Similar ability of FbaA with M protein to elicit protective immunity against group A streptococcus challenge in mice. *Cellular & molecular immunology* **6**, 73-7, doi:10.1038/cmi.2009.10 (2009).

198. Johansson, L., Thulin, P., Low, D.E. & Norrby-Teglund, A. Getting under the skin: The immunopathogenesis of streptococcus pyogenes deep tissue infections. *Clinical Infectious Diseases* **51**, 58-65, doi:10.1086/653116 (2010).

199. Kaplan, E.L., Anthony, B.F., Chapman, S.S., Ayoub, E.M. & Wannamaker, L.W. The influence of the site of infection on the immune response to group A streptococci. *The Journal of clinical investigation* **49**, 1405-1414, doi:10.1172/JCI106358 (1970).

200. Dale, J.B. *et al.* Protective immunogenicity of group a streptococcal M-related proteins. *Clinical and vaccine immunology : CVI* **22**, 344-50, doi:10.1128/cvi.00795-14 (2015).

201. Bessen, D. & Fischetti, V.A. Passive acquired mucosal immunity to group A streptococci by secretory immunoglobulin A. *The Journal of experimental medicine* **167**, 1945-50 (1988).

202. Norrby-Teglund, A. *et al.* Evidence for the presence of streptococcal-superantigen-neutralizing antibodies in normal polyspecific immunoglobulin G. *Infection and immunity* **64**, 5395-5398 (1996).

203. Hall, M.A. *et al.* Intranasal immunization with multivalent group A streptococcal vaccines protects mice against intranasal challenge infections. *Infection and immunity* **72**, 2507-12 (2004).

204. Lancefield, R.C. Current knowledge of type-specific M antigens of group A streptococci. *J Immunol* **89**, 307-13 (1962).

205. Quinn, R.W., Vander Zwaag, R. & Lowry, P.N. Acquisition of group a streptococcal M protein antibodies. *Pediatric Infectious Disease* **4**, 374-378, doi:10.1097/00006454-198507000-00008 (1985).

206. Flores, A.E., Johnson, D.R., Kaplan, E.L. & Wannamaker, L.W. Factors influencing antibody responses to streptococcal m proteins in humans. *Journal of Infectious Diseases* **147**, 1-15, doi:10.1093/infdis/147.1.1 (1983).

207. Von Bernuth, H. *et al.* Pyogenic bacterial infections in humans with MyD88 deficiency. *Science (New York, N.Y.)* **321**, 691-696, doi:10.1126/science.1158298 (2008).

208. Wang, B. *et al.* Induction of TGF- β 1 and TGF- β 1-dependent predominant Th17 differentiation by group A streptococcal infection. *Proceedings of the National Academy of Sciences of the United States of America* **107**, 5937-5942, doi:10.1073/pnas.0904831107 (2010).

209. Dileepan, T. *et al.* Robust antigen specific th17 t cell response to group a streptococcus is dependent on il-6 and intranasal route of infection. *PLoS pathogens* **7**, doi:10.1371/journal.ppat.1002252 (2011).

210. Dileepan, T. *et al.* Group A Streptococcus intranasal infection promotes CNS infiltration by streptococcal-specific Th17 cells. *The Journal of clinical investigation* **126**, 303-17, doi:10.1172/jci80792 (2016).

211. Mortensen, R. *et al.* Adaptive Immunity against Streptococcus pyogenes in Adults Involves Increased IFN-γ and IgG3 Responses Compared with Children. *The Journal of Immunology* **195**, 1657-1664, doi:10.4049/jimmunol.1500804 (2015).

212. Flanagan, J.G. & Rabbitts, T.H. Arrangement of human immunoglobulin heavy chain constant region genes implies evolutionary duplication of a segment containing gamma, epsilon and alpha genes. *Nature* **300**, 709-13 (1982).

213. Watson ME Jr., N.M., Caparon MG., *Animal Models of Streptococcus pyogenes Infection.*, in *Streptococcus pyogenes : Basic Biology to Clinical Manifestations* S.D. Ferretti JJ, Fischetti VA, Editor. 2016.

214. Bessen, D.E. Population biology of the human restricted pathogen, Streptococcus pyogenes. *Infection, genetics and evolution : journal of molecular epidemiology and evolutionary genetics in infectious diseases* **9**, 581-93, doi:10.1016/j.meegid.2009.03.002 (2009).

215. Alam, F.M., Turner, C.E., Smith, K., Wiles, S. & Sriskandan, S. Inactivation of the CovR/S virulence regulator impairs infection in an improved murine model of Streptococcus pyogenes naso-pharyngeal infection. *PLoS One* **8**, e61655, doi:10.1371/journal.pone.0061655 (2013).

216. Park, H.S., Francis, K.P., Yu, J. & Cleary, P.P. Membranous cells in nasal-associated lymphoid tissue: a portal of entry for the respiratory mucosal pathogen group A streptococcus. *J Immunol* **171**, 2532-7 (2003).

217. Mannam, P., Jones, K.F. & Geller, B.L. Mucosal vaccine made from live, recombinant Lactococcus lactis protects mice against pharyngeal infection with Streptococcus pyogenes. *Infection and immunity* **72**, 3444-50, doi:10.1128/iai.72.6.3444-3450.2004 (2004).

218. Medina, E., Goldmann, O., Rohde, M., Lengeling, A. & Chhatwal, G.S. Genetic control of susceptibility to group A streptococcal infection in mice. *The Journal of infectious diseases* **184**, 846-52, doi:10.1086/323292 (2001).

219. Husmann, L.K., Dillehay, D.L., Jennings, V.M. & Scott, J.R. Streptococcus pyogenesinfection in mice. *Microbial Pathogenesis* **20**, 213-224, doi:https://doi.org/10.1006/mpat.1996.0020 (1996).

220. Dale, J.B., Baird, R.W., Courtney, H.S., Hasty, D.L. & Bronze, M.S. Passive protection of mice against group A streptococcal pharyngeal infection by lipoteichoic acid. *The Journal of infectious diseases* **169**, 319-23 (1994).

221. Park, H.S. *et al.* Primary induction of CD4 T cell responses in nasal associated lymphoid tissue during group A streptococcal infection. *Eur J Immunol* **34**, 2843-53, doi:10.1002/eji.200425242 (2004).

222. Schrager, H.M., Rheinwald, J.G. & Wessels, M.R. Hyaluronic acid capsule and the role of streptococcal entry into keratinocytes in invasive skin infection. *The Journal of clinical investigation* **98**, 1954-8, doi:10.1172/jci118998 (1996).

223. Brenot, A., King, K.Y., Janowiak, B., Griffith, O. & Caparon, M.G. Contribution of glutathione peroxidase to the virulence of Streptococcus pyogenes. *Infection and immunity* **72**, 408-13 (2004).

224. Engleberg, N.C., Heath, A., Miller, A., Rivera, C. & DiRita, V.J. Spontaneous mutations in the CsrRS two-component regulatory system of Streptococcus pyogenes result in enhanced virulence in a murine model of skin and soft tissue infection. *The Journal of infectious diseases* **183**, 1043-54, doi:10.1086/319291 (2001).

225. Loughman, J.A. & Caparon, M. Regulation of SpeB in Streptococcus pyogenes by pH and NaCl: a model for in vivo gene expression. *Journal of bacteriology* **188**, 399-408 (2006).

226. Brenot, A., Weston, B.F. & Caparon, M.G. A PerR-regulated metal transporter (PmtA) is an interface between oxidative stress and metal homeostasis in Streptococcus pyogenes. *Molecular microbiology* **63**, 1185-96, doi:10.1111/j.1365-2958.2006.05577.x (2007).

227. Cusumano, Z.T., Watson, M.E., Jr. & Caparon, M.G. Streptococcus pyogenes arginine and citrulline catabolism promotes infection and modulates innate immunity. *Infection and immunity* **82**, 233-42, doi:10.1128/iai.00916-13 (2014).

228. Henningham, A., Barnett, T.C., Maamary, P.G. & Walker, M.J. Pathogenesis of group A streptococcal infections. *Discovery medicine* **13**, 329-42 (2012).

229. Shanley, T.P. *et al.* Streptococcal cysteine protease augments lung injury induced by products of group A streptococci. *Infection and immunity* **64**, 870-7 (1996).

230. Turner, P.V., Brabb, T., Pekow, C. & Vasbinder, M.A. Administration of substances to laboratory animals: routes of administration and factors to consider. *Journal of the American Association for Laboratory Animal Science : JAALAS* **50**, 600-13 (2011).

231. Bremell, T., Lange, S., Yacoub, A., Rydén, C. & Tarkowski, A. Experimental Staphylococcus aureus arthritis in mice. *Infection and immunity* **59**, 2615-2623 (1991).

232. Bremell, T., Abdelnour, A. & Tarkowski, A. Histopathological and serological progression of experimental Staphylococcus aureus arthritis. *Infection and immunity* **60** (1992).

233. Bremell, T. *et al.* Immunopathological features of rat Staphylococcus aureus arthritis. *Infection and immunity* **62**, 2334-2344 (1994).

234. Bremell, T. & Tarkowski, A. Preferential induction of septic arthritis and mortality by superantigen-producing staphylococci. *Infection and immunity* **63** (1995).

235. Tarkowski, A. *et al.* Model systems: modeling human staphylococcal arthritis and sepsis in the mouse. *Trends in microbiology* **9**, 321-6 (2001).

236. Tarkowski, A. Infectious arthritis. *Best Pract Res Clin Rheumatol* **20**, doi:10.1016/j.berh.2006.08.001 (2006).

237. Gjertsson, I., Jonsson, I.M., Peschel, A., Tarkowski, A. & Lindholm, C. Formylated peptides are important virulence factors in Staphylococcus aureus arthritis in mice. *The Journal of infectious diseases* **205**, 305-11, doi:10.1093/infdis/jir713 (2012).

238. Sakurai, A. *et al.* Streptococcus pyogenes Infection Induces Septic Arthritis with Increased Production of the Receptor Activator of the NF-κB Ligand. *Infection and immunity* **71**, 6019-6026, doi:10.1128/IAI.71.10.6019-6026.2003 (2003).

239. Tarkowski, A. *et al.* Model systems: modeling human staphylococcal arthritis and sepsis in the mouse. *Trends in microbiology* **9**, doi:10.1016/s0966-842x(01)02078-9 (2001).

240. Colavite-Machado, P.M. *et al.* Differential arthritogenicity of Staphylococcus aureusstrains isolated from biological samples. *BMC Infectious Diseases* **13**, 1-10, doi:10.1186/1471-2334-13-400 (2013).

241. Puliti, M., Bistoni, F., von Hunolstein, C., Orefici, G. & Tissi, L. Severity of group B streptococcal arthritis in selected strains of laboratory mice. *Infection and immunity* **69**, 551-5, doi:10.1128/iai.69.1.551-555.2001 (2001).

242. Puliti, M. *et al.* Role of macrophages in experimental group B streptococcal arthritis. *Cellular microbiology* **4**, 691-700 (2002).

243. Tissi, L. *et al.* Experimental model of type IV Streptococcus agalactiae (group B streptococcus) infection in mice with early development of septic arthritis. *Infection and immunity* **58**, 3093-100 (1990).

244. Tissi, L. *et al.* Role of Tumor Necrosis Factor Alpha, Interleukin-1β, and Interleukin-6 in a Mouse Model of Group B Streptococcal Arthritis. *Infection and immunity* **67**, 4545-4550 (1999).

245. Freiberg, J.A., McIver, K.S. & Shirtliff, M.E. In Vivo Expression of Streptococcus pyogenes Immunogenic Proteins during Tibial Foreign Body Infection. *Infection and immunity* **82**, 3891-3899, doi:10.1128/iai.01831-14 (2014).

246. Miller, R.L. Transgenic mice: beyond the knockout. *American journal of physiology. Renal physiology* **300**, F291-300, doi:10.1152/ajprenal.00082.2010 (2011).

247. Siemens, N. & Norrby-Teglund, A. Shocking superantigens promote establishment of bacterial infection. *Proceedings of the National Academy of Sciences of the United States of America* **114**, 10000-10002, doi:10.1073/pnas.1713451114 (2017).

248. Tilahun, A.Y. *et al.* Human leukocyte antigen class II transgenic mouse model unmasks the significant extrahepatic pathology in toxic shock syndrome. *The American journal of pathology* **178**, 2760-73, doi:10.1016/j.ajpath.2011.02.033 (2011).

249. Miethke, T. *et al.* T cell-mediated lethal shock triggered in mice by the superantigen staphylococcal enterotoxin B: critical role of tumor necrosis factor. *The Journal of experimental medicine* **175**, 91-98, doi:10.1084/jem.175.1.91 (1992).

250. Smiley, S.T., Laufer, T.M., Lo, D., Glimcher, L.H. & Grusby, M.J. Transgenic mice expressing MHC class II molecules with truncated A beta cytoplasmic domains reveal signaling-independent defects in antigen presentation. *International immunology* **7**, 665-77 (1995).

251. Zeng, Y. *et al.* Generation of human MHC (HLA-A11/DR1) transgenic mice for vaccine evaluation. *Human vaccines & immunotherapeutics* **12**, 829-36, doi:10.1080/21645515.2015.1103405 (2016).

252. Taneja, V. & David, C.S. HLA transgenic mice as humanized mouse models of disease and immunity. *The Journal of clinical investigation* **101**, 921-6, doi:10.1172/jci2860 (1998).

253. Norrby-Teglund, A., Nepom, G.T. & Kotb, M. Differential presentation of group A streptococcal superantigens by HLA class II DQ and DR alleles. *European Journal of Immunology* **32**, 2570-2577, doi:10.1002/1521-4141(200209)32:9<2570::AID-IMMU2570>3.0.CO;2-E (2002).

254. Sriskandan, S. *et al.* Enhanced Susceptibility to Superantigen-Associated Streptococcal Sepsis in Human Leukocyte Antigen-DQ Transgenic Mice. *Journal of Infectious Diseases* **184**, 166-173, doi:10.1086/322018 (2001).

255. Kasper, K.J. *et al.* Bacterial superantigens promote acute nasopharyngeal infection by Streptococcus pyogenes in a human MHC Class II-dependent manner. *PLoS pathogens* **10**, e1004155, doi:10.1371/journal.ppat.1004155 (2014).

256. Zeppa, J.J. *et al.* Nasopharyngeal Infection of Mice with Streptococcus pyogenes and In Vivo Detection of Superantigen Activity. *Methods in molecular biology (Clifton, N.J.)* **1396**, 95-107, doi:10.1007/978-1-4939-3344-0_8 (2016).

257. Miles, A.A., Misra, S.S. & Irwin, J.O. The estimation of the bactericidal power of the blood. *The Journal of Hygiene* **38**, 732-749 (1938).

258. Beall, B., Facklam, R. & Thompson, T. Sequencing emm-specific PCR products for routine and accurate typing of group A streptococci. *Journal of clinical microbiology* **34**, 953-8 (1996).

259. Birnie, G.D. The HL60 cell line: a model system for studying human myeloid cell differentiation. *The British journal of cancer. Supplement* **9**, 41-5 (1988).

260. Lam, J., Herant, M., Dembo, M. & Heinrich, V. Baseline mechanical characterization of J774 macrophages. *Biophysical journal* **96**, 248-54, doi:10.1529/biophysj.108.139154 (2009).

261. Romero-Steiner, S. *et al.* Standardization of an opsonophagocytic assay for the measurement of functional antibody activity against Streptococcus pneumoniae using differentiated HL-60 cells. *Clinical and diagnostic laboratory immunology* **4**, 415-22 (1997).

262. Gadjeva, M. *The Complement System: Methods and Protocols*. (Humana Press, 2014).

263. Stenslik, M.J. *et al.* Methodology and effects of repeated intranasal delivery of DNSP-11 in a rat model of Parkinson's disease. *Journal of neuroscience methods* **251**, 120-9, doi:10.1016/j.jneumeth.2015.05.006 (2015).

264. Fei, Y. *et al.* The combination of a tumor necrosis factor inhibitor and antibiotic alleviates staphylococcal arthritis and sepsis in mice. *The Journal of infectious diseases* **204**, 348-57, doi:10.1093/infdis/jir266 (2011).

265. Franklin, L. *et al.* The AgI/II family adhesin AspA is required for respiratory infection by Streptococcus pyogenes. *PLoS One* **8**, e62433, doi:10.1371/journal.pone.0062433 (2013).

266. Cornick, J.E. *et al.* Epidemiological and molecular characterization of an invasive Group A Streptococcus emm32.2 outbreak. *Journal of clinical microbiology*, doi:10.1128/jcm.00191-17 (2017).

267. Romero-Steiner, S. *et al.* Multilaboratory evaluation of a viability assay for measurement of opsonophagocytic antibodies specific to the capsular polysaccharides of Streptococcus pneumoniae. *Clinical and diagnostic laboratory immunology* **10**, 1019-24 (2003).

268. Melnick, N., Rajam, G., Carlone, G.M., Sampson, J.S. & Ades, E.W. Evaluation of a novel therapeutic approach to treating severe pneumococcal infection using a mouse model. *Clinical and vaccine immunology : CVI* **16**, 806-10, doi:10.1128/cvi.00120-09 (2009).

269. Alejandria, M.M., Lansang, M.A., Dans, L.F. & Mantaring, J.B., 3rd. Intravenous immunoglobulin for treating sepsis, severe sepsis and septic shock. *The Cochrane database of systematic reviews*, Cd001090, doi:10.1002/14651858.CD001090.pub2 (2013).

270. Krause, I. *et al.* In vitro antiviral and antibacterial activity of commercial intravenous immunoglobulin preparations--a potential role for adjuvant

intravenous immunoglobulin therapy in infectious diseases. *Transfusion medicine (Oxford, England)* **12**, 133-9 (2002).

271. Hemming, V.G. Use of intravenous immunoglobulins for prophylaxis or treatment of infectious diseases. *Clinical and diagnostic laboratory immunology* **8**, 859-63, doi:10.1128/cdli.8.5.859-863.2001 (2001).

272. Norrby-Teglund, A. *et al.* Successful management of severe group A streptococcal soft tissue infections using an aggressive medical regimen including intravenous polyspecific immunoglobulin together with a conservative surgical approach. *Scandinavian journal of infectious diseases* **37**, 166-172, doi:10.1080/00365540410020866 (2005).

273. Norrby-Teglund, A. *et al.* Varying titers of neutralizing antibodies to streptococcal superantigens in different preparations of normal polyspecific immunoglobulin G: implications for therapeutic efficacy. *Clinical infectious diseases : an official publication of the Infectious Diseases Society of America* **26**, 631-8 (1998).

274. Reglinski, M., Lynskey, N.N. & Sriskandan, S. Modification of the classical Lancefield assay of group A streptococcal killing to reduce inter-donor variation. *Journal of microbiological methods* **124**, 69-71, doi:10.1016/j.mimet.2016.03.015 (2016).

275. Harris, C.L., Heurich, M., Rodriguez de Cordoba, S. & Morgan, B.P. The complotype: dictating risk for inflammation and infection. *Trends in immunology* **33**, 513-21, doi:10.1016/j.it.2012.06.001 (2012).

276. Lancefield, R.C. Differentiation of group A streptococci with a common R antigen into three serological types, with special reference to the bactericidal test. *The Journal of experimental medicine* **106**, 525-44 (1957).

277. van den Akker, E.L. *et al.* Ficoll-separated mononuclear cells from sepsis patients are contaminated with granulocytes. *Intensive care medicine* **34**, 912-6, doi:10.1007/s00134-007-0989-0 (2008).

278. Martinez, J.E. *et al.* A flow cytometric opsonophagocytic assay for measurement of functional antibodies elicited after vaccination with the 23-valent pneumococcal polysaccharide vaccine. *Clinical and diagnostic laboratory immunology* **6**, 581-6 (1999).

279. Gallagher, R.E. *et al.* Characterization of differentiation-inducer-resistant HL-60 cells. *Leukemia research* **9**, 967-86 (1985).

280. Kim, K.-H., Seoh, J.Y. & Cho, S.J. Phenotypic and Functional Analysis of HL-60 Cells Used in Opsonophagocytic-Killing Assay for Streptococcus pneumoniae. *Journal of Korean Medical Science* **30**, 145-150, doi:10.3346/jkms.2015.30.2.145 (2015).

281. Manda-Handzlik, A. *et al.* The influence of agents differentiating HL-60 cells toward granulocyte-like cells on their ability to release neutrophil

extracellular traps. *Immunology & Cell Biology* **96**, 413-425, doi:doi:10.1111/imcb.12015 (2018).

282. Foley, M.J., Smith, M.R. & Wood, W.B., Jr. Studies on the pathogenicity of group A Streptococci. I. Its relation to surface phagocytosis. *The Journal of experimental medicine* **110**, 603-16 (1959).

283. Cole, J.N. *et al.* M protein and hyaluronic acid capsule are essential for in vivo selection of covRS mutations characteristic of invasive serotype M1T1 group A Streptococcus. *mBio* **1**, doi:10.1128/mBio.00191-10 (2010).

284. Moses, A.E. *et al.* Relative contributions of hyaluronic acid capsule and M protein to virulence in a mucoid strain of the group A Streptococcus. *Infection and immunity* **65**, 64-71 (1997).

285. Jarva, H., Jokiranta, T.S., Wurzner, R. & Meri, S. Complement resistance mechanisms of streptococci. *Molecular immunology* **40**, 95-107 (2003).

286. Turner, C.E. *et al.* Emergence of a New Highly Successful Acapsular Group A Streptococcus Clade of Genotype emm89 in the United Kingdom. *mBio* **6**, e00622, doi:10.1128/mBio.00622-15 (2015).

287. Flores, A.R. *et al.* Natural variation in the promoter of the gene encoding the Mga regulator alters host-pathogen interactions in group a Streptococcus carrier strains. *Infection and immunity* **81**, 4128-38, doi:10.1128/iai.00405-13 (2013).

288. Ji, Y., McLandsborough, L., Kondagunta, A. & Cleary, P.P. C5a peptidase alters clearance and trafficking of group A streptococci by infected mice. *Infection and immunity* **64**, 503-10 (1996).

289. Wexler, D.E., Chenoweth, D.E. & Cleary, P.P. Mechanism of action of the group A streptococcal C5a inactivator. *Proceedings of the National Academy of Sciences of the United States of America* **82**, 8144-8148, doi:10.1073/pnas.82.23.8144 (1985).

290. Okada, N., Geist, R.T. & Caparon, M.G. Positive transcriptional control of mry regulates virulence in the group A streptococcus. *Molecular microbiology* **7**, 893-903 (1993).

291. Kreikemeyer, B. *et al.* Genomic organization, structure, regulation and pathogenic role of pilus constituents in major pathogenic Streptococci and Enterococci. *International journal of medical microbiology : IJMM* **301**, 240-51, doi:10.1016/j.ijmm.2010.09.003 (2011).

292. Starr, C.R. & Engleberg, N.C. Role of hyaluronidase in subcutaneous spread and growth of group A streptococcus. *Infection and immunity* **74**, 40-8, doi:10.1128/iai.74.1.40-48.2006 (2006).

293. van der Maten, E., de Jonge, M.I., de Groot, R., van der Flier, M. & Langereis, J.D. A versatile assay to determine bacterial and host factors

contributing to opsonophagocytotic killing in hirudin-anticoagulated whole blood. *Scientific reports* **7**, 42137, doi:10.1038/srep42137 (2017).

294. Kadioglu, A. *et al.* Upper and lower respiratory tract infection by Streptococcus pneumoniae is affected by pneumolysin deficiency and differences in capsule type. *Infection and immunity* **70**, 2886-90 (2002).

295. Perry, M. & Whyte, A. Immunology of the tonsils. *Immunology today* **19**, 414-21 (1998).

296. Medzhitov, R. & Janeway, C.A., Jr. Innate immunity: impact on the adaptive immune response. *Current opinion in immunology* **9**, 4-9 (1997).

297. Chen, S.-M. *et al.* Streptococcal collagen-like surface protein 1 promotes adhesion to the respiratory epithelial cell. *BMC Microbiology* **10**, 1-11, doi:10.1186/1471-2180-10-320 (2010).

298. Malmstrom, J. *et al.* Streptococcus pyogenes in human plasma: adaptive mechanisms analyzed by mass spectrometry-based proteomics. *The Journal of biological chemistry* **287**, 1415-25, doi:10.1074/jbc.M111.267674 (2012).

299. Alouf, J.E. Streptococcal toxins (streptolysin O, streptolysin S, erythrogenic toxin). *Pharmacology & Therapeutics* **11**, 661-717, doi:https://doi.org/10.1016/0163-7258(80)90045-5 (1980).

300. Henry, B.D. *et al.* Engineered liposomes sequester bacterial exotoxins and protect from severe invasive infections in mice. *Nat Biotechnol* **33**, 81-8, doi:10.1038/nbt.3037 (2015).

301. Alhamdi, Y. *et al.* Circulating Pneumolysin Is a Potent Inducer of Cardiac Injury during Pneumococcal Infection. *PLoS pathogens* **11**, e1004836, doi:10.1371/journal.ppat.1004836 (2015).

302. Uchiyama, S. *et al.* Streptolysin O Rapidly Impairs Neutrophil Oxidative Burst and Antibacterial Responses to Group A Streptococcus. *Frontiers in immunology* **6**, 581, doi:10.3389/fimmu.2015.00581 (2015).

303. LaRock, C.N. & Nizet, V. Inflammasome/IL-1 β Responses to Streptococcal Pathogens. *Frontiers in immunology* **6**, doi:10.3389/fimmu.2015.00518 (2015).

304. Zhu, L. *et al.* A molecular trigger for intercontinental epidemics of group A Streptococcus. *The Journal of clinical investigation* **125**, 3545-59, doi:10.1172/jci82478 (2015).

305. Rezcallah, M.S., Boyle, M.D.P. & Sledjeski, D.D. Mouse skin passage of Streptococcus pyogenes results in increased streptokinase expression and activity. *Microbiology* **150**, 365-371, doi:doi:10.1099/mic.0.26826-0 (2004).

306. Kazmi, S.U. *et al.* Reciprocal, Temporal Expression of SpeA and SpeB by Invasive M1T1 Group A Streptococcal Isolates In Vivo. *Infection and immunity* **69**, 4988-4995, doi:10.1128/iai.69.8.4988-4995.2001 (2001).

307. Barnard, W.G. & Todd, E.W. Lesions in the mouse produced by streptolysins O and S. *The Journal of Pathology and Bacteriology* **51**, 43-47, doi:doi:10.1002/path.1700510108 (1940).

308. Coyle, E.A., Cha, R. & Rybak, M.J. Influences of Linezolid, Penicillin, and Clindamycin, Alone and in Combination, on Streptococcal Pyrogenic Exotoxin A Release. *Antimicrobial Agents and Chemotherapy* **47**, 1752-1755, doi:10.1128/aac.47.5.1752-1755.2003 (2003).

309. Drulis-Kawa, Z. & Dorotkiewicz-Jach, A. Liposomes as delivery systems for antibiotics. *International journal of pharmaceutics* **387**, 187-98, doi:10.1016/j.ijpharm.2009.11.033 (2010).

310. Nade, S. Septic arthritis. *Best Practice & Research Clinical Rheumatology* **17**, 183-200, doi:10.1016/S1521-6942(02)00106-7 (2003).

311. Koch, B. *et al.* Demonstration of interleukin-1beta and interleukin-6 in cells of synovial fluids by flow cytometry. *European journal of medical research* **1**, 244-8 (1996).

312. Abdelnour, A., Bremell, T., Holmdahl, R. & Tarkowski, A. Role of T lymphocytes in experimental Staphylococcus aureus arthritis. *Scandinavian journal of immunology* **39**, 403-8 (1994).

313. Abdelnour, A., Bremell, T., Holmdahl, R. & Tarkowski, A. Clonal expansion of T lymphocytes causes arthritis and mortality in mice infected with toxic shock syndrome toxin-1-producing staphylococci. *Eur J Immunol* **24**, 1161-6, doi:10.1002/eji.1830240523 (1994).

314. Norii, M. *et al.* Selective recruitment of CXCR3+ and CCR5+ CCR4+ T cells into synovial tissue in patients with rheumatoid arthritis. *Acta Med Okayama* **60**, 149-157, doi:10.18926/amo/30745 (2006).

315. Suzuki, N. *et al.* Selective accumulation of CCR5+ T lymphocytes into inflamed joints of rheumatoid arthritis. *International immunology* **11**, 553-9 (1999).

316. Ueno, A. *et al.* The production of CXCR3-agonistic chemokines by synovial fibroblasts from patients with rheumatoid arthritis. *Rheumatology international* **25**, 361-7, doi:10.1007/s00296-004-0449-x (2005).

317. Stanczyk, J. *et al.* RANTES and chemotactic activity in synovial fluids from patients with rheumatoid arthritis and osteoarthritis. *Mediators of inflammation* **2005**, 343-8, doi:10.1155/mi.2005.343 (2005).

318. Osiri, M., Ruxrungtham, K., Nookhai, S., Ohmoto, Y. & Deesomchok, U. IL-1beta, IL-6 and TNF-alpha in synovial fluid of patients with non-gonococcal septic arthritis. *Asian Pacific journal of allergy and immunology* **16**, 155-60 (1998).

319. Kwan Tat, S., Padrines, M., Theoleyre, S., Heymann, D. & Fortun, Y. IL-6, RANKL, TNF-alpha/IL-1: interrelations in bone resorption pathophysiology. *Cytokine Growth Factor Rev* **15**, 49-60 (2004).

320. Horowitz, M.C., Xi, Y., Wilson, K. & Kacena, M.A. Control of osteoclastogenesis and bone resorption by members of the TNF family of receptors and ligands. *Cytokine & Growth Factor Reviews* **12**, 9-18, doi:10.1016/S1359-6101(00)00030-7 (2001).

321. Corrado, A. *et al.* Staphylococcus aureus-dependent septic arthritis in murine knee joints: local immune response and beneficial effects of vaccination. *Scientific reports* **6**, 38043, doi:10.1038/srep38043 (2016).

322. Verdrengh, M. & Tarkowski, A. Role of macrophages in Staphylococcus aureus-induced arthritis and sepsis. *Arthritis and rheumatism* **43**, 2276-82, doi:10.1002/1529-0131(200010)43:10<2276::aid-anr15>3.0.co;2-c (2000).

323. Verdrengh, M. & Tarkowski, A. Role of neutrophils in experimental septicemia and septic arthritis induced by Staphylococcus aureus. *Infection and immunity* **65**, 2517-21 (1997).

324. Gjertsson, I., Hultgren, O.H., Stenson, M., Holmdahl, R. & Tarkowski, A. Are B lymphocytes of importance in severe Staphylococcus aureus infections? *Infection and immunity* **68**, 2431-4 (2000).

325. Dey, I. & Bishayi, B. Role of Th17 and Treg cells in septic arthritis and the impact of the Th17/Treg -derived cytokines in the pathogenesis of S. aureus induced septic arthritis in mice. *Microbial pathogenesis* **113**, 248-264, doi:10.1016/j.micpath.2017.10.033 (2017).

326. Gratz, I.K., Rosenblum, M.D. & Abbas, A.K., *The life of regulatory T cells*, in *Annals of the New York Academy of Sciences*. 2013. p. 8-12.

327. Qin, S. *et al.* The chemokine receptors CXCR3 and CCR5 mark subsets of T cells associated with certain inflammatory reactions. *The Journal of clinical investigation* **101**, 746-54, doi:10.1172/jci1422 (1998).

328. Nevius, E., Gomes, A.C. & Pereira, J.P. Inflammatory Cell Migration in Rheumatoid Arthritis: A Comprehensive Review. *Clinical reviews in allergy & immunology* **51**, 59-78, doi:10.1007/s12016-015-8520-9 (2016).

329. Aziz, R.K. *et al.* Microevolution of group A streptococci in vivo: capturing regulatory networks engaged in sociomicrobiology, niche adaptation, and hypervirulence. *PLoS One* **5**, e9798, doi:10.1371/journal.pone.0009798 (2010).

330. Sumby, P., Whitney, A.R., Graviss, E.A., DeLeo, F.R. & Musser, J.M. Genome-wide analysis of group a streptococci reveals a mutation that modulates global phenotype and disease specificity. *PLoS pathogens* **2**, e5, doi:10.1371/journal.ppat.0020005 (2006).

331. Rothbard, S. & Watson, R.F. Variation occurring in group A streptococci during human infection; progressive loss of M substance correlated with increasing susceptibility to bacteriostasis. *The Journal of experimental medicine* **87**, 521-33 (1948).

332. Molinari, G. & Chhatwal, G.S. Invasion and survival of Streptococcus pyogenes in eukaryotic cells correlates with the source of the clinical isolates. *The Journal of infectious diseases* **177**, 1600-7 (1998).

333. Dinkla, K. *et al.* Rheumatic fever-associated Streptococcus pyogenes isolates aggregate collagen. *The Journal of clinical investigation* **111**, 1905-12, doi:10.1172/jci17247 (2003).

334. Sriskandan, S. *et al.* Streptococcal pyrogenic exotoxin A release, distribution, and role in a murine model of fasciitis and multiorgan failure due to Streptococcus pyogenes. *The Journal of infectious diseases* **173**, 1399-407 (1996).

335. Sriskandan, S. *et al.* Enhanced susceptibility to superantigen-associated streptococcal sepsis in human leukocyte antigen-DQ transgenic mice. *The Journal of infectious diseases* **184**, 166-73, doi:10.1086/322018 (2001).

336. Courtney, H.S., Hasty, D.L. & Dale, J.B. Anti-phagocytic mechanisms of Streptococcus pyogenes: binding of fibrinogen to M-related protein. *Molecular microbiology* **59**, 936-47, doi:10.1111/j.1365-2958.2005.04977.x (2006).

337. Chiavolini, D., Pozzi, G. & Ricci, S. Animal models of Streptococcus pneumoniae disease. *Clinical microbiology reviews* **21**, 666-85, doi:10.1128/cmr.00012-08 (2008).

338. Kalia, A. & Bessen, D.E. Natural Selection and Evolution of Streptococcal Virulence Genes Involved in Tissue-Specific Adaptations. *Journal of bacteriology* **186**, 110-121, doi:10.1128/jb.186.1.110-121.2004 (2004).

339. Svensson, M.D. *et al.* Role for a secreted cysteine proteinase in the establishment of host tissue tropism by group A streptococci. *Molecular microbiology* **38**, 242-253, doi:10.1046/j.1365-2958.2000.02144.x (2000).

340. Sasaki, S. *et al.* Interleukin-4 and interleukin-10 are involved in host resistance to Staphylococcus aureus infection through regulation of gamma interferon. *Infection and immunity* **68**, 2424-30 (2000).